



**The Complexities of Long Distance:
a relationship between the gut microbiota and breast cancer**

Alastair Matthew McKee

Student Registration #100181882

A thesis submitted for the degree of Doctor of Philosophy (Ph.D.) in Biomolecular Science.

University of East Anglia
School of Biological Sciences

Quadram Institute Bioscience
Gut Microbes and Health

Word Count: 89 851

February 2023

Abstract

Antibiotic induced perturbations of the gut microbiota are increasingly associated with the progression of several cancers. In contrast, the promotion of a healthy microbiota, often through probiotic supplementation, can improve treatment outcomes and bolster anti-cancer immune responses in tumours. However, studies involving breast cancer specifically are relatively limited. In 2020, breast cancer was the most frequently diagnosed cancer globally and carried one of the highest mortality rates among all cancer types. Additionally, the use of antibiotics in breast cancer treatment pathways is common. Thus, the research presented in this thesis aims to expand the current understanding of the influences the microbiota has on breast cancer, particularly regarding the downstream effects of antibiotic administration. The results demonstrate that antibiotic-induced perturbations of the microbiota promote primary breast cancer tumour progression in at least two different orthotopic models of the disease. Antibiotics did not influence tumour progression in germ-free animals, confirming that this progression was microbiota dependent. Single cell transcriptomics and histological analysis identified mast cells as being increased in tumours from antibiotic treated animals and, subsequently, inhibiting mast cell function rescued tumour growth in antibiotic treated animals to sizes similar to those observed in a control group at the same timepoint. Shotgun metagenomic sequencing of caecal samples identified reductions in several bacterial species in antibiotic treated animals. One such species, *Faecalibaculum rodentium*, has known anti-tumourigenic influence in colorectal cancer models and, when supplemented to antibiotic treated animals, rescued tumour growth. Efforts were made to investigate how perturbation of the microbiota influenced breast cancer metastasis, but the results obtained suggest further research is required to fully understand such influences. The implications of this research suggest that the use of antibiotics in breast cancer treatment pathways should be cautious and clinical guidance regarding their administration may need to be revised.

Access Condition and Agreement

Each deposit in UEA Digital Repository is protected by copyright and other intellectual property rights, and duplication or sale of all or part of any of the Data Collections is not permitted, except that material may be duplicated by you for your research use or for educational purposes in electronic or print form. You must obtain permission from the copyright holder, usually the author, for any other use. Exceptions only apply where a deposit may be explicitly provided under a stated licence, such as a Creative Commons licence or Open Government licence.

Electronic or print copies may not be offered, whether for sale or otherwise to anyone, unless explicitly stated under a Creative Commons or Open Government license. Unauthorised reproduction, editing or reformatting for resale purposes is explicitly prohibited (except where approved by the copyright holder themselves) and UEA reserves the right to take immediate 'take down' action on behalf of the copyright and/or rights holder if this Access condition of the UEA Digital Repository is breached. Any material in this database has been supplied on the understanding that it is copyright material and that no quotation from the material may be published without proper acknowledgement.

Contents

ABSTRACT	2
CONTENTS.....	3
ACKNOWLEDGMENTS	8
LIST OF FIGURES	9
LIST OF TABLES.....	12
1 INTRODUCTION	13
1.1 PREFACE	13
1.2 BREAST CANCER	14
1.2.1 <i>Breast Physiology</i>	14
1.2.2 <i>Risk factors influencing breast cancer occurrence</i>	15
1.2.3 <i>Epidemiology</i>	16
1.2.4 <i>Staging and disease progression</i>	18
1.2.5 <i>Disease molecular pathophysiology</i>	21
1.2.6 <i>Current treatment approaches</i>	24
1.2.6.1 Surgery.....	24
1.2.6.2 Hormone therapies.....	25
1.2.6.3 Anti-HER2.....	26
1.2.6.4 Chemotherapy	26
1.2.6.5 Radiotherapy	27
1.3 THE IMMUNE SYSTEM	28
1.3.1 <i>Haematopoiesis</i>	28
1.3.2 <i>Innate immune cells and their functions</i>	31
1.3.2.1 Granulocytes and Mast Cells.....	31
1.3.2.2 Monocytes and Macrophages	35
1.3.2.3 Dendritic Cells	37
1.3.2.4 Natural Killer cells	39
1.3.3 <i>Adaptive immune cells and their functions</i>	40
1.3.3.1 CD4-expressing T-cells	40
1.3.3.2 CD8-expressing T-cells	44
1.3.3.3 B-Cells	45
1.4 IMMUNOGENICITY OF CANCER	48
1.4.1 <i>Immune influence on tumour growth and metastasis</i>	49
1.4.1.1 T-reg cells.....	49
1.4.1.2 Myeloid derived suppressor cells	51
1.4.1.3 M2 macrophages	52
1.4.1.4 Mast cells	54

1.4.2	<i>The anti-tumour immune response</i>	56
1.4.2.1	Cytotoxic T-cells and NK cells.....	56
1.4.2.2	Dendritic cells and macrophages	57
1.4.3	<i>Immune evasion and Immunotherapies</i>	58
1.5	THE GUT MICROBIOTA	64
1.5.1	<i>Establishment</i>	64
1.5.2	<i>Composition and equilibrium</i>	65
1.5.3	<i>Functional influences that benefit the host</i>	67
1.5.3.1	Protection from pathogens.....	67
1.5.3.2	Protein and carbohydrate metabolism	68
1.5.3.3	Regulation of the intestinal barrier	69
1.5.3.4	Immune education.....	70
1.5.4	<i>Influence on disease</i>	72
1.6	LINKS BETWEEN THE GUT MICROBIOTA AND CANCER	75
1.6.1	<i>The microbiota and its influence on intra-GI cancers</i>	75
1.6.2	<i>Current evidence of the microbiota's effect on cancers at distant sites</i>	78
1.6.3	<i>The gut microbiota and breast cancer</i>	80
1.7	PRELIMINARY RESEARCH FORMING THE FOUNDATION OF THE STUDIES UNDERTAKEN IN THIS THESIS.....	83
1.8	RESEARCH AIMS AND OBJECTIVES	86
2	MATERIALS AND METHODS	87
2.1	ANIMALS.....	87
2.2	PYMT-BO1 AND EO771 <i>IN VIVO</i> TUMOUR GROWTH ASSAYS	87
2.3	BREAST CANCER CELL CULTURE FOR <i>IN VITRO</i> AND <i>IN VIVO</i> EXPERIMENTS	87
2.4	ANTIBIOTIC ADMINISTRATION	87
2.5	CROMOLYN SODIUM ADMINISTRATION.....	88
2.6	PROBIOTIC ADMINISTRATION	88
2.6.1	<i>Faecalibaculum rodentium (F. rod)</i>	88
2.6.2	<i>Bifidobacterial Cocktail</i>	88
2.6.3	<i>Bacterial Load Enumeration</i>	88
2.6.4	<i>Bacterial Treatment Regimens</i>	88
2.7	<i>IN VIVO</i> TUMOUR GROWTH ASSAYS AND ANTIBIOTIC REGIMENS UNDERTAKEN BY INTERNATIONAL COLLABORATORS AND USED FOR MAST CELL COUNTING	89
2.7.1	<i>Spontaneous HER2 model</i>	89
2.7.2	<i>Orthotopic Luminal A model</i>	89
2.8	SERUM IGE ENZYME-LINKED IMMUNOSORBENT ASSAY (ELISA)	89
2.8.1	<i>Serum Collection</i>	89
2.8.2	<i>Running of Assay</i>	89
2.8.3	<i>Quantification of Serum IgE levels</i>	90

2.9	WESTERN BLOT	90
2.9.1	<i>Western Blot Sample Preparation</i>	90
2.9.2	<i>8% Polyacrylamide Gel (SDS-PAGE) Electrophoresis</i>	90
2.9.3	<i>Protein Transfer and Immunoblot</i>	90
2.10	<i>IN VIVO AND EX VIVO BIOLUMINESCENCE IMAGING</i>	91
2.11	CRYO-SECTIONING OF SNAP FROZEN TUMOURS	92
2.12	TOLUIDINE BLUE STAINING	92
2.13	PICRO-SIRIUS RED STAINING	92
2.14	TUNEL STAINING	92
2.15	IMMUNOFLUORESCENCE STAINING	93
2.16	TISSUE PROCESSING AND EMBEDDING	93
2.17	IMMUNOHISTOCHEMICAL STAINING	94
2.18	FLOW CYTOMETRY	95
2.18.1	<i>In vitro VNMAA effects on PyMT-BO1 cell proliferation and apoptosis</i>	95
2.18.2	<i>Animal Tissue</i>	95
2.18.3	<i>Blood Samples</i>	96
2.18.4	<i>Data Collection</i>	98
2.19	CAECAL DNA EXTRACTION	98
2.20	SHOTGUN METAGENOMICS	98
2.21	CAECAL METABOLOMICS	99
2.22	SINGLE CELL RNA SEQUENCING	100
2.22.1	<i>Loupe Cell Browser Analysis</i>	100
2.22.2	<i>Earlham Institute Expert Bioinformatic scRNAseq Analysis</i>	101
2.22.3	<i>Bulk RNAseq Deconvolution</i>	101
2.23	MESOSCALE DISCOVERY (MSD) MULTIPLEX IMMUNO-ARRAYS	102
2.24	STATISTICAL ANALYSIS	102

3 ANTIBIOTIC ADMINISTRATION PROMOTES PRIMARY BREAST CANCER TUMOUR GROWTH THROUGH A DISRUPTION OF GUT MICROBIOTA HOMEOSTASIS 103

3.1	GROWTH KINETICS OF PYMT-BO1 TUMOURS FOLLOWING VNMAA ANTIBIOTIC TREATMENT	104
3.2	INCREASED TUMOUR PROGRESSION IS MICROBIOTA-DEPENDENT AND NOT THE DIRECT RESULT OF ANTIBIOTIC ADMINISTRATION	107
3.3	EARLY TUMOUR IMMUNE INFILTRATION SHOWS NO DIFFERENCES FOLLOWING VNMAA ANTIBIOTIC TREATMENT .	109
3.4	VNMAA-INDUCED MICROBIOTA PERTURBATION PROMOTES TUMOUR GROWTH IN AT LEAST TWO MODELS OF BREAST CANCER	110
3.5	A CLINICALLY RELEVANT ANTIBIOTIC, CEPHALEXIN, PROMOTES PYMT-BO1 TUMOUR GROWTH IN A SIMILAR FASHION TO VNMAA	112
3.6	TUMOUR CELL PROLIFERATION IS INCREASED FOLLOWING ANTIBIOTIC TREATMENT	115

3.7	BLOOD VESSEL DENSITY IS UNCHANGED FOLLOWING ANTIBIOTIC TREATMENT	116
3.8	BOTH VNMAA AND CEPHALEXIN PERTURB THE MURINE GUT MICROBIOTA WITH THE COMMON LOSS OF SEVERAL BACTERIAL SPECIES	118
3.9	ANTIBIOTIC TREATMENTS ALTER THE METABOLIC PROFILE OF THE GUT MICROBIOTA	121
3.10	DISCUSSION	123
4	SINGLE CELL SEQUENCING REVEALS DISTINCT DIFFERENCES IN TUMOUR STROMA OF ANTIBIOTIC TREATED ANIMALS.....	130
4.1	SINGLE CELL TRANSCRIPTOMICS OF TUMOUR CELLS ALLUDES TO DIFFERENCES IN POPULATION DENSITY OF SEVERAL CELL TYPES.....	132
4.1.1	<i>Preliminary analysis identified differences in several cell clusters following VNMAA treatment.</i>	132
4.1.2	<i>Expert bioinformatic analysis highlights differences with Loupe Cell Browser analysis and identified increases in stromal gene signatures following VNMAA treatment.....</i>	135
4.1.3	<i>Deconvolution of historic whole tumour bulk RNA-sequencing data also identifies increases in stromal gene expression following VNMAA treatment.</i>	137
4.2	HISTOLOGICAL STAINING IDENTIFIES THE INCREASED ABUNDANCE OF GRANULAR CELLS IN TUMOURS FROM ANTIBIOTIC TREATED ANIMALS AS MAST CELLS.	139
4.3	MAST CELL DENSITIES ARE INCREASED IN SEVERAL BREAST CANCER MODELS AND FOLLOWING DIFFERENT ANTIBIOTIC TREATMENT REGIMENS.....	141
4.3.1	<i>Flow cytometry of tumour resident mast cells does not show significant changes in mast cell abundance.....</i>	141
4.3.2	<i>Histological staining reveals mast cell densities are increased following VNMAA treatment.</i>	142
4.3.3	<i>International collaborators identify similar increases in mast cell densities in different models of breast cancer following different antibiotic treatment regimens.</i>	144
4.4	INCREASED TUMOUR MAST CELL DENSITIES ARE NOT ASSOCIATED WITH AN INCREASE IN SERUM IGE LEVELS	146
4.5	INHIBITION OF MAST CELL DEGRANULATION REDUCES PYMT-BO1 TUMOUR GROWTH IN VNMAA TREATED ANIMALS.	147
4.6	DISCUSSION	149
5	ANTIBIOTIC INDUCED PERTURBATIONS OF THE GUT INFER INCREASED INCIDENCE AND SIZE OF SECONDARY BREAST CANCER METASTATIC LESIONS IN LUNG TISSUE.....	154
5.1	EPITHELIAL TO MESENCHYMAL TRANSITION (EMT).....	158
5.1.1	<i>Immunostaining of EMT markers suggests a largely mesenchymal tumour dynamic in PyMT-BO1 tumours.....</i>	158
5.1.2	<i>Western blot analysis supports histology and shows no differences in EMT markers between treatment conditions.....</i>	159
5.1.3	<i>Late-stage tumours do exhibit reductions in E-cadherin and increases in vimentin</i>	161

5.2	TREATMENT WITH CEPHALEXIN, BUT NOT VNMAA, SIGNIFICANTLY INCREASES THE INCIDENCE OF PYMT-BO1 METASTASIS TO THE LUNGS DURING THE RELATIVELY EARLY STAGES IN PRIMARY TUMOUR DEVELOPMENT	163
5.2.1	<i>In situ imaging of mice to identify metastasis was unsuccessful</i>	163
5.2.2	<i>Difficulties identifying circulating tumour cells and disseminated tumour cells due to low numbers in peripheral blood and digested lung tissue.</i>	165
5.2.3	<i>Ex situ imaging of lungs identifies increased incidence of metastasis in antibiotic treated animals</i>	169
5.3	AT LATER STAGES OF DISEASE PROGRESSION, THERE IS NO INFLUENCE ON THE INCIDENCE OR PROGRESSION OF METASTASIS FOLLOWING EITHER ANTIBIOTIC TREATMENT	173
5.4	IMMUNE ACTIVITY IN THE LUNG FOLLOWING ANTIBIOTIC TREATMENT AS AN INDICATION FOR METASTATIC INVASION AND SECONDARY TUMOUR INITIATION	177
5.4.1	<i>Antibiotics do not influence immune cell infiltration of lungs from tumour bearing mice</i>	177
5.4.2	<i>Targeted analysis of pro-inflammatory cytokines does not highlight any changes in their abundance in lungs of tumour bearing mice following antibiotic treatment</i>	181
5.5	DISCUSSION	183
6	LIVE BIOTHERAPEUTIC PRODUCTS AS MICROBIOTA REGULATORS TO RESCUE TUMOUR PROGRESSION IN PATIENTS IN DYSBIOSIS	188
6.1	<i>FAECALIBACULUM RODENTIIUM</i> SUPPLEMENTATION RESCUES PYMT-BO1 TUMOUR GROWTH IN VNMAA TREATED ANIMALS	191
6.2	A PROPRIETARY COCKTAIL OF BIFIDOBACTERIAL STRAINS RESCUES PYMT-BO1 TUMOUR GROWTH IN VNMAA TREATED ANIMALS IN A SIMILAR FASHION TO <i>F. ROD</i>	194
6.3	NO SIGNIFICANT DIFFERENCES IN LYMPHOID INFILTRATION OR MAST CELL DENSITY IN TUMOURS FROM <i>BIF</i> TREATED ANIMALS	196
6.4	<i>BIF</i> ADMINISTRATION APPEARS TO PROMOTE APOPTOSIS IN FCER1A-EXPRESSING CELLS.....	200
6.5	DISCUSSION	203
7	FINAL DISCUSSION AND FUTURE PERSPECTIVES	208
8	REFERENCES	214
9	ABBREVIATIONS	283
10	SUPPLEMENTARY FIGURES	287

Acknowledgments

It feels an impossible task to convey the gratitude I have towards those people who have supported me along this journey.

I must start by thanking Breast Cancer Now for funding the work undertaken during this project and their funding flexibility during the Covid-19 pandemic. I truly hope my research contributes in some way to the united fight against breast cancer. Dr Rebecca Ansorge and Matt Madgwick, I am so thankful for your expert support with the bioinformatic analyses. Without your expertise, several of the major findings in this thesis would not have been realised. To Prof Lindsay Hall, you are a role model to so many young scientists and your drive, confidence and vast scientific knowledge have inspired me completely, but I am especially grateful for your kindness and guidance during my time as one of your students.

Now to my fellow Robinson lab members. Sally, I thank you for sharing your experience and expertise with me and teaching me to think with scientific critique. To Wes, JT, Pricey and Benwell, above all, your friendship kept me focused, motivated and reassured. You are the reason I was fortunate enough to “work with friends, not colleagues”. To Kate and Ben, you went above and beyond in your support of me, on more than one occasion! I hold you as dear friends and your guidance throughout has meant the world to me.

Kerry, you are my rock, my best friend and my love. You have been a constant support to me in all aspects of my life and I can hand-on-heart say, without you, I would not have managed this feat. Mom, where do I start? I am grateful for your bravery, patience, generosity, guidance, kindness and love. Your commitment to Calum and I go beyond the responsibilities of a mother. Know that I am grateful for every part of you. You are an inspiration to me, and this thesis is the result of your hard work and sacrifice as much as it is mine.

Finally, saving the best for last, Dr Stephen Robinson, a.k.a. Boss. I am so privileged to have worked alongside you for so many reasons. The sharing and teaching of your knowledge and scientific approach will benefit me professionally for the rest of my career. You are a truly progressive scientist with a burning passion for your research that is infectious to all those around you. However, your supervision goes so far beyond the call of duty. You are selfless to a flaw! You never fail to ensure the success and acknowledgment of your staff and students and my experience of your kindness and support is not unique. All who enter the Robinson lab feel your empowerment and leave stronger and better people for it. I am eternally grateful to you. Thank you, my friend.

List of Figures

Figures are listed according to the section in which they are presented

Figure 1.2.1. Basic physiology of the mature human breast.....	14
Figure 1.2.4. The hallmarks of cancer: the next generation.....	18
Figure 1.2.5. Schematic describing receptor and Ki67 status of the molecular subtypes of breast cancer.....	22
Figure 1.3.1. Cytokine exposure drives haematopoiesis and the differentiation of haematopoietic stem cells.....	30
Figure 1.3.2.1. IgE dependent induction of mast cell degranulation.....	34
Figure 1.3.2.2. Cytokine induced macrophage polarisation.....	37
Figure 1.3.3.1. Cytokine release regulates CD4 T-cell polarization.....	42
Figure 1.3.3.3. T-cell dependent activation of B-cells.....	47
Figure 1.4.3.1. The influence of CTLA4 on CD8 T-cell activation and anti-cancer function.....	59
Figure 1.4.3.2. The influence of PD-1/PD-L1 on effector cell function and anti-cancer activity.....	60
Figure 1.4.3.3. Immune checkpoint inhibitors facilitate T-cell activation and effector activity to promote anti-cancer immunity.....	62
Figure 3.1. VNMAA administration influences tumour growth kinetics in PyMT-BO1 tumours.....	105
Figure 3.2. Antibiotic administration does not directly promote cancer cell proliferation <i>in vitro</i> or tumour progression <i>in vivo</i> in germ free mice.....	108
Figure 3.3. VNMAA administration does not influence immune cell tumour infiltration at an early timepoint.....	109
Figure 3.4. VNMAA treatment promotes tumour growth in the EO771 basal-like model of breast cancer without influencing infiltrating immune cell populations traditionally associated with tumourigenesis.....	111
Figure 3.5. Treatment with a clinically relevant antibiotic, cephalexin, promotes tumour growth without influencing tumour infiltration of immune cells.....	113
Figure 3.6. Expression of the proliferation marker, Ki67, is increased in tumours following antibiotic treatments.....	115
Figure 3.7. Blood Vessel density in tumours is unchanged following respective antibiotic treatment.....	117
Figure 3.8. Both VNMAA and cephalexin antibiotic treatment perturb the gut microbiota but to varying degrees, with the common loss of several bacterial species.....	120
Figure 3.9. ¹ H NMR spectroscopy of caecal samples show VNMAA and cephalexin treatments alter metabolic profiles to varying degrees.....	122
Figure 4.1.1. Preliminary analysis of tumour scRNA-seq outputs identified changes in the abundance of several cell types following VNMAA treatment.....	134

Figure 4.1.2. Bioinformatic analysis reveals an increase in the density of a cluster representing cells with a stromal-associated transcriptome.....	136
Figure 4.1.3 Deconvolution of historical bulk RNA-seq identifies a similar increase in gene expression associated with stromal cells following VNMAA treatment.....	138
Figure 4.2. Picosirius red staining shows no changes in collagen deposition but aids in identifying mast cells as potentially increased in abundance in tumours from antibiotic treated animals.....	140
Figure 4.3.1. Flow cytometry of intra-tumoural mast cells does not show an increase in their cell abundance following antibiotic treatment.....	142
Figure 4.3.2. VNMAA antibiotic treatment is associated with increased tumour mast cell density in PyMT-BO1 and EO771 tumours.....	143
Figure 4.3.3. Mast cell densities are increased in different tumour models following different antibiotic treatments in animals housed at different facilities.....	145
Figure 4.4. Serum IgE concentrations are not influenced by antibiotic treatment.....	146
Figure 4.5. Inhibition of mast cell degranulation via cromolyn sodium i.p. injection rescues tumour growth in VNMAA treated animals but not in vehicle treated controls.....	148
Figure 5.1.1. Immunostaining of tumour sections for the EMT markers E-cadherin and vimentin.....	159
Figure 5.1.2. Western blot analysis of tumour lysates obtained 15 days post tumour induction from VNMAA and cephalixin treated animals for E-cadherin and vimentin alongside subsequent densitometry analysis.....	160
Figure 5.1.3. Western blot analysis of tumour lysates obtained 18 days post tumour induction from VNMAA and cephalixin treated animals for E-cadherin and vimentin alongside subsequent densitometry analysis.....	162
Figure 5.2.1. <i>In situ</i> bioluminescence imaging was unable to identify metastasis <i>in vivo</i>	164
Figure 5.2.2.1 Flow cytometry was unable to reliably identify metastatic cells in blood samples of animals irrespective of treatment group.....	167
Figure 5.2.2.2 Flow cytometry was unable to reliably identify metastatic cells in lung samples of animals irrespective of treatment group.....	168
Figure 5.2.3. Metastatic incidence in the lungs appears increased in animals treated with antibiotics compared to vehicle treated controls.....	171
Figure 5.3. At later stages, metastasis is not influenced by antibiotic treatment.....	175
Figure 5.4.1. Antibiotic treatments do not influence immune populations in the lungs of tumour bearing animals.....	179
Figure 5.4.2. Cytokine production is not affected by antibiotic treatments in tumour bearing mice.....	182
Figure 6.1. <i>F. rod</i> administration rescues PyMT-BO1 tumour growth compared to growth in animals treated with VNMAA.....	193

Figure 6.2. *Bif* administration rescues PyMT-BO1 tumour growth compared to growth in animals treated with VNMAA.....195

Figure 6.3. Tumour infiltrating lymphoid and mast cell populations are unaffected by *Bif* supplementation.....198

Figure 6.4. *Bif* supplementation is associated with apoptosis in FCεR1α-expressing cells in PyMT-BO1 tumours.....202

List of Tables

Tables are listed according to the section in which they are presented

Table 1.2.4. Crude indications used to determine breast cancer staging as part of the TNM system.....	20
Table 2.9. Antibody information relevant to western blot assays.....	91
Table 2.15. Antibody information relevant to immunofluorescent staining.....	93
Table 2.17. Antibody information relevant to immunohistochemical stained sections.....	94
Table 2.18. List of flow cytometry antibodies and viable cell staining reagents.....	97

1 Introduction

1.1 Preface

The influence of the gut microbiota on regulating host health and response to disease is now an established concept. However, how far these influences stretch and the mechanisms by which they operate are poorly described. Fortunately, the efforts being put into studying such relationships are vast and since the turn of the millennium the body of research describing associations between the microbiota and an array of diseases, which include those local to the gut and at sites distant from it, as well as the mechanisms involved in these associations, continues to grow exponentially. Furthermore, the technological advances made in the same timeframe have supported these studies in profiling the microbial communities as well as assessing how these profiles may be associated with changes in host cell activity. Cancer research is one area in which the microbiota has been increasingly featured. Studies involving several types of cancers have shown that a diverse microbiota is generally associated with an improved prognosis and, in some cases, has even been linked with improved treatment efficacy. Although it is the most frequently diagnosed cancer globally, to date there is less than a handful of studies which have considered the role of the microbiota in regulating breast cancer progression. Therefore, the research presented in this thesis hopes to support and further the limited body of work describing the complex relationship between the gut microbiota and breast cancer. In support of this hope, several of the results presented in chapters three, four and six have formed the basis of a publication entitled “Antibiotic-induced disturbances of the gut microbiota result in accelerated breast tumour growth” published in iScience in 2021 in which this author was a co-first author [1].

1.2 Breast Cancer

1.2.1 Breast Physiology

Vertebrates of the taxonomic class Mammalia are characterised based on the presence of mammary glands which produce milk used to nurse their offspring. In humans, these glands form appendages comprising both epithelial and adipose structures and tissues called breasts.

At birth, both male and female infants will have already developed a small network of lobules within breast tissue [2]. Shortly after birth, the reduction in maternally derived oestrogen promotes the infant's own prolactin production that triggers early remodelling of breast tissue [3]. Early remodelling occurs in the first two years of life at which point the breast tissue becomes dormant until puberty [4]. At this point, due to changes in sex hormone production, physiology diverges between males and females whereby increased testosterone retains a dormant breast tissue in men while increases in oestrogen in women drive further breast tissue production and development, ultimately resulting in the formation of the mature breast and nipple (Figure 1.2.1) [5,6]. The mature breast sits atop the pectoral muscle and is comprised of several tissues including a branched network of lobes, which themselves are comprised of smaller lobules which produce milk, and lactiferous ducts, which transport milk from the lobules to the nipple where it is secreted [7]. These structures are both surrounded by a layer of adipose tissue that offers other cells within the tissues a fuel source in the form of lipids, a particularly important role during breast development [8,9]. Figure 1.2.1 depicts these major tissues and glands that makeup the mature breast.

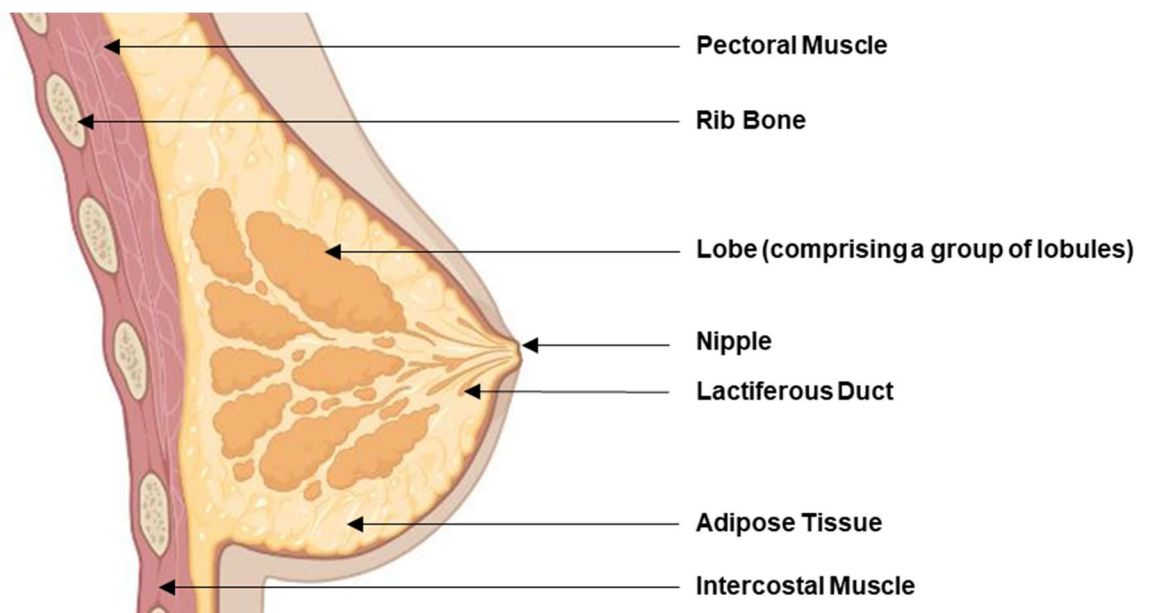


Figure 1.2.1. Basic physiology of the mature human breast. Graphic labelling the major structures and tissues that define the mature human breast. Created in part using BioRender.com.

1.2.2 Risk factors influencing breast cancer occurrence

The term “cancer”, with the exception of blood cancers, usually refers to the uncontrolled division of cells in a specific organ or tissue, causing the formation of a malignant mass of abnormal tissue called a tumour [10]. Once a malignant tumour is formed within an organ or tissue, there is an ongoing risk of tumour cells disseminating to and proliferating in distant organs, a process termed metastasis, which can ultimately lead to organ failure and eventually death [11]. The uncontrolled division of cells is triggered by genetic mutations in DNA which act to promote cell proliferation and reduce apoptosis [12,13]. These mutations can be hereditary, meaning they are inherited from parent to offspring via germline transmission, or somatic, where mutations arise after conception either spontaneously or following exposure to mutagens [10]. The historical perception regarding the causes of cancer was heavily weighted towards hereditary mutations [14]. However, studies are increasingly linking causality with somatic mutations associated with an array of risk factors. For example, in breast cancer specifically, hereditary mutations in the *BRCA1* and *BRCA2* oncogenes have long been associated with increased risk of breast cancer incidence in later life [15]. However, these and other germline mutations only account for around 5 to 10% of breast cancer incidence [16,17].

The somatic risk factors associated with breast cancer incidence can be subdivided into intrinsic and extrinsic groups. Intrinsic risk factors are those which one has no real control over and include age, gender, the body’s own hormone production and nodal state within breast tissue [18]. Extrinsic factors are those that involve lifestyle choices and are often controllable elements such as diet, alcohol consumption, smoking status and exposure to certain drugs such as hormone based contraceptives [18]. Of the intrinsic risk factors, age is the most significant indicator of risk. In 2015, the American Cancer Society estimated that between the ages of 50 to 59, 1 in 48 woman would experience a breast cancer diagnosis, between 60 to 69 years of age this increased to 1 in 29, and after the age of 70, 1 in 15 woman would be diagnosed with breast cancer [19]. These statistics are concerning and while it is difficult to prevent disease presentation associated with ageing, ever improving methods for early disease detection has improved long term survival in the populations of women with the appropriate access to them [20,21].

Major extrinsic risk factors for breast cancer include alcohol consumption, exposure to hormone-based treatments and other drugs, low activity lifestyles, unbalanced diets and obesity [22–25]. Despite the consistent positive correlation between alcohol consumption and cancer incidence, the molecular mechanism for a causative role in breast cancer is not well described. However, several possibilities have been hypothesised and include the increase in oestradiol and estrone hormones triggered by alcohol consumption which, over a prolonged time, results in overactive oestrogen

receptors in breast epithelial tissue, ultimately triggering mutagenesis which in turn causes cancer [26]. Similarly, several epidemiological studies have shown that postmenopausal women treated with hormone replacement therapies (HRT), such as oestrogen and/or progestin therapies, are more likely to present with breast cancer than those women who do not receive HRT [27–29]. The use of contraceptive drugs which increase oestrogen and progesterone levels in the blood are also thought to have similar links to breast cancer in later life [30,31]. Again, the exact molecular mechanisms by which these therapies drive mutagenesis are yet to be comprehensively described but are likely linked to promoting overactivity of hormone receptors in breast epithelium, triggering increased cell proliferation [32]. Diet and obesity are also strongly associated with breast cancer incidence. In the late 90's an investigation considered patient-reported pre-diagnosis diets and concluded that post-surgical disease recurrence was reduced in patients with low-fat diets and increased in those with higher body mass index (BMI) scores [33]. Several other studies have also shown that obesity promotes breast cancer incidence [34–36]. One mechanistic insight suggests that increased adiposity catalyses hormone production which in turn promotes hormone receptor activity and cell proliferation in breast epithelium as well as offering cancer cells a fuel source in the form of fatty lipids, which would also aid cellular proliferation [37–39].

Fortunately, the public awareness of the extrinsic risk factors associated with breast cancer incidence is increasing, particularly in the developed world [40,41]. Through education and appropriate medical intervention, many of these extrinsic risk factors can be managed to reduce a woman's risk of developing the disease. For example, a recent study has linked high fibre diets to an improved response to an anti-PD1 immunotherapy in patients suffering from skin cancer demonstrating that lifestyle changes have a potential to influence cancer progression and overall treatment outcomes [42]. This finding, coupled with the influences of obesity and high fat diets discussed already, support the evidence showing healthy eating and exercise may in part be a suitable preventative measure against breast cancer occurrence [43,44].

1.2.3 Epidemiology

In 2020 a global investigation of cancer incidence and mortality rates spanning 185 countries estimated that female breast cancer was the most diagnosed cancer across the globe with 2.3 million cases comprising nearly 12% of all cancer diagnoses [45]; a surprising statistic when considering female breast cancer affects only half the world's population. In the same year, an estimated 690,000 women succumbed to the disease worldwide, an increase from ~627,000 deaths estimated in 2018, [17,45]. These figures make breast cancer the worldwide leading cause of cancer-related deaths among women [46]. In the United Kingdom (UK), there were 53,889

incidence of breast cancer and 11,839 deaths resulting from the disease over the course of 2020 [46].

Incidence and mortality of breast cancer appears to be heavily affected by global socioeconomic disparities. In an analysis of the “GLOBOCAN cancer today” database, Lei *et al.* (2021) found that between the years 2000 and 2015 there was a slow but gradual increase in breast cancer incidence in developed nations with strong economies and established healthcare systems [46]. The increase observed in developed western countries, including the UK and the United States of America (USA) was slower than those observed in developed eastern countries, namely China and South Korea. Additionally, while developing nations generally had lower rates of breast cancer incidence compared to developed nations, their mortality rates were significantly higher [46].

These patterns may in part reflect the effects of lifestyle on cancer incidence and healthcare availability on cancer-related mortality. In developed societies, the extrinsic risk factors discussed are more commonly indulged or experienced than in developing nations. Alcohol consumption, high fat diets, administration of hormonal contraceptives and replacement therapies as well as jobs with low activity requirements are often the societal “norm” in the western world [47–49]. In the developing world, many of these factors are either culturally taboo or simply unaffordable and so have a lower influence on breast cancer incidence as a result. Furthermore, one population-based case-control study identified East-Asian American woman born in the US and exposed to western diets from a younger age had a 60% higher risk of presenting with breast cancer in their lifetime than East-Asian American migrants that had grown up on eastern in diets, suggesting that extrinsic factors are stronger drivers of breast cancer incidence than genetic predispositions in this context [50]. However, while these extrinsic differences may reduce incidence in the developing world, sadly, there are two key factors that increase mortality rates in these areas. Firstly, there are often societal and cultural stigmas associated with both cancers and visiting hospitals, resulting in reduced early stage detection and higher incidences of late stage detection at points where treatment options are usually extremely limited [51]. Secondly, the government funded healthcare systems in developing nations are often slow to advance treatment pathways and technologies due to the costs involved and where there are suitable private treatments available, the costs to the general population is often such that patients cannot afford it [52]. In 2018, Sun *et al.* carried out a systematic review of 20 studies from countries of varying economic wealth to assess the cost of breast cancer treatment at several stages of disease progression. They found that the mean cost ranged from £21,250 for a single patient in early stages of the disease up to £115,000 for one in its later stages, demonstrating how challenging it can be for poorer nations to accommodate patient treatment [53].

1.2.4 Staging and disease progression

In 2000, Hanahan and Weinberg defined six functional alterations in cellular physiology that malignant tumours must acquire to be classed as a cancer. These characteristics were coined “the hallmarks of cancer” [54,55]. They were: self-sufficiency in growth signals, insensitivity to growth-inhibitory (antigrowth) signals, evasion of programmed cell death (apoptosis), limitless replicative potential, sustained angiogenesis (formation of blood vessels), and tissue invasion and metastasis [54]. In 2011, the same authors updated these hallmarks to include two “emerging hallmarks”, tumour-promoting inflammation and genome instability and mutation, and two “enabling factors”, deregulating cellular energetics and avoiding immune destruction (Figure 1.2.4) [55]. These hallmarks govern the efforts involved in the research and development of novel diagnostic, prognostic and therapeutic approaches in oncological medicine.

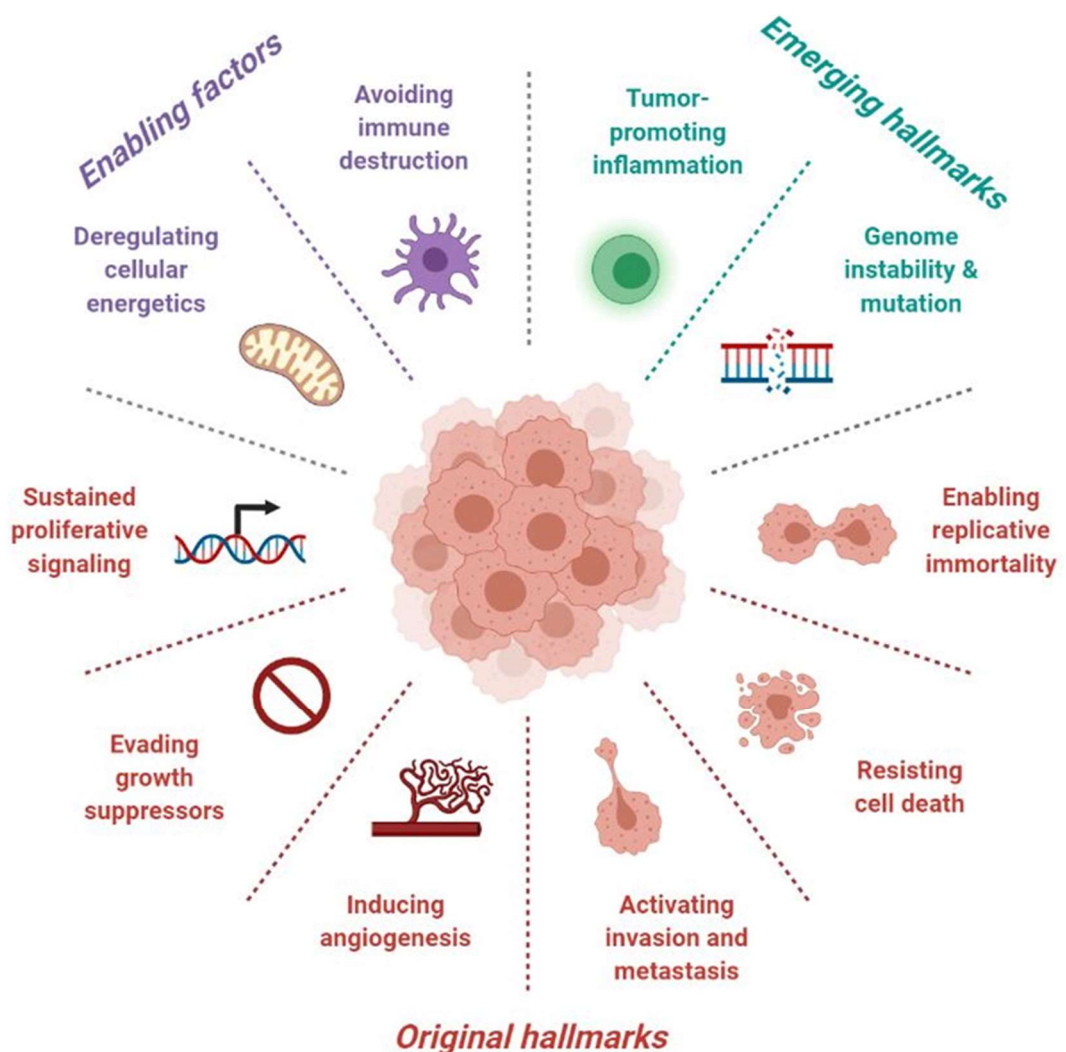


Figure 1.2.4. The hallmarks of cancer: the next generation. Diagram depicting the original hallmarks of cancer (red) as well as the updated enabling factors (purple) and emerging hallmarks (green) described by Hanahan and Weinberg in 2011 [55]. Adapted from “Hallmarks of Cancer: Circle”, by Biorender.com (2021). Retrieved from <https://app.biorender.com/biorender-templates>.

During a period of nine years between 1943 and 1952, Pierre Denoix, a French surgeon, developed a classification system by which all solid tumour cancers could be “staged” to assess pathophysiological features of the disease and determine a patient’s prognosis [56]. The tumour-node-metastasis (TNM) staging system is still used today across the globe, with some updated elements since its initial publication in 1958, and considers three anatomical features of cancer relating to the size of the primary tumour (T), invasion of tumour cells in regional axillary lymph nodes (N) and whether the disease has metastasised to distant organs (M) [57,58]. Each of these three factors is assessed either clinically (c), denoting assessment prior to or without surgery, or pathologically (p), denoting a post-surgical assessment. Tumours are sub-classed according to size, ranging from T1 to T4 where T1 would refer to a small primary tumour and T4 would refer to large primary tumour. T1 and T4 stages can be further sub-classed according to either the size of the primary tumour within the range set by the T1 staging definition (T1 only) or the disease-specific physiological effect of a large tumour at a T4 stage, such as swelling of the breast or redness of the breast surface caused by inflammation. These third-tier sub-stages are described using the lower-case letters “a”, “b” or “c”, where “a” would suggest a better prognosis than “b” and “b” a better prognosis than “c” [59,60]. Nodal subclasses range from N0 to N3 and refer to the number of lymph nodes affected by cancer cell invasion, again with N0 referring no cancer cells in the regional lymph nodes and N3 describing significant nodal invasion [59,60]. Similarly to T1 and T4 staging, nodal assessment in breast cancer is further defined by the number of lymph nodes affected, the size of nodal lesions and the location of the lymph nodes affected using the same lettering system where “a” would suggest a better prognosis than “b” and “b” a better prognosis than “c” [59,60]. Metastasis is sub-classed as a “yes or no” assessment describing either that there is no identifiable spread of the cancer to distant organs (M0) or there is metastatic disease in distant organs (M1) [59,60].

The TNM staging system aids clinicians in understanding exactly what stage the disease has progressed to and what the prognosis is likely to be for a patient. However, describing to a patient, particularly those of a non-clinical background, that their cancer is at a “T4a, pN2a, M1” stage is not an effective method of communication. Thus, the various assessments made using the TNM system are condensed to a simple number-based system describing the “overall stage” of disease progression, ranging from stage I to stage IV, with prognoses progressively worsening from stage to stage [58]. Table 1.2.4 summarises these TNM-based physiological parameters which determine the overall stage of a breast cancer. Stage I is generally when a primary tumour might be considered in its early growth phase and does not exceed 2cm in diameter with no spread to the lymph nodes or no more than one nodal lesion which does not exceed 0.2mm in diameter. Stage II is defined by

a primary tumour of a diameter between 2 to 5cm and/or tumours in up to three axillary lymph nodes (nodal tumours) which are no more than 2mm in size. Stage III is defined by a large primary tumour of greater than 5cm in diameter, often accompanied by redness or inflammation in the skin at the surface of the breast, and/or up to nine nodal tumours of no more than 2mm in diameter. Finally, stage IV refers to any metastatic spread of breast cancer to distant organs or tissues, irrespective of primary tumour size or number of nodal tumours. Major metastatic sites of breast cancer include the brain, lungs and bones [61,62].

Table 1.2.4. Crude indications used to determine breast cancer staging as part of the TNM system.

Stage	Tumour Diameter (T)	Lymph Node Disease (N)	Lesions in Distant Organs (M)
Stage I	Up to 2 cm	Up to 0.2 mm	No
Stage II	2 to 5 cm	Up to 2 mm in 1 to 3 axillary lymph nodes	No
Stage III	>5 cm	Up to 2 mm in 4 to 9 axillary lymph nodes and/or lesions in lymph nodes near/on the breastbone	No
Stage IV	Any size	Any spread to lymph nodes	Yes, metastatic lesions observed in distant organs.

As stated above, patients diagnosed at an earlier stage of the disease usually experience better prognostic outcomes than those diagnosed in the more advanced stages. Globally, the five-year survival rate for patients diagnosed between stage I and stage II is ~85 to 98% while those patients diagnosed between stage III and stage IV have very poor five year survival rates, less than ~30% in 2018 [53]. Furthermore, once the disease progresses to stage IV, it is considered incurable and clinicians focus on treatments to slow progression and manage symptoms of the disease, including pain management, to maintain a patient’s quality of life for as long as possible [63]. Thus, disease prevention and early diagnosis are important in reducing the mortality of breast cancer.

While this system has aided both clinicians and patients in understanding disease progression and predicting prognosis for many years, it is heavily leveraged towards anatomical features and does not consider the significant heterogeneity of the molecular characteristics of breast cancer [64]. Molecular pathophysiology not only contributes to tumour aggressiveness but also, and arguably

more importantly, determines the most appropriate therapeutic approach to treating breast cancer [65]. Therefore, in 2017, the American Joint Committee on Cancer updated the breast cancer staging manual, now in its eighth edition, to include assessments of hormone and HER2 receptor expression, in addition to TNM factors, to improve the prognostic scoring of breast cancers [64,65]. Additionally, the use of several multigene panels to assess oncogenic gene expression in tumours has been incorporated in the updated system [65,66]. Of particular interest is the Oncotype DX Breast Recurrence Score assay which assesses the expression of 21 genes associated with breast cancer prognosis and recurrence potential in early stage hormone receptor positive, HER2 negative breast cancers [66]. However, how the addition of these factors fit into the numeric staging (stage I to stage IV) of breast cancer is currently quite complex.

1.2.5 Disease molecular pathophysiology

Breast tumours are often named according to the tissue in which they originate. There are two major malignant breast cancer tumour types, invasive ductal and invasive lobular carcinoma. Invasive ductal carcinomas are the most common type of breast tumour, contributing ~75 to 80% of all breast cancer cases, and form in the lactiferous ducts [67]. Invasive lobular carcinomas are the second most common malignant breast tumour type, contributing ~5 to 15% of breast cancer cases, and form in the milk producing lobules within the mature breast [67,68]. The remaining cases are either less-invasive carcinomas, such as most ductal carcinoma *in situ* (DCIS), which rarely breach the ductal tissues in which they form and are therefore not usually malignant, or sarcoma tumours which form in the muscles and connective tissues within the breast [69,70].

Carcinomas are further classified into one of five molecular subtypes of breast cancer, namely luminal A, luminal B, HER2-enriched, normal-like and basal-like or triple negative breast cancer (TNBC). These subtypes are so classed according to the expression, or lack thereof, of three receptor proteins: oestrogen receptor (ER), progesterone receptor (PR) and human epidermal growth factor receptor 2 (HER2), and determine patient prognosis as well as which treatment pathways are likely to be the most effective (Figure 1.2.5) [71,72]. The hormone receptor positive luminal subtypes (luminal A and B) account for the largest proportion of cases, ~70%, while normal-like breast cancer account for only ~8% and HER2-enriched and TNBC account for between 15 to 20% and 10 to 15% of cases respectively [72,73].

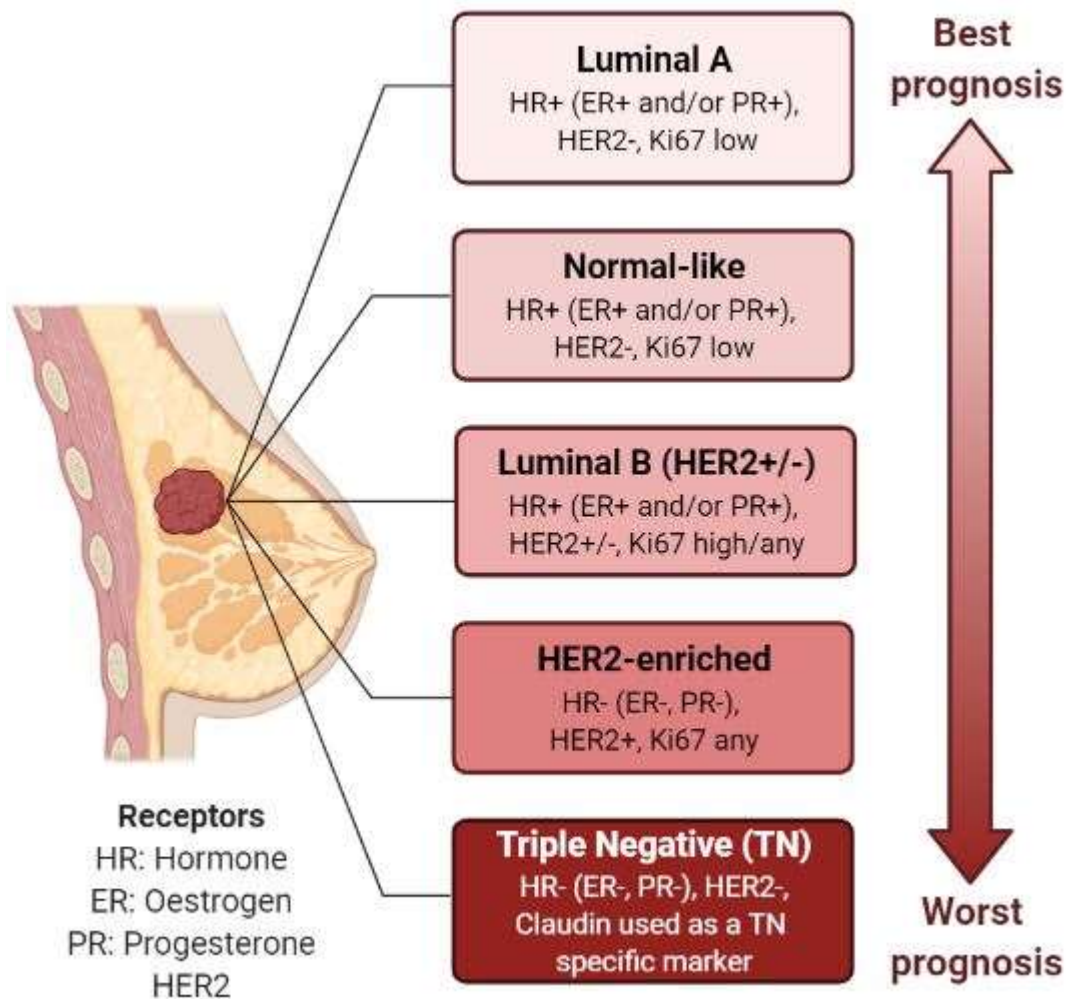


Figure 1.2.5. Schematic describing receptor and Ki67 status of the molecular subtypes of breast cancer. Molecular subtypes are characterised according to the expression of several receptors as well as the proliferation marker protein Ki67. Prognosis generally worsens as the number of receptors expressed reduces, the exception being Luminal B HER2+ compared to Luminal B HER2-. Adapted from “Intrinsic and Molecular Subtypes of Breast Cancer”, by Biorender.com (2021). Retrieved from <https://app.biorender.com/biorender-templates>.

Luminal A and normal-like breast cancers share the same expression profiles for hormone receptors, HER2 receptor and Ki67. However, genetically, normal-like tumours resemble more closely the gene expression profiles of normal non-neoplastic cells than luminal A breast cancer cells do and as a result are slightly more challenging to target, carrying a comparatively poorer prognosis [72].

ER and PR are intracellular receptors which bind the sex hormones oestrogen and progesterone respectively. These sex hormones are present in both males and females but play an integral role in female sexual development and influence menstruation, pregnancy and menopause [74,75]. In the breast, oestrogen has been shown to regulate the formation of lactiferous ducts while progesterone regulates alveolar formation in milk-producing lobules and ductal branching [76]. The

oestrogen receptors are nuclear transcriptional factors with two distinct forms, oestrogen receptor- α (ER α) and oestrogen receptor- β (ER β) [77,78]. When oestrogens bind these receptors, they promote the epigenetic regulation of gene expression associated with several cellular pathways, including cell proliferation [79]. ER α is associated with increasing activity of genes associated with proliferation while ER β generally restricts cell division and is linked to regulating apoptotic pathways [80–82]. Thus, it is the upregulation of ER α which has more widely been linked to the growth and progression of breast cancer[83].

Most hormone receptor positive breast cancers are both ER α and PR positive. This is because ER α activity regulates the transcription of PR mRNA [84]. Thus, the expression of PR in tumour tissues indicates the activity of ER α and can be used as prognostic marker regarding the likely efficacy of hormone based therapeutic approaches to treating breast cancer [84,85]. Similarly to ER, PR is a transcriptional factor protein which when activated by binding of its ligand, progesterone, regulates gene expression [86]. There are three isoforms of the PR: PR-A, PR-B and PR-C. PR-A and PR-B are usually co-expressed but have different transcriptional influences, PR-A regulates uterine reproductive functions while PR-B aids in normal mammary gland development [87,88]. The understanding of functional influences of PR-C is not well described but there is some evidence showing this isoform may promote proliferation of PR-expressing human breast cancer cells (T47D) *in vitro* through interactions that interfere with DNA binding by PR-B, resulting in irregular cell division in breast epithelial cells [89].

HER2 is a transmembrane protein belonging to the family of four epidermal growth factor receptors (EGFR) [90,91]. While HER2 does not have a known ligand to which it binds, when neighbouring a EGFR proteins, namely HER1, HER3 and HER4, bind their ligands, HER2 dimerizes with them in a ligand independent manner, triggering intracellular signalling pathways, such as the mitogen-activated protein kinase (MAPK) pathway which is involved in the regulation of transcription and translation of genes and proteins that promote proliferation and suppress apoptosis [92,93]. In ~20% of breast cancers, the HER2 protein is overexpressed, leading to the increased activation of signalling pathways and genes that promote proliferation and, in turn, progressing tumour development [94].

TNBC lacks the expression of all three of these proteins. Thus, while it is the least common subtype in terms of breast cancer incidence, it is also considered the most aggressive as the therapeutic approaches which target hormone receptor and HER2 activity are not applicable in these cases and only chemotherapeutic approaches currently have any influence on preventing cancer cell

proliferation [95]. These molecular characteristics also contribute to very high disease recurrence rates and poor overall survival relative to the other breast cancer subtypes [96,97].

In addition to the three receptors, there are several other intracellular proteins which allude to the aggressiveness of a breast tumour. The intranuclear protein Ki67 is a principal diagnostic marker used to identify the proliferative potential of breast cancer cells [98]. It is expressed only during the interphase stage of the cell cycle and is most abundant during S-phase when the cell is doubling its DNA content in preparation for cell division [99]. The presence or absence of these receptors and proteins are used by clinicians to determine the treatment routes most likely to be effective in fighting the disease [100,101]. The presence of hormone receptors are often associated with a better prognosis because neoadjuvant hormone therapies can be implored in addition to radiotherapy or surgical intervention while TNBC carries a poorer prognosis as, among other reasons, these neoadjuvant drugs do not have a target to inhibit [100,101].

1.2.6 Current treatment approaches

Treatment approaches in breast cancer are governed by staging and molecular pathophysiology of the disease [73]. Currently, these approaches include surgical intervention, endocrine therapy, HER2 inhibition therapy, chemotherapy and radiotherapy, and are often used in varying combinations to achieve the best patient outcomes [73,102].

1.2.6.1 Surgery

Most patients will undergo surgery to remove the primary tumour, often as the first step in the treatment pathway, as it is an effective method to halt tumour progression and reduce the risk of metastatic dissemination in all molecular subtypes of the disease [102]. Subsequent subtype specific adjuvant therapies are employed after surgery, and following biomedical analysis of tumour biopsies, to target metastatic cells and/or residual local tumour cells to limit or eradicate further progression [103]. In patients diagnosed with larger tumours (>2cm) or tumours of a complex morphology, neoadjuvant treatment can be employed prior to surgery to reduce tumour size and, in turn, the subsequent degree of invasiveness associated with surgery [104].

Surgical intervention can be either breast-conserving or a complete removal of the breast (Figure 1.2.6.1), again depending on tumour size and stage. At early stages, when tumours are small and with little or no local spread, a lumpectomy can be performed to resect only the tumour and a small amount surrounding healthy tissue (wide-excision) [105]. This surgery aims to remove malignant tissue to reduce risk of metastasis while conserving the morphology and appearance of the breast for the patients physical and mental well-being.

In rare cases, a quadrantectomy can be performed on tumours of larger sizes which are localised to one region of the breast. This approach is more invasive than a lumpectomy and up to a quarter of the breast can be removed, including a larger margin of healthy tissue surrounding the tumour [106,107]. Often surgeons will also remove axillary lymph nodes at the same time to investigate potential nodal spread [108].

In cases where primary tumours are larger and/or there is confirmed significant diffusion of cancer to axillary lymph nodes, usually at later stages of the disease, a mastectomy is often performed to remove the entire breast so as to limit the amount of residual cancer tissue which may otherwise be left behind [109,110]. Mastectomy surgery can also be an elective prophylactic procedure opted into by patients who have been identified as “high-risk” in terms of developing breast cancer, for example those with an identified mutation in the *BRCA1* and *BRCA2* oncogenes [111,112]. Unfortunately, this type of surgery is the most invasive and in addition to dramatically changing the physical appearance of a patient’s body, it can result in depression and anxiety caused by feelings of asexuality and unhappiness with the physical changes [113,114].

1.2.6.2 *Hormone therapies*

In hormone receptor positive breast cancers, namely the luminal A and luminal B molecular subtypes, the proliferative effects of activated ER and PR are responsible for driving tumour growth. This is achieved either by antagonistic action of the receptors, preventing the binding of hormone ligands, or by reducing the production of oestrogen, in turn reducing receptor activity [115,116]. There are several approved drugs which are used to these ends. Tamoxifen is the most common adjuvant hormone therapy and has been used for decades [117]. It antagonistically blocks ER, preventing oestrogen binding and thus inhibiting the mitogenic activity of the ER [118]. The length of tamoxifen administration varies but longer periods of treatment correlate with reduced recurrence. Five years of treatment reduce recurrence rates to 25.1% versus 21.4% following 10 years of treatment [119]. Unfortunately, tamoxifen often induces several side effects. Mild side effects include those often associated with menopause such as hot flushes, changes in menstruation, low mood and fatigue while more severe side effects include blood clotting [120].

Aromatase inhibitors are an alternate hormone therapy option and work by preventing the production of oestrogen, particularly in adipose tissues. Aromatase is an enzyme that regulates the rate-limiting step in the conversion of androgens to oestrogen, thus aromatase inhibitors prevent the activity of this enzyme and reduce oestrogen bioavailability, in turn reducing ER activation and in turn cancer cell proliferation [115,121]. There are several of these approved drugs including anastrozole, exemestane and the most common letrozole [122,123]. A major benefit of aromatase

inhibitors is that they have fewer side effects than tamoxifen. Additionally, some research shows that combining an initial period of tamoxifen treatment followed by the use of aromatase inhibitors further reduces recurrence rates to below those of tamoxifen alone [124]. However, aromatase inhibitors are not suitable for pre-menopausal patients due to initial reduction in systemic oestrogens triggering the secretions of gonadotrophins by the hypothalamus and pituitary gland which feeds back to the ovaries and increase oestrogen production, ultimately promoting oestrogen induced cell proliferation in breast tumours [125].

1.2.6.3 *Anti-HER2*

HER2-enriched, hormone receptor negative, breast cancers do not respond to hormone therapies. However, monoclonal antibodies against the HER2 receptor antagonistically inhibit their aberrant pro-tumour action by preventing receptor activation and inhibiting intracellular proliferative signalling cascades [126]. Trastuzumab is generally used alongside traditional chemotherapies as a combination treatment which tends to have more favourable outcomes for the patients [127]. For example, in patients with HER2-enriched metastatic breast cancer, combination therapies using both traditional chemotherapies and trastuzumab increased the median survival time by five months and reduced death rates at one-year post diagnosis by 11% [128]. More recently, new HER2-targeting therapeutics have shown promise in treating this particular subtype of breast cancer. Both pertuzumab, another monoclonal antibody against HER2, and lapatinib, a tyrosine kinase inhibitor which interferes with HER2 induced proliferative signalling, have been shown to improve overall survival when combined with trastuzumab relative to using trastuzumab alone [129–131].

1.2.6.4 *Chemotherapy*

Chemotherapy involves the administration of cytotoxic agents to promote cancer cell death and is a part of the vast majority of treatment pathways. In hormone receptor positive or HER2-enriched cancers, chemotherapy is generally combined with one or more of the alternate treatments discussed above, depending on receptor status [132]. However, for patients with TNBC, adjuvant chemotherapy is the only drug-based approach for post-surgical treatment [133,134]. There is an array of chemotherapeutic drugs which are often combined in treatments. Their specific methods of action vary but they all generally aim to cause DNA damage and promote cell death. The most commonly employed chemotherapeutic agents are anthracyclines, namely doxorubicin, and taxanes, namely docetaxel and paclitaxel. These are often combined, in varying concentrations and durations, with other chemotherapeutic agents such as the platinum-based carboplatin and/or 5-fluorouracil [135,136].

Unfortunately, most chemotherapies induce quite severe side effects which can be acute or chronic in nature [137]. Acute symptoms include nausea and vomiting, hair loss, fatigue, and diarrhoea. However, chronic side effects can be quite severe and may be life-limiting. For example, anthracycline based chemotherapies are known to be cardiotoxic and can cause cardiomyopathies while taxanes can induce neuropathies [138]. In the worst cases, delayed chronic symptoms can lead to congestive heart failure [139].

1.2.6.5 *Radiotherapy*

Radiotherapy, which utilises radiation to kill cancer cells, has been employed for over a century [140]. It can be used at almost any point in the treatment pathway but is regularly employed as an adjuvant treatment following breast conserving surgery and, in some cases, mastectomy [140,141]. This treatment bombards cells, often both malignant and healthy cells, with high doses of radiation which trigger DNA damage and ultimately cell death. Again, it is not uncommon for this treatment approach to be combined with other methods, predominantly chemotherapy and particularly in cases of TNBC [142].

1.3 The Immune System

An organism's immune system acts as its major defence against ill health. Exposure to infectious pathogenic organisms or signals generated by the abnormal activity of one's own cells can trigger immune responses which aim to remove or correct the threats posed and return the body to a state of homeostasis [143,144]. The major process by which this is achieved is through inflammation. Inflammation is the regulated and collective response of several immune cell types to a variety of foreign or irregular stimuli, such as pathogenic activity or damaged cells, that may otherwise cause harm to an organism [145]. Inflammation involves the removal of said stimuli and subsequent activity to repair any damage caused, making it an integral process in maintaining tissue and organ homeostasis [145]. It is usually acute and temporary, however, in some cases inflammatory responses can become unregulated and result in chronic inflammation, which is associated with an array of inflammatory diseases, including cancer [145].

1.3.1 Haematopoiesis

The immune system comprises a series of "white blood cells", collectively termed leukocytes, which differentiate into an array of cell types with specific functions that support a collective response against foreign threats. The immune response is divided into two compartments: innate and adaptive. The innate immune response is the body's immediate defence against pathogenic infections and occurs without prior exposure to antigenic threat, meaning it is not "learned" but is rather, as its name suggests, innate [146]. The adaptive immune response is more targeted and requires previous exposure to antigens to mount attacks against specific molecular patterns produced by particular organisms or cells [147]. The establishment of the various cell types from both of these immunogenic compartments occurs via a process of cell differentiation termed haematopoiesis. Haematopoiesis is responsible for the production of all the major cell types that comprise the blood, all of which stem from the same multipotent progenitor cells known as haematopoietic stem cells (HSCs) (Figure 1.3.1) [148].

The commitment of HSCs to a particular lineage and subsequent terminal differentiation to a particular type of leukocytes is largely governed by cytokine signalling [149–151]. Cytokines encompass a broad range of proteins and peptides produced by several different cell types including leukocytes, fibroblasts and endothelial cells among others, which act as signalling molecules to promote or inhibit certain cellular activities in the surrounding cells and tissues. These molecules bind their respective cell surface receptors and trigger intracellular signalling cascades that regulate a cell's function and taxonomy [150]. Thus, cytokines could be considered the major drivers of immune cell differentiation and activation.

HSCs differentiate into one of two major lineages, either the myeloid or lymphoid lineages, which themselves differentiate or commit to several sub-lineages [152]. Interleukin-3 (IL-3) is one of the major cytokines that stimulate the differentiation of HSCs to several lineages, including to myeloid progenitor cells [153]. Myeloid progenitor cells produce the only two blood cells not included in the 'leukocyte' class of immune cells. These are the megakaryocytes, which subsequently produce platelets in the blood and aid in blood clotting during wound healing, and erythroblasts which differentiate into erythrocytes which carry oxygen via the blood to the body's tissues and organs [154,155]. Myeloid progenitor cells can be stimulated by granulocyte-macrophage colony-stimulating factor (GM-CSF) to produce myeloblasts or by IL-6 and stem cell factor (SCF) to promote production of mast cell progenitor cells [156]. The latter enter the blood stream where they travel to target tissues and become mature mast cells, driven by binding of IL-4 [156,157]. The former are the precursors to many of the most common members of the innate immune response, such as the neutrophils and macrophages. Myeloblasts can bind G-CSF to promote a differentiation towards the granulocytic lineages which include neutrophils, eosinophils and basophils or IL-6 to drive differentiation to granulocytic myeloid derived suppressor cells [158–160]. Myeloblast binding of M-CSF promotes the differentiation to monocytic progenitor cells which themselves differentiate into monocytes which enter the blood stream and are transported to target tissues where they extravasate and differentiate to one of macrophages or monocytic myeloid derived suppressor cells depending on further exposure to an array of cytokines [160]. Monocytic progenitors can also differentiate into common dendritic progenitors in the presence of FMS-like tyrosine kinase 3 ligand FLT3L [161]. Common dendritic progenitors become pre-dendritic cells which migrate into the blood stream and travel to target tissues where they fully mature into either conventional dendritic cell 1 (cDC1) or conventional dendritic cell 2 (cDC2) [161].

Differentiation of HSCs to a lymphoid lineage is stimulated by the binding of IL-7 which produces common lymphoid progenitor cells (CLP) [162]. The binding of IL-15 promotes these cells to form natural killer (NK) cells while FLT3L promotes their differentiation to lymphoid derived dendritic cells [163–165]. Lymphoid progenitors also differentiate into lymphoblasts, with further exposure to IL-7, and subsequently produce naïve T-cells, mediated by IL-2 exposure, or naïve B-cells, mediated by IL-4 exposure [150]. Each of these lineages can themselves become activated or matured depending on exposure to an array of cytokines in target tissues or secondary maturation organs to produce cluster differentiation protein 4 (CD4)- expressing T-cells, which can further differentiate to T-helper or T-regulatory cells, CD8-expressing T-cells, plasma cells or memory B-cells [166].

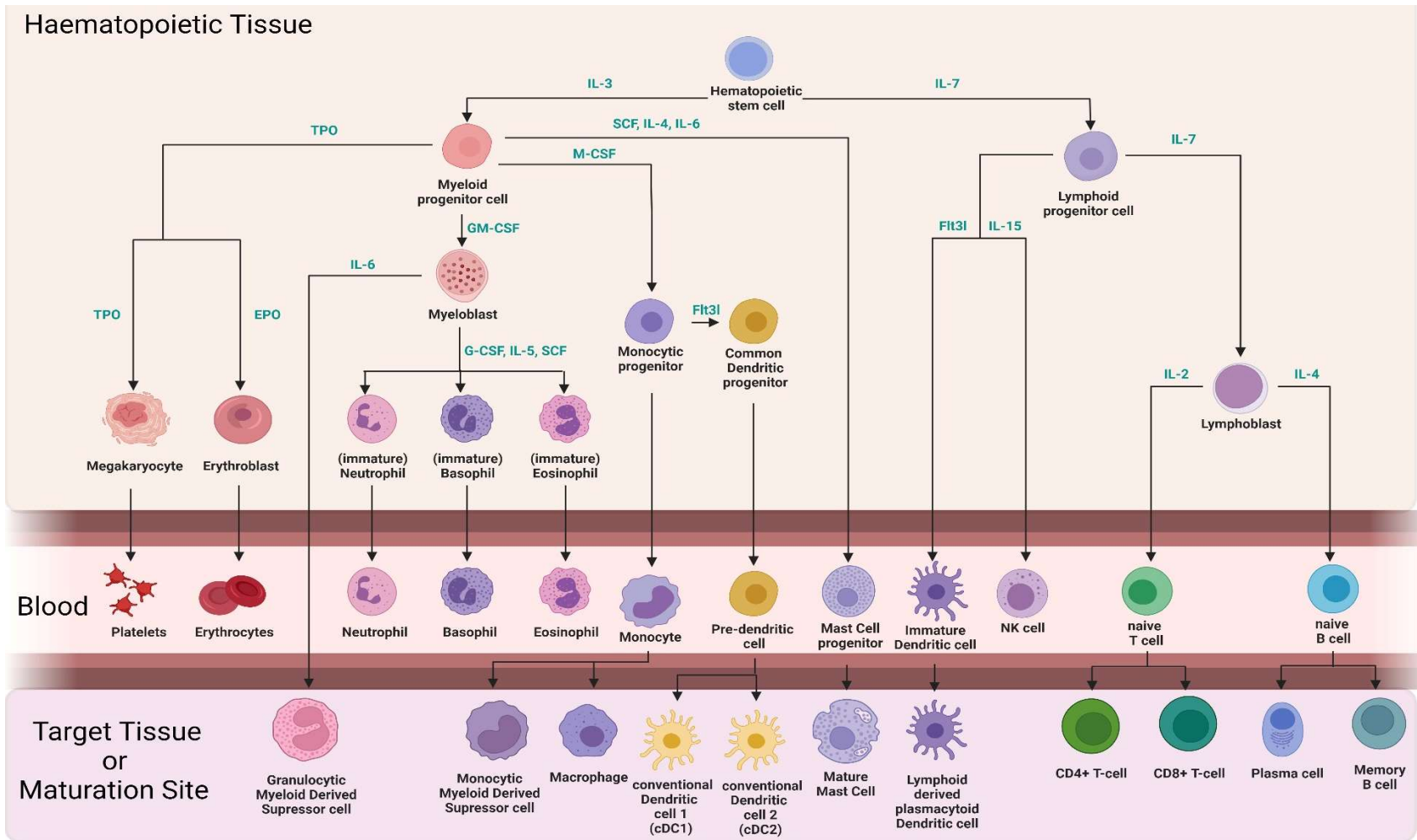


Figure 1.3.1. Cytokine exposure drives haematopoiesis and the differentiation of haematopoietic stem cells. Flow chart showing the various haematopoietic cell lineages, the major cytokines which drive cell differentiation and the locations in which differentiation occurs. Created in part using BioRender.com.

1.3.2 Innate immune cells and their functions

The innate immune response is the compartment of the immune system that is capable of mounting a defence from the moment an individual is born. This immune compartment refers to immune cells which respond to pathological challenge without having had prior exposure to a particular antigen [167]. In essence, cells of the innate immune system are the first line of defence against pathological threats, recognising and eliminating pathogens and distressed or infected 'self' cells as they come across them [168]. The efficacy of the innate immune response is governed by the expression of an array of germline encoded receptor proteins, called pattern recognition receptors (PRRs), against numerous highly conserved microbial proteins, called pathogen-associated molecular patterns (PAMPs), and proteins produced by an organism's own cells when damaged or distressed, called damage-associated molecular patterns (DAMPs) [169]. When PRRs on the surface of innate immune cells bind to either PAMPs or DAMPs on their targets' cell surfaces, a cascade of intracellular signalling occurs that triggers effector pathways to determine how the immune cell processes the threat [169]. The most common pathway by which innate immune cells can process the removal of pathogens or damaged cells is phagocytosis. Phagocytosis is the process by which several innate immune cells identify, engulf and digest their targets [170]. These cells are aptly named phagocytes. A number of phagocytes also act as antigen presenting cells (APCs) whereby, following phagocytosis, they translocate proteins isolated from the digested target to their cell surface membrane where they are 'presented' to other effector immune cells, particularly those within the adaptive immune compartment [171]. Thus, while early studies of the immune system labelled the innate immune response as 'non-specific' [169,172], the actions of APCs are now understood to be integral to educating and regulating downstream adaptive immunity [171]. Other mechanisms of innate immune activity include the release of an array of molecules with either microbicidal or cytotoxic effects. Exocytosis involves the intracellular packaging and subsequent secretion of proteins and peptides into the extracellular space where they interact directly with target microbes or target cells to exert their protective functions as well as promoting the activation of effector cells in the adaptive immune compartment [173].

1.3.2.1 Granulocytes and Mast Cells

The granulocytes encompass several innate immune cells characterised predominantly by the presence of granules within their cytoplasm which contain antimicrobial compounds used in the elimination of pathogens [174]. There are three types of granulocytes: neutrophils, eosinophils and basophils. However, mast cells are often considered within this grouping due to several physiological and functional similarities they have with granulocytes [175].

Neutrophils are the most abundant cell type of all the leukocytes, contributing up to 70% of the human white blood cell populations [176]. These cells are highly mobile and travel through the blood to sites of inflammation and infection where they play a significant role in eliminating pathogenic challenge. Unlike other members of the granulocytes, but similarly to some monocytic immune cells, neutrophils are considered professional phagocytes [177]. As described above, phagocytes identify pathogens or distressed cells via membrane bound PRRs and, once identified, engulf and digest their targets [178]. Many cell types, including non-immune cells such as fibroblasts, epithelial and endothelial cells, can undertake phagocytosis. However, professional phagocytes are those immune cells, predominantly, macrophages, monocytes and neutrophils, whose major function is phagocytosis and they undertake the process with improved efficiency compared to non-professional phagocytes [178]. Predominantly due to the increased expression of cell-surface receptors, PRRs, which promote phagocytosis of targets and the increased toxicity of the biomolecules involved in killing targets once engulfed in the phagosome [178]. The process by which pathogens or other foreign bodies are engulfed includes the formation of an envelope-like structure, called a phagosome, which is internalised to contain the target. The intracellular granules, containing toxic antimicrobial compounds and proteins, such as nitric oxide, reactive oxygen species, myeloperoxidase and matrix metalloproteinases (MMPs), fuse with phagosomes and release their contents into the intra-phagosomal space to exert their antimicrobial and cytotoxic activity and eliminate the phagocytosed target [178,179]. The high mobility and abundance of neutrophils as well as the efficiency by which they phagocytose their targets make these cells an integral line of defence, ahead even of other innate immune cells.

In contrast to highly abundant neutrophils, eosinophils and basophils contribute only ~3% and ~1% of circulating white blood cells respectively [180–182]. Eosinophils are associated with efficient response to parasitic infection, particularly in the case of helminth worms [183,184]. The granules in the cytoplasm of these granulocytes contain acidophilic proteins and bioactive compounds, including peroxidases, ribo- and deoxyribo- nucleases, which are toxic to the target parasites [185]. Eosinophils degranulate and release the toxic contents within their granules which target and kill parasites within their locale [183,186]. This can occur either by complete cytolysis which also ultimately kills the eosinophils as well as their target, or by controlled exocytosis of granules via secretory vesicles, called piecemeal degranulation, leaving eosinophils in a viable state after targeting parasites [186–188]. In either case, due to the high toxicity of the proteins present in eosinophilic granules, degranulation is often accompanied by negative effects on surrounding host tissues and, as a result, these immune cells have been shown to drive progression in several atopic diseases, including asthma and dermatitis [189,190].

The third and honorary fourth member of the granulocytes are basophils and mast cells respectively. These cells have numerous similarities in terms of both their physiology and function [191]. Early immunological studies, between the late 1800's and early 1900's, were only able to distinguish between them by the fact that one was only found in circulation, basophils, while the other was found in tissues, mast cells [192]. Like eosinophils, both have been described to play active roles in fighting parasitic infection and are poorly phagocytic, rather attacking parasites by releasing various components of their cytoplasmic granules into the extracellular space [193–196]. Morphologically, mast cell granules tend to be smaller than those of basophils but far more numerous, resulting in higher concentrations of certain granular molecules [191]. The granular contents of basophils and mast cells are largely very similar and comprise histamine, proteoglycans and a variety of serine proteases, including tryptase and chymase [197]. However, one key difference between the granular contents is that mast cell granules have a far higher concentration of the glycosaminoglycan, heparin, a molecule which acts as an anticoagulant to prevent the formation of blood clots [189]. Additionally, basophil granules contain lower concentrations of histamine when compared to mast cells [197]. That said, both mast cell and basophils are considered the major producers of histamine, a molecule contained within intracellular granules which, when released, promotes vasodilation and vascular permeability to increase blood flow to areas of infection and inflammation in an attempt to 'flush-out' parasites and facilitate the extravasation of phagocytes, namely neutrophils and monocytes [198,199]. However, histamine also has a significant influence in promoting hypersensitivity in response to allergen exposures, potentially resulting in atopic disease or, in the worst cases, anaphylaxis [200]. In addition to histamine, several other proteins released during the degranulation of basophils and mast cells can promote inflammation and recruitment of macrophages and other effector cells via cytokine signalling, such as CCL3, a chemotactic factor of both macrophages and neutrophils, and TNF α , a cytokine which drives proinflammatory activity in macrophages [191,201]. As a result, mast cells and basophils are understood to be key regulators of allergy and atopic disease [191].

The mast cells and basophils share a common mechanism by which they are activated, resulting in the degranulation of histamine and other inflammatory granule components. Both these cells express the FC ϵ R1 cell surface receptor which binds IgE immunoglobulins with very high affinity. IgE immunoglobulins are produced by plasma cells and Th2 T-cells, of the adaptive immune compartment, in response to allergenic antigens [202]. Once released into tissues or circulation, mast cells and basophils bind these antibodies via the FC ϵ R1 receptor and retain them on their cell surfaces. When these surface bound IgE antibodies bind their allergenic antigen, they become crosslinked with neighbouring IgE antibodies and trigger an intracellular signalling cascade which

triggers degranulation via exocytosis [203]. Figure 1.3.2.1 outlines the induction of mast cell degranulation via IgE crosslinking.

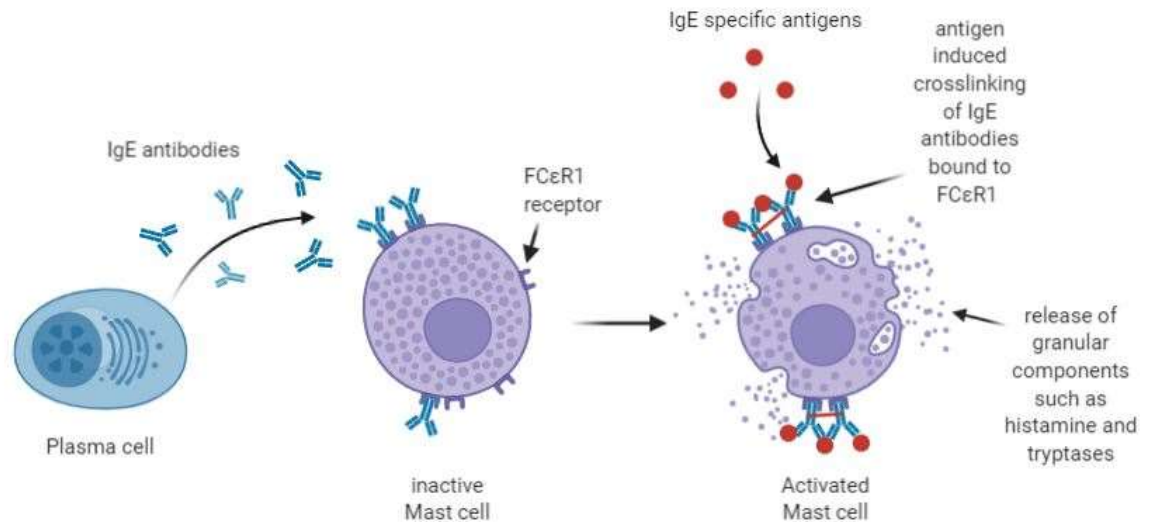


Figure 1.3.2.1. IgE dependent induction of mast cell degranulation. Cartoon schematic depicting the release of IgE immunoglobulins from plasma cells which bind FcεR1 receptor on the surface of mast cells and subsequently bind antigens specific to IgE binding sites. Antigen binding of neighbouring IgE on the surface of mast cells induces crosslinking of the immunoglobulins and the induction of intracellular signalling cascades that trigger degranulation of mast cell granules via exocytosis. Adapted from “Novel Pathway of IgE-Mediated Drug Allergy”, by Biorender.com (2022). Retrieved from <https://app.biorender.com/biorender-templates>.

Advances in immunological research has now identified several integral differences between basophils and mast cells. As stated above, basophils are primarily present within blood circulation while mature mast cells are only found in tissues [191]. Additionally, mast cells are generally larger than basophils. The former tend to be between 12 to 20µm in diameter while the latter do not tend to exceed 10µm [191]. Nuclei are another distinguishing feature whereby basophils exhibit the traditional segmented nucleus observed in their granulocytic counterparts while mast cells have an oval nucleus, suggestive of a monocytic lineage [191,204]. At a molecular level, mature mast cells express the receptor for SCF called KIT or CD117 [205]. This receptor is ubiquitously expressed in various stem cell types, including those of the haematopoietic lineages, but is reduced as cells differentiate and mature [206]. However, mast cells uniquely retain CD117 expression even when terminally differentiated and matured, and their ability to bind SCF is integral to their ability to proliferate and survive in tissues [205,207]. Functionally, basophils have an increased ability to rapidly synthesise IL-4, a cytokine which promotes the activation of Th2 T-cells and naive B-cells, making them key regulators of the cellular type 2 and humoral immune responses [208].

1.3.2.2 *Monocytes and Macrophages*

Monocytes and macrophages are cell types at different points along the same lineage and are both considered professional phagocytes within the mononuclear phagocyte system [209]. These cells are especially effective at the removal of pathogens and damaged or dying cells through recognition of PAMPs and DAMPs [210,211]. They also support adaptive immune responses by presenting antigens to lymphocytes on their cell surfaces [212]. Monocytes are produced in the bone marrow from common myeloid progenitor cells and migrate into circulation where they eliminate blood-borne threats through phagocytosis (Figure 1.3.1) [209]. They predominantly remain in circulation until recruited to tissues by chemotactic release of various cytokines and other signalling molecules by resident cells and/or other activated immune cells [213]. This chemotactic recruitment occurs in greater numbers following injury or infection but is also undertaken by undamaged tissues in order to maintain tissue homeostasis. Once monocytes extravasate from the blood and migrate into tissue, they differentiate into macrophages or dendritic cells where they become tissue resident [213]. Depending on the cytokines and signalling molecules present within the microenvironment, macrophages will undergo polarisation to one of two activation states or phenotypes. These are termed the classically activated macrophage (M1) and alternatively activated (M2) state [209]. Polarisation determines the functional role of macrophages within a tissue which can either be one of antimicrobial and pro-inflammatory activity, observed in M1 macrophages, or anti-inflammatory and tissue repair activity, as seen in M2 macrophages [214].

M1 macrophages, are effective at fighting infections and exhibit targeted antimicrobial activity [215]. Their activation is promoted by several mediators including the release of tumour necrosis factor α (TNF α) and interferon γ (IFN γ), by Th1 T-cells, among others, and PAMPs such as lipopolysaccharides (LPS) on the surface of certain bacteria. These molecular signals trigger proinflammatory stimuli and the activation of nitric oxide synthase 2 (NOS2), an enzyme involved in the metabolism of arginine, producing nitric oxide and reactive oxygen species (ROS) which exert strong microbiocidal influences and cytolytic activity on phagocytosed targets [216]. In addition to their phagocytic activity, classically activated macrophages also act as APCs and express higher levels of the transmembrane glycoprotein major histocompatibility complex class II (MHC-II) than their alternatively activated counterparts [215]. Following phagocytic degradation of microbes, intracellular MHC-II molecules, present along the phagosome membrane, bind the exogenous fragmented antigens and translocate to the cell surface where they present these antigens to members of the adaptive immune response, predominantly CD4+ T-helper cells, triggering their activation and downstream roles in fighting the infection [217]. These activities mean classically

activated (M1) macrophages are associated with pro-inflammatory roles and the production of microbiocidal and cytolytic products which often cause tissue damage [214].

In contrast to their classically activated counterparts, alternatively activated macrophages, or M2 macrophages, promote cell proliferation and anti-inflammatory activity to support tissue repair after injury or infection [218,219]. Cytokines, including IL-4, IL-10 and IL-13, produced in the tissue microenvironment in response to damage or infection stimulate macrophage polarisation to an M2-phenotype [220]. In contrast to NOS2 dependent arginine metabolism observed in M1 macrophages, M2 macrophages utilise arginase to enzymatically process arginine into ornithine which is subsequently processed to form proline, an amino acid with a role in collagen formation and tissue remodelling, and polyamines, which are integral to regulating cell proliferation [221]. In addition, M2 macrophages produce IL-10 in high abundance [222]. IL-10 is an immunosuppressive cytokine which reduces the expression of pro-inflammatory signalling proteins, such as MHC-II and several Th1 T-helper cell cytokines, in turn limiting the activity of cytotoxic cells, such as classically activated macrophages, while facilitating tissue repair through matrix remodelling and cell proliferation [223,224].

The increased expression of CD206, macrophage mannose receptor, is another marker of an M2 macrophage [225]. This cell surface protein acts as a molecular scavenger, binding antigen remnants produced following lysosomal degradation of pathogens or distressed cells during phagocytosis and exocytosis, and promoting their internalisation by endocytosis to reduce the potential for said antigens to induce activation of pro-inflammatory immune cells [226]. Additionally, recent studies have demonstrated that the binding of CD206 on the surface of macrophages with CD45 on the surface of CD8 cytotoxic T-cells inhibits phosphatase activities and promotes upregulation of immune-tolerance genes, including the immune checkpoint protein cytotoxic T-lymphocyte associated protein 4 (CTLA4), reducing their cytotoxic activity and promoting tissue repair [227]. These M2 functions may be considered beneficial in the context of reducing inflammation following local infections and returning tissues to a state of homeostasis, however, in the context of cancer, they may act to promote cancer cell proliferation and tumour growth, processes detrimental to one's health [228]. The key differences between M1 and M2 macrophage polarisation and function are summarised in Figure 1.3.2.2 below.

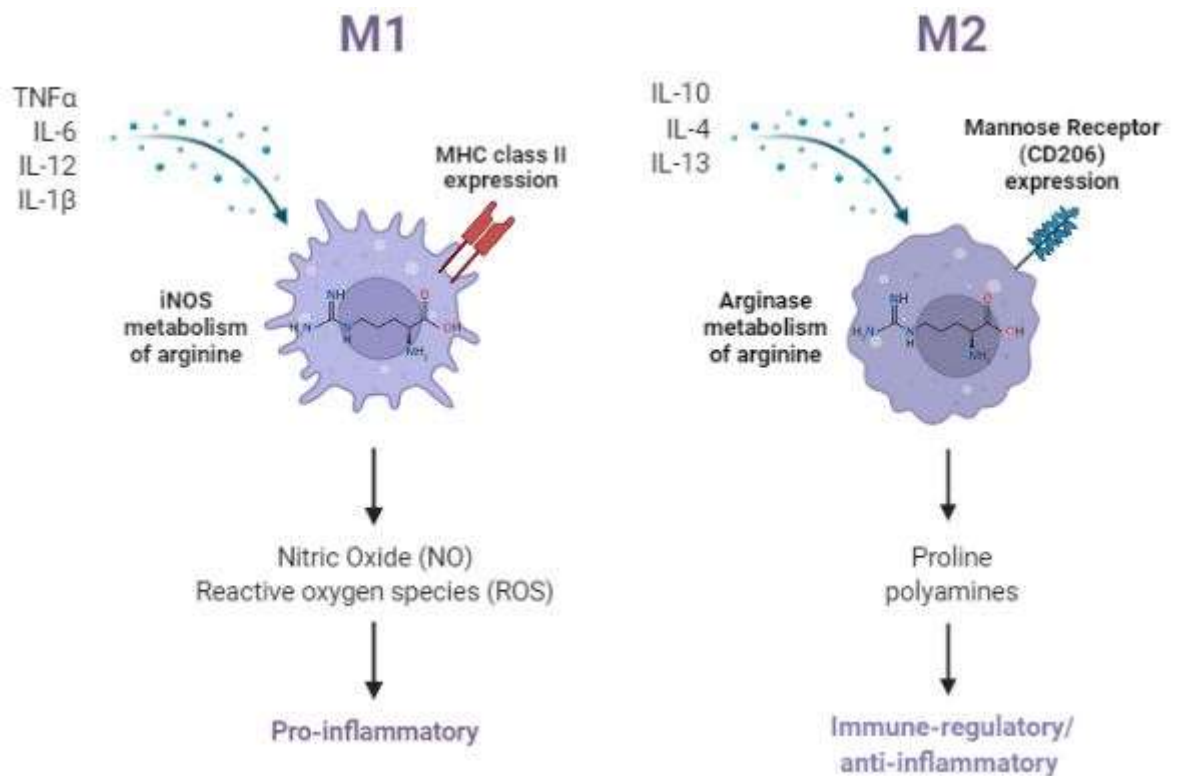


Figure 1.3.2.2. Cytokine induced macrophage polarisation. M1 macrophages are produced in the presence of TNF α , IL-6, IL-12 and IL-1 β , promoting expression of MHC-II and arginine metabolism via the iNOS pathway to produce pro-inflammatory ROS, including nitric oxide (NO). M2 macrophages are produced in the presence of IL-10, IL-4 and IL-13, promoting expression of the scavenging mannose receptor, CD206, as well as arginine metabolism via the arginase pathway to reduce production of ROS instead producing proline and polyamines involved in tissue repair and remodelling. Created in part using BioRender.com.

1.3.2.3 Dendritic Cells

Like monocytes and macrophages, dendritic cells are also members of the mononuclear phagocytic system and are so named due to the presence of protruding appendages along their cell surface, called dendrites [229]. While morphologically distinct, the roles of dendritic cells in regulating immune homeostasis are similar in many ways to those described for M1 macrophages [230]. The major difference between these two innate immune cells is the efficacy by which dendritic cells are able to act as APCs and their interaction with adaptive immune cells to mount targeted immune responses to specific antigens. In comparison to macrophages, phagosomal degradation of engulfed contents in dendritic cells occurs in a less severe manner, in part due to the slower rate of acidification within dendritic cell phagosomes [231]. Thus, it may be considered that dendritic cells might not be grouped in the “professional phagocyte” classification. However, this characteristic facilitates the preservation of antigenic components for presentation on MHC-II and MHC-I complexes, as in M1 macrophages, to CD4+ T-cells [232,233]. Additionally, while macrophages are tissue resident and do not migrate from their site of activation, dendritic cells are motile and able

to translocate from activation sites to lymphoid tissues where they can ubiquitously activate T-cells and mount an appropriate immune response in a scale greater than tissue resident macrophages would be able to [234,235]. It is this optimised functionality which defines dendritic cells as the most effective APC and why they are considered sentinels of the immune system, identifying invading pathogens and reporting their presence to the adaptive immune compartment. Thus, similarly to professional phagocytes, dendritic cells are considered professional APCs as their major function is to present antigens to the adaptive immune compartment and mount a targeted adaptive immune response to threats against homeostasis and are better equipped to do so due to their increased expression of MHC proteins and co-stimulatory proteins, namely CD80/86 [236].

Naïve or inactivated dendritic cells are generally located in peripheral tissues where the likelihood of exposure to invading pathogens is increased, such as mucosal tissues and skin epithelium [237]. As in other mononuclear phagocytes, dendritic cells become activated when binding antigens on the surface of invading cells PAMPs via PRRs such as toll-like receptors (TLR) or scavenge antigens released by other phagocytes following proteolytic degradation of a pathogen [238]. These antigens are internalised, and trigger increased production of MHC-II which binds endosomal antigen components before translocating to the cell surface to present the antigen to T-cell receptors (TCR) on the surface of naïve T-cells [239]. However, this interaction alone is not enough to promote T-cell activation. In addition to increased production of MHC-II, activated dendritic cells also increase expression of CD80 and CD86 which act as co-stimulatory molecules [240,241]. These transmembrane proteins bind receptors on the surface of T-cells to support MHC-TLR binding in regulating the activation of signal transduction pathways that promote or inhibit T-cell activation. Specifically, the binding of CD80/86 to CD28 on the surface of T-cells promotes T-cell activation while the same binding to CTLA4 would inhibit T-cell activation [242].

In addition to their role in T-cell priming, dendritic cells have an integral role in preventing autoimmunity through regulating tolerogenic signalling and inhibiting T-cell activation in response to self-antigens [243]. As mentioned above, the migratory ability of dendritic cells was highlighted as a key characteristic of their ability to prime T-cell responses within lymphoid organs. However, within lymphoid organs, particularly the thymus, exist resident dendritic cells which translocate from the bone marrow as progenitor cells and mature in these locations without ever migrating to peripheral tissues. These cells present a broad array of self-antigens, mostly obtained from medullary thymic epithelial cells to thymic naïve T-cells. Those T-cells which react with high affinity for the self-antigens are considered autoreactive and pose a threat to homeostasis. These are therefore directed to undergo apoptosis, via a process called negative selection, or towards T-cell differentiation into a T-regulatory (T-reg) cell with immunosuppressive functionality via a variety of

signalling pathways including CD70 on the surface of thymic dendritic cells to CD27 on the surface of T-cells [243,244].

1.3.2.4 *Natural Killer cells*

NK cells are one of only a few innate immune cells derived from CLPs [245]. Most innate immune cells stem from common myeloid progenitors while the progeny CLPs tend to be members of the adaptive immune compartment, requiring activation by antigen specific interaction with APCs to carry out their effector roles. However, unlike their lymphoid 'siblings', NK cells can be activated by an antigen-independent pathway [246]. The predominant niche of NK cells within the immune response is to eliminate cells signalling distress, often resulting from viral infection and proliferation within a cell [247]. NK cells express both activating and inhibitory receptors along their cell surface. When NK cells bind ligands of both these receptors simultaneously, NK cytolytic activity is inhibited and the cell with which they engage is left alone. However, in distressed cells, including cancer cells and those infected by viruses, the expression of inhibitory ligands is downregulated while activation ligand expression is unchanged, resulting in the increased signalling of activator proteins following binding of their ligands on the surface of distressed cells, triggering NK cell activation and the cytolytic actions that follow [248]. In humans, the major protein groups that contribute to inhibitory signalling are the binding of killer Ig-like receptors (KIRs) on the surface of NK cells to MHC class I (MHC-I) ligands on the surface of target cells [248]. When cells become distressed they reduce expression of MHC-I and thus the binding of activating receptors to their ligands on target cells promotes NK cell activation [248,249].

Once activated, intracellular signalling cascades promote the exocytosis of secretory vesicles containing cytolytic proteins, including perforin and several granzymes [250]. Perforin production is limited to just NK cells and CD8-expressing cytotoxic T-cells, and is integral to the cytolytic aspect of the overall cytotoxic activity of these cells [251]. Perforin molecules are integrated into phospholipid bilayer of the target cell membrane and polymerize with other perforin molecules to form transmembrane channels [252]. These 'pores' facilitate the unchecked influx and efflux of various ions, such as Na⁺ and Ca²⁺, and polypeptides which disturb intracellular mineral homeostasis and trigger pro-apoptotic pathways to cause cell death [252]. Granzymes are also released in response to NK cell and cytotoxic T-cell activation and are capable of passing through the transmembrane pores produced by perforin into the target cell cytosol [251]. These serine proteases comprise 90% of the granular contents within NK cells and cytotoxic T-cells and, when released into target cells, cleave peptide chains at specific amino acid residues, depending on the type of granzyme, to initiate several signalling pathways, including those which induce apoptosis [253]. There are five known granzymes to be active in human cells and eight in mice, but in both

species granzyme B is the most prominent pro-apoptotic of these and operates by proteolytically cleaving caspase proteins, particularly caspase 3, between aspartic acid and glutamic acid residues, to initiate their activity in apoptotic pathways to rapidly induce cell death [253,254]. Activated NK cells also produce IFN γ , a cytokine with key modulatory effects on macrophages and neutrophils, encouraging inflammatory responses of phagocytes which then identify and engulf any microbial antigens released following target cell lysis following apoptosis [255–257].

1.3.3 Adaptive immune cells and their functions

While innate immunity is ubiquitous in both the plant and animal kingdoms, adaptive immunity is a vertebrate specific response to pathological challenge [232]. Unlike innate immunity, adaptive immunity requires “learning” by exposure to said challenges. This is largely facilitated by the presentation of antigens to naïve or memory lymphocytes which become activated and pursue one of several avenues to mount a response. The avenue selected depends on the type of lymphocytic cell and governs their role in responding to the challenge.

In contrast to the molecular interactions that govern recognition of pathogens and damaged cells by the innate immune compartment, the adaptive immune system relies on somatic generation of its receptors, meaning different lymphocytes will express unique immunological proteins against a diverse array of antigens and only those receptors which recognise pathological challenges will be selected for clonal expansion [146]. The adaptive immune compartment can be divided into two broad cell groups based on their site of maturation: T-cells and B-cells. Thymus cell lymphocytes, or T-cells, are produced in the bone marrow but translocate to the thymus, an endocrine gland, where they mature into naïve CD4 or CD8 expressing T-cells [258,259]. T-cells mount immune responses either directly, via the targeted release of cytotoxins in response to antigen recognition, or indirectly, via the production of cytokines which promote the activity of effector immune cells. These responses are termed cellular immune responses due to their reliance on cell-to-cell interaction to engage pathological challenges. B-cells arise from the same CLP as T-cells but mature in the bone marrow [260]. B-cells and their subsets are the drivers of humoral immunity, as opposed to cellular immunity, via their production of antigen-specific macromolecular proteins, called antibodies, which are released into circulation and bind their target antigens, inhibiting pathological activation of specific proteins as well as aiding phagocytic cells in identifying these targets as entities that require phagocytosis [261,262].

1.3.3.1 CD4-expressing T-cells

T-cells are derived from CLPs that migrate from the bone marrow to the thymus where they mature and differentiate according to signalling molecules on, or released by, other members of the

immune system [263]. During periods of maintained homeostasis, T-cells exist in a naïve state. However, following immune challenge, APCs present antigens via MHC complexes which bind TCRs on the surface of naïve T-cells, triggering signalling transduction pathways which activate T-cells [264]. Additionally, costimulatory molecules expressed on APC cell surfaces as well as the cytokines they release influence T-cells activation pathways [264,265]. The types of cytokines released by innate immune cells are governed by the nature of the antigens responsible for their activation and are significant determinants of the polarisation pathways naïve T-cells will follow to become effector T-cells [266].

T-cells can be divided into two broad groups, classified by the expression of either CD4 or CD8. CD4-expressing T-cells (CD4 T-cells) are activated by exogenous antigens presented by MHC-II complexes on the surface of activated APCs [267]. Depending on which cytokines are concurrently released, CD4 T-cells polarise to one of several subsets, the major four of which are T-helper 1 (Th1), Th2, Th17 or T-reg cells [266]. When activated, all four subsets operate by themselves releasing different molecular signals to either promote or inhibit the activity of other immune cells, including innate immune cells like macrophages and other adaptive immune cells such as NK cells and cytotoxic T-cells. Each subset also targets different types of immune threats. Th1 cells tend to be associated with targeting intracellular pathogens, such as mycobacterial species, Th2 cells target extracellular parasites such as helminths, Th17 cells are linked to intracellular anti-bacterial and antifungal responses and T-reg cells exert a regulatory effect on other immune cells to maintain immune homeostasis [268]. Figure 1.3.3.1 below summarizes the major cytokines involved in driving CD4 T-cell polarization and the effector functions driven by the various CD4 T-cell subsets.

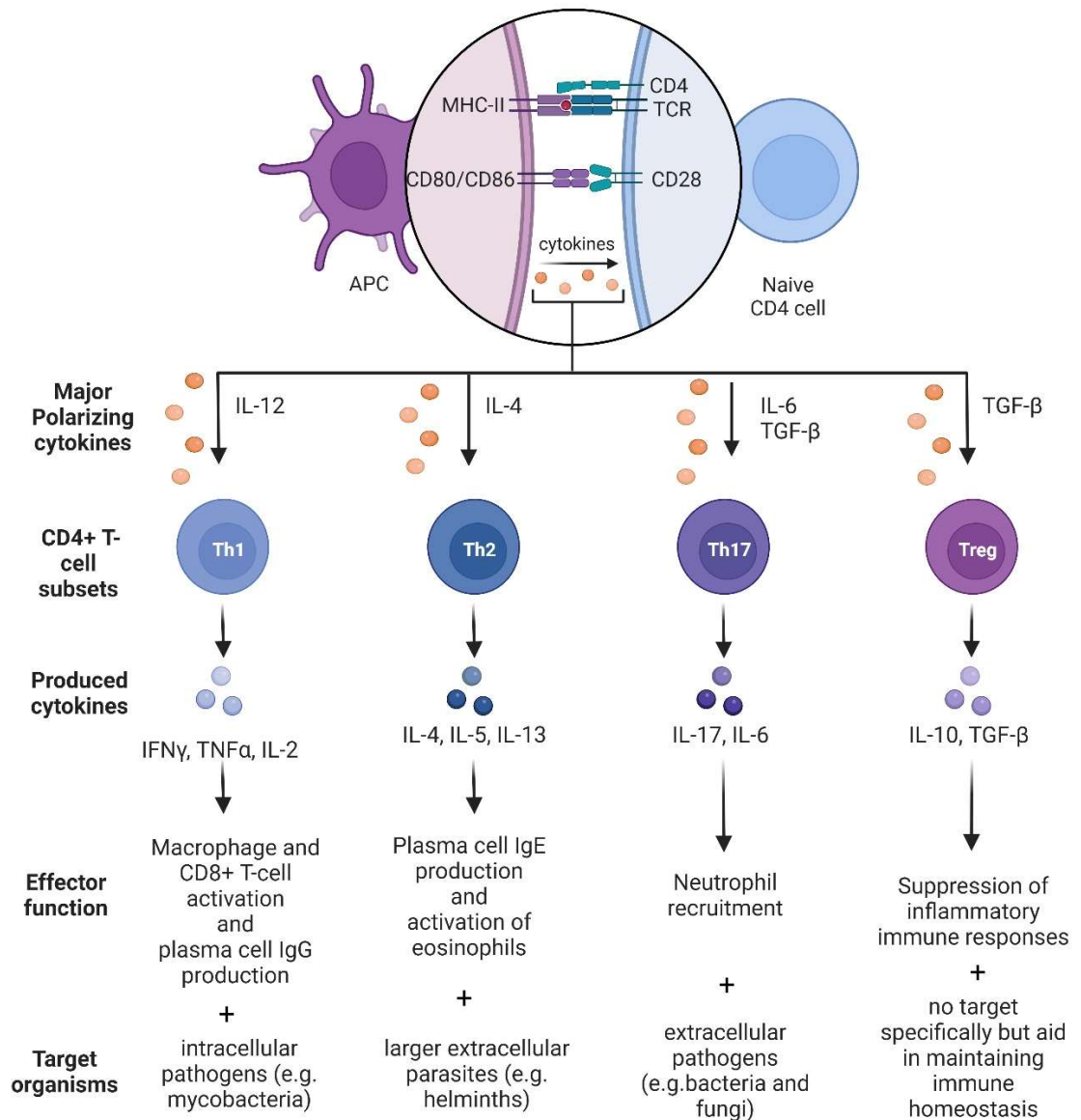


Figure 1.3.3.1. Cytokine release regulates CD4 T-cell polarization. Cartoon schematic summarising the receptor interactions and major cytokines released by APCs involved in activating and polarising naïve CD4 T-cells in to one of four major subsets and the effector functions the activity of those cells exert after polarization via their own cytokine production. Adapted from “T cell activation and differentiation”, by Biorender.com (2021). Retrieved from <https://app.biorender.com/biorender-templates>.

Th1 cells develop in response to IL-12, released by pro-inflammatory stimulated APCs, which promotes the activity of transcription factor signal transducer and activator of transcription 4 (STAT4) [269]. STAT4 induces Th1 cell production of IFN γ , which is itself a regulator of Th1 activation via STAT1, triggering a positive feedback loop that facilitates clonal expansion of Th1 cells [270,271]. Once a suitable population of Th1 cells is established, they drive effector activity in several other immune cells including the activation of professional phagocytes, plasma cell production of IgG antibodies and the activation of CD8-expressing cytotoxic T-cells. A major protein governing these

effects on macrophages, dendritic cells and B-cells is the expression of the costimulatory CD40-ligand (CD40L) in T-cells. CD40L is expressed on the surface of Th1 cells and binds to its receptor, CD40, on the surface of target immune cells to promote their activation, dependent on other signalling molecules concomitantly released by the T-cells. As mentioned, IFN γ is released in high abundance by Th1 cells and, in its presence, the binding of CD40L to CD40 on the surface of macrophages stimulates production of anti-microbial molecules associated with an M1 macrophage polarisation phenotype, namely NO and other ROS [272]. However, when binding CD40 on the surface of B-cells, it induces several signalling cascades which regulate a number of biological processes including B-cell maturation to antibody producing plasma cells, specifically of IgG isotype antibodies [262]. Th1 cells also play an integral role in the activation of CD8 expressing T-cells, via the production of IL-2, to undertake cytotoxic activities against distressed cells and cancer cells [273,274].

Cytokine release of IL-4 regulates Th2 polarisation, a T-cell state which is associated with inducing anti-parasitic immune activity but concurrently driving tissue hypersensitivity and allergic responses [275,276]. Initial IL-4 release by APCs promotes the activation of transcription factor STAT6 which further triggers Th2-associated gene transcription and subsequent production of increased levels of IL-4 as well as IL-5 and IL-13 [277,278]. IL-4 and IL-13 cytokines both contribute to isotype class switching in B-cell production of antibodies from IgG to IgE isotypes [279]. As described above IgE antibody release stimulates basophils and mast cells to degranulate and release signalling molecules which promote vasodilation and inflammation which, when unchecked, can result in allergic responses and anaphylaxis. IL-5 release promotes eosinophil activation, another cell with established links to allergenic activity, and antibody production in B-cells, complementing the release of IgE following isotype class switching induced by IL-4 and -13 [280].

Th17 cells are the third major subset of Th cells, and their activation is stimulated by IL-6 and transforming growth factor β (TGF β) [281,282]. Th17 cells are pro-inflammatory and release several cytokines themselves, predominantly IL-17, which are potent activators of phagocytic neutrophils [283]. Several studies demonstrate particular influences Th17 cells have in mounting anti-fungal responses against filamentous and mucocutaneous fungi [284]. However, these cells have also been linked to driving autoimmune disease through their pro-inflammatory cytokine release promoting immune cell activity that can result in tissue damage [282,285].

The final major subset derived from CD4 expressing T-cells are the T-regs. These cells are also produced in response to TGF β but in the absence of IL-6 and, in contrast to Th17 cells, are

associated with preventing autoimmune disease [286,287]. T-reg cells can be identified by the increased expression of several surface-level and intra-nuclear proteins, such as IL-2 receptor (IL-2R). IL-2 is a pleiotropic cytokine released by several lymphocytes during inflammatory responses which modulates effector cell responses through regulating proliferation and polarisation [288,289]. Its receptor, IL-2R, comprises three heterotrimeric protein chains (IL2R α , IL2R- β IL2R γ_c) and T-reg cells express high levels of IL2R α , also called CD25, which, when combined with the - β and - γ_c subunits, promotes a high affinity for IL-2 [290,291]. This T-reg specific characteristic heightens their sensitivity to even low doses of IL-2 relative to other T-lymphocytes and is thought to reduce the activity of other effector T-cells by starving them of IL-2 and therefore inducing deprivation-mediated apoptosis [292,293]. Additionally, T-reg cells constitutively express FoxP3, a transcription factor which downregulates expression of several genes associated with proteins that promote effector cell activity in order to reduce inflammatory responses [294]. FoxP3 also upregulates expression of several genes encoding proteins such as CTLA4, a receptor which when bound to CD80/86 on the surface of APCs triggers inhibitory signalling in T-cells, in turn promoting immunosuppressive activity and reducing inflammatory effector pathways [294]. As well as CTLA4, T-reg cells produce IL-10 in abundance. IL-10 is a potent immunosuppressive cytokine that binds to IL-10 receptor (IL10R) on the surface of an array of cell types [295,296]. IL-10R is a heterodimeric protein comprising two α subunits (IL10R α) and two β subunits (IL10R β). On binding IL10, tyrosine kinase enzymes phosphorylate the intracellular domain of the two IL10R α dimers which promotes the recruitment of STAT3 proteins [297]. Once recruited, STAT3 proteins are themselves phosphorylated by tyrosine kinase enzymes, namely Janus kinase (JAK), to form homodimers which are translocated to the nucleus where they promote gene expression associated with anti-inflammatory activity, such as the expression of suppressor of cytokine signalling 3 (SOCS3) which is a negative regulator of cytokine signalling and reduces expression of genes that code pro-inflammatory TNF α and IL-6 [298]. In several immune cells, predominantly macrophages and dendritic cells, IL10R α production is upregulated in response to initial binding of IL-10, increasing STAT3 dimerization and promoting gene expression patterns associated with anti-inflammatory immune activity [299]. Thus, T-reg cell production of IL-10 reduces the activity of several proinflammatory innate immune cells.

1.3.3.2 *CD8-expressing T-cells*

CD8-expressing T-cells (CD8 T-cells) play a largely similar role to NK cells in regulating immune homeostasis. Like NK cells, they are integral to the elimination of distressed cells, such as those subject to viral infection, or cancer cells which inadvertently express antigens that identify them as malignancies [300,301]. The major difference between CD8 T-cells and NK cells is that the former

relies on an adaptive antigen-dependent activation pathway while the latter are activated in an antigen-independent manner, as described in section 1.3.2 [302]. Naive CD8 T-cells circulate in the blood and lymphoid organs, including lymph nodes and mucosal tissues, until they are activated through the binding of endogenous pathological antigens presented on the surface of distressed cells via MHC-I with TCR on the surface of the CD8 T-cell [303]. The CD8 protein itself acts as a co-receptor for MHC-I and binds the non-antigen presenting extracellular domain to enhance the activation pathway [303]. Additionally, and in similarity to CD4 T-cells, CD8 T-cell activation is also supported by the signalling cascade triggered by the co-stimulatory protein CD28 binding to CD80/86 on the surface of APCs [304]. Once activated, CD8 T-cells undergo clonal expansion, producing a population of cytotoxic T-cells specific to the antigen that caused their activation [305]. Cytotoxic T-cells continue to bind MHC-I presented antigens on the surface of target cells via TCR and in doing so trigger the exocytosis of cytolytic and cytotoxic proteins, predominantly perforin and granzymes respectively, which permeate the target cell membrane and induce apoptosis, in much the same way as that described for the action of NK cells in section 1.3.2.4 [306,307]. Additionally, recognition of MHC-I presented antigens trigger cytotoxic T-cells to release IFN γ and TNF α , both of which promote inflammatory responses in other effector cells against distressed or malignant cells [308]. Cytotoxic T-cells are extremely effective at targeting distressed cells and if left unchecked have the potential to cause autoimmune pathologies. Therefore, it is important these cells have a mechanism by which their response can be self-regulated. Cytotoxic T-cells express two members of the TNF-receptor family called Fas and Fas-ligand (FasL) [309]. When Fas binds FasL on the surface of an opposing cell, it triggers the caspase cascade, a series of proteolytic cleavages involving various proteins which ultimately act to induce apoptosis [309]. Thus, when two cytotoxic T-cells bind via their respective Fas/FasL surface proteins, apoptosis is induced in both cells causing cell death and reducing the potential for autoimmune activity once a pathology has been suitably addressed [309].

1.3.3.3 B-Cells

The other major adaptive immune cells are the B-cells, which are responsible for humoral immunity through the production of soluble macromolecular proteins called immunoglobulins, or more commonly, antibodies [261,262]. The 'B' in B-cell is often mistakenly assumed to stand for 'bone' due to their derivation and maturation in the bone marrow. It actually refers to the 'bursa of Fabricius', a lymphoid organ found only in birds, and in which B-cells were first identified as being responsible for antibody production [310]. Like T-cells and NK cells, B-cells arise from CLPs in the bone marrow [260]. B-cell development largely occurs in the bone marrow via a series of intermediate stages to support the major function of B-cells, the production antigen specific

antibodies [311]. Antibody specificity is regulated by the somatic recombination of several genes associated with three regions of an immunoglobulin, the variable (V), diversity (D) and joining (J) regions [312]. This process is termed V(D)J rearrangement and governs the structural and molecular ability of an antibody to bind to specific antigens as well as facilitating antibody diversity to enable humoral responses against an array of antigen-dependent pathological threats [313].

Naive B-cells express unique B-cell receptors (BCR) which bind antigens and trigger B-cell activation [314]. Each BCR comprises a membrane bound version of an immunoglobulin associated with a transmembrane signal transduction moiety, CD79, a heterodimeric protein consisting of an α and β subunit [315]. The binding of a specific antigen at the binding sites on the membrane bound immunoglobulin promotes phosphorylation of CD79 and subsequent signal transduction pathways that activate the B-cell [316]. Part of these signalling pathways includes the internalisation and processing of BCR-antigen complexes via endocytosis so that the antigen can be presented via MHC-II complexes to T-cells, via their TCRs, to activate T-cells [317,318]. In doing so, B-cells bind CD40L on the surface of the T-cells via CD40, an interaction which promotes B-cell proliferation [319]. The activated T-cells also release cytokines, namely IL-4, which bind their receptors on the surface B-cells to further support proliferation as well as inducing antibody isotype class switching, a process which governs the structural specificity of the antibodies to be produced downstream [278]. Figure 1.3.3.3 outlines the T-cell dependent activation of B-cells via these interactions.

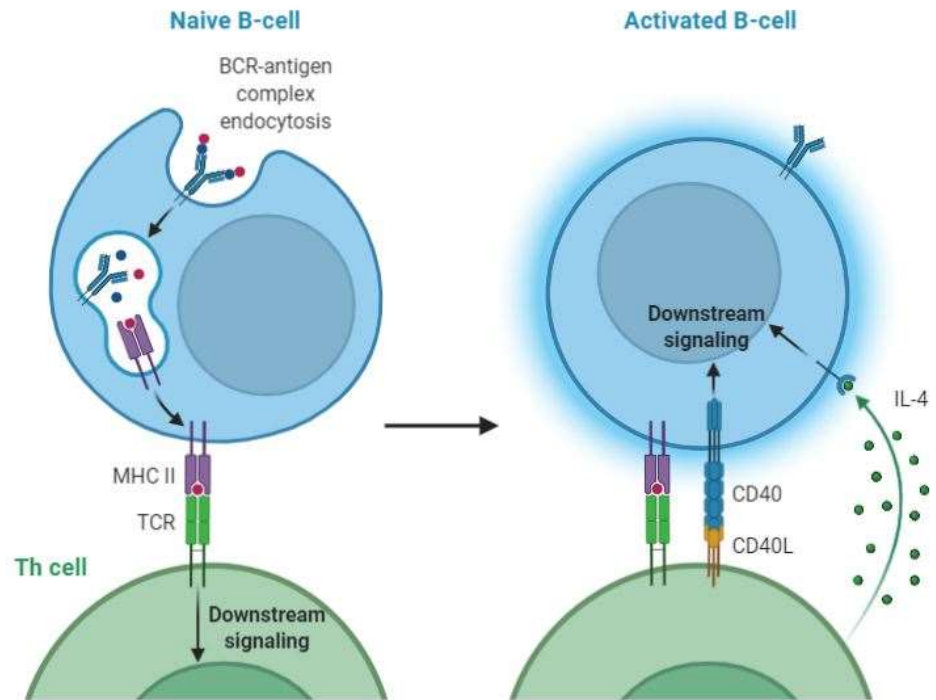


Figure 1.3.3.3. T-cell dependent activation of B-cells. Cartoon schematic summarising the key molecular interactions between naïve T-cells and B-cells that result in activation of both cells. Adapted from “Tfh Cells Help B Cells Secrete Antibodies Leading to ‘Linked Recognition’”, by Biorender.com (2021). Retrieved from <https://app.biorender.com/biorender-templates>.

Upon activation and proliferation, naïve B-cells differentiate into either long-lived memory B-cells or plasmablasts, an intermediate short-lived precursor to the mature antibody-producing plasma cells [320]. Clonal selection ensures only plasma cells producing antibodies which bind their targets with high specificity and affinity proliferate via clonal expansion to produce mature plasma cells that themselves produce highly antigen-specific antibodies [58].

1.4 Immunogenicity of Cancer

The previous section described and discussed the types and functions of the various immune cells in the context of their 'normal' roles and how these roles influence immune homeostasis or, in certain circumstances, disrupt it. This section aims to frame these various immune cells in the context of how they may influence cancers, specifically solid tumour cancers, and explore how the 'normal' roles of these cells can be exploited by cancer cells to promote tumour growth and metastasis as well as how some of these immune cells utilise their typical function to target and kill cancer cells.

The first hypothesis that inflammation was involved in cancer pathogenesis was made by the German physician Rudolf Virchow in 1863 [321]. Today, chronic inflammation is considered one of the 'hallmarks of cancer' and the understanding of the roles that various immune cells play in tumour initiation, growth and metastasis is much improved and further understanding is constantly emerging [55]. As outlined in section 1.2.2, cancers arise from the abnormal growth and proliferation of cells following DNA mutations [12,13]. Thus, while inflammation itself does not initiate carcinogenesis, it creates an environment in which malignant cells can proliferate and evade anti-cancer immune cells. Balkwill and Mantovani (2001) outlined this concept well using the analogy that if DNA mutations are the "match that lights the fire" to initiate cancers, inflammation is the "fuel that feeds the flames" [322].

The immunogenicity of a tumour refers to the extent to which it interacts with the immune system to elicit or prevent an immune response [323]. These interactions include both pro- and anti-tumour responses and the understanding of how these interactions occur is integral to several clinical facets associated with a given cancer, including disease diagnosis, predicting patient prognosis and informing appropriate treatment pathways. However, cancer is an incredibly heterogenous disease and the label of 'cancer' refers to an array of malignancies which affect different tissues and organs in the body. The influence of the immune system on these various types of cancer is itself heterogenous and as such this influence can vary greatly between different types of the disease. Thus, while certain immune cells may be influential in promoting or inhibiting tumour growth in one tissue or organ, it does not mean that that immune cell type will have the same influence on a different tumour type at a different location within the body.

The role that different immune cells play within the tumour microenvironment and surrounding tissues is a complex topic. The tumour milieu and surrounding tissues comprise an array of different cell types, both immune and non-immune, each of which influence tumour survival, either to promote it or to attack it [324]. Additionally, several immune cells can change their activity in

tumours in response to signalling either directly with neighbouring cells or through the production of signalling molecules such as cytokines and chemokines [321]. These changes mean it is often difficult to broadly categorise a cell type as exclusively pro- or anti-tumourigenic, macrophages being one such example [325]. However, advances in technologies, such as RNA-sequencing and flow cytometry, have aided greatly in identifying changes in a given cell type's activity within a tumour based on the expression or change in expression of various marker genes and proteins. This section aims to discuss how those functions promote or mitigate tumour progression and how those understandings can potentially be used as markers for prognosis and potential therapeutic targets.

1.4.1 Immune influence on tumour growth and metastasis

Although the immune system is largely evolved to support and maintain homeostasis, in some circumstances, it can malfunction, disrupting homeostasis and potentiating disease. In solid tumours, the immune system is often manipulated by cancer cells and their signalling pathways to promote tumour success [321]. During early stages of tumour initiation, the main objective of cancer cells is to avoid detection by anti-cancer cytotoxic effector cells, particularly cytotoxic T-cells and NK cells [326]. To this end, tumour cells engage with various other immune cells via direct cell to cell interactions as well as via the release of an array of signalling molecules to avoid immune attack and promote the activity of immunosuppressive cells [326]. Two immunosuppressive cell types commonly associated with the success of solid tumours regarding both growth and metastasis are T-reg cells and myeloid-derived suppressor cells (MDSCs) [327].

1.4.1.1 T-reg cells

As their name suggests, T-regulatory cells are integral to the regulation of inflammation and effector immune cell activity [328]. While these functions are protective against autoimmune diseases, in the context of cancer, T-reg cells are arguably the most influential immune cell in promoting tumour growth as they inhibit the activity of cytotoxic cells via an array of mechanisms [328]. The abundance of tumour infiltrating T-reg cells is a common prognostic marker in several murine and human solid tumours, including breast and ovarian cancers, with higher numbers generally being associated with poorer outcomes [329]. For example, Bates *et al.* (2006) observed a positive correlation between intratumoral T-reg abundance and tumour invasiveness in human ER-positive breast cancer tumour sections [330]. Using immunohistochemical staining of FoxP3 expressing cells and histological analysis of tumour sections, the study described that those patients with more than 15 T-reg cells per frame had poorer relapse-free survival and overall survival than patients with fewer than 15 T-reg cells per frame [330]. This association was only made in ER-positive tumours and T-reg abundance did not influence survival metrics in ER-negative patients.

T-reg recruitment into tumours is governed by chemotaxis gradients involving the tumoural release of several chemokines and the binding of these by chemokine receptors on the surface of T-reg cells [328]. These include binding of chemokine ligand 17 (CCL17) and CCL22 by chemokine receptor 4 (CCR4), CCL1 by CCR8 and CCL28 by CCR10 to name a few [328]. Once in the tumour, T-reg cells begin to undertake several immunosuppressive activities. T-reg cells are major producers of the anti-inflammatory and pro-tumorigenic cytokine IL-10 [296]. IL-10 down regulates the anti-tumorigenic activity of several effector cells including macrophages, dendritic cells, and cytotoxic T-cells [295]. When IL-10 binds its receptor, IL-10R, on the surface of APCs, it downregulates the expression of co-stimulatory proteins such as CD80/86, resulting in a reduced ability of these cells to activate CD8 effector T-cells and ultimately reducing cytotoxic activity within the tumour [331,332]. It also reduces the production of pro-inflammatory cytokines by APCs, such as IL-12, which otherwise activate Th1 cells and promote their recruitment of M1 macrophages and CD8 T-cells [333]. In addition to secreting interleukins, T-regs also bind them. Relative to other T-cells, T-regs highly express the IL-2R α receptor for IL-2, a key cytokine involved in naïve T-cell proliferation and activation [328]. The overexpression of this receptor means T-regs bind IL-2 with high affinity, thus removing it from the tumour microenvironment and preventing other T-cells from binding it, reducing their activation and proliferation, and subsequently their ability to perform anti-cancer functions [334]. FoxP3 expression in T-reg cells increases the expression of the co-inhibitory protein CTLA4 relative to other T-cell subsets [335]. While the interaction between CTLA4 and CD80/86 on the surface of APCs is typically associated with inhibiting T-cell activation, there is now evidence demonstrating the ability of T-regs to deplete CD80/86 abundances via trogocytosis, a process that involves the T-reg 'nibbling' part of the APC, removing the protein and internalising it [336,337]. This process reduces the availability of CD80/86 to stimulate activation of other T-cell subsets, including anti-cancer Th1 and cytotoxic T-cells. One study by Tekguc *et al.* (2021) demonstrated that T-reg cells formed an immune synapse with dendritic cells in a CTLA4-dependent manner and removed the section of the dendritic with which this synapse had formed, internalising the CD80 co-stimulatory protein [337]. Additionally, the trogocytosis of CD80 was associated with an increase in free PD-L1 on the surface of the dendritic cells, a ligand which when bound PD-1 on the surface of T-cells promotes immunosuppression and T-cell apoptosis [337]. CD80 forms heterodimers with PD-L1 on the surface of APCs and in doing so prevents PD-L1 from binding PD-1 on T-cells [337]. Thus, by removing CD80, T-regs prevent dimerization of these two cell surface proteins and facilitate the immunosuppressive activity of PD-L1 on T-cells, resulting in unchecked tumour cell proliferation. Combined, these various immune functions arguably make T-reg cells the most

effective cell type at reducing inflammation and anti-cancer effector cell activity, ultimately promoting tumour cell proliferation and disease progression.

1.4.1.2 Myeloid derived suppressor cells

In section 1.3.2 the major innate immune cell types and their functions were introduced in the context of regulating immune homeostasis without reference to carcinogenesis. However, myeloid derived suppressor cells (MDSCs) were not introduced or discussed. This was because MDSCs are almost exclusively linked to cancer progression and are not commonly discussed in the context of a supportive role in maintaining homeostasis [338]. These cells are derived from a myeloid progenitor as the result of defective haematopoiesis during myeloid cell differentiation [339]. Due to the heterogeneity of tumours and the production of signalling molecules that govern immune cell maturation and differentiation between individuals, the current mechanism by which haematopoiesis becomes defective in patients with cancer remains unclear [339]. However, the mechanisms by which these cells exert immunosuppressive influences on anti-cancer effector cells, particularly cytotoxic T-cells and pro-inflammatory macrophages, are becoming better understood. MDSCs are currently classed into two subtypes, granulocytic MDSCs (gMDSCs) and monocytic MDSCs (mMDSCs) according to the differential expression of several cell surface markers, usually identified by flow cytometry [340]. In mice, MDSCs are classified as CD11b⁺ Ly6C^{low} Ly6G⁺⁺ for gMDSCs while mMDSCs are CD11b⁺ Ly6C⁺⁺ Ly6G^{low} [340]. In humans, both MDSC subsets are identified by cell-surface expression profiles of CD11b⁺ CD33⁺ HLA-DR⁻ and subsequently CD14⁺ CD15⁻ for mMDSCs and CD14⁻ CD15⁺ for gMDSCs [340].

Casbon *et al.* (2015) observed that in a murine PyMT model of breast cancer, there were significantly more gMDSCs present in several tissues, including mammary gland, lung, blood and spleen when compared to wild-type controls; mMDSC abundance was also significantly increased in blood and spleen relative to controls. However, the abundance of gMDSC compared to mMDSCs was consistently higher in all tissues in PyMT tumour-bearing animals compared to wild-type controls [341]. Subsequently, the study investigated how these gMDSCs may alter the proliferation of effector T-cells. gMDSCs were isolated from spleens of both PyMT tumour-bearing animals and wild-type animals and cultured, separately, with the fluorescent dye carboxyfluorescein diacetate succinimidyl ester (CFSE) labelled splenocytes. As cells proliferate, the CFSE label is excreted, and thus increased cell proliferation should result in reduced CFSE fluorescence. Casbon and colleagues observed that splenocytes cultured with gMDSCs from PyMT tumour-bearing animals had an almost 50% reduction in proliferation in both CD4 and CD8 T-cell populations compared to those cultured with gMDSCs from wild-type animals. Additionally, the splenocytes cultured with wild-type gMDSCs did not exhibit changes in proliferation relative to control splenocytes cultured in the

absence of gMDSCs [341]. This latter result supports the idea that myeloid cells with a cell marker expression profile indicative of MDSCs, specifically gMDSCs in this case, are only immunosuppressive in cancer settings and do not exert immunosuppressive activity in healthy animals. Supporting the observations that MDSC activity is cancer specific.

Although not in the context of solid cancers, observations by Ferrer *et al.* (2021) described a similar role of gMDSCs in chronic lymphocytic leukaemia patients when they observed gMDSC abundances were increased in blood samples relative to healthy patient samples while mMDSCs were not significantly different between patients and healthy controls [342]. The study went on to investigate the efficacy of the immunosuppressive influences of gMDSCs versus mMDSCs, both isolated from the same cancer patient, on autologous T-cell proliferation. The results showed a significant reduction in T-cell proliferation following incubation with gMDSCs while mMDSCs did not alter T-cell proliferation [342]. Additionally, while gMDSCs expressed higher abundances of proteins associated with T-cell stimulations, such as CD80, compared to mMDSCs, they also had a significant increase in the expression of proteins that block T-cell function, namely PD-L1 [342]. Thus, it is likely the immunosuppressive activity of gMDSCs in chronic lymphocytic leukaemia is driven by both their increased abundance as well as the overexpression of co-inhibitory proteins. Together these two studies highlight the cancer-specific immunosuppressive roles of gMDSCs, with the latter study offering a mechanism relating to immune checkpoint involvement. Such insights may lead to future therapeutic targeting of these pro-tumourigenic immune cells, and recent studies have begun to consider methods by which to prevent their recruitment to and inhibit their proliferation in tumour tissues [343].

1.4.1.3 M2 macrophages

The roles of macrophages in tumour progression are some of the most well studied regarding immune cell influences on cancer. However, these roles are indeed complex and can be both anti- and pro-tumourigenic depending on the stage of tumour development [344]. Typically, macrophages of an M1 polarisation state tend to be associated with an anti-tumourigenic influence and are more numerous in and around solid tumours during early stages of tumour development as the tumour battles with an effective immune response to become established [344]. However, as cancer cells overcome the initial immune attack during tumour initiation, cytokine signalling, particularly of IL-4, IL-10 and IL-13, and endogenous antigen presentation promote polarisation of infiltrating macrophages towards an M2 macrophage phenotype [222,345]. This polarisation state exerts immunosuppressive influences on several effector cells, particularly T-cells, encouraging the formation of new blood vessels by angiogenesis and promotes pathways usually associated with

wound-healing, resulting in the remodelling of the surrounding extracellular matrix (ECM), a process which is integral to tumour growth and metastasis [346,347].

Angiogenesis is the process by which new blood vessels are formed [348]. As tumours grow, they require blood vessel formation to supply areas of the tumour with nutrients and oxygen via the blood [348]. Thus, angiogenesis and blood vessel density are integral to tumour growth and survival. Lin *et al.* (2015) described that in tumour sections from breast cancer patients with invasive ductal carcinoma, blood vessel density was positively correlated with the presence of tumour associated macrophages expressing the chemokine CCL18 [349]. To query whether these macrophages were of a M1 or M2 polarization, *in vitro* activation of macrophages with IL-4 to induce an M2 polarisation and subsequent CCL18 production was measured using an enzyme-linked immunosorbent assay (ELISA). Compared to unstimulated macrophages, CCL18 production was significantly increased [349]. Subsequent migration and proliferation assays using human umbilical vascular endothelial cells (HUVEC) in the presence or absence of CCL18 showed that CCL18 significantly increased proliferation and migration of endothelial cells. This was later confirmed *in vivo* using chicken chorioallantoic membrane assays including CCL18 treatments versus controls and demonstrated again that angiogenesis was increased as a result of CCL18 [349]. These findings suggest M2 macrophages increase angiogenesis in breast tumours in a CCL18 dependent manner and as a result promote tumour growth by improving blood flow and nutrient availability to the tumour.

Another process that promotes disease tumour progression and metastasis is the remodelling of the ECM [350]. This is predominantly performed by fibroblasts which produce collagens, MMPs and other matrix components that facilitate tumour expansion and cell motility and migration in the stromal compartments of tumours [351]. However, M2 macrophages are also involved in remodelling of the ECM to promote tumour growth and metastasis [218]. For example, Chen *et al.* (2017) identified that compared to M1 macrophages, M2 macrophages in gastric and breast cancers increased the expression of chitinase 3-like protein 1 (CHI3L1) [352]. Using a glutathione-S-transferase (GST)-pulldown assay to screen the cell surface membrane of breast cancer cell lines that were interacting with CHI3L1, the study identified IL-13 receptor α 2 (IL-13R α 2) as a candidate. Subsequent culture of cancer cells with CHI3L1 and microscopic analysis identified colocalization of CHI3L1 and IL-13R α 2 at the plasma membrane, indicative of binding of CHI3L1 by IL-13R α 2 [352]. This binding was later shown to activate the mitogen activated protein kinase (MAPK) signalling pathway, which has previously been linked to MMP expression [353]. Gene expression analysis of RNA extracts from breast cancer cells (MDA-MB-231 cells) cultured in the presence of CHI3L1 identified the increase in the expression of several MMPs in following CHI3L exposure, including of

MMP-2, -3, -7 and -9 [352]. These MMPs are all involved in ECM remodelling via the cleaving matrix components to facilitate cell motility and migration, which in a tumour setting facilitates expansion and metastasis. Chen and colleagues went on to investigate the effect of CHI3L1 on metastasis in an *in vivo* experiment using MDA-MB-231 cells in mice and observed injections of the protein increased metastatic burden in the lungs of animals compared to vehicle treated controls. Additionally, analysis of sera from patients with breast cancer revealed increased levels of CHI3L1 compared to healthy donors. Together, these results highlight the role of M2-induced matrix remodelling by cancer cells to promote metastasis in breast cancer.

1.4.1.4 Mast cells

Macrophages, MDSCs and T-reg cells are the immune cells most commonly linked to pro-tumour activity. However, the tumour milieu is a complex network of cell types and, increasingly, several other immune cells have been identified as potentially playing pro-tumorigenic roles in addition to the 'usual suspects', mast cells being one such cell type. Although these cells are typically associated with atopic responses and diseases via their IgE-dependent activation by allergenic antigens, they are increasingly being associated with tumour progression and metastasis due to the functional ability they have to promote inflammation, angiogenesis and tissue remodelling [354]. To date, mast cells have been associated with poorer prognosis in melanoma, prostate and pancreatic cancers [355–357]. Tumour cells express an array of proteins which promote immune cell tumour infiltration by chemotaxis. SCF is one of these proteins and binds the c-kit tyrosine kinase receptor with high affinity, a receptor highly expressed in mast cells [354,358]. Using a BALB/c murine model of hepatocarcinoma, Huang *et al.* (2008) injected bone marrow-derived mast cells into the tail vein and demonstrated that mast cell injections increased tumour mass relative to a control [359]. Subsequently, the study found that inhibiting SCF activity via antibody treatments against either SCF or c-kit, after a tail vein injection of mast cells, resulted in a reduced mast cell infiltration in tumours and corresponded with a reduced tumour mass relative to animals that did not receive the an antibody therapy [359]. Additionally, real-time polymerase chain reaction (PCR) and flow cytometric analysis identified that T-reg cell abundance and the abundance of their immunosuppressive and tumour promoting proteins, namely IL-10 and TGF β , were increased relative to controls and that NK cell and effector T-cell activation was reduced [359]. These later observations suggest mast cells play an immunoregulatory role by reducing the anti-tumorigenic activity of cytotoxic immune cells and increasing immunosuppressive functions in T-reg cells.

In a separate study, Saleem *et al.* (2012) later observed that mast cells were integral to the activation of MDSCs and their pro-tumour immunosuppressive influences in a murine model of metastatic melanoma [360]. MDSCs are known to support antiparasitic immunity in mucosal tissues

and are recruited in response to mast cell derived molecular signalling, including the release of IL-17 and 5-lipoxygenase [361,362]. Thus, having observed T-cell impaired responses in metastatic organs, specifically the lungs, resulting from increased activity of MDSC in a transgenic mouse model (A10Tg), the researchers employed a mast cell deficient mouse model (C57 BL/6 Kit^{Wsh/Wsh}) to investigate if adoptive transfer of MDSCs would affect metastatic melanoma lesion formation to the same extent as in wild-type mice. Interestingly, while the transfer indeed increased lesion formation in wild-type C57 BL/6 mice, in the mast cell deficient model the MDSC transfer had no influence on lesion formation [360]. While these results further support the existing evidence of a pro-tumourigenic role of mast cells, the specific mechanism by which this regulation occurs remains to be elucidated. However, even in the absence of a complete mechanism, the results of the two studies described highlight a strong pro-tumourigenic role of mast cells in both these models.

In breast cancers, the roles of mast cells in tumour progression are still under debate. Several studies have linked their presence within mammary tissues and tumours to be a marker of a good prognosis while others observe them to be associated with a poor prognosis; in recent years there has been a shift in consensus towards a more pro-tumourigenic role [357,363]. One of the mast cell-derived factors thought to be linked to breast cancer progression is the release of tryptase, among other proteins, a serine protease involved in immune cell recruitment, angiogenesis and ECM remodelling [364]. Xiang *et al.* (2010) described that histological analysis of tissue sections from breast cancer patients identified increased abundance of tryptase in peri-tumoural tissues compared to normal breast tissue [364]. The same study also observed that increasing concentrations of tryptase, modelled *in vitro* via trans-well migration assays, resulted in increased migration of human MDA-MB-231 breast cancer cells [364]. Additionally, culturing the same cell line in the presence of tryptase increased the cellular production of MMP-2, an MMP with a functional role in ECM remodelling, a process used by tumours to grow and metastasise effectively [365]. He *et al.* (2016) observed that when a Kit^{Wsh/Wsh} mouse was crossed with mouse model of spontaneous breast cancer, mammary tumour virus-polyoma middle tumour-antigen (MMTV-PyMT), tumour growth and metastasis was reduced relative to MMTV-PyMT/Wild-type animals, however primary tumour occurrence was not affected [366]. The same study also described a reduced blood vessel density in mast cell deficient animals relative to controls, suggesting a reduction in tumour associated mast cells resulted in reduced angiogenesis, a biological mechanism integral to tumour success [366]. These studies are suggestive of pro-tumourigenic roles of mast cells in breast cancer but the body of literature in this area is light and further research into their effects on breast cancer is required to understand these roles more completely.

1.4.2 The anti-tumour immune response

The heterogeneity of cancer in its many forms means the understanding of its pathogenesis is ever evolving, including how the immune system influences disease progression. However, the broad understanding of the anti-cancer immune response has mostly remained consistent and largely revolves around the activity of a small number of immune cells with effective mechanisms for targeting and killing cancer cells. These include dendritic cells, macrophages, Th1 cells, cytotoxic T-cells and NK cells.

1.4.2.1 Cytotoxic T-cells and NK cells

While there are several immune cell types involved in the anticancer immune response, cytotoxic T-cells and NK cells are arguably the most effective of these, using a conserved mechanism to specifically target cancer cells without disturbing surrounding healthy cells and tissues [367]. The activation pathways for these cells are different and was outlined in detail in sections 1.3.2.4 and 1.3.3.2. Briefly, Cytotoxic T-cells are activated in an antigen dependent manner involving the recognition of endogenous antigens presented via MHC-I on APCs while NK cells are activated in an antigen independent manner by recognising changes in the expression of specific endogenous activator or inhibitory proteins on the surface of target cells [248,303].

Once activated, both cytotoxic T-cells and NK cells migrate to the tumour via the blood stream and begin exerting their anti-cancer functions. Intracellular vesicles containing perforin and granzymes are delivered from the Golgi apparatus to the part of the plasma membrane in contact with the target cell [368]. Exocytosis of the vesicles releases the cytolytic proteins into the narrow intercellular space, called the immunological synapse, between either of these immune cells and target cancer cells [369]. This targeted and controlled release of the vesicular contents is important as it limits the potential for the cytotoxic proteins to affect surrounding tissue, protecting healthy cells from unsolicited immune attack [370]. The release of perforin molecules forms pores in the plasma membrane of cancer cells and subsequently facilitates the passive movement of granzymes from the immunological synapse through the pores into the cell where they initiate the caspase signalling pathway via the cleaving of several caspase proteins, namely caspase 3, to initiate apoptosis and ultimately cancer cell death [254]. The effective response of NK cells and cytotoxic T-cells, particularly in the early stages of tumour formation, is indicative of a strong anti-cancer response and the abundance of both of these immune cells are considered markers of an improved prognosis in an array of cancers, including colorectal, prostate, ovarian and breast cancers [371–374].

1.4.2.2 *Dendritic cells and macrophages*

As mentioned, the anti-cancer efficacy of cytotoxic T-cells relies on the presentation of antigens by APCs, namely dendritic cells and macrophages [304]. These cells phagocytose and present antigens associated with cancer cells to naïve CD8 T-cells, triggering their activation in an MHC-I dependent manner. Therefore, these innate immune cells have an integral role in regulating anti-cancer immunity. Due to their highly efficient ability to conserve and present antigens, dendritic cells in particular are considered the major drivers of such responses and have even been tested in several trials aiming to produce 'cancer vaccines'. These trials isolate immature dendritic cells from an individual patient, expose them to cancer cell antigens to initiate antigen presentation and then autologously inject them back into the same patient where they present the cancer antigens to effector cells, promoting their activation and priming anti-cancer responses, particularly in CD8 cytotoxic T-cells. One phase II clinical trial undertaken by Wilgenhof *et al.* (2016) combined an immune checkpoint inhibitor against CTLA4, ipilimumab, with synthetic mRNA dendritic cell vaccine and observed an increase in the abundance of several lymphocyte populations, including CD4 and CD8 T-cells, as well as a correlative improvement in overall response to therapy, 38% of 39 patients [375]. However, this was a single armed trial and subsequent studies plan to compare between patients receiving ipilimumab with or without the dendritic cell vaccine. In early results from an ongoing phase III study, a similar administration of tumour antigen activated dendritic cells was administered to patients with glioblastoma receiving an adjuvant standard treatment of care regimen, including radiotherapy and chemotherapy (temozolomide). The administration of the primed dendritic cells alongside standard treatments (223 patients) increased the median overall survival by 8.1 months compared to a cohort of patients that only received the radio- and chemotherapies (99 patients) [376]. These results are promising in terms of extending life, but further work is required to improve complete response to treatments moving forward.

While M2 macrophages are associated with promoting tumour growth, M1 macrophages are known to support anti-tumour responses in several ways, predominantly via anti-cancer effector cell activation and to a lesser extent by direct cytotoxic interaction with cancer cells [377]. Although not as effectively as dendritic cells, M1 macrophages can exert anticancer immunity in much the same way, via MHC-dependent antigen presentation [378]. M1 macrophages are extremely effective phagocytes, breaking down ingested organisms or cells and presenting the isolated antigens on their cell surface via MHC complexes to naïve T-cells, triggering T-cell activation [379,380]. These activation pathways are further supported by the release of several cytokines that polarise T-cell differentiation towards one of the several T-cell subtypes, previously described in section 1.3.3.1. Specifically, M1 macrophages are potent producers of IL-12, a cytokine which drives

polarisation of naïve CD4 T-cells towards a pro-inflammatory anti-tumourigenic Th1 T-helper cell subtype. Subsequently, Th1 cells produce IFN γ , a cytokine integral to the activation and function of M1 macrophages and promotes M1 macrophage cytotoxic anti-cancer activity in tumours [377,381,382].

As described in section 1.3.2.2, macrophages identify invading pathogens by a series of proteins on the surfaces of target organisms. In addition to pathogen derived proteins, macrophages are capable of recognising a number of host derived surface proteins, including Tn antigen and carcinoembryonic antigen, which are expressed in increased abundance by tumour cells [377,383]. When M1 macrophages recognise these proteins via their highly conserved PRRs, they can induce phagocytosis pathways as described previously, but they can also directly secrete NO, and other ROS, which is produced during NOS2 dependent arginine metabolism [344,384]. The secretion of these molecules, as well as the simultaneous production of TNF α , is cytotoxic to surrounding cells, however, can reduce the proliferation of cancer cells it comes into contact, supporting other anti-tumour effector cells in inhibiting tumour growth and killing cancer cells [385].

1.4.3 Immune evasion and Immunotherapies

There have been several proteins identified which influence how the immune system interacts with cancer. These proteins are often referred to as immune checkpoints as they function to regulate immune responses to promote tissue homeostasis, often to reduce inflammation and repair damaged tissues [386]. However, in several cancers, the expression of these immune checkpoints can act to promote tumourigenesis by down regulating the anti-cancer immune activity, specifically cytotoxic T-cells [386]. Effectively, the action of these proteins could be compared to putting a 'break' on the immune response to slow its activity and facilitate cell proliferation, wound healing and, in the context of cancer, tumour growth. Of the identified immune checkpoints, the two which have received much attention in recent years as potential therapeutic targets are CTLA4 and the programmed death 1 / programmed death ligand 1 (PD-1/PD-L1) proteins.

The role of CTLA4 in regulating immune homeostasis was introduced in section 1.3.3.1. Briefly, this protein is expressed on the surface of T-cells and acts as an inhibitor of activation during interactions between naïve T-cells and APCs [294]. Specifically, when CTLA4 expression is increased, it out competes CD28, a co-stimulatory protein, in the binding of CD80/86 on the surface of dendritic cells and inhibits intracellular signalling that would otherwise activate naïve T-cells. While this is an important function in preventing over activation of T-cells which may lead to autoimmune conditions, in the context of cancer this mechanism often facilitates immune evasion and tumour outgrowth by reducing the numbers of active cytotoxic T-cells able to target tumour cells [387].

Figure 1.4.3.1 outlines these interactions and how CTLA4 expression alters the ability of CD8 T-cells to target cancer cells.

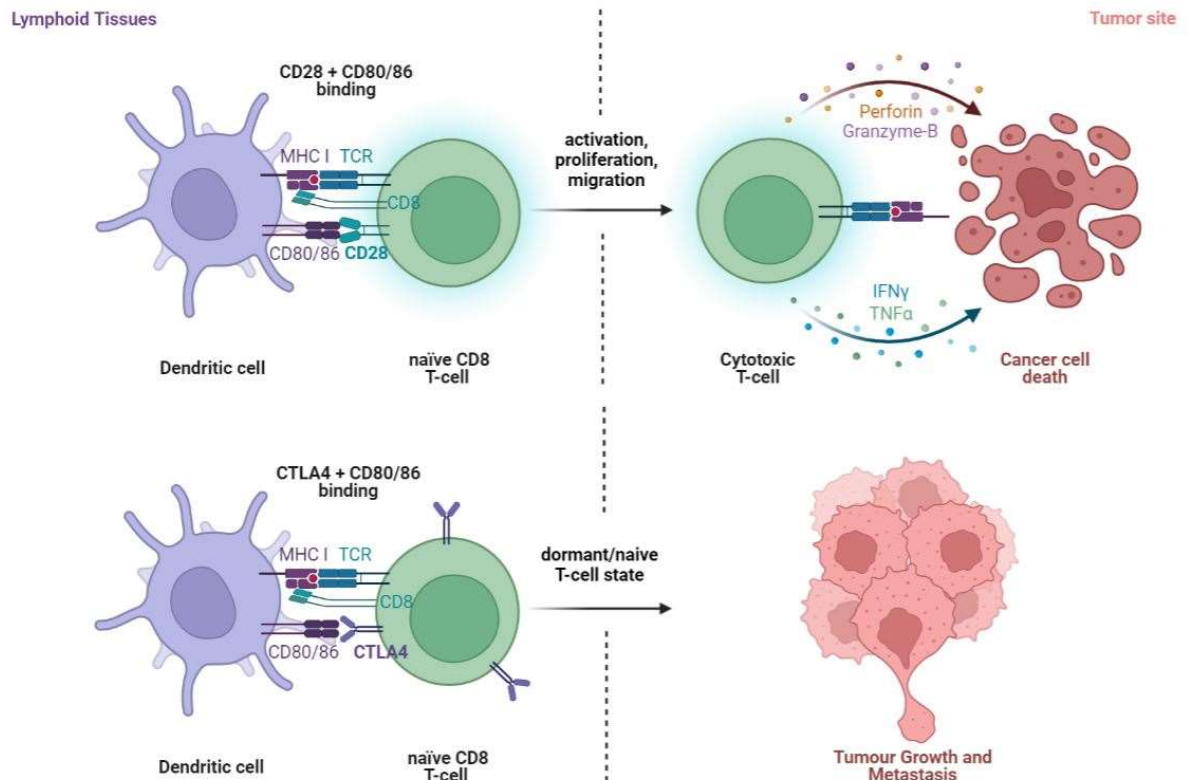


Figure 1.4.3.1. The influence of CTLA4 on CD8 T-cell activation and anti-cancer function. Cartoon schematic depicting typical activation of naïve CD8 T-cells to cytotoxic T-cells via co stimulatory interactions of T-cell CD28 with CD80/86 on the surface of APCs, promoting anti-cancer activity (top), and the inhibition of this pathway by CTLA4 binding CD80/86 in place of CD28, facilitating tumour growth (bottom). Adapted from “T Cell Activation in Cancer”, by Biorender.com (2022). Retrieved from <https://app.biorender.com/biorender-templates>.

While CTLA4-dependent immune evasion occurs by preventing activation of naïve T-cells during the immune priming stage, where innate immune cells interact with naïve adaptive immune cells, the PD-1/PD-L1 mechanism occurs directly between effector cells, including cytotoxic T-cells and NK cells, and tumour cells [388]. The role of this interaction, like CTLA4, is to regulate immune responses and promote immune homeostasis during periods of inflammation [388]. However, as described for CTLA4, in the context of cancer this pathway can act to facilitate immune evasion and tumour growth [389]. Specifically, when effector T-cells expressing the PD-1 receptor on their cell surface engage a cell expressing PD-L1 it promotes signalling pathways that act to inhibit effector cell activity and reduce their proliferation [388]. This again aids tumour cells in the evasion of cytotoxic anti-cancer activity and facilitates their growth and metastasis. Figure 1.4.3.2 outlines the effects of PD-1/PD-L1 interactions on cancer cell survival.

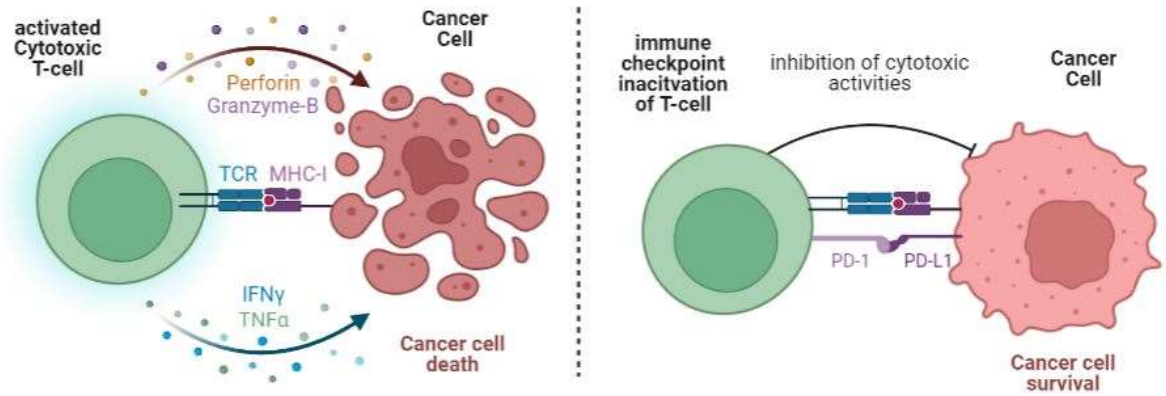


Figure 1.4.3.2. The influence of PD-1/PD-L1 on effector cell function and anti-cancer activity. Cartoon schematic depicting typical anti-cancer activity of cytotoxic T-cells following endogenous antigen recognitions via TCR to MHC-I protein complex (left) and the effect of PD-1/PD-L1 binding on inhibiting this activity to facilitate cancer cell survival and tumour growth (right). Adapted from “T Cell Activation in Cancer”, by Biorender.com (2022). Retrieved from <https://app.biorender.com/biorender-templates>.

Although these immune checkpoint mechanisms benefit the survival and growth of tumours, they also pose a significant therapeutic target. By inhibiting the function of these checkpoint inhibitor proteins with monoclonal antibodies the ‘break’ is released and the immune system is enabled to pursue typical activation pathways, resulting in the targeting and killing of cancer cells. There is currently an ongoing expansion in the number of treatments that aim to support anti-cancer immune activity, but those targeting the two pathways discussed above appear to be the most effective to date [390]. A pioneering study by Leach *et al.* (1996) used antibodies against CTLA4 to study the effects of CTLA4 inhibition on the growth of a syngeneic murine colon carcinoma in BALB/c mice. The study identified a marked reduction in tumour growth following treatment with anti-CTLA4 antibodies compared to both an untreated cohort as well as a cohort of mice treated with anti-CD28 antibodies [391]. A subsequent human study tested an anti-CTLA4 monoclonal antibody, branded ipilimumab, in combination with a melanoma-specific immune-boosting vaccine, called gp100, against late stage melanoma and described promising results [392]. The study recruited 676 patients with unresectable stage III or IV melanoma and divided them into one of three arms: ipilimumab with gp100 treatment (403 patients), ipilimumab alone (137 patients) or gp100 only treatment (136 patients). In comparison to the gp100 only treatment, overall survival increased by 3.6 months in the combined therapy group and by 3.7 months in the ipilimumab only cohort [392]. In 2011, ipilimumab became the first checkpoint inhibitor immune therapy to be approved by the Food and Drug Administration (FDA) in the US and has since been employed in the treatment of several other cancers including renal and lung cancers [393,394].

While such results are promising, it is desirable to extend overall survival beyond the three months observed in this study. Fortunately, antibody therapies targeting the PD-1/PD-L1 immune checkpoint proteins have improved patient outcomes and generally seem to prolong patient survival more effectively than CTLA4 therapies alone [393]. Of these, nivolumab, a monoclonal antibody against PD-1, has shown most promise. Larkin *et al.* (2015) carried out a phase III clinical trial to investigate the differences in treatment efficacy of both ipilimumab and nivolumab [395]. The study divided 945 patients, with stage III or IV metastatic melanoma, equally into one of three treatment cohorts due to receive either ipilimumab, nivolumab or a combination of the two. The cohort that received ipilimumab alone (anti-CTLA4) had a median disease-free progression of 2.9 months while the nivolumab (anti-PD-1) cohort had a median disease-free progression of 6.9 months, an improvement of four months compared to the anti-CTLA4 treatment [395]. Moreover, the combination of the two resulted in an even greater improvement of 11.5 months median disease-free survival, showing that by preventing binding of immune checkpoint proteins to their ligands during both the 'priming phase' and 'effector phase' of immune evasion, the anti-cancer activity of the patients' own immune cells was significantly stronger when targeting both stages simultaneously. Figure 1.4.3.3 illustrates how each antibody therapy facilitates the priming and effector function of T-cells in this context.

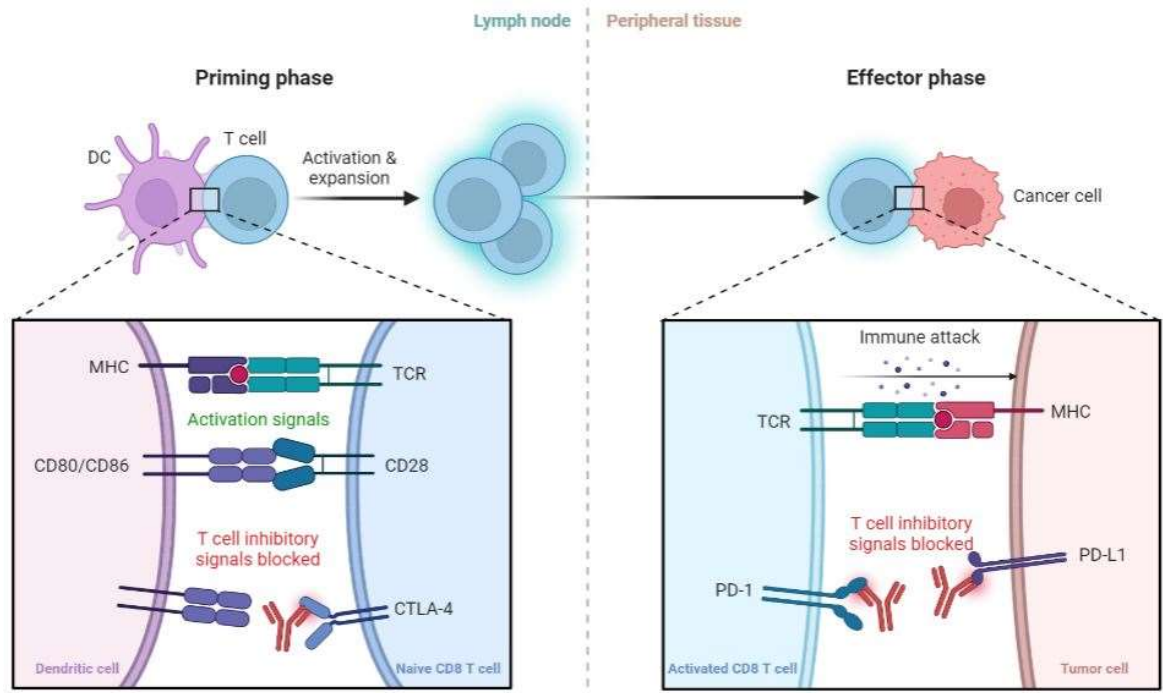


Figure 1.4.3.3. Immune checkpoint inhibitors facilitate T-cell activation and effector activity to promote anti-cancer immunity. During the 'priming phase' (left), monoclonal antibodies against CTLA4 inhibit immunosuppressive function of the protein and allow for costimulatory binding of CD28 with CD80/86 and subsequent activation of naive T-cells. During the 'effector phase' (right), anti-PD-1 and/or anti-PD-L1 monoclonal antibodies inhibit the binding of these two immune checkpoint proteins and thus prevent pro-apoptotic signalling in the activated T-cell, allowing for the T-cell to carry out its cytotoxic function against the cancer cell. Reprinted from "Blockade of CTLA-4 or PD-1 Signalling in Tumour Immunotherapy", by BioRender.com (2022). Retrieved from <https://app.biorender.com/biorender-templatesn>

Although the immune system exerts some influence on almost all solid tumours, tumour immunogenicity is extremely variable between cancer types and subtypes, and thus there is no one-size-fits-all approach to targeting immunogenicity as a potential therapeutic target [323]. Breast cancer, for example, comprises several molecular subtypes and most of these, predominantly ER-positive tumours, are not generally considered to be immunogenic [396,397]. However, in some TNBC tumours, a subtype often associated with poor prognoses due to difficulty in treating it with traditional anti-cancer therapeutics, PD-L1 expression appears to be increased; an indicative target for immunotherapy [398].

So far none of the treatments described are capable of curing late-stage breast cancer. However, there is constant research focussing on therapies which are most effective at reducing metastatic outgrowth and prolonging life while maintaining a high quality of life for patients with breast cancer. As discussed, TNBC is the most difficult of the subtypes to treat due to treatments against hormone receptors or HER2 proteins being ineffective. Fortunately, recent advances in immunotherapies for breast cancer may be improving prognoses for patients with TNBC [399].

Breast cancer is not generally considered a highly immunogenic cancer. One reason is due to the lower expression of MHC I in hormone receptor positive and HER2 enriched breast cancers which results in a reduced presentation of cancer specific antigens and thus poorer activation of effector T-cells [397]. Additionally, the production of oestrogen is associated with the polarising of T-helper cells to an immunosuppressive Th2 state rather than an inflammatory Th1 state, resulting in reduced effector function and subsequent activation of other anticancer immune cells [397]. However, TNBC tumours, in comparison to receptor positive sub-types, are generally more immunogenic and often exhibit enrichment of tumour infiltrating lymphocytes [400]. Additionally, in some TNBC patients the expression of PD-L1 in tumour tissues is increased, offering a potential immunotherapeutic target [398]. Recently, Schmid *et al.* (2020) described that the combination of neoadjuvant chemotherapy with the checkpoint inhibitor pembrolizumab, an anti-PD-1 therapy, improved pathological complete response by 13.6% compared to a cohort of patients that received neoadjuvant treatment only [401]. Thus, while current treatment pathways for breast cancer do not typically employ immunotherapies, emerging evidence is suggesting they may support traditional therapies to improve treatment outcomes in some cases.

1.5 The Gut Microbiota

The 'average' person comprises ~30 trillion human cells [402]. The human GI tract is home to a population of ~38 trillion microbial organisms, comprising several thousand species, meaning there are more microbes in the GI tract than there are cells in the human body [402]. While these organisms encompass several classes of microbes, including viruses and fungi, bacteria are widely considered to have the most influential roles in human health [403]. Thus, for the purposes of the research presented here, the term 'microbiota' will refer to the bacterial populations inhabiting the gut and will encompass the functional elements of the microbiome.

Under homeostatic conditions, the microbiota exist as a symbiotic community in mutualism with its host. The benefits it infers include aiding in the metabolism of food and drug components as well as preventing bacterial infection through various competition based mechanisms with pathobiont and pathogenic bacteria [404,405]. However, the capacity of the microbiota to educate and prime the immune system to fight disease is arguably one of its most influential roles in supporting host health [406]. Unfortunately, picking apart the specific bacterial candidates responsible for this education as well as the mechanisms involved is extremely challenging due to the high fluidity of the microbiota's composition and the difficulty in linking local events to systemic changes respectively [407].

1.5.1 Establishment

The environment within the womb during foetal development is typically considered to be sterile, meaning it is free from the presence of microorganisms [408]. Recently, this concept has been challenged following the isolation of several microbial organisms, or their DNA, from *in utero* tissue samples including placenta, umbilical blood and amniotic sack fluid [408–410]. Thus, it is likely that the infant microbiota begins its development *in utero* [411]. However, the literature widely agrees that it is the vertical transmission from mother to infant via exposure to microbes during birthing which plays an essential role in shaping the infant microbiota and aligning its further development to one associated with a variety of beneficial health outcomes [412–414].

During vaginal birth, the initial colonisation of facultative anaerobic bacteria, transmitted via the vaginal canal, promotes the colonisation of strict anaerobes which begin to shape the early life microbiota [414]. The major genera associated with early-life microbial profiles are *Bifidobacterium*, *Bacteroides* and *Clostridium* [414,415]. Of these species, *Bifidobacterium* spp. are the most dominant and are particularly important for their ability to metabolise the oligosaccharides present in milk [416–418]. As infants grow and begin to eat solid foods, new bacterial species are introduced to the gut, increasing species diversity and shaping a more mature

microbial profile [419]. The neonatal microbiota is characterised by a relatively low biodiversity in comparison to one of an adult and their composition is known to fluctuate as they are regularly exposed to new microbes [420]. These fluctuations reduce over time and between three and five years of age the microbiota matures and resembles more closely an adult's microbiota profile, although there is still relative fluidity in its composition [416].

Several factors associated with birth are able to exert influence over the colonisation of microbial communities and influence early homeostasis within the gut. These include birthing method, a mother's age and exposure to antibiotics [411,414]. For example, babies born via caesarean section, as opposed to via the vaginal canal, have increased abundances of bacteria from the genus *Staphylococcus* as well as a reduced overall gut microbial load, while those born through the vaginal canal are colonised by lactic acid producers, such as *Lactobacillus* sp. [421,422]. Additionally, babies subject to antibiotic treatment in the first week of life exhibit lower diversity of Bacteroidetes species and delayed Bacteroidetes colonisation, a pattern linked to the presentation of atopic diseases and type I diabetes in later stages of life [423]. Differences such as these can mean babies born via caesarean are more susceptible to developing chronic inflammatory conditions such as asthma, eczema and other atopies compared to those born via the vaginal canal [424–426]. These cases demonstrate the importance of supporting the appropriate development of the gut ecosystem during the first few years of an infant's life and how exposure to microbes should not always be considered unhealthy.

1.5.2 Composition and equilibrium

No two people share the same microbiota profile, and it is often compared to that of one's fingerprint due to its uniqueness. Thus, it is not possible to define exactly what the composition of a microbiota should be in order to deem it "healthy". However, the consensus amongst scientists and clinicians alike is that diversity is key [427,428]. The parameters that govern diversity are defined by ecologists as a balance between the species richness and species evenness of a given biological community [429]. Richness refers to the number of different species that participate within a community while evenness considers the number of individuals within a particular species present in the same community [430,431]. Therefore, while an individual's microbiota may consist of many different types of bacteria, if the abundances of respective species are not in ratios that promote homeostasis, the risk of infection and development of disease is greatly increased. Likewise, if there is a suitable abundance of bacteria but that abundance is comprised of few health-promoting species this can also compromise homeostasis. Hence, the understanding of how these two components both effect diversity, and ultimately gut health, is incredibly important.

A common marker of change in gut homeostasis is a shift in the abundance of two dominant microbiota phyla, Firmicutes and Bacteroidetes, which together contribute up to 80% of the total taxonomic profile at a phyla level [432,433]. Often, the abundance of one of these phyla will increase while the other conversely decreases. These shifts define the Firmicutes to Bacteroidetes ratio (F/B ratio) which has been linked to several health implications. Namely, an increased F/B ratio is often associated with obesity while a reduction in the F/B ratio is associated with promoting inflammatory disorders such as inflammatory bowel disease (IBD) [434–436].

There are many factors that contribute to the composition, and ultimately function, of the host microbiota. Diet is thought to be the most influential of these [437,438]. The saying “you are what you eat” somewhat describes the dietary influence on the microbiota because what the host consumes determines which microbes thrive within the gut, and ultimately the metabolites they produce in return. Thus, what one eats may be considered a filter for whom one ‘houses’. Changes in diet are therefore capable of changing the profile of the microbiota. Fortunately, the microbiota is fluid and manages temporary shifts readily by promoting metabolic and immunologic activities that allow its profile to return to a state of homeostasis over relatively short periods of time [437,439]. However, persistent perturbations of the gut can result in long term disturbances to the equilibrium within the microbial communities and ultimately promote infection and inflammation, causing and driving disease [440].

The discovery of penicillin by Sir Alexander Fleming in 1928 paved the way for discovery and development of an array of antimicrobial compounds which have been incomprehensively beneficial to modern medicine and undoubtedly saved millions of lives. These drugs were so successful in treating otherwise deadly bacterial infections, that in 1967 the US Surgeon General at the time, Dr William H. Stewart, was believed to have suggested that the advent and development of antibiotic drugs had largely “closed the book on infectious diseases” [441]. Unfortunately, by the early 1990’s this widely popular consensus began to falter and the rapid increase in antibiotic-resistant bacterial pathogens in the early 2000’s raised widespread concern over how antibiotics were being prescribed [442]. Sadly, although clinical understanding of how and when antibiotics should be used is much improved, public perception regarding antibiotic usage has largely remained poor since the issue of antibiotic resistance was first raised [443,444]. However, antibiotic resistance is not the only concern regarding the use of antibiotics. Research over the past two decades has increasingly identified the important role of the microbiota in regulating host health. Part of this body of research has also begun to highlight the risks antibiotics pose to the composition and, ultimately, the function of the gut microbiota and the resulting effects these have on host health [25].

Antibiotics encompass an array of drugs prescribed to prevent or treat a bacterial infection and can be broad or narrow regarding the spectrum of bacterial species they target. These drugs can dramatically disturb the equilibrium of the microbiota and are known to promote several inflammatory conditions, both local to the gut and at sites distant from it, particularly when used repeatedly or over prolonged periods of time [440,445,446]. This is in part due to the dramatic loss of bacterial diversity that follows antibiotic administration. The severity of the loss is dependent on the type of antibiotics used, the length of the treatment regimen and the regularity of exposure to them [447–449]. Broad spectrum antibiotics target a greater number of bacterial species and are often able to kill both gram-positive bacteria, or those encased by a peptidoglycan layer, and gram-negative, those species without a peptidoglycan layer [450,451]. Narrow spectrum antibiotics effect fewer species and are often used to target a particular bacterial pathogen known to cause the infection [452–454]. An example of this is fidaxomicin, a narrow spectrum antibiotic used to selectively target *Clostridium difficile*, a pathogenic bacteria which causes severe diarrhoea that can be fatal without treatment [455,456]. Prior to the discovery of this drug, vancomycin, a strong broad-spectrum antibiotic, was used to treat such infections and caused major reductions in diversity of microbiota [457]. Fidaxomicin, relative to vancomycin, significantly reduces the effects of treatment on the diversity of the gut microbiota and facilitates and improves rate of recovery as well as reducing the incidence of recurrence [455,456].

1.5.3 Functional influences that benefit the host

The composition and diversity of the microbiota dictates how well it is able to serve its host in terms of its functional outputs. These functions include protection from pathogens, carbohydrate and protein metabolism, regulation of the gut-epithelial barrier and immune education [458–460].

1.5.3.1 Protection from pathogens

Our microbiota is regularly exposed to an array of potentially pathogenic bacteria. Even some of the resident species of the microbiota have the potential to act pathogenically should the equilibrium within the gut be disturbed, these species are known as pathobionts [461–463]. Fortunately, under normal homeostatic conditions our microbiota is equipped to manage these potential threats through several mechanisms [440]. As in any ecosystem, particularly in ones as densely populated as the gut, there is constant competition to occupy the available ecological niches [440,464]. Thus, one method by which pathogens and pathobionts are prevented from colonising the intestinal barrier is by the sheer numbers of mutualistic and commensal species occupying space and consuming available nutrients, inhibiting pathogens and pathobionts from doing so, causing their death and passage through the gut without causing infection [465]. Another protective action of the microbiota is the production of antimicrobial products by many symbiotic

species [466]. The production of proteinaceous toxins, called bacteriocins, facilitate the deliberate killing of neighbouring bacteria to prevent them from colonizing the epithelium and occupying a competitive niche [467]. As an example, Corr *et al.* (2007) demonstrated that administrating the probiotic species *Lactobacillus salivarius* inhibited colonisation and infection of the food-borne pathogenic bacteria *Listeria monocytogenes* in mice [468]. However, mice supplemented with a stable mutant of the same *L. salivarius* strain, which did not produce bacteriocins, did not inhibit *L. monocytogenes* from infecting the host mice. Additionally, mice exposed to a strain of *L. monocytogenes* expressing an immunity gene against the bacteriocin produced by *L. salivarius* were not inhibited from colonising and infecting their murine hosts, confirming the involvement of the bacteriocins in preventing pathogen infection [468].

1.5.3.2 Protein and carbohydrate metabolism

Dietary fibre comprises several biomolecules including complex carbohydrates or polysaccharides which the host digestive system is incapable of digesting on its own [469]. The microbiota facilitates fermentation of these macromolecular fibres, as well as proteins and peptides, via anaerobic enzymatic catabolism involving a series of redox reactions to generate adenosine triphosphate (ATP), the primary energy unit used in both pro- and eukaryotes, via substrate-level phosphorylation [470]. In addition to ATP, this process also produces several biproducts which are beneficial to host metabolism and other cellular processes, short-chain fatty acids (SCFA) arguably being the most beneficial of these [471].

SCFAs are organic monocarboxylic acids and are a product of anaerobic fermentation of both complex carbohydrates and amino acids, although the latter account for only 1% of SCFA production [472]. Acetate, propionate and butyrate are the three most abundantly produced SCFAs during anaerobic fermentation and are usually present in a percentage ratio of 60:20:20 respectively [473]. Although produced in abundance in the gut, only a small fraction of microbiota-derived SCFAs enter systemic circulation [472]. The majority of SCFAs are themselves metabolised by the epithelial colonocytes that line and form the colon while a small minority passage into circulation where they disperse to a variety of tissues and organs. One of these organs includes the liver where propionate and butyrate have been shown to influence several metabolic pathways including glucose synthesis via the gluconeogenesis pathway as well as improving responses to insulin and reducing liver steatosis [474,475]. One study by Besten *et al.* (2013) infused mice caeca with a propionate isotope ($2\text{-}^{13}\text{C}$ propionate) and observed that 62% of the SCFA isotope was used as a gluconeogenic substrate to produce glucose and that 69% of total glucose production was attributed to propionate metabolism within the gluconeogenesis pathway [476]. Similarly, Mollica *et al.* (2017) observed that in obese mice, butyrate supplementation improved respiratory capacity,

fatty acid oxidation and the activation of the adenosine monophosphate activated protein kinase (AMPK) pathway, which is involved in regulating cell growth and autophagy, in the mitochondria of hepatocytes [477]. These mitochondrial activities subsequently resulted in improved insulin sensitivity, reduced steatosis and improved glucose metabolism in the liver [477]. In support of these findings, Vrieze *et al.* (2012) previously described that in humans the transferring of microbiota samples from lean donors to patients with metabolic syndromes was correlated with improved insulin sensitivity in those patients six weeks after the transfer [478]. Additionally, the same study observed that at the six-week timepoint post transfer, patients had increased abundances of butyrate producing bacteria in both faecal samples, including a 2.5-fold increase in *Roseburia intestinalis*, and the small intestine mucosa in comparison to samples from the same patients taken prior to the transfer [478]. These are just a few examples of many studies providing evidence of the beneficial effects bacterial-derived SCFAs offer their hosts.

1.5.3.3 Regulation of the intestinal barrier

The luminal contents of the gut are separated from the host circulatory system and local tissues by the intestinal barrier. This barrier is comprised of a mucus layer, a layer of columnar epithelial cells and the lamina propria, a layer of connective tissues that supports blood and lymph vessels as well as housing an array of resident immune cells, from both the innate and adaptive immune compartments [479–481]. The major function of the intestinal barrier is to facilitate the absorption of nutrients from the lumen into the host circulatory system whilst at the same time preventing pathogens, and their pathogenic products, from passing across the barrier into circulation where they may otherwise cause ill health [482,483]. When in a state of homeostasis, the microbiota and intestinal barrier support one another's functional activities. The regulation of these functions is facilitated by a bi-directional crosstalk that takes place between gut microbes and the host cells comprising the barrier [484]. The recognition of microbial associated molecular patterns, such as PAMPs, on the surface of microbes, including LPS and peptidoglycans, by PRRs on the surface of host cells, triggers the release of signalling molecules which promote intercellular junction integrity and production of mucus to sustain defences against pathogens [482,485]. However, when the microbiota is perturbed, these signals become dysregulated and barrier integrity can become compromised, leading to a 'leaky gut', allowing for the passage of microbes across the gut epithelium where they colonise the lamina propria and/or enter circulation, causing infection and inflammation [485,486]. In addition to direct interactions between PAMPs and PRRs, indirect interactions via commensal metabolites, particularly the SCFA butyrate, also promote intestinal barrier integrity by binding G-protein coupled receptors (GPCRs) on the surface of colonic crypt cells, in turn promoting gene activation via transcription factor Kruppel-like factor (KLF) 4 (KLF4)

and cell differentiation to mucin-producing goblet cells [487]. Thus, supporting the production of the mucous membrane and preventing pathogens from penetrating the epithelial layer of the barrier.

1.5.3.4 Immune education

Arguably, one of the most important roles of the microbiota is its ability to regulate host immune homeostasis. The intestinal barrier acts as a bidirectional communication line between these populations of microbes and immune cells. In particular, the lamina propria acts as a site in which various immune cells can interact both with bacterial antigens and each other to prime immune responses that promote homeostasis within the gut and reduce inflammatory responses both local to and at sites distant from the gut and gut microbiota [488].

In section 1.3.3.1, the immunosuppressive role of T-reg cells was introduced. The function of these cells has been observed to be integral to maintaining immune homeostasis and preventing over stimulation effector immune cell populations within intestinal barrier. Several studies have described their importance in this context and identify specific activation patterns of colonic T-reg cells as being important in their regulation of immune activity. For example, using a TCR transgenic mouse model, which was reactive to bacterial flagellin proteins on the surface of commensal bacterial species, Cong *et al.* (2009) described the role of intestinal-specific T-reg mediated IgA antibody production to prevent the mucosal uptake of microbiota-derived flagellin, in turn reducing activation of proinflammatory effector cells at the gut intestinal barrier [489]. Later, Lathrop *et al.* (2011) compared the TCR repertoire of T-reg cells in the lamina propria versus those at a peripheral level and identified an improved specificity for microbiota-derived antigens in TCRs on the surface of colonic T-reg cells compared to peripheral T-reg cells [490]. A subsequent adoptive transfer study identified that naïve T-cells, which were transduced with these colon-specific TCRs prior to T-reg differentiation, resulted in polarization of naïve T-cells to effector T-cells and subsequently inflammation and colitis in the murine colon [490]. These results suggest that post-thymic education of differentiated immunosuppressive T-reg cells in the colon was integral to the prevention of potential inflammation caused by uneducated naïve T-cells, expressing the same TCRs, from differentiating into proinflammatory effector T-cells [490]. Together these studies demonstrate how a bidirectional cross talk between the microbiota and immunosuppressive T-reg cells, in combination with IgA producing plasma cells, act to maintain gut homeostasis and support mutualism between the host and the microbiota.

The role of microbiota derived SCFAs in regulating carbohydrate metabolism was briefly mentioned above. However, SCFAs exhibit immune regulation functionality through their ability to bind GPCRs

on the surface of the gut epithelium and immune cells in the lamina propria. Although produced in least abundance, butyrate seems to be the most influential regarding its beneficial effects on host health [491]. These beneficial interactions include the activation of certain GPCRs, such as GPR41 on epithelial cells and GPR43 in leukocytes, which trigger intracellular signalling that reduces the expression of several pro-inflammatory cyto- and chemokines, including IL-1 and TNF α , and promoting expression of the GPR109A GPCR receptor which activates the immunosuppressive activity of T-reg cells and other IL-10 expressing T-cells [487,492,493]. In addition to regulating adaptive immunity, butyrate has been shown to influence several innate immune cells to the benefit of the host. As described in section 1.3.2.1, neutrophils are integral members of the phagocytic system but also produce several proinflammatory cytokines associated with colitis and promotion of inflammatory diseases both in the gut and at sites distant from it [487]. Hazem *et al.* (2018) demonstrated that in an inducible mouse model of hepatitis, via concanavalin-A treatment, butyrate supplementation, specifically β -hydroxybutyrate, resulted in the reduction of neutrophil and monocyte derived proinflammatory cytokines, namely TNF α , IL-6 and IL-12 [494]. Furthermore, using an knockout mouse model of the butyrate target GPCR receptor GPR43, Pan *et al.* (2018) identified GPR43 on the surface of neutrophils as the mediator for reducing the production of the proinflammatory cytokine in the presence of butyrate, further supporting the role of this SCFA in mediating inflammatory immune activity [495]. Finally, monocytes and macrophages are perhaps two of the most influential innate immune cells involved in regulating inflammation based on the combination of their relatively prolonged lifespan, the efficiency of their phagocytic activity, the array of their key cytokine products upon activation and their ability to present antigens to the adaptive immune compartment to trigger effector cell activity [496].

Thus, one might argue that the influence of butyrate in regulating macrophage activation and function is its most important role in promoting host immune homeostasis. There are several ways in which it is capable of doing so and include indirect and direct mechanisms. As described above, butyrate promotes T-reg cell activation and production of IL-10 and other anti-inflammatory signalling molecules. In section 1.3.2.2, IL-10 was described as a key regulator of polarizing macrophages towards an M2 phenotype with anti-inflammatory functions including a reduction in cytotoxic activity of cytotoxic T-cells as well as promoting tissue repair and matrix remodelling [227]. However, butyrate can also act directly on macrophages through their function as histone deacetylase inhibitors (HDACi). This characteristic of butyrate applies to an array of largely beneficial functions involving multiple cell types and biological pathways and will be discussed as part of several topics within this thesis. However, in the context of its HDACi activity in macrophages, butyrate prevents the deacetylation of histones in the nucleus and thus alters

transcriptional activity resulting in downregulation of the expression of several genes, including that of the transcription factors nuclear factor κ B (NF- κ B) and STAT1 [487,497]. NF- κ B has been shown to be a key regulator of cytokine gene transcription in macrophages, including of proinflammatory TNF α and IL-6, while STAT1 has been shown to promote proinflammatory phenotypes seen in M1 polarised macrophages, as well as of Th1 effector T-cells, including the production of the intraphagosomal cytolytic product NO [498,499]. Thus the inhibition of these proteins through HDACi activity reduces macrophage dependent inflammatory pathways and supports the maintenance of host homeostasis [487].

1.5.4 Influence on disease

Section 1.5.3 outlines various functions of the commensal microbiota which are beneficial to their host; the importance of maintaining gut homeostasis is paramount. However, there are various intrinsic and extrinsic factors that can have deleterious effects on the composition and function of the gut microbiota, ultimately influencing its ability to support its host and potentially even become pathogenic or drive inflammatory pathologies.

While the gut microbiota is a relatively fluid and adaptive community, capable of coping with compositional shifts resulting from temporary/transient changes in extrinsic factors, such as nutrient availability or drug exposure, prolonged alterations to such factors can result in severe perturbations which carry the potential to cause long-term disruption of gut homeostasis, inducing a state coined 'dysbiosis' [445,500,501]. When in a state of dysbiosis, the body is at an increased risk of both local and systemic disease, often resulting from the amplification of pathobionts [502–504]. In addition, the resulting breakdown in communication between the microbiota and the immune system interrupts immune education, leading to local and systemic inflammation [502]. Fortunately, short-term changes in nutrient availability or exposure to medications, including short and necessary courses of antibiotics, generally result in temporary dysbiosis which is almost always reversible and exhibits only mild symptoms, such as diarrhoea or constipation, which are generally fully alleviated when gut homeostasis returns, usually a matter of weeks after the said extrinsic change [502]. However, as described in section 1.5.2, research broadly agrees that the use of antibiotics, particularly for prolonged or repetitive treatment courses, poses one of the greatest risks to the gut microbiota and the induction of severe gut dysbiosis [440,445,446,501]. Specifically, prolonged period of dysbiosis are known to promote the pathogenesis of inflammatory conditions, two of the most common are irritable bowel syndrome (IBS) and IBD [405,505]. There are several similarities regarding the symptoms of these two conditions, namely fluctuations between diarrhoea and constipation, abdominal pain and increased flatulence [506]. However, these are distinct and separate conditions. The major difference being that IBD is associated with chronic

inflammation of the lower GI-tract, particularly in the number of intraepithelial lymphocytes, while in IBS patients often don't present with any inflammation and their intestines generally appear healthy after investigation via colonoscopy [506]. Unfortunately, IBD also carries an increased risk of developing colon cancer while IBS does not carry such a risk, likely due to the differences in inflammation between the two [506].

Ulcerative colitis and Crohn's disease, the two most prevalent forms of IBD, are thought to be caused by the dysregulation of the immune response to microbes at the intestinal barrier [507,508]. Patients suffering these conditions generally present with altered bacterial composition compared to healthy individuals; whether these differences are causative or correlative remains unclear [507][509]. Several studies have found the use of antibiotics during childhood increases the likelihood of developing Crohn's disease later in life [509–511]. Such observations highlight the importance of the microbiota in educating the immune system to appropriately respond to challenges by commensal bacterial species during infancy and childhood so as to avoid the development of pathologies later in life [511]. In addition, the novel use of probiotics in combination with traditional treatments has shown some potential in alleviating symptoms of IBD and IBS [512–514]. Zaylaa *et al.* (2018) identified that the administration of several strains of *Bifidobacterium* and *Lactobacillus* bacterial species to a mouse model of colitis, 2,4,6-trinitrobenzene sulfonic acid (TNBS)-induced, resulted in reduced inflammation [512]. Additionally, the supplementation of *Bifidobacterium infantis* strain 35642 has been shown in multiple blinded randomized studies to alleviate symptoms of IBS in human patient cohorts [515,516]. IBS patients often present with an abnormal ratio of IL-10/IL-12 cytokine production in comparison to healthy subjects [517,518]. Often IL-12 is elevated promoting proinflammatory Th1 effector cell activity while IL-10 is reduced resulting in a reduction in the immunosuppressive activity of T-regs and polarisation of macrophages to an inflammatory M1 phenotype [518]. Thus, when O'Mahony *et al.* (2005) identified that the alleviation of IBS symptoms in patients following supplementation of *B. infantis* 35642 was linked to the rescue of an abnormal proinflammatory IL-10/IL-12 ratio, they supported the notion of beneficial bacteria being capable of regulating immune and microbial homeostasis to treat disease and support host health [518]. Together, results such as these highlight the important roles microbes play in regulating gut inflammation as well as presenting evidence of their potential in supporting treatment of disease.

While diseases local to the gut have historically received more attention than those of a systemic nature, there is now a growing body of research identifying how alterations to the microbiota affect disease occurrence and progression at distant sites [519–521]. Some of the earliest of these investigations focused on the presentation of asthma in children resulting from variability in their

exposure to microbes [522]. One route of exposure gaining a lot of interest is the method of delivery during birthing [523,524]; several studies have identified an increased risk of children developing asthma when delivered by caesarean section versus through the vaginal canal [524]. This is thought to be due to a reduction in the exposure to beneficial genera, predominantly *Bifidobacterium*, and an increased exposure to pathobionts, namely species from the genera *Clostridium* and *Staphylococcus*, predominantly found on human skin [525]. Similarly, observations have been made that when infants are raised in the presence of siblings and/or pets they are exposed to an increased diversity of microbes and subsequently develop a more diverse microbiota, leading to the reduced presentation of atopies compared to infants raised without the same exposures [522]. The general consensus on the reason for these observations is that an 'abnormal' or reduced exposure to microbes results in the sub-optimal education of the adaptive immune system [522,523]. Specifically, it reduces the activation of Th1 cells while facilitating activation of the Th2 specific pathways, including those triggered by IL-4, IL-5, IL-6 and IL-13, resulting in isotype class switching in plasma cells to produce IgE immunoglobulins and activation of immune cells, such as mast cells and eosinophils, associated with allergenic activity and atopic disease [523,526,527]. Interestingly, there is some evidence to show that probiotic supplementation both prenatally to the mother and postnatally to the infant reduces the risk of developing atopic asthma by reducing total levels of IgE [528,529]. These findings once again provide evidence of the potential for probiotic use in the prevention and treatment of disease.

1.6 Links Between the Gut Microbiota and Cancer

Over the past two decades, as microbial research has begun to focus on the complex interactions between the gut microbiota and their host, the stigma around bacteria as always being pathogenic and infectious has begun to shift and the understanding of how these microbes are integral to supporting an array of beneficial functions within their host has improved greatly and continues to do so. Section 1.5.4 outlined how perturbations of the microbiota, both during development and when matured, can result in inflammatory atopies and diseases, but conversely, supporting a healthy microbiota, for example via the administration probiotic species, can alleviate symptoms and some cases cure disease. To date, the body of literature describing such interactions has largely focussed on local sites within the GI tract, predominantly the small and large intestines, but increasingly studies are beginning to elucidate the microbiota's potential to influence diseases at distant sites, including the skin, lungs and liver to name just three [424–426,494]. Considering these findings, it is arguably unsurprising that there is now a growing body of research investigating the microbiota's role in distal cancers and diseases. In fact, a recent review published in 2021 by Senga and Grose discussed the possibility of including an “altered microbiome” to the list of the “hallmarks of cancer” and discussed the “tug-of-war” hypothesis whereby shifts in the abundances of commensal bacterial populations within the gut leads to changes in immune activity and epigenetic instability of host cells, ultimately influencing the success or removal of neoplastic cells [530].

1.6.1 *The microbiota and its influence on intra-GI cancers*

In the context of causation and progression, it is estimated that ~20% of the global cancer burden is linked to infectious agents including viruses, bacteria and other microbes [504]. For example, one of the earliest bacterial species to be identified as a major carcinogen in the presentation of stomach cancers was *Helicobacter pylori* [531]. Specifically, *H. pylori* appears to increase the expression of β -catenin target genes, such as the proto-oncogenes *Myc* and *CCND1*, ultimately causing aberrant Wnt/ β -catenin signalling and interfering with the epithelial (E)-cadherin - β -catenin - actin cytoskeleton complexes which regulate cell-to-cell adhesion, facilitating the formation of gastric carcinomas within the stomach epithelium [531,532].

The colon houses the most dense population of bacteria within the GI tract and so it is perhaps unsurprising that initial interest of the microbiota's potential relationship with cancers focused on colorectal cancers (CRC) [533]. There is already an array of bacteria, including several species commonly considered to be commensals within a ‘healthy’ microbiota, which have been identified to be enriched within CRC patients [504]. These include *Streptococcus bovis*, *Bacteroides fragilis*, *Enterococcus faecalis*, *Clostridium septicum* and *Fusobacterium* spp. [504]. Wu *et al.* (2013)

observed that in faecal samples taken from patients suffering from CRC there was an increase in the abundance of bacteria from the *Bacteroides* genus in comparison to samples from healthy individuals [503]. This genus is known to produce an oncogenic bacterial compound, fragilysin, an enterotoxin that stimulates IL-8 production by epithelial cells leading to a pro-inflammatory signalling cascade, attracting neutrophils and other innate immune cells to the site where they promote further inflammation and facilitate tumourigenesis [503]. Additionally, fragilysin has been linked to an increase in epithelial cell proliferation via activation of the *C-Myc* oncogene, the same oncogene mentioned in the oncogenesis of *H. pylori* induced stomach cancers [532,534]. In a separate study, Castellarin *et al.* (2012) observed a similar over representation of *Fusobacterium nucleatum*, a bacterium naturally present in the oral microbiota, in CRC tumour tissue in comparison to healthy tissue [535]. Furthermore, the same study highlighted a positive correlation between *F. nucleatum* abundance and the occurrence of lymph node metastasis [535]. Yu *et al.* (2017) furthered the understanding of the pathogenesis of *F. nucleatum* in CRC when they showed that not only was the bacterium enriched in tumour tissues but it was associated with chemotherapy-resistance through the activation of autophagy in anti-cancer innate immune cells, predominantly macrophages, via TLR binding, specifically TLR4, and intracellular miRNA signalling, resulting immune cell death and immune evasion during chemotherapy [536].

Interestingly, it is not only immunological changes resulting from alterations in the microbiota that have been linked to cancer progression, or at least not directly. As aforementioned, the by-products of bacterial metabolism and fermentation produce an array of metabolites which can be beneficial or detrimental depending on the bacterial species involved [537–539]. For example, an increased abundance of *Bacteroidetes* and *Firmicutes* are associated with the fermentation of proteins, the products of which can be carcinogenic, such as phenol [540]. However, species of *Roseburia* and *Butyricoccus* are known producers of the SCFA butyrate, a metabolite described in section 1.5.4 to have anti-inflammatory properties, which epigenetically regulates cell proliferation and supports the integrity of the intestinal barrier, all of which aid in reducing cancer incidence [503,540,541]. In particular, the ability of butyrate to act as a HDACi is suspected to evoke the strongest anti-cancer effects. Briefly, butyrate prevents the de-acetylation of histone molecules which subsequently prevents RNA polymerase accessing DNA. In turn this inhibits gene transcription, interferes with the expression of genes involved in cell proliferation and ultimately promotes cell apoptosis [542–545]. For example, Thangaraju *et al.* (2009) described that the binding of butyrate GPR109A down-regulates activity of the anti-apoptotic proteins cyclin-D1 and BCL-2 while up-regulating proteins involved in promoting apoptosis [546]. However, the same study described that in both mouse and human colorectal tumour tissue, the GPR109A receptor was silenced, suggesting that one method

by which colorectal cancer cell may avoid being pushed into an apoptotic state by bacterial metabolites, such as butyrate, is through altering their transcriptome to avoid expression of proteins which might bind them.

Considering this causative association between bacterial communities and CRC development, investigations started to question whether altering the composition of said communities may in fact offer a protective effect. Results from several animal studies infer that probiotic supplementation may reduce CRC through the dampening of inflammatory pathways and regulating cell proliferation and apoptosis [547–549]. One such study performed by Mousavi Jam *et al.* (2021) demonstrated a role of a potentially probiotic bacterial species, *Lactobacillus paracasei*, in reducing the pathogenesis of CRC [550]. Specifically, Wistar rats, with dimethylhydrazine induced CRC, were supplemented with *L. paracasei* and exhibited reduced CRC associated symptoms such as diarrhoea and rectal bleeding [550]. More importantly, histological analysis identified fewer dysplastic regions within the colon when compared to rats that did not receive the probiotic supplement [550]. Finally, the combination of *L. paracasei* supplementation with a common colorectal chemotherapy, 5-fluorouracil (5-FU), significantly increased treatment efficacy, quantified as an increase in apoptotic cells, compared to rats treated with 5-FU only [550]. Chang *et al.* (2018) has previously described that, in BALB/c mice induced with a syngeneic model of CRC, a bacterium from the same genus as *L. paracasei*, *Lactobacillus casei* variety *rhamnosus* (Lcr35), attenuated chemotherapy-induced mucositis following postsurgical 5-FU treatment [551]. Additionally, the supplementation with Lcr35 reduced the levels of proinflammatory IL-6 and TNF α in comparison to 5-FU treated animals which did not receive the same supplementation. Of note, probiotic supplementation rescued the skewed F/B ratio observed in 5-FU treated animals that did not receive the probiotic [551].

In humans, a randomised double-blind placebo-controlled study carried out on 52 post-surgical colorectal cancer patients observed that the supplementation of probiotic bacterial species from the genera of *Lactobacillus* and *Bifidobacteria* reduced levels of a number of pro-inflammatory cytokines, namely TNF- α , IL-6, IL-10, IL-17 and IL-22, compared to pre-treatment levels [552]. A result which offers improved prognostic outlook as inflammation is commonly associated with increase recurrence rates and poorer disease-free survival rates [552]. Taken together, these pre-clinical and clinical studies point to a likely immunological interaction between the probiotic supplementation and the host immune cells to reduce inflammatory activities and highlight the possibility of utilising the microbiota's influences on host cells to support CRC therapies and can even result in the alleviation of some of the morbid symptoms that follow chemotherapies.

1.6.2 Current evidence of the microbiota's effect on cancers at distant sites

Naturally, identifying the links between the microbiota and cancer pathogenesis within the GI tract has led researchers to question as to whether similar observations may be made in organs and tissues at sites distant from it [520,553]. It is both surprising and promising that many studies asking such questions have mostly identified beneficial influences of the microbiota, and the manipulation of it, in slowing or treating cancers outside the GI tract. The immunogenicity of cancer was broadly outlined in section 1.4 and the role of the microbiota in priming immune responses was done so in section 1.5.3.4. Thus, considering the immune system's association with both the microbiota and cancer, it was sensible that initial studies of the relationship between the two began with typically immunogenic cancers such as melanoma.

The use of immune checkpoint inhibitors against PD-1 and PD-L1 proteins on the surface of T-cells and some cancer cells respectively has been outlined in section 1.4.2. This form of immunotherapy is an established approach in the treatment of melanoma, a malignant cancer caused by the abnormal development of melanocytes in skin due to an overexpression of PD-L1 [554]. One of the early studies investigating the potential of probiotic microbiota therapies in supporting immunotherapeutic treatments was undertaken by Sivan *et al.* (2015). This comprehensive preclinical study identified that a combination therapy incorporating a *Bifidobacterium* probiotic supplementation alongside a traditional PD-L1 inhibitor produced an anti-tumourigenic response that significantly reduced tumour outgrowth in a subcutaneous syngeneic melanoma model (B16.SIY) [555]. Subsequent *in vitro* experiments, exposing bone marrow derived murine DCs to *Bifidobacterium*, showed that *Bifidobacterium* directly evokes maturation and activation of the cells [555]. Furthermore, DCs obtained from lymphoid tissues of mice treated with *Bifidobacterium* showed an increased ability to activate CD8 cytotoxic T-cells as well as increasing IFN γ production by T-cells when compared to animals which were not treated with the probiotic [555]. These results therefore concluded that *Bifidobacterium* supplementation supported PD-L1 checkpoint inhibitor therapy by promoting DC maturation and, in turn, promoting CD8 cytotoxic T-cell activation and function to target and kill melanoma cancer cells.

More recently, Tanoue *et al.* (2019) produced a similar conclusion when supplementing germ-free mice, engrafted with a syngeneic adenocarcinoma (MC38) tumour model, with a consortia of 11 bacterial species and combining this with an anti-PD1 checkpoint inhibitor therapy [556]. The combination treatment markedly reduced tumour volumes relative to animals that were treated with only anti-PD-1 and significantly increased the number of activated CD8 T-cells within tumour tissues. Metabolomic analysis of both caeca and sera identified the abundance of several

metabolites, namely mevalonate and dimethylglycine, were increased in the animals supplemented with the bacterial consortia relative to those that were not. Mevalonate has been linked to both pro- and anti-tumour influences but there is some evidence suggesting that increased mevalonate metabolism promotes the activation of several effector cells including anti-cancer CD8 T-cells, alluding to a pathway by which the naïve T-cells may become activated following consortia-induced microbial changes in the gut [556,557].

Furthermore, the same study subsequently described similar results when using specified pathogen free (SPF) mice, in place of germ-free animals, engrafted with a subcutaneous melanoma model (*Braf*^{V600E} *Pten*^{-/-}) and subjected to supplementation with the same bacterial consortia but treated in combination with either an anti-PD-1 or anti-CTLA4 immune checkpoint inhibitor therapies [556]. Again, the combination of probiotic supplementation with either checkpoint inhibitor therapy resulted in reduced melanoma tumour, further demonstrating the beneficial potential of biotherapeutics in combination with more traditional cancer therapies.

Both the above studies by Sivan and Tanoue described the beneficial effects of using probiotic microbes to support anti-cancer immunological responses during immune checkpoint inhibitor therapies. However, a common practice within the treatment pathways of many cancers is the prophylactic use of antibiotics to avoid bacterial infections during periods where the immune system may be weakened, such as during chemotherapies or following surgery [558,559]. Thus, Pinato *et al.* (2019) investigated how antibiotic use may influence the efficacy of anti-PD-1 or anti-PD-L1 immune checkpoint therapies in an observational study considering patient overall survival following the various treatments in patients with either lung or melanoma metastatic disease [560]. The study admits to several limitations including a small sample size (196 patients) and lack of correlative analyses of the downstream translational effects of antibiotics on microbiota composition. Despite this, the study presented compelling evidence showing a correlation of worsened diagnosis in patients treated with antibiotics and subjected to immune checkpoint inhibitor therapy compared to those that did not receive antibiotics [560]. Specifically, it outlined that pre-treatment antibiotics, rather than concurrent antibiotic treatment, were most influential in reducing checkpoint inhibitor efficacy. Their analyses identified that mean overall survival was just 2.5 months in patients that received pre-treatment antibiotics while it was 26 months in those that did not receive antibiotics [560]. Although concerning based on the current clinical guidelines for antibiotic use in cancer patients, this finding supports the work of Tanoue and Sivan demonstrating that a healthy microbiota is integral in supporting immunomodulatory effects against cancers.

1.6.3 The gut microbiota and breast cancer

Due to the high morbidity and mortality rates of breast cancer globally, it is imperative that any and all possible influences on the progression of the disease are considered. In comparison to cancers local to the GI tract, and to highly immunogenic cancers such as melanoma, there are relatively few studies detailing links between changes in the microbiota and subsequent influences on breast cancer. However, considering the evidence of both pro- and anti-tumourigenic effects of those changes, some of which have been discussed above, there is now a growing interest in the potential influences of the microbiota on breast cancer.

Rao *et al.* (2006) were some of the first to undertake such studies and observed an increased occurrence of breast tumours in C57/BL6 *Apc*^{min/+} mice, usually used as models for CRC, infected with *Helicobacter hepaticus*, an enteric bacterial species known to cause chronic hepatitis in mice [561]. Subsequent cytokine analysis of the gut mucosa identified increased production of several proinflammatory molecules, including TNF α . Further experimentation using *Rag2*-deficient *Apc*^{min/+} animals, which lack mature lymphocytes, showed even greater increase in breast tumour burden and increased tumour infiltrating F4/80+ myeloid populations, a marker of murine macrophages, in *H. hepaticus* infected animals, suggesting a protective role of lymphocytes in breast cancer pathogenesis. Additionally, dosing *Rag2*-deficient mice with T-reg cells isolated from wild-type animals significantly reduced breast tumourigenesis [561]. When these T-reg cells were isolated from animals which had survived previous infection with *H. hepaticus*, the tumour counts were reduced even further, highlighting not only their immune influence on breast tumourigenesis but also the role microbes have in priming the immune response, particularly regarding the adaptive components, in regulating carcinogenesis distant to the gut. The same authors went on to review the literature for similar associations between the microbiota and breast cancer. While important observations were discussed, they were largely linked to pathogen and pathobiont outgrowth, and less so on the loss or gain of mutualistic bacterial species on breast cancer progression [562]. Additionally, the metabolomic influence of the microbiota on breast cancer progression in terms of bacterial-derived metabolite abundance and availability had, at the time, not been described.

However, the influence of the microbiota on cancer-associated immune activity is just one area to consider, with a specific regard to its potential to effect disease progression. As discussed in section 1.5.4, several microbiota-derived metabolites have been shown to influence inflammatory diseases and there is evidence suggesting that these influences stretch to several cancers, including breast cancer. Species from the genera *Roseburia* and *Butyricoccus* are known producers of butyrate, a SCFA previously described as having anti-inflammatory properties and regulating gut mucosa permeability [503,540,541]. However, in the context of cancer, its epigenetic activity, particularly

as a HDACi, is of particular importance. The HDACi activity of butyrate involves the silencing of genes with roles in promoting cell proliferation and angiogenesis, hallmarks of tumour growth and progression [563,564]. Therefore, an increase in the abundance of butyrate producing species may contribute to slowing tumour growth and reducing tumour cell dissemination [565]. *In vitro*, butyrate has been shown to induce apoptosis in human hormone receptor positive (MCF-7) and triple negative (MDA-MB-468) breast cancer cell lines through increasing production of intracellular ROS, caspase activity and reducing mitochondrial membrane potential [543]. Thus, it is possible that manipulating the microbiota to increase butyrate production may aid in preventing tumour growth *in vivo*, but this hypothesis is yet to be tested.

An *in vivo* study of the effects of a lesser researched microbial metabolite, cadaverine, a polyamine not produced by human cells, on breast cancer progression has been undertaken. Kovács *et al.* (2019) observed that when BALB/c mice challenged with syngeneic orthotopic 4T1 triple negative-like breast cancer cells were supplemented with cadaverine, they exhibited a reduced primary and metastatic tumour burden relative to vehicle controls [566]. Further *in vitro* investigation of 4T1 cells grown in cadaverine supplemented media revealed an increased resistance when subjected to electric cell-substrate impedance sensing, suggesting improved cellular adhesion, as well as having a more epithelial actin cytoskeleton, shown through Phalloidin-Texas Red staining, relative non-supplemented cells [566]. These observations suggest that cadaverine is involved in inhibiting epithelial to mesenchymal transition (EMT), a process associated with tumour cell dissemination and increased metastasis.

These findings highlight a potential protective role of the microbiota in breast cancer pathogenesis. Thus, considering the current use of antibiotics in cancer clinics, it is important to ask whether antibiotic-induced perturbations of the microbiota might influence the progression of the disease. Already, these drugs have been associated with oncogenesis in several cancers [560,567,568]. Unfortunately, recent pre-clinical studies, including a publication by this author and colleagues, advise that perturbations of the microbiota both increase growth kinetics of the primary breast tumours and the metastatic dissemination of cells to distant organs [1,569].

In a comprehensive study, Buchta Rosean *et al.* (2019) administered C57/BL6 mice with a robust cocktail of antibiotics, including vancomycin, neomycin, metronidazole, gentamycin and ampicillin (VNMGA), to significantly reduce the microbial load in the gut. Following a four-day re-colonisation period, effectively establishing a perturbed microbiota, mice were subject to an orthotopic transplantation with a syngeneic breast cancer model of either a poorly metastatic hormone receptor positive BRPKp110 cell line, derived from a p53/KRas/PI3K driven primary breast

adenocarcinoma, or the more aggressive PyMT-derived model [356]. While, the primary tumour growth kinetics were not affected, metastasis of breast cancer cells to the lungs was significantly increased in both models [354]. Furthermore, when animals with pre-perturbed microbiotas were engrafted with autochthonous weight-matched tumour fragments, grown in in wild-type C57/BL6 mice using GFP-labelled cells, they similarly suffered increased dissemination to the lungs compared to non-perturbed animals engrafted in the same way. Subsequent cytokine analysis of mammary tissue from animals subjected to the VNMGA cocktail, but not induced with cancer cells, identified elevated levels of myeloid recruitment components, namely CXCL10 and CCL2, and flow cytometry found increased abundance of infiltrating myeloid cells. These results suggest that the microbiota may have a protective role over metastasis through regulating the immune responses which may otherwise act to promote tumour cell dissemination.

1.7 Preliminary research forming the foundation of the studies undertaken in this thesis

Preliminary work undertaken and interpreted by this author's predecessor, Benjamin Kirkup, formed the bedrock of the research presented in this thesis [570]. Thus, to establish what was known at the starting point of this study, it is imperative those results are briefly discussed prior to presenting results subsequent to this research.

Through attempted amplification of bacterial 16S rRNA genes in faeces, Kirkup identified that the administration of a broad-spectrum cocktail of antibiotics, comprising vancomycin, neomycin, metronidazole, amphotericin-B and ampicillin (VNMAA), knocks down the bacterial component of the murine gut microbiota and that this gut level disturbance was associated with increased primary tumour growth in two orthotopic murine models of breast cancer in C57 BL6 mice [570]. These models were the MMTV-PyMT derived PyMT-BO1 model which resembles a luminal-B-like molecular subtype and the basal EO771 model isolated from a spontaneous basal-like breast carcinoma in a C57 BL/6 mouse. Flow cytometry of tumour associated leukocytes in PyMT-BO1 tumours found no differences in the numbers of tumour infiltrating macrophages, including those of a classical M1 or alternate M2 activation state, or lymphoid populations (CD8⁺ or CD4⁺). Furthermore, a targeted intra-tumoural pro-inflammatory cytokine profiling showed no changes between VNMAA treated and control animals. However, several pro-inflammatory cytokines were reduced in the intestines of VNMAA treated animals compared to a control cohort.

In the absence of an obvious difference between immune activity and tumour growth, bulk RNA-sequencing of whole tumours was undertaken to identify gene expression patterns which may be associated with an increase in tumour growth. This revealed the tumours from VNMAA treated animals had increased expression of several genes associated with lipid metabolism, gluconeogenesis and, surprisingly, apoptosis. It also identified a reduced expression in genes linked to protein metabolism and cell migration. These results arguably led to more questions than answers as pathways such as gluconeogenesis and apoptosis are usually associated with an anti-tumorigenic effect, yet were upregulated in the larger tumours [571,572].

Following these results, Kirkup asked how VNMAA treatment influenced the metabolic output of the gut microbiota. ¹H-Nuclear Magnetic Resonance (¹HNMR) spectroscopy of faecal samples identified major reductions in abundances of bacterial derived metabolites in samples from VNMAA treated animals. This was partly expected due to the significant knockdown in bacterial load caused by the antibiotic treatment. However, the observed reduction in the bacterial derived SCFAs butyrate, acetate and propionate in the gut were interesting due to their known roles in regulating

human metabolic health [542]. Although butyrate has been shown to have anti-cancer effects, as mentioned in section 1.6.1, linking these reductions at a gut level to influences at distant sites would prove difficult and beyond the scope of the study at that time.

Another consideration was whether increased tumour growth following robust antibiotic treatment was the result of the loss of symbiotic bacterial members of the microbial community or was it facilitating the amplification of a pathobiont/s by reducing overall competition for a particular niche in the gut. Kirkup setup an experiment which facilitated what this author would describe as passive faecal microbiota transplants (pFMT). Mice are coprophagic, meaning they will consume faeces as a food source and thus ingest the bacteria present in it. Therefore, by transferring bedding, which was littered with faecal pellets, from animals treated with either a vehicle or VNMAA to cages where animals receive the opposite treatment, one can facilitate microbiota transfer. Kirkup observed that VNMAA treated animals receiving pFMT from vehicle treated animals had significantly reduced tumour volumes compared to VNMAA treated animals not receiving pFMT. In fact, tumours returned to similar volumes observed in the control cohort. However, vehicle treated animals receiving pFMT from VNMAA treated animals did not show increased tumour growth when compared to the control cohort. This suggests that the increased tumour growth observed following VNMAA treatment is the result of losing a protective member, or members, of the gut microbiota. Unfortunately, due to the severe knockdown caused by the treatment, it would not be possible to identify these members as there would be too many candidates to consider.

While these results demonstrate that antibiotics perturb the microbiota, which in turn promotes breast cancer tumour growth, the VNMAA combination is not one which would be prescribed to patients. Thus, in order to show the clinical translation of these observations, an experiment was undertaken which substituted the VNMAA antibiotic combination for a clinically relevant cephalosporin antibiotic, cephalexin, which was suggested to us by our clinical colleagues as it is regularly prescribed in breast cancer clinics to prophylactically treat patients undergoing chemotherapy and/or mastectomy or reconstructive surgery. Administration of this drug also resulted in a significantly increased rate of tumour growth in the PyMT-BO1 model, an important observation in the context of clinical relevance. However, this was only performed once and thus required repeating to support the reliability of the observations.

16S rRNA sequencing of DNA isolated from faecal pellets showed significant reduction in bacterial load and diversity following cephalexin treatment. Notable genera reduced in abundance were *Lactobacillus*, a genus known to include several probiotic species, and *Faecalibaculum*, a genus with recent traction as a possible protective member in the context of colorectal cancers [573,574].

Thus, it is possible that members of the microbiota belonging to either, or both, of these genera may be protective against this model of breast cancer.

Finally, Kirkup used a cocktail of several proprietary *Bifidobacterial* strains as a live biotherapeutic product (LBP) and showed that in mice subject to PyMT-BO1 tumours, administration of this cocktail reduced primary tumour growth compared to a vehicle treated cohort. Again, this supports the hypothesis that a healthy microbiota plays a protective role in breast cancer progression.

These results act as the foundation on which this research hoped to build upon. However, many of the animal experiments described by Kirkup (2019) were only able to be performed once or, at the most, twice due to time constraints and shifts in project focus. Thus, in some cases, to ensure the reliability and robustness of observations previously described, experiments were repeated by this author. Where such data was pooled with previous results, this has been clearly stated.

1.8 Research Aims and Objectives

Changes to the composition of the host gut microbiota has been implicated in affecting the progression and regression of carcinogenesis in several *in vivo* models representing a variety of cancer types, including melanoma and colorectal cancers. However, the understanding of how these microbes influence breast cancer is relatively poor in comparison. Preliminary data produced by the Robinson lab suggested the microbiota plays a protective role in breast cancer tumourigenesis. Based on these early findings, the aims of this project were two-fold. Firstly, to support and confirm the early-stage findings discussed above, particularly regarding clinical relevance in the context of antibiotic administration; and secondly, to underpin the cellular and molecular components likely to be involved in driving the observations made. The objectives laid out to achieve these aims were as follows:

- To further explore the effect of antibiotic-induced perturbations of the gut microbiota on breast cancer progression with a particular focus on clinically relevant antibiotic administration.
- To demonstrate that a perturbed gut microbiota acts as a driving force behind shifts in tumour growth kinetics.
- To identify the key cellular, molecular and microbial components involved in driving tumour progression following antibiotic administration.
- To investigate the effect of antibiotic administration on breast cancer metastasis and the immunological profiles of the metastatic niche.
- To determine whether supplementation of gut-established commensals as well as probiotic bacterial species are capable of rescuing the pro-tumorigenic effects of antibiotic administration.

2 Materials and Methods

2.1 Animals

C57 BL6 mice, of either SPF or germ-free microbiota status, were sourced in-house from the University of East Anglia's Disease Modelling unit. Germ-free animals were maintained in an aseptic environment throughout their lives. All animals were age matched at 8-12 weeks old and were cage mixed prior to experiments. Animals in separate cages but part of the same treatment group were cage mixed prior to dosing to reduce the influence of cage effects. All animal experiments were performed in accordance with UK Home Office regulations and the European Legal Framework for the Protection of Animals used for Scientific Purposes (European Directive 86/609/EEC).

2.2 PyMT-BO1 and EO771 *in vivo* Tumour Growth Assays

Syngeneic mouse breast carcinoma (PYMT-BO1 or EO771) cells were injected at 1×10^5 per $50 \mu\text{l}$ of a 1:1 mixture of phosphate buffered saline (PBS) and Matrigel (Corning Life Sciences, Corning, USA, 354234) into the left inguinal mammary fat pad (MFP) of age matched female mice. Upon conclusion of the experiment or once tumours reached *in situ* volumes of $\sim 1000 \text{mm}^3$, animals were sacrificed by cervical dislocation and tissues harvested for various downstream analyses. Tumour dimensions were measured using digital callipers and volume calculated according to the following formula: length x width² x 0.52 [575].

2.3 Breast Cancer Cell Culture for *in vitro* and *in vivo* Experiments

PYMT-BO1 and EO771 cells were cultured in high glucose Dulbecco's Modified Eagle Medium (DMEM) (Invitrogen, Carlsbad, D1145-500ML) supplemented with 10% foetal bovine serum (FBS) (Hyclone, Invitrogen) and 100units/ml penicillin/streptomycin (Pen/Strep) (Invitrogen, 15140-122). Cells were maintained at the following conditions: 37°C, 5% CO₂ and 95% humidity. Tissue culture plastic was coated with 0.1% porcine gelatin (Sigma-Aldrich-Aldrich, St-Louis, USA, G2500) in water for one hour at 37°C prior to culture.

2.4 Antibiotic Administration

Animals were treated with antibiotics three times weekly by oral gavage ($200 \mu\text{l}$ in dH_2O). Animals were treated with either an antibiotic cocktail consisting of 1mg/ml Amphotericin B (Sigma-Aldrich, A4888), 25mg/ml Vancomycin (Sigma-Aldrich, 11956911), 50mg/ml Neomycin (Sigma-Aldrich, PHR1491), 50mg/ml Metronidazole (Sigma-Aldrich, PHR1052) with drinking water being supplemented with 1mg/ml Ampicillin (Sigma-Aldrich, A9518) or 8.64mg/ml Cephalexin (Sigma-Aldrich, C4895). Antibiotic treatment began one week prior to tumour cell injection and was maintained throughout animal experiments.

2.5 Cromolyn Sodium Administration

Animals were treated with cromolyn sodium (Sigma-Aldrich, 15826-37-6) daily for the final five days of respective experiments at a dosage of 10mg/kg administered via intraperitoneal (i.p.) injection (100µl in physiological saline). Any antibiotic treatments were continued alongside cromolyn administration as described in Section 2.4.

2.6 Probiotic Administration

2.6.1 *Faecalibaculum rodentium* (*F. rod*)

F. rod (Leibniz Institute DSMZ, Braunschweig, Germany, Type strain 103405) was cultured in Peptone Yeast Glucose (PYG) (Thermo Fisher, 16289761) broth under anaerobic conditions and harvested at optical density (OD) 0.6 (~48 hours growth time) via centrifugation 2770 relative centrifugal force (rcf) for 10 minutes at 4 °C. Bacterial pellets were washed twice in sterile PBS before final resuspension in 2.5ml of sterile PBS ready for oral gavage administration.

2.6.2 *Bifidobacterial Cocktail*

Four proprietary *Bifidobacterium* strains, previously isolated from healthy human infants by Lindsay Hall's group, were each cultured for 48 hours in MRS broth (Thermo Fisher, 11713553) containing mupirocin (50mg/L) (Sigma-Aldrich, 07188) and L-cysteine (50mg/L) (Sigma-Aldrich, C7880) under anaerobic conditions and harvested via centrifuge at 2770 rcf for 10 minutes at 4 °C. Bacterial pellets were washed twice in PBS before final resuspension in 2ml of sterile PBS. Equal volumes of each strain were then combined to form the cocktail (*Bif*) ready for oral gavage administration.

2.6.3 *Bacterial Load Enumeration*

Following resuspension of bacterial pellets in the stated volumes of sterile PBS, enumeration of each strain was determined by colony forming units (CFU) per millilitre (CFU/ml). Each individual bacterial suspension was subject to a 10-fold dilution series in sterile PBS down to a factor of between 1×10^{-13} and 1×10^{-16} mean CFU. These were then plated on agar plates comprising the respective media elements described for the specific bacteria (Section 2.5.1 and 2.5.2) by pipetting three 20µl droplets for each dilution. Mean colonies per droplet were calculated for each dilution and this was multiplied by 50 to account for volume in 1ml and then again by the respective dilution factor to produce a CFU/ml concentration. For clarity the calculation was: mean colonies in three 20µl droplets X 50 X dilution factor = CFU/ml.

2.6.4 *Bacterial Treatment Regimens*

Animals were treated with either a vehicle control or the VNMAA cocktail (See section 2.4) for the first week of the experiment, at which point tumours were induced (PyMT-BO1, see section 2.2 and

2.3) and one of four treatment regimens were adopted, either: vehicle control continued (control); vehicle was switched to bacterial oral gavages (control to bacteria); VNMAA was switched to vehicle control (VNMAA to control); or VNMAA was switched to bacterial oral gavages (VNMAA to bacteria). All administrations were via oral gavages (250µl for *F. rod* experiments, 200µl for *Bif* experiments) and administered three times weekly.

2.7 *in vivo* Tumour Growth Assays And Antibiotic Regimens Undertaken By International Collaborators And Used For Mast Cell Counting

2.7.1 *Spontaneous HER2 model*

The Tagliabue laboratory (Fondazione IRCCS Istituto Nazionale di Tumori, Milan, Italy) treated Delta16HER2 transgenic FVB mice, previously described by Marchini *et al.* (2011) [576,577], with Vancomycin (200mg/L) in drinking water starting when mice were 4 weeks of age and continued to 6 weeks post tumour onset.

2.7.2 *Orthotopic Luminal A model*

The Rutkowski laboratory (University of Virginia, Virginia, USA) treated C57 BL6 mice by oral gavage with antibiotic cocktail comprising 0.5 mg/ml Vancomycin, 1 mg/ml Ampicillin, 1 mg/ml Metronidazole, 1 mg/ml Neomycin, and 1 mg/ml Gentamicin (VNMGA) (100 µl in dH₂O) for 14 days or water. After 14 days of treatment, mice were left untreated for four days before initiation of mammary tumours, at which point 5x10⁵ BRPKp110 cells were injected orthotopically into the left inguinal MFP, as previously described by Buchta Rosean *et al.* (2019) [569].

2.8 Serum IgE Enzyme-linked Immunosorbent Assay (ELISA)

2.8.1 *Serum Collection*

Blood was collected via cardiac puncture immediately after mice were euthanised by CO₂ overdose. After being left to coagulate in Eppendorf tubes at RT for 30 minutes, blood was spun down at 2600 rcf for 15 minutes at 10°C. Serum was carefully collected off of the top of pelleted blood and stored at -80°C until required.

2.8.2 *Running of Assay*

The assay was performed according to the manufacturer's protocol (Abcam, ab157718) with the exception that serum samples were loaded without dilution due to low levels of IgE observed during assay optimisation. Briefly, standards and samples were loaded in duplicate into the manufacturer's 96-well plate and incubated for 30 minutes at RT. Wells were aspirated and washed four times with wash buffer before enzyme-antibody conjugates were added to wells and incubated for 30 minutes at RT in the dark. Following aspiration and four more washes, chromogen substrate was added and

incubated for precisely 10 minutes at RT in the dark. Stop solution was added and absorbance measured using a VERSAmax microplate reader (Molecular Devices, San Jose, USA) at 450nm.

2.8.3 Quantification of Serum IgE levels

The mean of duplicates for both standards and samples were calculated and the reading for a blank well was subtracted from these means. Readings from the standards and their known concentrations were used to establish a standard curve using a four-parameter (4PL) algorithm in Prism 9.0.0 (GraphPad, San Diego, USA) and IgE concentrations of samples were extrapolated from this curve.

2.9 Western Blot

2.9.1 Western Blot Sample Preparation

Tissue samples were kept frozen using liquid nitrogen and dry ice while being cut and weighed to obtain ~50mg of tissue. Samples were placed in Safe-Lock Eppendorf tubes (Eppendorf, Hamburg, Germany, 0030120086) containing acid washed glass beads (Sigma-Aldrich, Z273619-1EA) and mechanically homogenised using plastic pestles. Electrophoresis sample buffer (Tris-HCl, 65mM, pH 7.4), sucrose (60mM), SDS (Sodium Dodecyl Sulfate) (3%) was added and samples were then further homogenised using a TissueLyser LT (Qiagen, Hilden, Germany, 85600) at 50 Hz for two minutes. Once lysed, samples were centrifuged at 16, 800 rcf for five minutes at 4°C and lysate supernatant transferred to new Eppendorf tubes. Protein concentration was then quantified using the BioRad DC protein assay (Bio-Rad, Hercules, USA, 5000112) and samples read using the VERSAmax microplate reader (Molecular Devices, San Jose, USA) at 666nm. Prior to loading, the required volume of each sample for a given mass of total protein (25µg) was reduced by the addition of lithium dodecyl sulphate sample buffer (Invitrogen, NP0007) and sample reducing agent (Invitrogen, NP0009) to a final concentration of 1X then boiled at 98°C for three minutes.

2.9.2 8% Polyacrylamide Gel (SDS-PAGE) Electrophoresis

Prepared lysates were loaded and run on homemade gels (5% stacking, 8% resolving) alongside 3µl of Spectra™ Multicolour Broad Range Protein Ladder (Thermo Fisher, 26623). Gels were run until sufficient resolution of proteins was achieved. Running buffer was used at 1X concentration in distilled water (dH₂O): 10X running buffer stock (glycine (1.92M), Tris (250mM), SDS (1%) in dH₂O).

2.9.3 Protein Transfer and Immunoblot

Resolved proteins were transferred onto nitrocellulose at 30V for three hours. Transfer buffer used at 1X concentration in dH₂O with the addition of methanol (MeOH) (20%): 10X transfer buffer stock (glycine (1.92M), Tris (250mM) in dH₂O). Post-transfer, membranes were incubated with Ponceau

S stain (0.1% in 5% acetic acid) for five minutes to confirm the presence of proteins. Subsequently, membranes were blocked in 0.1% Tween-20/PBS (PBST) containing 5% milk powder for one hour. Once blocked, membranes underwent three five-minute washes in PBST prior to incubation with the appropriate primary antibody, prepared in 5% milk/PBST, o/n at 4°C. Primary Antibodies were used at dilutions sated in Table 2.9. Following this incubation, membranes were washed three times for five minutes in PBST then incubated with the appropriate horseradish peroxidase (HRP) conjugated secondary antibody (Table 2.9) for two hours at room temperature (RT) in the dark. Secondary antibodies were prepared in 5% milk/PBST and used at dilutions stated in stated in Table 2.9. Membranes were again washed three times for five minutes in PBST, treated with Pierce® ECL Western Blotting Substrates (Thermo Fisher, 32106) and imaged via detection of chemiluminescence on a ChemiDoc XRS+ (Bio-Rad, 1708265). Chemiluminescence was converted to densitometric readings and quantified using Fiji ImageJ [578].

Table 2.9. Antibody information relevant to western blot assays.

Primary Antibodies						
Antigen	Host Species	Conjugate	Manufacturer	Product Code	Clone	Dilution
E-cadherin	Rat	none	Thermo Fisher	10199532	ECCD-2	1:1000
Vimentin	Rabbit	none	Abcam	ab92547	EPR3776	1:1000
Firefly Luciferase	Rabbit	none	Thermo Fisher	PA5-32209	polyclonal	1:1000
β-actin	Rabbit	none	CST	8457P	D6A8	1:2000
Secondary Antibodies						
Target Species	Host Species	Conjugate	Manufacturer	Product Code	Clone	Dilution
Rabbit	Goat	HRP	Agilent	P044801-2	polyclonal	1:2000
Rat	Goat	HRP	Thermo Fisher	31470	polyclonal	1:2000
Mouse	Goat	HRP	Agilent	P044701-2	polyclonal	1:2000

2.10 *In Vivo* And *Ex Vivo* Bioluminescence Imaging

Animals received an i.p. injection containing 2mg of VivoGlo™ luciferin (Promega, P1041) diluted in 150µL of sterile PBS (13.34 mg/ml). For *in vivo* imaging, animals were then anaesthetised using isoflurane and imaged in the prone position on the Bruker *In Vivo* Xtreme instrument (Bruker, Billerica, MA, USA). For *ex vivo* imaging, following an incubation period of seven to 10 minutes after the i.p., animals were cervically dislocated and lungs and bones immediately harvested. Once all tissues from all animals were harvested, tissues were placed in 1.5ml of 300µg/ml VivoGlo™

luciferin in a 24-well plate and imaged using the Bruker *in vivo* Xtreme instrument. Metastatic burden was calculated in *ex vivo* tissues using photons/sec/mm².

2.11 Cryo-sectioning Of Snap Frozen Tumours

Tumours were harvested from humanely killed animals, immediately placed in Eppendorf tubes, snap frozen in liquid nitrogen and stored at -80°C. Tumours were subsequently sectioned at a thickness of 5µm on a Cryostat NX70 (Thermo Fisher, Waltham, USA) and sections were stored at -80°C until staining.

2.12 Toluidine Blue Staining

Frozen sections were air dried for 10 minutes at RT then fixed in ice cold MeOH for 10 minutes. A stock solution of Toluidine Blue O (Merck, 198161) was prepared in 70% ethanol and then added to 1% NaCl, pH 2.5 in ratio 1:10. Following fixation, sections were placed in the working solution of toluidine blue for three minutes before three subsequent washes in distilled water, a gradual dehydration through quick changes of 95% and two change of 100% ethanol for ~20 seconds per change then cleared in two changes of xylene (Sigma-Aldrich, 534056) for three minutes per change. Sections were mounted with an anhydrous mounting medium then left to air dry.

2.13 Picro-Sirius Red Staining

Frozen sections were air dried for 10 minutes at RT then fixed in 4% PFA for 10 minutes. Sections were covered with picro-Sirius red solution (Abcam, ab150681) and incubated for one hour at RT. Sections were washed twice in a 0.5% acetic acid solution for ~30 seconds each, dehydrated in three quick changes of 100% ethanol of ~20 seconds each and cleared in xylene (Sigma-Aldrich, 534056) for three minutes. Sections were mounted with an anhydrous mounting medium and allowed to air dry.

2.14 TUNEL Staining

All sections were air dried before fixing in ice cold MeOH for 10 minutes and washed in PBST. For sections requiring both TUNEL and antibody staining, TUNEL was performed first followed by antibody staining.

TUNEL staining was performed according to the manufacturer's protocol using the Click-iT™ Plus TUNEL Assay for In Situ Apoptosis Detection with Alexa Fluor™ 647 as the fluorescent reporter (Thermo Fisher, C10619). Briefly, sections were fixed and permeabilised in ice cold methanol, washed with dH₂O, incubated in the deoxyuridine triphosphate (dUTP) and terminal deoxynucleotidyl transferase (TdT) reaction solution, washed with 3% bovine serum albumin (BSA) and 0.1% Triton™ X-100 in PBS followed by PBS alone, incubated with the Click-iT™ Plus TUNEL

reaction mixture containing the fluorescent reporter and washed with 3% BSA in PBS followed by PBS alone. A negative control was established by not incubating a section with the dUTP and TdT reaction solution and a positive control was established by incubating a section with DNase I recombinant solution (~3000U/ml in 50mM Tris-HCl, pH 7.5, 1mg/ml BSA) (10 minutes, RT).

All images were obtained using a Zeiss Axioplan 2ie widefield microscope and processed using Fiji imageJ [578].

2.15 Immunofluorescence Staining

Either directly after MeOH fixation or immediately following TUNEL staining (see Section 2.13 above for both methodologies), sections were blocked using Dako serum-free protein block (Agilent Dako, X0909) and incubated over-night at 4°C with respective primary antibodies (Table 2.15) diluted in PBS/2% donkey serum. Where unconjugated primary antibodies were used, sections were then incubated in species appropriate secondary antibodies, diluted in PBS, for two hours at RT in the dark (Table 2.15). All sections were blocked in Sudan Black B (Sigma-Aldrich, 199664-25G) for five minutes and, finally, mounted with Fluoromount-G with DAPI (eBiosciences, E115189).

All images were obtained using a Zeiss Axioplan 2ie widefield microscope and processed using Fiji imageJ [578].

Table 2.15. Antibody information relevant to immunofluorescent staining.

Primary Antibodies						
Antigen	Host Species	Conjugate	Manufacturer	Product Code	Clone	Dilution
Vimentin	Rabbit	None	Abcam	ab92547	EPR3776	1:200
FCεR1α	Hamster	FITC	Invitrogen	11-5898-82	MAR-1	1:200
Secondary Antibodies						
Target Species	Host Species	Conjugate	Manufacturer	Product Code	Clone	Dilution
Rabbit	Donkey	AlexaFluor© 488	Thermo Fisher	A-21206	polyclonal	1:500

2.16 Tissue Processing And Embedding

Tissues were fixed overnight in 4% PFA at 4°C. Using the Leica Tissue Processor ASP-300-S (Leica Biosystems, Milton Kenes, UK), tissues were placed in formalin (one hour) and dehydrated in solutions of increasing concentrations of ethanol (70% for five minutes, 90% for five minutes and four changes of 100% ethanol for one hour per change), then into xylene (Sigma-Aldrich, 534056) (three changes of one hour per change) and finally paraffin wax (Sigma-Aldrich, 327212) (three

changes of one hour per change at 62°C). Tissues were embedded in paraffin wax and cooled overnight (o/n) at 4°C. Paraffin blocks were sectioned using a rotary microtome (Leica Biosystems, RM2235) at a thickness of 6µm and mounted onto positively charged glass slides (Thermo Fisher) and incubated o/n at 37°C. Prior to staining and using an automated multistainer (Leica Biosystems, ST5020), sections were deparaffinised in xylene (Sigma-Aldrich, 534056) (two changes for five minutes per change) followed by rehydration through gradually decreasing concentrations of ethanol (100%, 80% and 70% for two minutes each) into dH₂O.

2.17 Immunohistochemical Staining

Deparaffinised sections were blocked for endogenous peroxidases (3% H₂O₂ in MeOH) for 10 minutes at RT prior to antigen retrieval in citrate buffer (2mM citric acid, 9.5 mM trisodium citrate, pH 6) using a microwave to boil sections followed by blocking in Tris-buffered saline, 10% goat serum, 0.1% Triton-X100 (Merck, 93443) solution. Staining was performed using primary antibodies at dilutions stated in Table 2.17 o/n at 4°C. Following a one-hour incubation with respective secondary antibodies (Table 2.17), sections were developed with 3,3'-Diaminobenzidine chromogen (2BScientific, SK-4100) and quenched in water. The Leica ST5020 multistainer was used to perform counterstaining with Harris Hematoxylin followed by a graded alcohol dehydration. Sections were mounted in an anhydrous mounting medium and left to air dry.

Table 2.17. Antibody information relevant to immunohistochemical stained sections.

Primary Antibodies						
Antigen	Origin Species	Conjugate	Manufacturer	Product code	Clone	Dilution
E-cadherin	Rat	None	Thermo Fisher	10199532	ECCD-2	1:100
Ki67	Rabbit	None	Abcam	ab15580	polyclonal	1:200
Endomucin	Rabbit	None	Santa Cruz	sc-65495	V.7C7	1:200
GFP	Rabbit	None	Abcam	ab290	polyclonal	1:100
Luciferase	Rabbit	None	Thermo Fisher	PA5-32209	polyclonal	1:100
Secondary Antibodies						
Anti-Rabbit	Goat	HRP	Agilent	P044801-2	polyclonal	1:1000
Anti-Rat	Goat	HRP	Thermo Fisher	31470	polyclonal	1:500

2.18 Flow Cytometry

2.18.1 In vitro VNMAA effects on PyMT-BO1 cell proliferation and apoptosis

PyMT-BO1 cells were seeded at 25 000 cells per well in 12-well tissue culture plates (Thermo Fisher, 150628) and grown for 18 hours under conditions described in Section 2.3. A 2-fold serial dilution of media containing the VNMAA antibiotic cocktail was established, starting at the concentrations described in Section 2.4 and ending at a 1/512th concentration of the starting media. A control media containing no antibiotics was also prepared. Spent media was aspirated and, in triplicate, media containing the various concentrations of VNMAA was applied to cells. Cells were cultured for 24 hours before detachment using Ethylenediaminetetraacetic acid (EDTA) (50µM) and resuspension in normal media (High Glucose DMEM, 10% FBS, 1% Pen/Strep) and left to recover for one hour at 37°C and 5% CO². Following recovery, cells were centrifuged at 300 rcf for 4°C for five minutes and resuspended in 100µL of Annexin V binding buffer (BioLegend, 422201) before being transferred to a 96-well v-bottom plate. Annexin V conjugated to allophycocyanin (APC) (Table 2.18) was added to relevant wells at dilution 1:50 and propidium iodide (Merck, P4864) at 1:100 or 100µg/ml. Cells were stained at RT in the dark for 10 minutes followed by gentle fixation in 2% PFA made up in 1/2X Annexin V binding buffer for 10 minutes at RT and then further fixed and permeabilised in 1X fixation/permeabilization buffer from the Foxp3/Transcription Factor Staining Buffer kit (eBioscience, 00-5523-00) o/n at 4°C. Cells were centrifuged (400 rcf, 4°C, five minutes) and washed twice in 1X permeabilization buffer from the Foxp3/Transcription Factor Staining Buffer kit (eBioscience, 00-5523-00). Cells were blocked in 2% goat serum in 1X permeabilization buffer for five minutes at RT followed by addition of anti-Ki67 antibody (Table 2.18) and stained for 30 minutes in the dark at RT. Cells were centrifuged at 400 rcf at 4°C for five minutes and washed once with 1X permeabilization buffer before being resuspended in FACS buffer (2% FBS in PBS) ready for analysis.

2.18.2 Animal Tissue

Organs were excised from humanely killed animals and tissues were mechanically homogenised using scalpels. Dependent on tissue and cells of interest, homogenate was incubated in either a collagenase IV solution (tumours looking at basic myeloid and lymphoid populations) or a collagenase I solution (tumours looking at mast cells and lung immune infiltrates). These collagenase solutions comprised either 0.2% Collagenase IV (Thermo Fisher, 10780004) or 0.2% Collagenase I (Thermo Fisher, 17100017) as well as 0.01% Hyaluronidase (Sigma-Aldrich, H6254) & 2.5U/ml DNase I (Sigma-Aldrich, D4263) in Hanks' Buffered Salt Solution (HBSS). All samples were

digested for one hour at 37°C with regular agitation. Following digestion, supernatant was passed through a 70µm cell strainer and centrifuged at 300 rcf at 4°C for five minutes. Pellets were washed twice in PBS and resuspended in 10ml 1X RBC lysis buffer (Invitrogen, 00-4333-57) and incubated for five minutes at RT. Cells were washed once in PBS, counted using a haemocytometer and 1 million cells per sample transferred to a 96 well plate for staining. Remaining cells were combined to produce a heterogenous population for use as fluorescence minus one (FMO) controls.

Cells were incubated in a fixable Live/Dead stain (Thermo Fisher) for 30 minutes at RT, washed twice and blocked in TruStain FcX™ (BioLegend, 101320) Fc block made in FACS buffer for 10 minutes at 4°C. For cell surface protein targets, cells were resuspended in 100µl antibody solutions (

Table 2.18) and incubated in the dark for 30 minutes at 4°C followed by fixation in 4% PFA for 20 minutes at 4°C. Once fixed, cells were resuspended in FACS buffer. Where intracellular staining was required, following surface level staining, cells were subject to gentle fixation in 2% PFA for 10 minutes at RT and then further fixed and permeabilised in 1X fixation/permeabilization buffer from the Foxp3/Transcription Factor Staining Buffer kit (eBioscience, 00-5523-00) o/n at 4°C. Cells were centrifuged at 400 rcf at 4°C for five minutes and washed twice in 1X permeabilization buffer provided in the Foxp3/Transcription Factor Staining Buffer kit (eBioscience, 00-5523-00). Cells were blocked in 2% goat serum in 1X permeabilization buffer for five minutes at RT followed by addition of respective intracellular antibodies (Table 2.18) and stained for 30 minutes in the dark at RT. Cells were centrifuged at 400 rcf at 4°C for five minutes and washed once with 1X permeabilization buffer before being resuspended in FACS buffer ready for analysis.

UltraComp eBeads™ Compensation Beads (Thermo Fisher, 01-2222-41) were used according to the manufacturer's instructions to establish single stained controls for each antibody used. For Live/Dead stains, the ArC™ Amine Reactive Compensation Bead Kit (Thermo Fisher, A10346) was used according to the manufacturer's instructions to establish single stained controls for each Live/Dead stain used.

2.18.3 Blood Samples

Animals were sacrificed via carbon dioxide overdose and blood samples collected immediately after via cardiac puncture. Blood was collected into 1 ml syringes precoated with 0.5M EDTA and transferred to eppendorfs containing 100µl of 0.5M EDTA to prevent coagulation. The same volume of blood per animal was transferred to 10ml of 1X red blood cell (RBC) lysis buffer (Invitrogen, 00-4333-57) and incubated for five minutes at RT. Samples were centrifuged at 300 rcf at 4°C for five minutes and the cell pellet subject to one repeat of the RBC lysis. Following centrifugation once

more, cells were resuspended in 2ml circulating tumour cell (CTC) media comprising a 1:1 mix of high glucose DMEM (Invitrogen, D1145-500ML) and Nutrient Mixture F-12 Ham (Sigma-Aldrich, N6658-500ML) with 20% FBS (Hyclone, Invitrogen) and 100units/ml Pen/Strep (Invitrogen, 15140-122). The cell suspension for each blood sample was transferred to one well of a 6-well plate, pre-coated with 0.1% porcine gelatin (Sigma-Aldrich-Aldrich, G2500) in sterile dH₂O. Cells were incubated at 37°C, 5% CO₂ and 95% humidity for seven days with media changed accordingly.

Staining was carried out in the same way as described for those isolated from solid tissues and included the steps described for intracellular staining (see section 2.18.2) and antibodies used presented in Table 2.18.

Table 2.18. List of flow cytometry antibodies and viable cell staining reagents.

Antigen	Conjugate	Manufacturer	Product code	Clone	Dilution
Live/Dead Red	N/A	Thermo Fisher	L34971	N/A	1:200
CD45	PerCP-Cy5.5	Thermo Fisher	45-0451-82	30-F11	1:200
CD11b	BV605	BD	563015	M170	1:200
Ly-6C	eFluor450	Thermo Fisher	48-5932-82	HK1.4	1:200
Ly6G	APC-Cy7	BD	560600	1A8	1:200
F4/80	APC	Thermo Fisher	17-4801-80	BM8	1:200
MHCII	PE-Cy7	Thermo	25-5321-82	M5/114.15.2	1:200
CD206	FITC	BioLegend	141703	C068C2	1:200
CD11c	BUV395	BD	564080	HL3	1:200
FCεR1α	BUV395	BD	751762	MAR-1	1:200
C-kit	BV421	BD	562609	2B8 (RUO)	1:200
CD3e	APC	Thermo Fisher	17-0031-81	145-2C11	1:200
CD4	FITC	Thermo Fisher	11-0043-81	RM4-4	1:200
CD8a	APC-Cy7	Thermo Fisher	A15386	53-6.7	1:200
CD19	BV650	BioLegend	115541	6D5	1:200
NK1.1	PE-Cy7	BioLegend	108713	PK136	1:200
Foxp3	eFluor450	Thermo Fisher	48-5773-82	FJK-16s	1:100
Ki67	APC	BioLegend	652405	16A8	1:100
Ki67	BUV395	BD	564071	B56	1:100
Annexin V	APC	BioLegend	640920	N/A	1:50
Firefly Luciferase	AlexaFluor647	Abcam	ab23752	EPR17789	1:100
green fluorescent protein (GFP)	PE-Cy7	BioLegend	338014	FM264G	1:100

2.18.4 Data Collection

All data was collected using a Becton Dickinson (BD, Franklin Lakes, NJ, USA) LSRFortessa™ cell analyser with standard filter sets and five lasers. Data was analysed using FlowJo V10.2 software (BD). Gating strategies are detailed in Supplementary Figures 5.2.2, 5.4.1 and 5.4.2.

Briefly, single cells were gated via FSC-A against FSC-H followed by viable cell selection as a Live/Dead® negative population. For immune cell identification, leukocytes were identified by CD45⁺ staining. Pan-myeloid cells were gated as CD11b⁺ and subsequent populations including monocytic cells (Ly6C^{high} Ly6G⁻), granulocytic cells (Ly6C^{low} Ly6G^{high}), and macrophages (Ly6C^{low} F4/80^{high}) were identified from them. Metastasis associated macrophages (MAM) (Ly6C^{low} CD11b⁺), metastasis associated macrophage progenitor cells (MAMPC) (Ly6C^{high} CD11b⁺) and resident macrophages (RMAC) (Ly6C⁻ CD11b^{low}) were identified from CD45⁺ F4/80⁺ populations. Mast cells (FCεR1α⁺ CD117 (c-kit)⁺) were gated from CD45⁺ populations. Lymphocytes (CD3e⁺) were gated from a CD45⁺ population and divided into Cytotoxic T-cells (CD8⁺) and T-helper cells (CD4⁺) populations. Where possible T-regulatory cells (Foxp3⁺) were gated from CD4⁺ T-helper cells. B-Cells (CD19⁺) were also gated directly from CD45⁺ populations. Pan-dendritic cells (CD11c⁺) were also gated directly from CD45⁺ populations. For identification of metastatic cells in the lung, PyMT-BO1 cells were identified as CD45⁻ Native green fluorescent protein (GFP)⁺ anti-GFP⁺ Firefly Luciferase⁺. For metastatic cells in the blood and lung, PyMT-BO1 cells were identified as being CD45⁻, Native GFP⁺, Anti-GFP⁺, Anti-Firefly Luciferase⁺.

2.19 Caecal DNA Extraction

Caecal material or faeces was weighed into MPBio Lysing Matrix E bead beating tubes (MPBio, Santa Ana, USA, 116914050-CF) and extraction was completed according to the manufacturer's protocol for the MPBio FastDNA™ SPIN Kit for Soil (MPBio, 116560200-CF) but extending the beat beating time to three minutes. The DNA recovered from these samples was assessed using a Qubit® 2.0 fluorometer (Invitrogen) and samples diluted using nuclease free water to a concentration of 5ng/μL. Samples were then sent to Illumina for sequencing.

2.20 Shotgun Metagenomics

A modified Illumina Nextera low input tagmentation approach was used. 9μL of TD Tagment DNA Buffer was mixed with 0.09μL TDE1, Tagment DNA Enzyme and 4.01μL PCR grade water in a master mix and 3μL added to a chilled 96 well plate. Genomic DNA was normalised to 0.5ng/μL with 10mM Tris-HCl. 2μL of normalised DNA (1ng total) was pipette mixed with the 5μL of the tagmentation mix and heated to 55 °C for 10 minutes in a PCR block.

A PCR master mix was made up using 4 μ L kapa2G buffer, 0.4 μ L dNTP's, 0.08 μ L Polymerase and 4.52 μ L PCR grade water, contained in the Kap2G Robust PCR kit (Merck Life Science) per sample and 9 μ L added to each well need to be used in a 96-well plate. 2 μ L of each P7 and P5 of Nextera XT Index Kit v2 index primers (Illumina) were added to each well. Finally, the 7 μ L of Tagmentation mix was added and mixed. The PCR was run with 72°C for three minutes, 95°C for one minute, 14 cycles of 95°C for 10 seconds, 55°C for 20 seconds and 72°C for three minutes.

Following the PCR reaction, the libraries were quantified using the Quant-iT dsDNA Assay Kit, high sensitivity kit and run on a FLUOstar Optima plate reader. Libraries were pooled following quantification in equal quantities. The final pool was double-SPRI size selected between 0.5 and 0.7X bead volumes using KAPA Pure Beads (Roche, Burgess Hill, UK). The final pool was quantified on a Qubit 3.0 instrument and run on a D5000 ScreenTape (Agilent) using the Agilent TapeStation 4200 to calculate the final library pool molarity.

The pool was run at a final concentration of 1.5 pM on an Illumina Nextseq500 instrument using a Mid Output Flowcell (NSQ® 500 Mid Output KT v2(300 CYS)) following the Illumina recommended denaturation and loading recommendations which included a 1% PhiX spike in (PhiX Control v3 Illumina Catalogue FC-110-3001). Data was uploaded to Basespace (www.basespace.illumina.com) where the raw data was converted to 8 FASTQ files for each sample.

Dr Rebecca Ansorge, the Gut Microbes and Health in house Bioinformatician at the Quadram Institute, performed the various analyses on data files. Raw reads were trimmed to a quality of phred 20, and adapters and PhiX Illumina standards removed with BBDuk v38.76 (sourceforge.net/projects/bbmap/). Human and mouse contamination was removed from raw reads by using Kraken2 v2.1.0 [579] with a confidence setting of 0.5 and minimum base quality 22 using the human genome GRCh38.p12 and mouse genome GRCm39 as reference databases. Decontaminated reads were trimmed to a quality of phred 20 and adapters removed using fastp v0.21.0 [580]. Clean reads from single samples were concatenated. Taxonomic profiling was performed on the filtered reads using MetaPhlan v3.0 using the settings --unknown_estimation and --add_viruses and the Chocophlan database v30 [581]. Functional profiling was performed with HUMAnN2 v3.0.0.alpha with search mode uniref90, a uniref90 translated search database and using DIAMOND v0.9.24 [582]. The results were normalized to relative abundances and these visualised using a combination of GraphPad Prism V6 and Qlucore Omics Explorer V3.7.

2.21 Caecal Metabolomics

Caecal contents (50-100 mg) were thoroughly mixed with 600-1200 μ L NMR buffer made up of 0.1M phosphate buffer (0.51 g Na₂HPO₄, 2.82 g K₂HPO₄, 100 mg sodium azide and 34.5 mg sodium 3-

(Trimethylsilyl)-propionate-d₄ (1 mM) in 200ml deuterium oxide), centrifuged at 12,000 rcf for five minutes at 4°C and supernatant transferred to 5-mm NMR tubes. Samples were then passed to Dr Gwenaëlle Le Gall of the University of East Anglia who obtained ¹H NMR spectra using a 600MHz Bruker Avance spectrometer fitted with a 5 mm TCI cryoprobe (Bruker, Rheinstetten, Germany). Sample temperature was controlled at 300K. Each spectrum consisted of 64 scans of 65,536 complex data points with a spectral width of 12.5 ppm (acquisition time 2.67 s). The noesypr1d pre-saturation sequence was used to suppress the residual water signal with low power selective irradiation at the water frequency during the recycle delay (D1 = 3 s) and mixing time (D8 = 0.01 s). A 90° pulse length of 9.6µs was set for all samples. Spectra were manually phased, and baseline corrected using the TOPSPIN 2.0 software (Bruker). Dr Le Gall identified and quantified metabolites using Chenomx[®] software NMR suite 7.0[™].

Data interpretation and statistical analysis was subsequently performed by this author using Qlucore Omics Explorer 3.6 software. A two-way way ANOVA test with post-hoc Tukey's range test was performed with a pre-set limit for the respective q-values of ≥0.05 to identify statistically significantly different metabolites.

2.22 Single Cell RNA sequencing

Organs were excised from cervically dislocated animals and tissues were mechanically homogenised using no. 10 scalpels. Homogenate was incubated in collagenase solution (0.2% Collagenase IV (Invitrogen), 0.01% Hyaluronidase (Sigma-Aldrich) & 2.5U/ml DNase I (Sigma-Aldrich) in HBSS) for one hour at 37°C with regular agitation. Supernatant was passed through a 70µm cell strainer and centrifuged for five minutes at 300 rcf/4°C. Pellet was washed twice in PBS and resuspended in 10ml 1X red blood cell lysis buffer (Invitrogen) and incubated for five minutes at RT. Cells were washed once in PBS and resuspended in 10ml FACS buffer (2% FBS in PBS) before being handed to the Earlham Institute sequencing facility where they were run on the 10X Genomics Chromium platform.

2.22.1 Loupe Cell Browser Analysis

BAM files were generated using 10X Genomics Cell Ranger pipeline and imported into Loupe Cell Browser V3.1.0 which generated interactive t-distributed stochastic neighbour embedding (t-SNE) dimension reduction plots. Marker genes expressed by cells of interest, predominantly leukocytes, were searched, by this author, using the "Gene ID" search function to identify in which clusters they were highly expressed. For clusters in which known marker genes were not expressed, gene ontology (GO) searches were subsequently performed on the top 50 upregulated genes using the GO search engines DAVID [583] and PANTHER [584] to ascertain the cell types of which they are

comprised. Finally, the numbers of cells in each cluster between treatment conditions (vehicle control and VNMAA) were compared to identify overt differences in specific cell populations between treatments.

2.22.2 Earlham Institute Expert Bioinformatic scRNAseq Analysis

Matthew Madgwick, a postgraduate student under the supervision of Dr Tamás Korcsmáros, undertook the bioinformatic data analysis of these datasets. BCL files were processed using `bcl2fastq` to create FASTQ files which were demultiplexed using Cell Ranger v2.0 aligned to the mm10 (GRCm38) mouse transcriptome and their = cell and unique molecular identifier (UMI) barcodes extracted. The resulting digital gene expression (DGE) matrices were processed using the R package V1.2.5019 and Seurat V3.0 package [585]. As a quality control step, the DGE matrices were filtered to remove low-quality cells (genes detected in less than five cells and cells where < 200 genes had non-zero counts) and library size normalization to obtain the normalized counts.

Matthew integrated the datasets in Seurat v3.0 [585] using a non-linear transformation of the underlying data and identified anchors from `FindIntegrationAnchors` used to integrate across the datasets. The top 2500 highly variable genes were selected, and the integrated dataset was scaled. Initial clustering was performed using a Louvain algorithm with default parameters within Seurat's `FindClusters` function [585] and a single principle component analysis (PCA) applied to datasets to project onto two dimensions with UMAP clustering.

Matthew performed differential expression analysis using the combined datasets. Genes were identified as differentially expressed in each cluster by comparing the gene expression of cells in the cluster with that of all the other cells. The top differentially expressed genes for each cluster were identified as cluster marker genes and ranked by their adjusted p-values, obtained via Wilcoxon rank sum test and adjusted based on Bonferroni correction, and mean log-fold change. The top cluster marker genes were compared to cell type marker genes identified in the literature and used for cell-type identification [586–588].

2.22.3 Bulk RNAseq Deconvolution

Bulk RNAseq was performed by Matthew Madgwick on samples previously obtained from whole tumours as described in McKee *et al.* (2021) [1]. To estimate the cell type abundances from the heterogeneous bulk expression, BisqueRNA V1.0.5 [589] was used. The reference-based method was implemented which utilizes single-cell data to generate a signature matrix and transformation of bulk expression. These were then plotted using a stacked-bar graph to compare the estimated abundances of the various cell types against those found in the single-cell datasets.

2.23 Mesoscale Discovery (MSD) Multiplex Immuno-arrays

Tissue samples were weighed into Safe-Lock Eppendorf tubes with acid washed glass beads (Sigma-Aldrich Aldrich) with 1ml of homogenisation buffer (500 mM NaCl, 2 mM EDTA, 1% Triton X-100, 0.5% Sodium Deoxycholic Acid, 0.1% SDS, 50 mM Tris HCl and Halt™ Protease and Phosphatase Inhibitor Cocktail (4X) (Thermo Scientific, 78446). Tissues were homogenised using TissueLyser LT at 50 Hz for two minutes and repeated once. Samples were centrifuged at 12,000 rcf for 12 minutes at 4°C and subsequently stored at -80°C until analysed. Protein concentration was then quantified using the BioRad DC protein assay (BioRad) and samples diluted using the Diluent 41 solution from the Mesoscale Discovery V-PLEX Pro-Inflammatory Panel 1 Mouse Kit (MSD, Rockville, MD, USA) so that 100µg of total protein was loaded in a 50µl volume per well on 96-well spot assay plate. Samples were incubated at 4°C on a shaker overnight and the remaining protocol was performed according to the manufacturer's instructions. The plate was read using an MSD QuickPlex SQ 120 imager and data analysed on the MSD Discovery Workbench software V4.0.

2.24 Statistical Analysis

Unless otherwise stated, normality testing was undertaken via a Kolgorov-Smirnov test and P values were generated using Student's t-test (GraphPad Prism, version9) (unpaired, two-tailed, at 95% confidence interval). Where multiple t-tests were performed, a false discovery rate (FDR) of $q < 0.05$, calculated using Bonferroni's method, was used to consider significant observations and the associated P-value presented. All significant observations ($P < 0.05$) have been stated on relevant figures. Where no P-value is presented, it should be assumed that statistical analysis did not identify a significant observation. Where alternate statistical analysis was undertaken, statements regarding such tests are described in the relevant figure legends.

3 Antibiotic administration promotes primary breast cancer tumour growth through a disruption of gut microbiota homeostasis

Unfortunately, many of the clinical treatment pathways used to treat patients with cancer carry with them an increased risk of infection [590,591]. Chemotherapies cause enormous stress on the body and often result in a compromised immune system. For example, a well-documented side effect caused by several chemotherapies is the systemic reduction in neutrophil populations. This induces a state called neutropenia, and significantly increases the risk of bacterial infection [592]. Surgical interventions, such as lumpectomy, mastectomy and breast reconstruction, also carry increased risk of post-surgical infection. Therefore, it is common for clinicians to prophylactically administer antibiotics in an attempt to prevent bacterial infections from occurring [593]. These drugs are usually broad-spectrum, meaning they target both gram-positive and gram-negative bacteria and can therefore kill multiple different species which may otherwise cause an infection [594].

The clinical understanding of the influence prophylactic antibiotic use may have on breast cancer, either directly or indirectly through the effects on the gut microbiota, is poorly described [595]. However, there are several pre-clinical studies involving different cancer types which have shown antibiotic usage increases the factors associated with poor prognoses, such as increased metastasis and reduced response to immunotherapies [555,596]. There is also evidence suggesting that observations like these may translate to humans. Several studies have identified reduced efficacy of immune checkpoint inhibitor therapies, such as anti-PD-1 therapy, in treating melanoma patients with a perturbed microbiota [597,598].

This study sought to assess the effects of an antibiotic induced perturbation of the gut microbiota on breast cancer progression in mouse models. Administration of either a robust antibiotic cocktail or a clinically relevant antibiotic to C57/BL6 animals induced with a luminal-B-like breast cancer model resulted in increased primary tumour volumes in both cases. The robust antibiotic cocktail elicited the same effects in a basal-like model. *In vitro* application of antibiotics did not alter cancer cell proliferation or apoptosis, nor did they promote tumour growth *in vivo* in germ free animals lacking a microbiota. In SPF mice, treatments appeared to increase the proliferative potential of tumour cells but did not influence tumour vascular density or infiltration of immune cell populations traditionally associated with tumourigenesis. Finally, treatments altered the composition and metabolic profile of the gut microbiota, but to varying degrees dependent on the antibiotic administered. This chapter details and discusses these results.

3.1 Growth kinetics of PyMT-BO1 tumours following VNMAA antibiotic treatment

The PyMT-BO1 model had been used in preliminary studies as described in Section 1.5 and has been described by Kirkup (2019) [570]. Briefly, this orthotopic murine model of breast cancer was derived from a spontaneous MMTV-PyMT tumour and resembles a luminal-B subtype of human breast cancer. It also shows similar metastatic patterns compared to human breast cancers in that it metastasises readily to lung and bone tissues in mice.

To support previous experimental data and explore mechanistic links driving increased tumour growth following antibiotic treatment, experiments were setup as previously described by Kirkup (2019). Animals were subject to either a vehicle control (water) or VNMAA treatment one week prior to inducing a PyMT-BO1 breast tumour, with treatment continuing from this point three times weekly until a pre-determined endpoint (10, 13, 15 or 18 days post tumour induction) (Figure 3.1A). Previous experience highlighted inaccuracies of tumour volumes measured *in situ* when compared to measurements obtained post dissection *ex situ*. Therefore, to better understand the growth kinetics of our model, it was necessary to undertake experiments concluding at earlier timepoints to reliably measure tumours *ex situ* and plot more accurately the changes in tumour volumes overtime. Several experiments were setup independently, with tumours harvested at endpoints of either 10-, 13-, 15- or 18-days post tumour induction.

At the earliest timepoint, day 10, the mean tumour volumes of both control and VNMAA groups were similar ($\sim 200\text{mm}^3$) with the VNMAA arm non-significantly reduced relative to the control group (Figure 3.1B). At day 13, the means were almost identical ($\sim 350\text{mm}^3$) but after this timepoint a shift in growth rate appears to occur and, at day 15, tumour growth from VNMAA treated animals increase significantly relative to controls (Figure 3.1B). While the difference in tumour growth between control and VNMAA treated animals continues to day 18, at this timepoint the tumours reach sizes beyond ones deemed ethically appropriate and no further primary tumour experiments were taken to this timepoint under the VNMAA treatment regimen. Figure 3.1C presents these changes in growth kinetics overtime and includes the associated P-values from unpaired t-tests relevant to each timepoint.

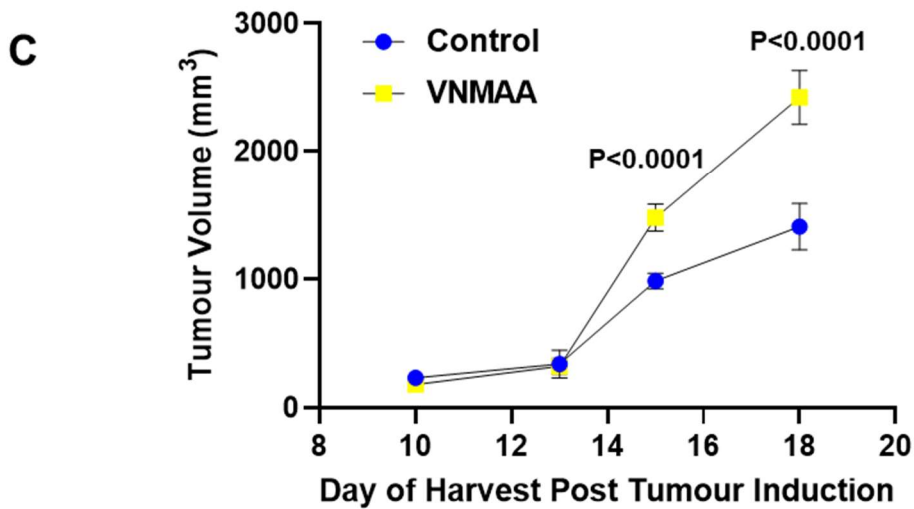
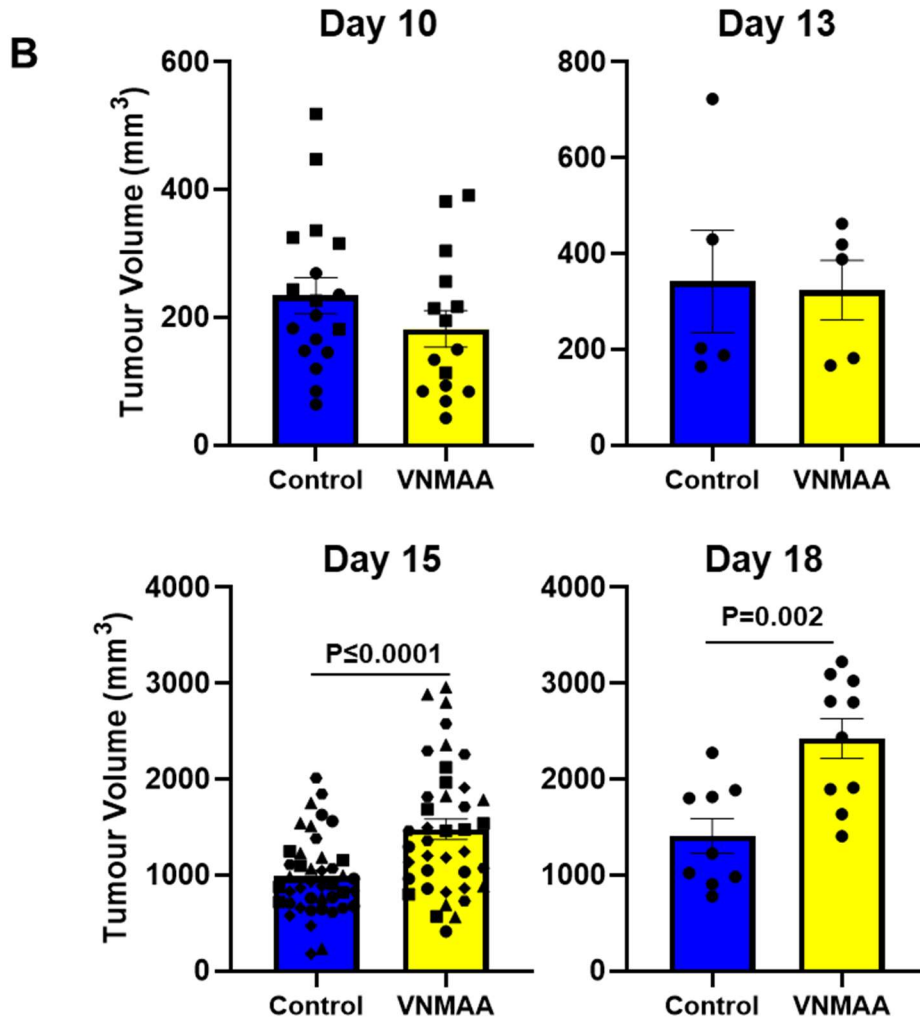
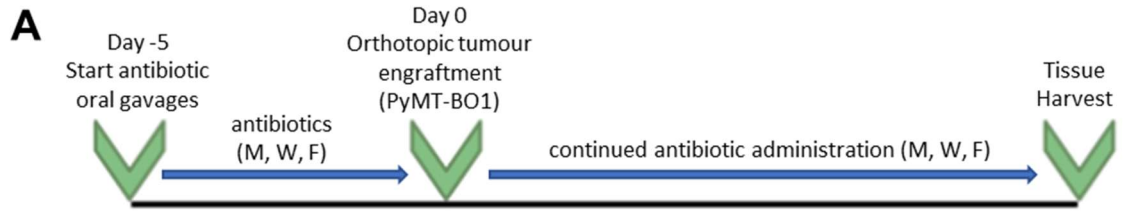


Figure 3.1. VNMAA administration influences tumour growth kinetics in PyMT-BO1 tumours. **A)** Schematic of VNMAA antibiotic treatment regimen detailed in Section 2.4. Antibiotic administration begins one week prior to PyMT-BO1 tumour induction and continues for the duration of the experiment three times per week until experiment cessation. **B)** Bar graphs depicting PyMT-BO1 tumour volumes measured *ex situ* at different timepoints. Graphs show the mean (\pm SEM) tumour volumes from control and VNMAA treated animals at day 10 (N=2, n \geq 15 animals per condition, P=0.2085, difference between means (DBM)=-52.15, SEM=40.6), day 13 (N=1, n=5 animals per condition, P=0.8887, DBM=-17.83, SEM=123.5), day 15 (N=5, n \geq 40 animals per condition, P \leq 0.0001, DBM=492.5, SEM=120.9) and day 18 (N=1, n \geq 9 animals per condition, P=0.002, DBM=1015, SEM=278.9) post tumour induction. Significantly different P-values are stated on relevant graphs. Points of the same shape between conditions are from the same experiment (N). **C)** XY plot showing differences in tumour growth kinetics overtime based on mean tumour volumes (\pm SEM) from VNMAA and control animals at different timepoints based on tumour volume data presented in panel **B** with respective P-values following a two-way ANOVA (p<0.0001) and Sidak's multiple comparison test (Day10 P=0.9965, DBM=52.15; Day13 P>0.9999, DBM=17.83; Day 15 P<0.0001, DBM=-492.5; Day18 P<0.0001, DBM=-1015).

3.2 Increased tumour progression is microbiota-dependent and not the direct result of antibiotic administration

While it was clear that the administration of antibiotics promoted primary tumour growth, it was unclear whether this was the direct influence of the antibiotic compounds or their downstream disruption of the gut microbiota. The proliferative potential of breast cancer is used to indicate the aggressiveness of tumours and, particularly in oestrogen receptor positive (ER+) breast cancer, is often used to guide clinical decisions regarding treatment pathways. The expression of the nuclear protein, Ki67, is positively associated with cell proliferation and is used as a proliferative index when diagnosing patients with breast cancer [98,599]. Conversely, the presence of phosphatidylserine on the surface of cells occurs during apoptosis. Annexin V binds cell surface phosphatidylserine in the presence of calcium and can be used to identify apoptotic cells [600]. Thus, to investigate any potential direct effects of antibiotics on cancer cell proliferation, PyMT-BO1 cells were cultured in media containing reducing concentrations of the VNMAA antibiotic cocktail, starting at the same concentration administered to animals, and subjected to flow cytometric analysis of Ki67 and Annexin V staining to investigate any changes in cell proliferation or occurrence of apoptosis respectively.

Analysis found there were no significant changes in the median fluorescence intensity (MFI) of Ki67 (Figure 3.2A) nor was there a clear trend suggesting an antibiotic-dependent effect on apoptosis ($P > 0.05$; t-test) (Figure 3.2B). While these results begin to support the hypothesis that the microbiota is a key player in regulating tumour progression, this work alone is insufficient to confirm this hypothesis due to the complex nature of the multiple systems involved in this model.

Germ free animals are born and bred in sterile conditions and are completely free of any microbes meaning they do not have a gut microbiota [601,602]. Therefore, an experiment, identical in workflow to previous experiments, was setup to investigate the effect of the VNMAA cocktail in tumour progression in germ free animals. At 15-days post tumour induction tumour volumes showed no significant differences between antibiotic treated animals and control counterparts (Figure 3.2C). Taken together with the *in vitro* study, these results suggest that antibiotics are not directly responsible for the increased tumour growth but that the effects they have on the gut microbiota are driving the increased rates of tumour progression.

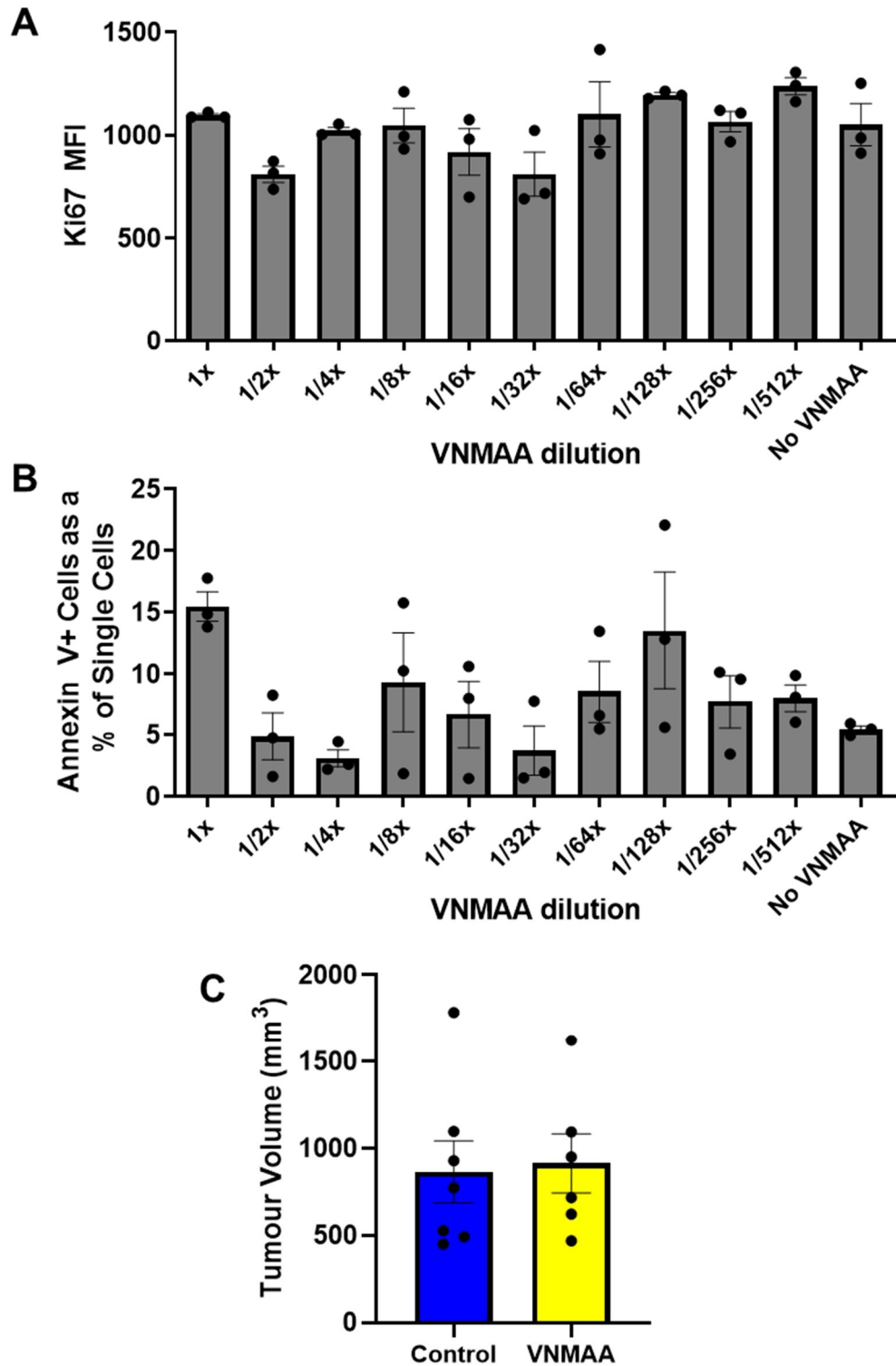


Figure 3.2. Antibiotic administration does not directly promote cancer cell proliferation *in vitro* or tumour progression *in vivo* in germ free mice. Bar graphs showing mean (\pm SEM) **A**) MFI of Ki67 expression and **B**) the percentage of single cells which bound Annexin V in PyMT-BO1 cells cultured in media containing reducing concentrations of VNMAA, starting at the concentrations administered to animals during *in vivo* experiments (1X) (N=1, n=3 animals per condition). **C**) Bar graph showing mean (\pm SEM) PyMT-BO1 tumour volumes from tumours taken from control and VNMAA treated germ free animals 15 days post tumour induction (N=1, n \geq 6 animals per condition, P=0.849, DBM=48.4, SEM=248.3).

3.3 Early tumour immune infiltration shows no differences following VNMAA antibiotic treatment

Previous studies considered immune influence on tumour progression at late stages in tumour progression [570]. At these timepoints there was no evidence that antibiotic-induced disturbances of the gut microbiota resulted in changes to the abundance of immune cell types typically associated with tumourigenic influence. Due to the known pro-tumour role that inflammation plays in the early stages of tumour establishment it was possible that later timepoint experiments had missed early differences in immune activity. Additionally, immune infiltration observations may be skewed when comparing cell abundances in tumours with significantly different sizes. Therefore, the day-10 timepoint was used to consider early immune activity in tumours from VNMAA and control groups due to both its early stage of tumour development and the similarity in tumour volumes observed at this stage. As had been previously observed in experiments which ended at the later stage of 15 days post tumour induction, flow cytometry of whole tumours did not identify any evidence of significant changes in either myeloid or lymphoid immune compartments following VNMAA treatment which may have been involved in driving tumour growth (Figure 3.3).

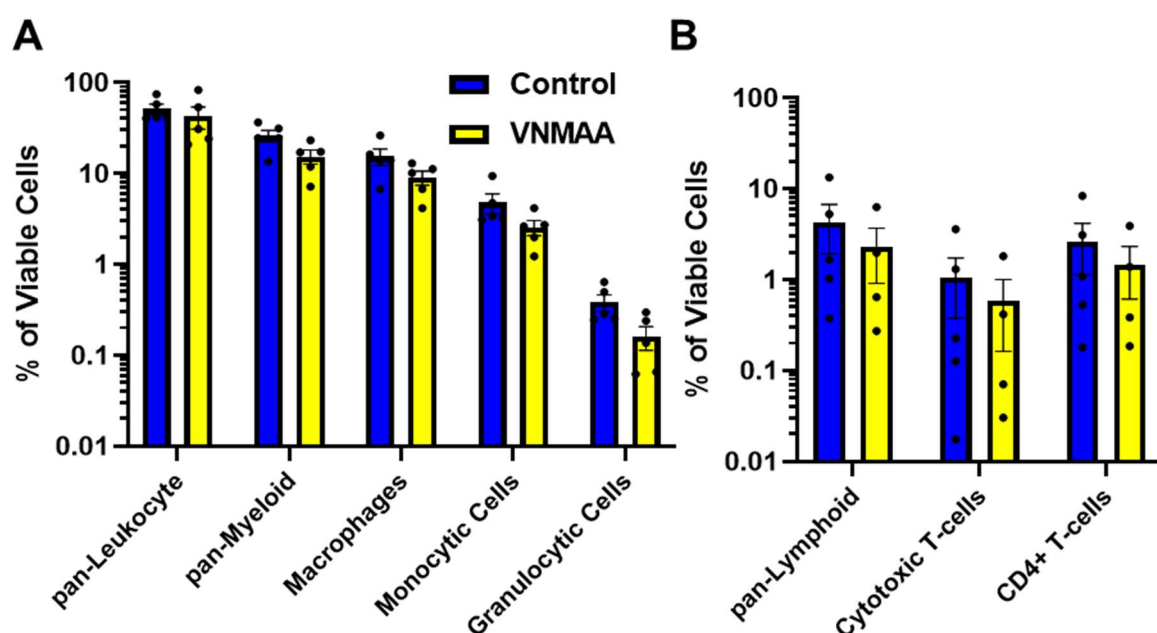


Figure 3.3. VNMAA administration does not influence immune cell tumour infiltration at an early timepoint. Bar graphs showing mean abundances (\pm SEM) of tumour infiltrating **A**) myeloid cells ($N=1$, $n=5$ animals per condition) including pan-Leukocytes ($P=0.546$, $q=0.551$), pan-Myeloid ($P=0.053$, $q=0.135$), Macrophages ($P=0.107$, $q=0.153$), Monocytic cells ($P=0.122$, $q=0.153$) and Granulocytic cells ($P=0.041$, $q=0.135$) and **B**) lymphoid cells ($N=1$; $n\geq 4$ animals per condition), including pan-Lymphoid cells ($P=0.516$, $q=0.604$), Cytotoxic T-cells ($P=0.598$, $q=0.604$) and CD4+ T-cells ($P=0.549$, $q=0.604$), in PyMT-BO1 tumours from control and VNMAA treated animals harvested 10 days post tumour induction. Abundances are presented as a percentage (%) of viable cells.

3.4 VNMAA-induced microbiota perturbation promotes tumour growth in at least two models of breast cancer

Breast cancer is an extremely heterogenous disease with several molecular subtypes classed according to the presence or absence of several receptors (see Section 1.1.3). The pathophysiology of the disease is dependent on these classifications as is patient prognosis and treatment pathway. Therefore, to assess whether or not the observations made in Section 3.1 were exclusive to the luminal model used previously, it was necessary to substitute the PyMT-BO1 model for one resembling an alternate molecular subtype of the disease. Kirkup (2019) had shown that, in two experiments, VNMAA treatment also increased tumour growth in an orthotopic basal-like model of breast cancer induced using spontaneously-derived murine breast cancer cells, coined EO771 [570,603,604]. However, no immune profiling of the tumour infiltrating immune cells were performed in this model. To improve the robustness of those observations and to assess possible differences in immune infiltration between treatment groups, a third experiment was undertaken with the addition of immune profiling through flow cytometry. The same experimental workflow was undertaken but due to the slower growth kinetics of this model, a longer growth phase of 26 days compared to 15 days in the PyMT-BO1 model was required (Figure 3.4A). Upon excision, and when combined with measurements from the two previous experiments, tumour volumes were again significantly increased relative to controls (Figure 3.4B). This confirms that the observations regarding tumour growth are not limited to just one model. Additionally, similarly to observations made in the PyMT-BO1 model, low-level flow cytometric immune profiling of tumour infiltrating leukocytes did not identify evidence of changes in the abundances of cells from either the myeloid or lymphoid immune compartments being associated with the increased rate of tumourigenesis (Figure 3.4 C and D).

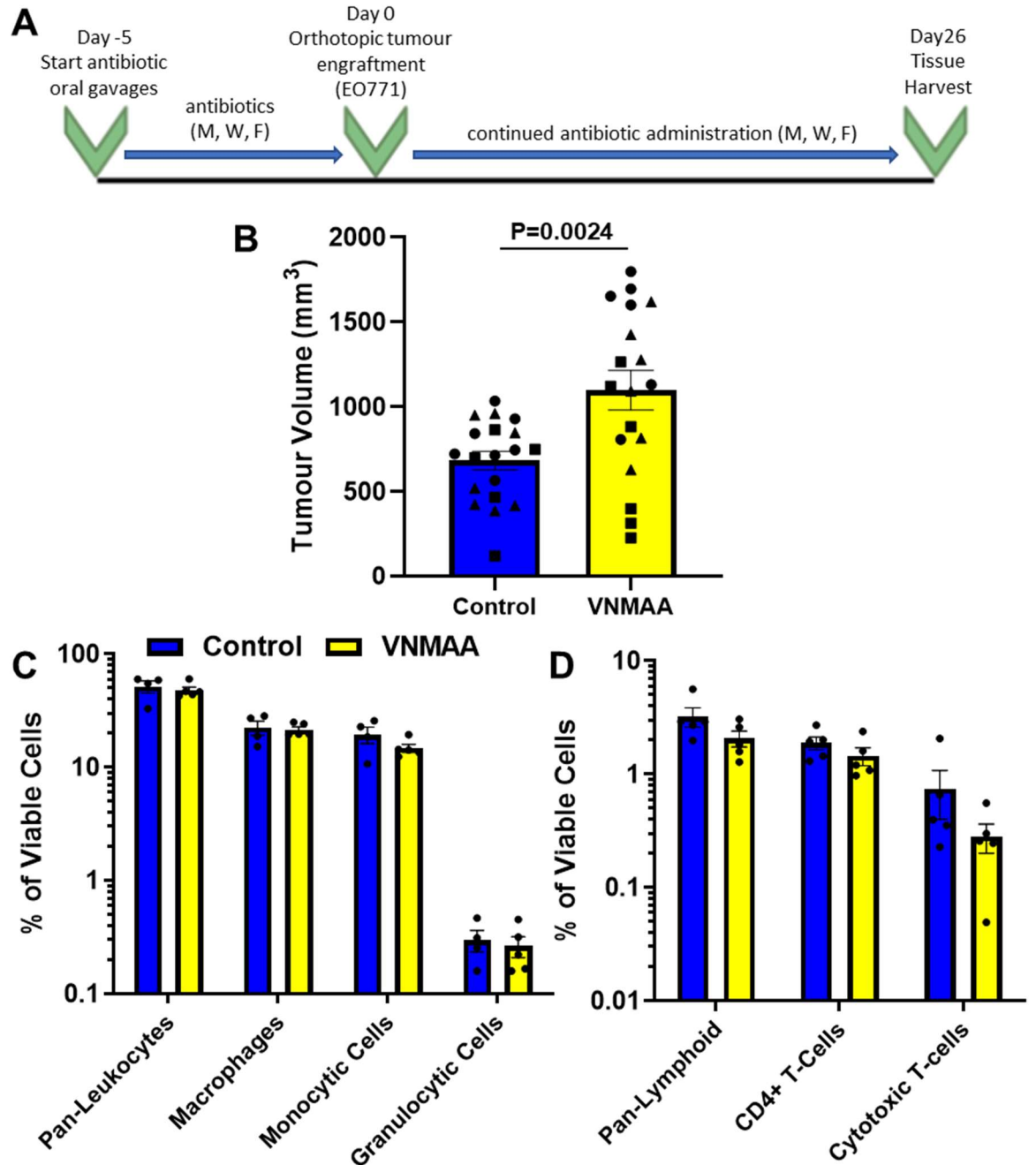


Figure 3.4. VNMAA treatment promotes tumour growth in the EO771 basal-like model of breast cancer without influencing infiltrating immune cell populations traditionally associated with tumourigenesis. **A)** Schematic of VNMAA antibiotic treatment regimen detailed in Section 2.4. Antibiotic administration begins one week prior to EO771 tumour induction and continues for the duration of the experiment three times per week until experiment cessation at 26 days post tumour induction. **B)** Bar graph showing mean (\pm SEM) *ex situ* EO771 tumour volumes following VNMAA treatment (N=3, $n \geq 18$ animals per condition, $P=0.0024$, $DBM=414.9$, $SEM=126.7$). Bar graphs showing mean (\pm SEM) abundances of **C)** myeloid cells (N=1; $n \geq 4$ animals per condition), including pan-Leukocytes ($P=0.599$, $q=0.812$), Macrophages ($P=0.803$, $q=0.812$), Monocytic cells ($P=0.183$, $q=0.738$) and Granulocytic cells ($P=0.695$, $q=0.812$) and **D)** lymphoid cells (N=1; $n=5$ animals per condition), including pan-Lymphoid cells ($P=0.139$, $q=0.258$), Cytotoxic T-cells ($P=0.224$, $q=0.258$) and CD4+ T-cells ($P=0.256$, $q=0.258$), in EO771 tumours harvested 26 days post tumour induction following VNMAA treatment. Abundances are presented as a percentage (%) of viable cells.

3.5 A clinically relevant antibiotic, cephalexin, promotes PyMT-BO1 tumour growth in a similar fashion to VNMAA

The VNMAA cocktail combines several broad-spectrum antibiotics which, when administered together, severely perturb the gut microbiota to a degree unlikely to be experienced by patients in clinic. Therefore, to strengthen the clinical relevance of these observations, clinical collaborators in the UK and the US were consulted and advised that cephalexin, a broad-spectrum first-generation cephalosporin antibiotic, is often used at various stages within the breast cancer treatment pathway, including prophylactically. Thus, cephalexin was substituted in place of the VNMAA cocktail.

Patient relevant doses (35mg/kg) [605] were administered in the same fashion as described in Figure 3.1A and, upon harvest at 15 days post tumour induction, the tumour volumes of cephalexin treated animals were significantly increased compared to tumours from animals treated with a vehicle control (Figure 3.5A). Additionally, flow cytometry of tumour infiltrating immune cells did not highlight any evidence of either the myeloid (Figure 3.5B) or lymphoid (Figure 3.5C) immune compartments being involved in driving tumour growth. A result consistent with those from VNMAA experiments in both PyMT-BO1 and EO771 breast cancer models.

There is a relatively large difference between the number of tumour volumes presented and the number of tumours subject to flow cytometry (5 per treatment). This is largely due to samples being required for other applications in addition to flow cytometry, such as histology and western blot. Additionally, previous attempts at running flow cytometry of tumours had failed due to poor antibody staining hence the number of individual experiments stands at one for this treatment comparison. However, based on the relatively tight grouping of samples in terms of consistently small SEM values for all profiled cell types as well as observations made in previous flow cytometry experiments for the VNMAA treatment experiments, in both PyMT-BO1 and EO771 models, these data strongly support that there is no evidence that the profiled immune cells are involved in driving the increase in tumour growth.

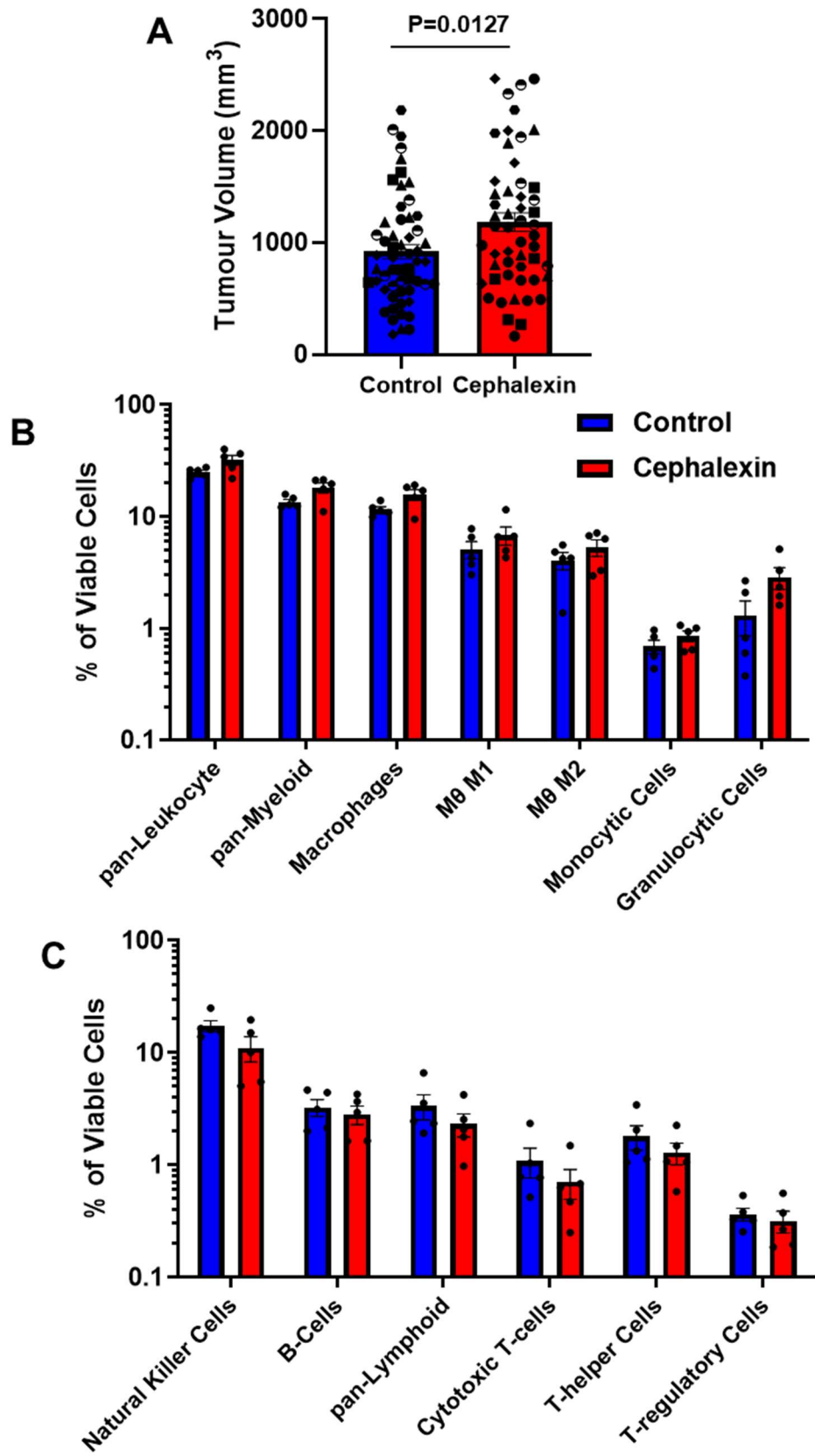


Figure 3.5. Treatment with a clinically relevant antibiotic, cephalexin, promotes tumour growth without influencing tumour infiltration of immune cells. **A)** Bar graph showing mean (\pm SEM) *ex situ* PyMT-BO1 tumour volumes from control and cephalexin treated animals 15 days post tumour induction (N=7, n \geq 53 animals per condition, P=0.0127, DBM=263.3, SEM=103.9). Points of the same shape between conditions are from the same experiment (N). Bar graphs showing mean (\pm SEM) abundances of tumour infiltrating **B)** myeloid cells (N=1; n=5 animals per condition), including pan-Leukocytes (P=0.071, q=0.143), pan-Myeloid (P=0.052, q=0.143), Macrophages (P=0.055, q=0.143), M1 Macrophages (P=0.297, q=0.312), M2 Macrophages (P=0.309, q=0.312), Monocytic cells (P=0.256, q=0.312) and Granulocytic cells (P=0.081, q=0.143) and **C)** lymphoid cells (N=1; n=5 animals per condition), including Natural Killer cells (P=0.104, q=0.543), B-cells (P=0.585, q=0.6), pan-Lymphoid (P=0.326, q=0.543), Cytotoxic T-cells (P=0.346, q=0.543), T-helper cells (P=0.358, q=0.543) and T-regulatory cells (P=0.594, q=0.6), in PyMT-BO1 tumours from control and cephalexin treated animals harvested 15 days post tumour induction. Abundances are presented as a percentage (%) of viable cells.

3.6 Tumour cell proliferation is increased following antibiotic treatment

The use of Ki67 as a diagnostic and prognostic tool has been described in Section 3.2 [98,599]. To assess the effect of both antibiotic treatments on the proliferative potential of our model *in vivo*, tumour sections were immunohistochemically stained for Ki67 (Figure 3.6A). Quantification of the proliferative potential of tumour cells was calculated by the mean percentage of Ki67 positive (Ki67⁺) cells per frame from two frames per tumour. Both VNMAA and cephalixin treatments resulted in significantly increased numbers of Ki67⁺ cells in tumour sections, showing antibiotic administration promoted tumour cell proliferation *in vivo* (Figure 3.6B).

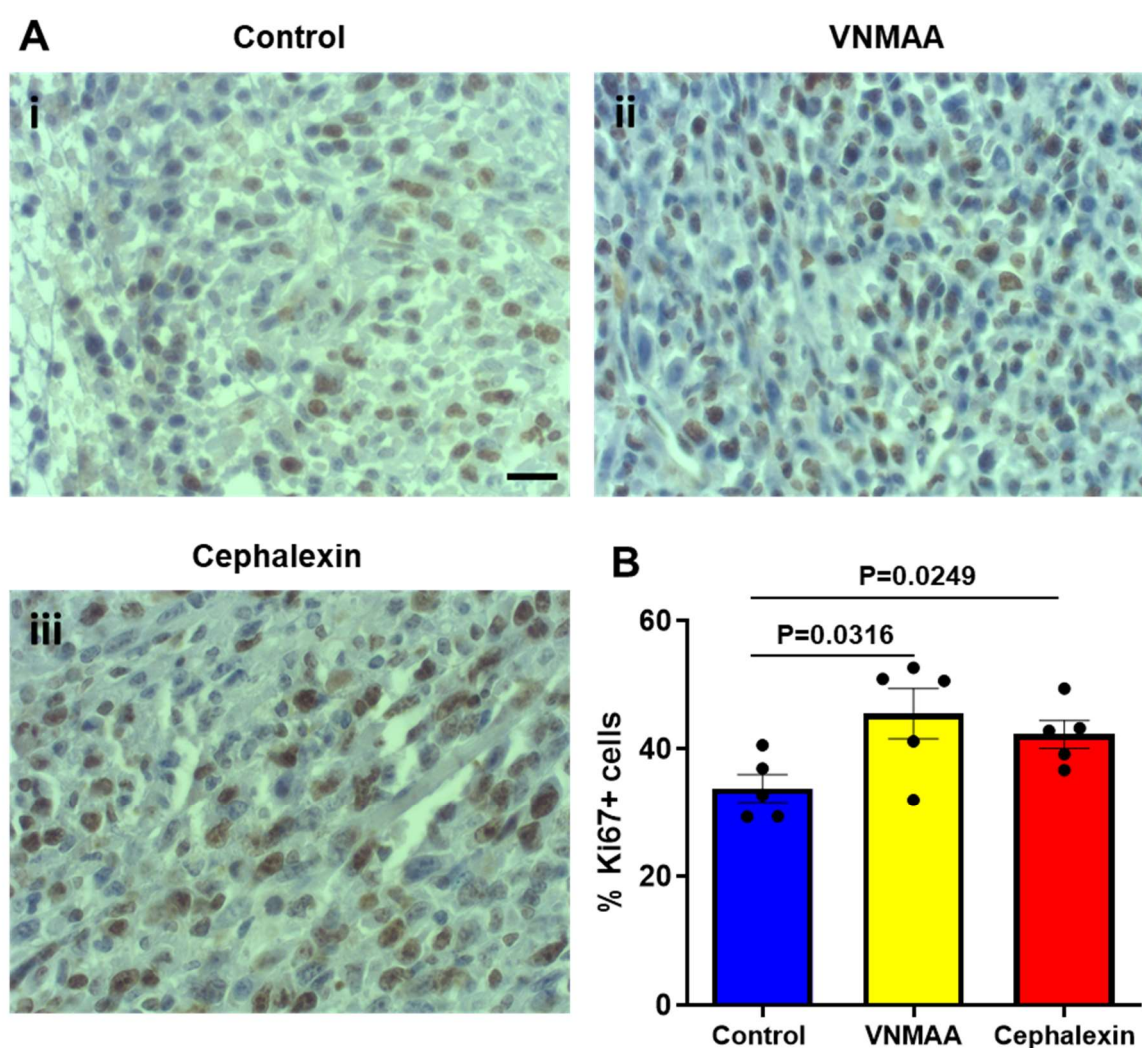


Figure 3.6. Expression of the proliferation marker, Ki67, is increased in tumours following antibiotic treatments. A) Representative immunohistochemical staining of Ki67 (denoted by presence of brown stain) in tumour sections from i) control, ii) VNMAA and iii) cephalixin treated animals; scale bar = 20 μ m. **B)** Bar graph showing the mean (\pm SEM) percentage of Ki67⁺ cells from two frames per tumour from animals treated with a vehicle control, VNMAA or cephalixin (N=1, n=5 animals per condition; Control Vs. VNMAA P=0.0316, DBM=11.72, SEM=4.505; Control Vs. Cephalixin P=0.0249, DBM=8.494, SEM=3.083).

3.7 Blood vessel density is unchanged following antibiotic treatment

A classical hallmark of tumour growth and progression is the expansion of the tumour vasculature; angiogenesis [606,607]. Angiogenesis can be considered a rate limiting step in tumour growth and is often hijacked by tumours to overcome the limited oxygen supply, associated tissue growth, whilst also serving as a source of growth factors and means of metastatic dissemination. One measure of angiogenesis is the histological evaluation of intra-tumoural micro vessel density [608,609]. Staining of endomucin, a protein expressed by endothelial cells, was undertaken to identify vascular structures in tumour sections from control, VNMAA or cephalixin treated animals (Figure 3.7A). In all treatment groups, vessel density was at its highest around tumour peripheral edges. Thus, four frames per tumour were acquired from the top, bottom, left and right of tumour sections along the section periphery for quantification. Blood vessels were counted in each of the four frames from one section per tumour and the mean vessel count calculated for each tumour prior to quantifying vessel density relative to control tumours (Figure 3.7B). While vessel densities in the cephalixin treatment arm were similar to those in the control cohort, there was a slight increase in vessel densities in tumours from the VNMAA treatment arm. However this was statistically non-significant.

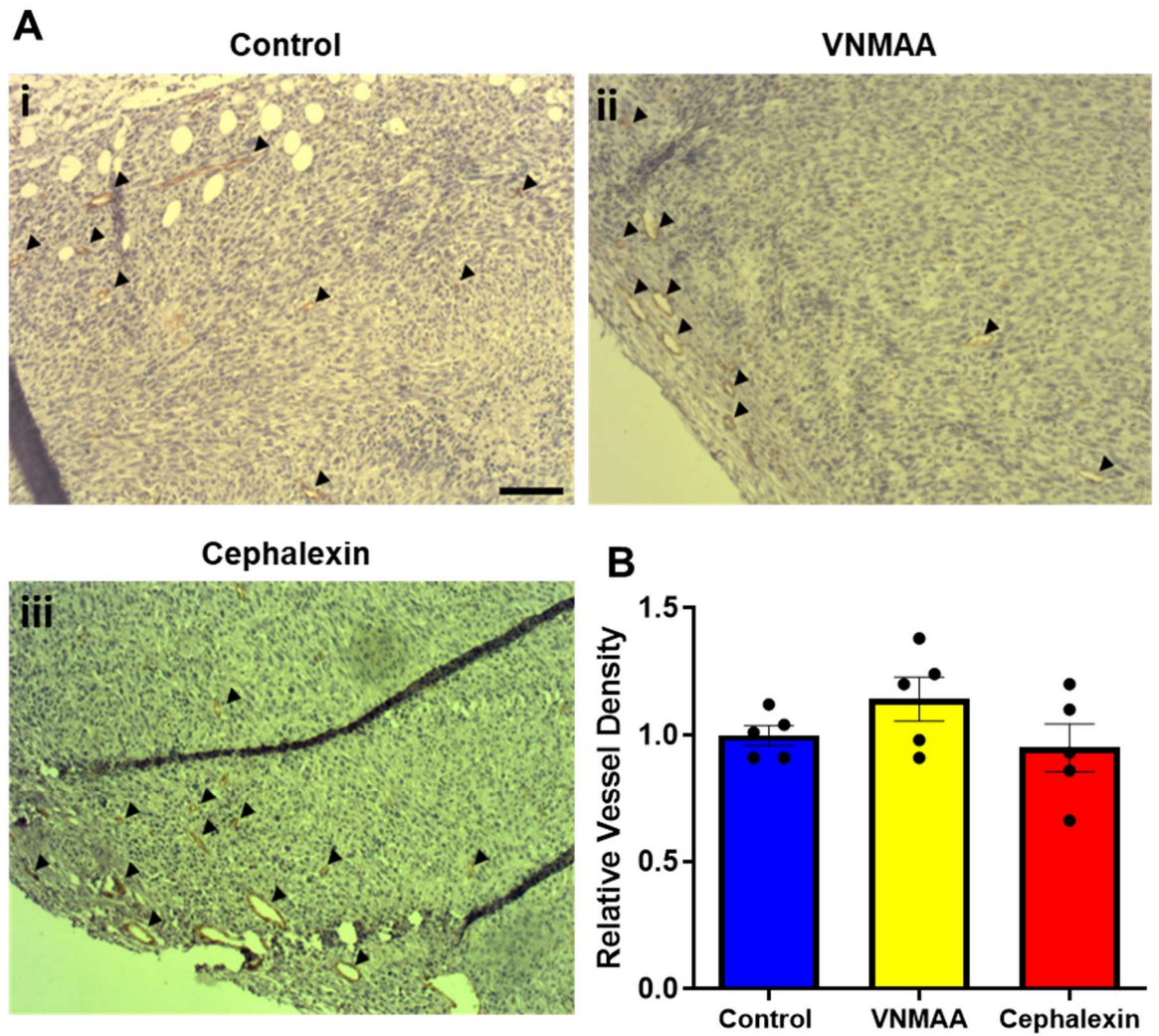


Figure 3.7. Blood Vessel density in tumours is unchanged following respective antibiotic treatment. A) Representative immunohistochemical staining of endomucin (denoted by black arrow heads) in tumour sections from **i)** control, **ii)** VNMAA and **iii)** cephalixin treated animals; scale bar = 100 μ m. **B)** Bar graph showing mean (\pm SEM) vessel density of tumours relative to the mean of control tumours calculated from mean vessel counts in four frames per tumour from animals treated with a vehicle control, VNMAA or cephalixin (N=1, n=5 animals per condition; Control Vs. VNMAA P=0.17, DBM=0.144, SEM=0.095; Control Vs. Cephalixin P=0.652, DBM=-0.048, SEM=0.102).

3.8 Both VNMAA and cephalexin perturb the murine gut microbiota with the common loss of several bacterial species

Previous studies had employed 16S rRNA sequencing of faecal samples in an attempt to profile the bacterial communities of the microbiota in antibiotic treated animals. Following VNMAA treatment, there was no detectable amplification of 16S rRNA from faecal pellets, suggesting an antibiotic-induced bacterial knockdown, while cephalexin treatment was shown to reduce the abundances of bacteria from the genera *Lactobacillus*, *Faecalibaculum* and *Alistipes* [570]. However, at the time of sequencing, this method of taxonomic profiling was limited to the genus level and could not infer species specific changes. Shotgun whole genome sequencing (WGS) sequences all genomic DNA in a sample, rather than just the 16S rRNA genes, provides a species and strain level taxonomic classification as well as detailing metabolic function based on the abundances of associated gene reads [610]. Therefore, for an improved profiling of the microbiota, following either VNMAA or cephalexin treatment, caecal DNA was subject to shotgun WGS and taxonomic profiles compared to those from a control cohort. Support was provided by the Quadram bioinformatics team, predominantly Dr Rebecca Ansoorge, who sent the extracted DNA samples for sequencing and undertook bioinformatic analysis. Subsequent data interpretation was undertaken by this author.

A total of 52 species were identified from the 21 samples sequenced. Similar to results described by Kirkup (2019), in which VNMAA treatment appeared to cause a near complete ablation of the bacterial element of the gut microbiota [570]. WGS identified that, of the genetic material present in samples from VNMAA treated animals, the vast majority of it was viral as well as a small portion from the fungal phyla of Ascomycota (Figure 3.8A). Relative to these two taxonomic groups, a miniscule number of reads were identified as being from the bacterial phyla of Bacteroidetes and Firmicutes which are typically the two major phyla contributing to the bacterial component of a normal microbiota. Cephalexin treatment resulted in a far less aggressive reduction of bacterial communities but did cause a shift in the ratio of Firmicutes to Bacteroidetes (F/B) in favour of Bacteroidetes, from 3:1 to 1:2, as well as an increase in the relative abundance of Verrucomicrobia compared to control samples (Figure 3.8A).

Due to the ablation of the microbiota following VNMAA treatment, and in order to identify bacterial species which are mutually reduced in both VNMAA and cephalexin, a two-group comparison of control samples versus antibiotic samples, from both VNMAA and cephalexin, was undertaken. Setting a threshold FDR of 5% ($q=0.05$) identified only two species which were significantly reduced ($P<0.0011$) in both antibiotic groups compared to control: *Anaerotruncus* sp. G3(2012) and *Enterorhabdus caecimuris* (Figure 3.8B). Review of these species in current literature did not link

them to cancer or any other inflammatory diseases associated with microbiota changes. However, when the FDR threshold was relaxed ($q=0.2085$) to consider all species where $P<0.05$, an additional nine species were observed to be reduced in both VNMAA and cephalixin groups relative to controls, namely *Turicimonas muris*, *Faecalibaculum rodentium*, *Asaccharobacter celatus*, *Adlercreutzia equolifaciens*, *Lactobacillus reuteri*, *Lactobacillus taiwanensis*, *Lachnospiraceae bacterium*, *Jeotgalicoccus halotolerans* and *Corynebacterium stationis* (Figure 3.8C). These include two species of the genus *Lactobacillus*, *L. reuteri* and *L. taiwanensis*, as well as *F. rodentium* which links well with the previous 16S data described by Kirkup who identified reductions in both *Lactobacillus* and *Faecalibaculum* genera in faecal samples following cephalixin treatment.

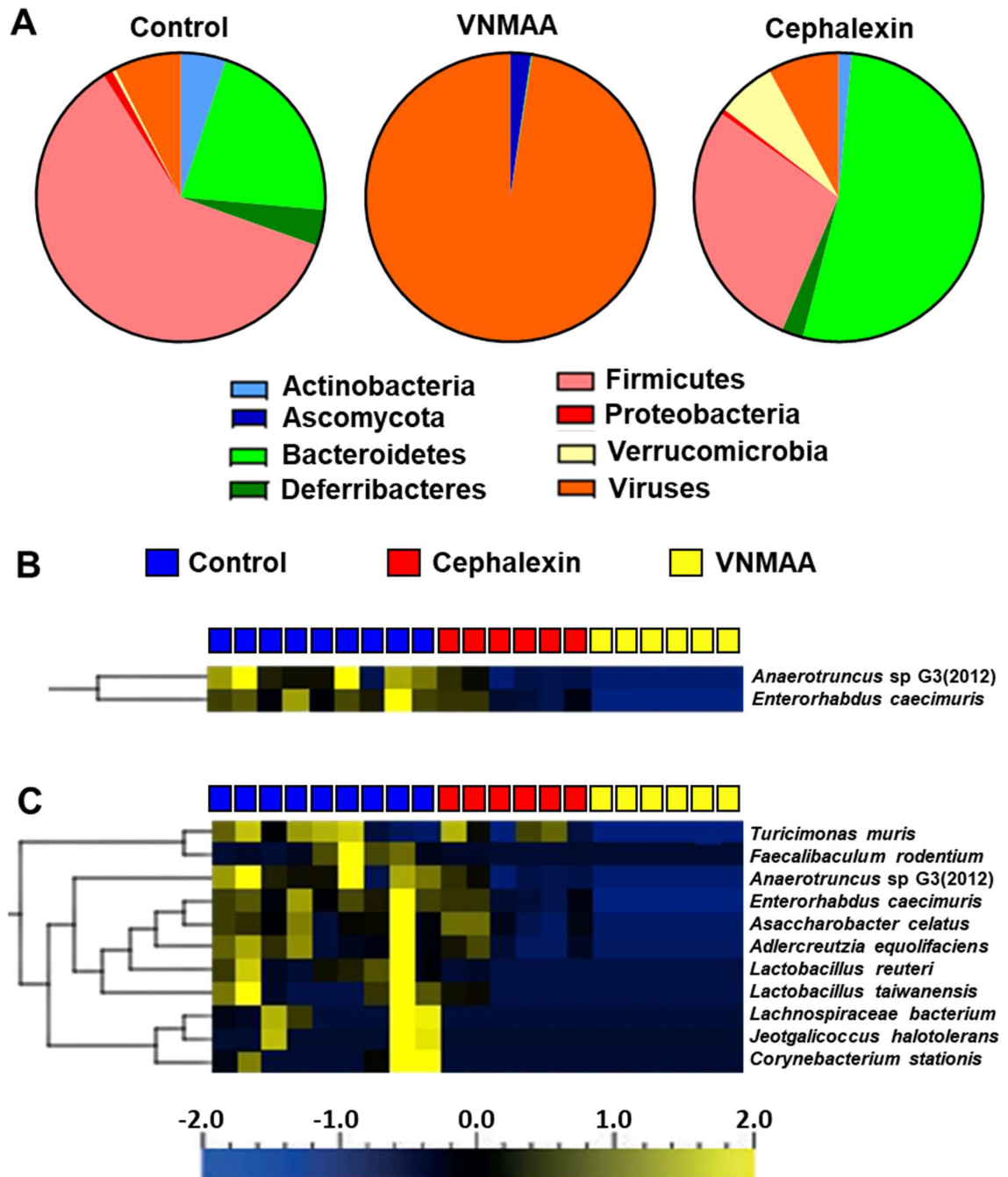


Figure 3.8. Both VNMAA and cephalixin antibiotic treatment perturb the gut microbiota but to varying degrees, with the common loss of several bacterial species. **A)** Pie charts of WGS datasets (N=2) showing the mean phyla-level relative abundances of microbes in caecal samples from control (n=9), VNMAA (n=6) and cephalixin (n=6) treated animals. **B)** Filtered heatmap showing hierarchically clustered bacterial species with significantly different relative abundances following a two-group comparison of both VNMAA and cephalixin samples versus controls ($P < 0.001$, $q \leq 0.05$); (N=2, $n \geq 6$); colour ratio shown according to Log_2 fold change. **C)** Filtered heatmap showing hierarchically clustered relative abundances of bacterial species following a two-group comparison, with a relaxed FDR q-statistic, of both VNMAA and cephalixin samples versus controls ($P = 0.05$, $q = 0.2085$); (N=2, $n \geq 6$); colour ratio shown according to Log_2 fold change.

3.9 Antibiotic treatments alter the metabolic profile of the gut microbiota

The function of the gut microbiota depends largely on its metabolic activity in processing nutrients, such as complex carbohydrates, into metabolites which can be used in cellular processes such as glucose regulation and lipid metabolism [611–613]. Many of these metabolic products are associated with beneficial health outcomes. For example, the SCFA butyrate has been shown to reduce proliferation of cancer cells through epigenetically inhibiting histone deacetylase (HDAC), preventing gene transcription and promoting apoptosis [542,563,564]. Therefore, disruption of gut homeostasis could lead to a “loss of function” in the microbiota and facilitate disease progression. Thus, profiling of metabolites in caecal samples from control, VNMAA and cephalixin treated animals was undertaken using ^1H NMR spectroscopy. To achieve this, support was sought from Dr Gwenaelle Le Gall of the University of East Anglia who performed undertook the sample running on the spectrophotometer and downstream metabolite identification and quantification. All subsequent analysis was undertaken by this author.

Principal components analysis (PCA) illustrated that while the samples from VNMAA treated animals clustered together and separately from the other treatment groups, the cephalixin samples generally had a metabolite profile more similar to control samples than to those of the VNMAA group (Figure 3.9A), demonstrating the dramatic influence of VNMAA treatment on the microbiota compared to a clinically relevant antibiotic. A total of 93 metabolites were identified across the 14 samples sent for analysis. A one-way analysis of variance (ANOVA) test with a pre-set corrected FDR ($q < 0.05$) identified that, of these 93 metabolites, 50 were significantly different from each other ($P < 0.025$). Heat mapping of these metabolites with hierarchal clustering clearly illustrated the changes in metabolite abundances between the VNMAA and control treatment groups (Figure 3.9B). VNMAA treatment results in an increase in several amino acids including valine, leucine, tryptophan and glutamine, and complex carbohydrates, including raffinose and stachyose. Conversely, it causes a depletion in the SCFAs, acetate, propionate and butyrate, as well as in simple sugars such as glucose and ribose. However, the metabolic impact of cephalixin is less clear, and samples do not appear to follow the same trend observed in the VNMAA samples. While two of the four samples did show a similar increase in the amino acids observed in VNMAA samples, generally there were few differences between the control and cephalixin samples. Thus, a post-hoc Tukey’s range test was performed to better identify how these abundances differ between groups and showed that only three metabolites, caprylate, adenosine monophosphate and 2-methylbutyrate, were significantly reduced in both VNMAA and cephalixin treatment groups (Supplementary Figure 3.9).

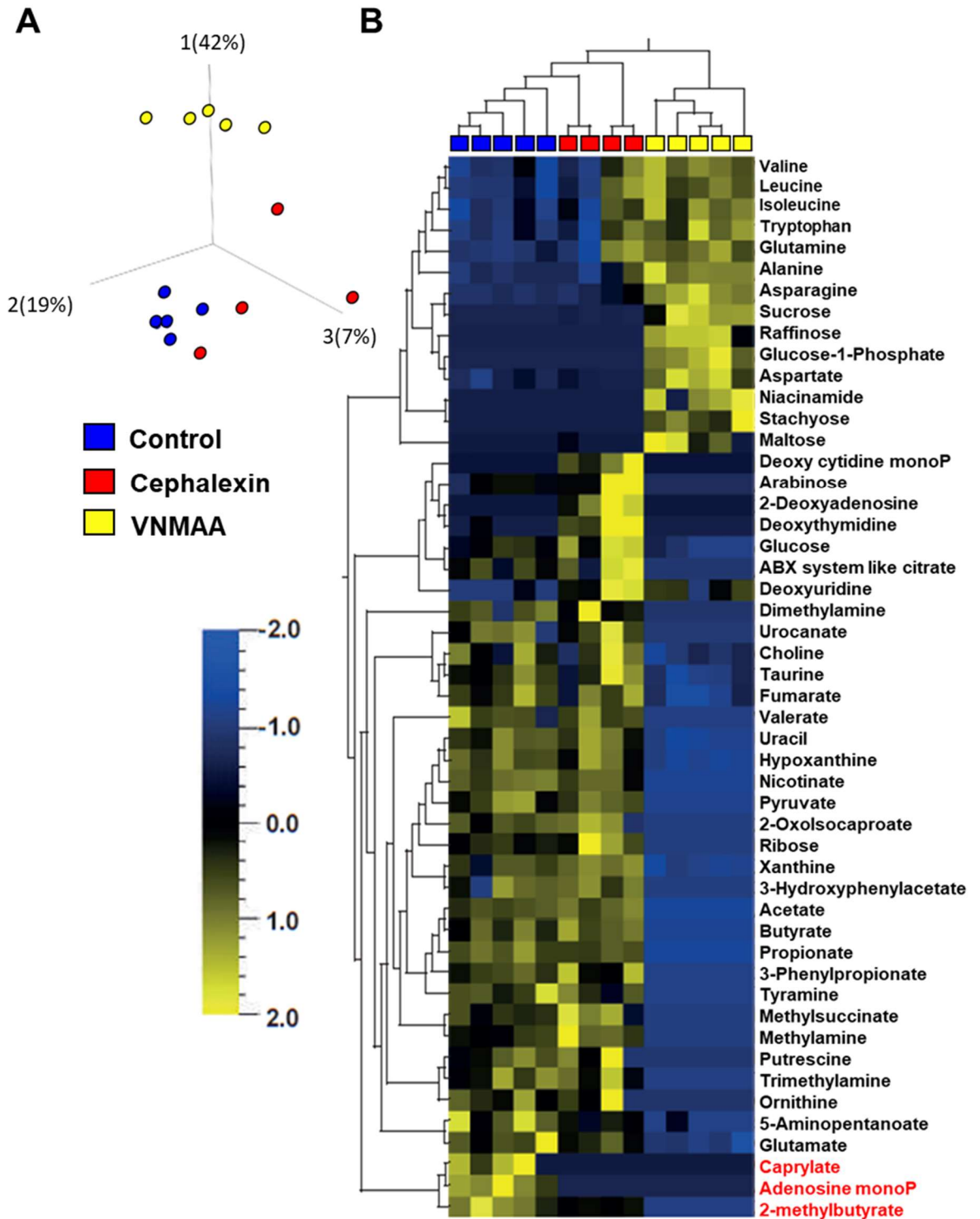


Figure 3.9. ^1H NMR spectroscopy of caecal samples show VNMAA and cephalalexin treatments alter metabolic profiles to varying degrees. **A)** Three-dimensional PCA clustering of metabolite abundances in caecal samples from control, VNMAA and cephalalexin treated animals. **B)** Heatmapping and hierarchal clustering of the 50 metabolites identified as significantly different following a one-way ANOVA test ($P < 0.026$, $q \leq 0.05$), metabolites in red font denote those which were significantly reduced by a post-hoc Tukey's range test in both VNMAA and cephalalexin samples relative to controls ($P < 0.05$).

3.10 Discussion

With the advent of antibiotic-resistance, the administration of antibiotics to treat bacterial infections has become an area of increasing clinical debate. While the importance of these drugs is undeniable, a layman's misunderstanding and naivety associated with their use can result in bacterial mutagenesis and development of bacterial strains which are resistant to antibiotic treatments [614]. These "super-bugs" often lead to increased mortality in patients and pose serious epidemiological risks [615]. However, it is not just antibiotic resistance that should concern clinicians. The understanding of the gut microbiota's role in regulating human health has grown exponentially over the past decade and continues to do so [616,617]. Due to the largely "broad-spectrum" targeting approach of many antibiotics, their use often reduces symbiotic bacterial populations and causes large shifts in community composition, ultimately influencing the functional capabilities of the microbiota, including those which are beneficial to human health [618].

As outlined in Section 1.4, the gut microbiota is involved in regulating human health in several ways. One such role is the processing of plant-derived polysaccharides into simple sugars and fermentation products such as SCFAs, which are used in cellular metabolism and regulation of gene transcription respectively [472,619,620]. Additionally, the microbiota interacts both directly and indirectly with elements of the immune system to educate it regarding which antigens and molecular signals should trigger inflammatory responses and which of these should be tolerated [507]. These interactions can involve signalling in local environments, such as the gut epithelium, as well as at distant sites [520,621]. Disruption of gut homeostasis has been shown to have negative consequences on human health. In the context of cancer, microbial dysbiosis has been associated with worsened prognoses and reduced efficacy of anti-cancer therapies, particularly in immunogenic cancers such as melanoma, in both pre-clinical and clinical studies [503,568,622]. However, how these disturbances might influence breast cancer is, so far, poorly described.

To confirm and support the previous observations made by Kirkup (2019) and improve the understanding of the antibiotic effects on tumour growth kinetics, several experiments ending at different timepoints were undertaken. These identified that until 13 days post tumour induction, growth of PyMT-BO1 tumours from VNMAA treated animals was almost identical to control cohorts. However, after this time, tumour progression in animals treated with VNMAA antibiotics was dramatically increased and by day 15 tumours were significantly larger in antibiotic treated animals. Separation in tumour volumes between groups became even greater by day 18, at which point tumours become too large to ethically continue experiments.

The question was then: was this increase in tumour growth the direct result of antibiotic compounds interacting with tumours or was the gut microbiota an integral “middleman” regulating the change in growth kinetics? The lack of detected changes in either cell proliferation or apoptosis *in vitro* following culturing of PyMT-BO1 cells with VNMAA supplemented media combined with the lack of any differences in tumour volumes between control and VNMAA treated germ free animals, which do not have a microbiota, suggests that the increased tumour growth observed in the specified pathogen free animals following treatment was not directly caused by VNMAA but likely by the downstream antibiotic-induced perturbation of the gut microbiota.

The tumour microenvironment plays a major role in regulating cancer progression through promoting cell metabolism and proliferation as well as supporting immuno-evasion from anti-cancer immune cells such as cytotoxic T lymphocytes and natural killer cells [623,624]. In contrast, some immune cells present in the tumour microenvironment, including macrophages and T regulatory cells, can promote cancer progression by stimulating angiogenesis and suppressing anti-cancer immune responses [625,626]. Profiling the abundances of these cancer-associated immune cells in tumours between treatments could identify possible players involved in increased tumour growth following antibiotics. Previous experiments had not identified changes in tumourigenic immune populations at a late timepoint in tumour growth but had not considered this possibility in early-stage tumours. However, even in tumour infancy, the key immune members generally associated with influencing tumour progression were not significantly different in VNMAA treated animals versus controls, suggesting the profiled cell types are unlikely the culprits promoting the increase in tumour growth observed at later timepoints following VNMAA administration.

The lack of obvious differences in tumour associated leukocytes at either an early or later timepoint was surprising. However, “number of cells present” is a crude measurement of their involvement in tumourigenesis. Immune cells change their functional behaviours in response to environmental cues, so it might be that these cues are different in tumours from antibiotic treated animals versus controls and, as a result, certain immune cells might change their activity in a way that may be pro-tumourigenic [321]. Previous research by Kirkup (2019) had looked at intra-tumoural pro-inflammatory cytokines but saw no significant changes between conditions, a result which supports the observations regarding immune cell abundances. However, recent developments in single cell proteomics and transcriptomics technologies, such as scRNA sequencing, will better aid in assessing differences in activity and behaviour of specific cell types based on gene expression profiles [627,628].

The heterogeneity of breast cancer means there is no one-size-fits-all approach to treating it and therapies require tailored approaches based on the different molecular and physiological characteristics of the disease. Therefore, it was important to confirm the increased tumour volumes associated with antibiotic treatment were not limited to just the luminal model. Replacing the PyMT-BO1 model with the EO771 basal-like model generated a similar increase in tumour volume following VNMAA treatment and immune profiling also produced comparable results between the two cancer models suggesting, that in both models, these immune cells are unlikely to be the driving forces behind the change in growth kinetics. Additionally, these results allude to the potential that the mechanism involved in increasing tumour growth might be the same or similar between the models. In the context of improving the understanding of how cancer is regulated, this is an important result as it demonstrates that the microbiota may play a role in cancer regulation in multiple molecular subtypes. Ideally, this would be further tested in several more models, such as triple negative and HER2 positive murine breast cancer lines, to confirm this hypothesis, but these models were not available to me at the time this research was undertaken.

Although these results demonstrate the microbiota does indeed play a role in regulating tumour progression, their clinical relevance may be questioned due to the combination of antibiotics used in the VNMAA cocktail. While the individual various components, described in Section 2.4, might be prescribed to patients during a bacterial infection, they would not generally be prescribed together. Thus, to strengthen the relevance of these observations, the VNMAA treatment was replaced with cephalexin, a cephalosporin antibiotic used by our clinical colleagues to prophylactically treat breast cancer patients. Again, tumour volumes, measured at the same timepoint as those from VNMAA - PyMT-BO1 experiments, were significantly increased compared to controls following treatment. Furthermore, the flow cytometric profiling of tumour infiltrating immune cells did not identify changes in either myeloid or lymphoid immune compartments, again suggesting the increase in tumour growth are not linked by classical tumour immune cell recruitment, or lack thereof, which has traditionally been associated with disease progression.

As described in Section 1.1.4, the hallmarks of cancer are a set of physiological alterations that cancer cells acquire during tumour development which dictate their malignant success [54,55]. Sustained cellular proliferation is one of these alterations. Proliferative potential, assessed through histological quantification of ki67 expression, is used as a diagnostic tool in the identification of breast cancer molecular subtypes as well as assessing tumour aggressiveness [98]. Staining of this marker in tumours from both VNMAA and cephalexin treated animals found significantly increased numbers of Ki67 expressing cells compared to controls, suggesting a higher proliferative potential

of tumours from antibiotic treated groups which is likely involved in promoting the increases in tumour volumes observed following these treatments.

Cell proliferation is important for tumour establishment and growth, but sustained growth largely depends on an adequate blood supply. Blood vessels carry the components required to support tumour cell proliferation, remove waste products that might otherwise trigger apoptosis and offer a route by which cells can metastasise to distant target organs. The process by which blood vessels are formed is called angiogenesis and the induction of this process is considered another one of the hallmarks of cancer [55,606]. Therefore, looking at the vasculature within a tumour might offer some insight into how likely it is to both continue to grow as well as metastasise. Interestingly, while tumours were larger following antibiotic treatment and had higher proliferative potential quantified through Ki67 staining, quantification of blood vessel density, following endomucin staining to identify endothelial cells, I did not find increased vessel density in either VNMAA or cephalixin tumours relative to controls. This was surprising as it might be expected that for the tumours to grow more quickly and to larger sizes, they would require an increased blood supply.

Antibiotics can have severe influences on the composition and function of the microbiota, particularly if administered over an extended period of time [501]. While previous research had used 16S sequencing of faecal DNA to profile the changes made to the bacterial composition in our model, these profiles were limited to genus level observations resulting in no more than speculation over the species specific members which might be involved in driving tumour growth. Thus, shotgun whole genome sequencing was employed in its stead to resolve taxonomic identities to a species and strain level in order to better define changes in specific populations of microbes following antibiotic treatment. The results showed that while VNMAA essentially ablates bacterial microbes in the gut, cephalixin has a far less aggressive effect with a relatively diverse bacterial community remaining when compared to VNMAA samples. However, phyla level shifts did occur in the form of an increase in relative abundances of Bacteroidetes and Verrucomicrobia but reductions in Actinobacteria and Firmicutes relative to control samples. Species level resolution facilitated the identification of several bacteria being mutually reduced in both antibiotic treatment groups. Of note were two *Lactobacillus* species, *L. taiwanensis* and *L. reuteri*, and *Faecalibaculum rodentium*.

The probiotic *Lactobacillus* genus is widely linked with beneficial influences on supporting a healthy microbiota and maintaining gut epithelial integrity [629,630]. These lactic acid bacteria play a major role in the fermentation of complex carbohydrates which generates ATP, a key molecule used in many host metabolic pathways [631]. Additionally, lactobacilli produce several antimicrobial factors including hydrogen peroxide, reuterin and bacteriocins which either kill or inhibit the growth

of microbes which might otherwise act pathogenically [632,633]. The latter of these functions has been associated with improving inflammatory conditions in the gut, predominantly during early life, such as necrotizing enterocolitis, colic and paediatric diarrheal disease [634–636]. Furthermore, several species from this genera have more recently been associated with anti-cancer effects in several cancers including pancreatic, colon and cervical cancer [637–639]. It is therefore plausible that in the context of our observations, their reduction might be involved in the mechanism driving antibiotic-induced tumorigenesis. Neither *L. taiwanensis* nor *L. reuteri* have so far been specifically linked with protective roles against cancer, though the later has been linked to improved bone mineral density in older women [640], illustrating the potential for health benefits.

The reduction in *Faecalibaculum rodentium* was interesting as this species has recently been identified as having protective influences against colorectal cancer in a mouse model of the disease. Research identified its underrepresentation in samples from *APC^{min/+}* tumour bearing mice relative to controls [574]. The same study also found the human homologue of *F. rodentium*, *Holdemanella biformis*, was underrepresented in adenomas from patients. Furthermore, subsequent supplementation experiments, using spent media from either *F. rodentium* or *H. biformis* cultures, resulted in reduced tumour multiplicity, relative to vehicle treated controls, via the inhibition of two proteins involved in T-cell activity and cell proliferation, calcineurin and nuclear factor of activated T cells cytoplasmic 3 (NFATc3), in a SCFA dependent mechanism [574]. The novelty surrounding this member, and its human homologue, in relation to such functions make it an exciting microbe to consider as a possible candidate for investigating its biotherapeutic potentials against cancer.

Microbial influences on their host can be either direct, through microbe-cell interactions, or indirect through production of metabolic compounds which regulate host pathways such as gene expression, apoptosis and cell proliferation. Host defences at the gut epithelium largely prevent bacterial cells from accessing the blood stream. However, many bacterial-derived metabolites are able to freely cross this barrier and enter blood vessels, facilitating systemic movement to distant organs where they can influence local changes in immune and/or metabolic activity [641]. Therefore, understanding how antibiotics influence the production of these metabolites can infer the effect on the functional capability of the disturbed microbiota. Targeted ¹H NMR identified changes in the abundances of various metabolites in faecal samples from both VNMAA and cephalixin treated animals. Based on the dramatic ablation of microbes following VNMAA treatment, it was unsurprising the metabolic profiles between VNMAA and control animals were essentially opposite. Complex carbohydrate molecules require bacterial processing to be broken into simple sugars resulting in increased polysaccharide levels and reduced abundances of

monosaccharides like glucose following bacterial ablation. SCFAs are also produced by the bacterial driven anaerobic fermentation of polysaccharides and so their reduction was also relatively unsurprising following VNMAA treatment. Considering that there was still a relatively diverse microbiota post cephalixin treatment, it was expected that samples from this treatment group would contain more bacterial-derived metabolites than VNMAA samples. However, the degree of similarity between the metabolic profiles of samples from cephalixin treated animals compared with controls was surprising, especially due to the increases in tumour growth following cephalixin treatment being comparable with that observed in VNMAA cohorts. The only clear similarities in metabolite reduction between the two antibiotic treatment groups were in caprylate, adenosine monophosphate (AMP) and 2-methyl butyrate.

The number of studies investigating the roles of gut derived caprylate, a medium chain fatty acid, are few. Although, one study has linked it to an improved gut mucosal function and antioxidant capacity but also showed it to reduce lactobacilli abundance in C57 BL/6 mice [642]; there have so far been no studies linking it to cancer progression.

Increases in the nucleotide AMP triggers the activation of the AMP kinase signalling pathway which regulates an array of cellular processes in the host, including glucose and lipid metabolism, autophagy and RNA transcription [643]. While all of these processes could be linked to cancer progression in some way, there is no literature linking gut derived AMP to changes in local or distant disease progression.

Gut barrier integrity, auto immune disease, allergy, immune response and bacterial colonisation resistance are just a handful of the roles with which gut derived SCFA have been associated [644]. Acetate, propionate and butyrate are the three major SCFA produced in the gut and of these butyrate has been robustly linked to anti-cancer effects through its epigenetic regulation of gene transcription [542,564,565,645]. Our analysis identified a reduction of all three major SCFA in samples from VNMAA treated animals, but none were significantly reduced, relative to controls, in cephalixin samples. However, the branched SCFA, 2-methylbutyrate, was reduced in both the treatment groups. While the nomenclature of this molecule might elude to a relationship with butyrate, it is in fact derived from different precursor molecules [646]. Butyrate is derived from two molecules of acetyl coenzyme A but 2-methylbutyrate is formed by the oxidation of isoleucine [647,648], a branched chain amino acid which was conversely increased in abundance in two of the four cephalixin samples. Although the functions of butyrate are well described, the functions of 2-methylbutyrate are far less so and no evidence currently links them to similar functions of those

described for butyrate. Thus, again, it is unclear how this metabolite might be involved in driving the mechanism in question for in this study.

In conclusion, the observations made in this research demonstrate that an antibiotic-induced perturbation of the microbiota results in increased tumour growth with significant clinical relevance. Although increased tumour growth was not associated with changes in immune cell populations traditionally associated with tumourigenesis, antibiotic administration was associated with changes in bacterial composition in the gut and highlighted several species which may be involved in the tumour-level observations. Gut metabolomic profiles were also consequently influenced by antibiotic administration but this was heavily dependent on the strength of the drugs used. However, the metabolites which were consistently reduced in both treatment groups are not currently associated with significant influences on host health, but future supplementation or exclusion studies may aid in assessing their importance in this context.

4 Single Cell Sequencing reveals distinct differences in tumour stroma of antibiotic treated animals

Solid tumour tissues are comprised of a complex milieu of different cell types and structures, each exerting their own influence on tumour progression. A broad classification of the major cell types active in tumours would include epithelial and endothelial cells, mesenchymal stromal cells, leukocytes and fibroblasts [649,650]. The function and behaviours of these cells is dependent on the activity of surrounding cells. The release of intercellular signalling molecules, such as chemokines and cytokines which bind receptors on the surface of neighbouring cells, trigger signalling cascades that ultimately promote sustained tumour growth and survival through a variety of mechanisms [651].

Immune cells are particularly active in promoting the pathways and interactions that govern the success of cancer. Several innate immune cells, including macrophages, produce the major proangiogenic molecule, vascular endothelial growth factor (VEGF), which stimulates vascular development and, in turn, increases nutrient availability within tumours [625,652]. Additionally, some immune cells, namely T-reg cells, play a major role in promoting immune evasion of cancer cells through their suppression of anticancer effector T-cells and cytotoxic T-cell activity [653,654]. Mesenchymal cells and fibroblasts, often associated with stromal regions in tumour tissues, are also heavily influential in regulating tumour progression and metastasis [655–659]. Profiling cell types present in tumours following antibiotic treatment may identify shifts in abundances which could suggest possible candidates involved in the mechanism driving tumour growth. Furthermore, gene expression profiling of specific cell types enables the assessment of a cell's functional capabilities, often alluding to whether a given cell might act pro- or anti-tumourigenically.

Previous attempts have been made to identify changes in both cell abundance and gene expression in tumours from VNMAA treated animals through the use of flow cytometry and bulk RNA-sequencing, respectively [570]. Flow cytometry did not identify significant differences in cell numbers of several of the immune cell types typically associated with tumorigenesis. However, there are two main limitations of using flow cytometry to measure potential immune influences in tumour tissue. Firstly, it is a targeted approach and is limited by the size of the antibody panel compatible with the instrument being used. Secondly, an increase in cell abundance is not necessarily an indication of a functional effect on tumour progression, it may simply be a result of it. Bulk RNA-seq was used to investigate whole tumour transcriptomics in an attempt to identify possible differences in the activity of functional pathways between treatment conditions. The limitation of using “bulk” transcriptomics is that it profiles the entire transcriptome within a given

sample and is not designed to identify differences in transcription patterns between specific cell types within a tissue. Thus, while differences in gene expression may be observed, it would not be immediately clear which cell types are specifically responsible for those differences.

Fortunately, the recent advancements in single cell (sc) transcriptomic technologies, through scRNA-sequencing (scRNA-seq), have significantly improved the resolution of gene expression studies by facilitating the exploration of cell specific transcriptomes [660,661]. A major benefit of single cell sequencing technologies over their bulk sequencing counterparts is their capability for untargeted cell identification through the quantification of the expression of marker genes at a single cell level [662]. In studies where cell types of interest are yet to be identified, this capability is beneficial over targeted cell identification methods such as flow cytometry. However, the use of these technologies is still being developed in studies involving solid tumours and the more complex a tissue, the more challenging it is to clearly resolve rare cell types and, subsequently, their functional outputs, particularly where short-read sequencing is employed [663]. Nonetheless, an attempt was made to identify the effect of VNMAA treatment on single cell transcriptomics of cells isolated from whole tumours.

Following the sequencing of four tumour samples, two from VNMAA treated animals and two from a vehicle control group, two analyses were undertaken which ultimately identified differences in cluster densities of cells with transcriptomes associated with T-cells, B-cells, mast cells and stromal cells. Subsequent histology confirmed that VNMAA treatment was associated with increased tumour resident mast cell densities in PyMT-BO1 and EO771 tumours. Additionally, collaborators working with different breast cancer models and antibiotic treatment regimens presented data showing increases in mast cells in tumours from their experiments. Finally, *in vivo* functional inhibition of mast cells, through administration of the mast cell stabilizer, cromolyn sodium, rescued PyMT-BO1 tumour growth in VNMAA treated animals but did not influence tumour growth in vehicle treated controls.

4.1 Single cell transcriptomics of tumour cells alludes to differences in population density of several cell types

4.1.1 Preliminary analysis identified differences in several cell clusters following VNMAA treatment.

Four samples, two from VNMAA and two from vehicle control treated animals, were sequenced using the 10X Genomics Chromium X platform at the Earlham Institute (Norwich, England). The readout format from this hardware facilitates an initial data visualisation using Loupe Cell Browser, a software produced by 10X Genomics for this purpose. This software generates interactive t-SNE dimension reduction plots through the comparison of gene expression profiles for each cell against all other cells, irrespective of treatment, and assigns them to a cluster with cells most similar to themselves. These clusters are used to assign cell types through in software searches of marker genes as well as GO searches. Subsequently, the densities of the various cell types within a cluster can be compared between treatment groups to identify differences in cell abundance post treatment.

A total of 10,054 cells were sequenced and the aggregated data assigned to 17 clusters (Supplementary Figure 4.1.1.1). Of these, 4,981 cells were from the two control tumours (2,773 and 2,208, respectively) and 5,073 were from the tumours taken from VNMAA treated animals (2,474 and 2,599, respectively). Using the Loupe Cell Browser gene expression search function, which allows searching the t-SNE plot for the expression of a particular gene across clusters and visualised as a heatmap (Supplementary Figure 4.1.1.2), as well as two gene ontology search sites, DAVID [583] and PANTHER [584], the top 50 upregulated genes of each cluster (Supplementary Figure 4.1.1.3) were used to assign cell types (Figure 4.1.1A); the density of given cell types per treatment condition were noted. Using the t-SNE plots based on sample IDs allowed for a visual assessment of the differences in densities for the respective cell types identified between treatment conditions. This assessment showed a reduction in the number of cells assigned to the T-cell (cluster 1) and B-cell (cluster 2) clusters following VNMAA treatment as well as a more obvious increase in the number of cells in the cluster associated with mast cell specific genes (cluster 3) (Figure 4.1.1B i and ii), namely *Mcpt1*, *Mcpt2*, *Mcpt4*, *Tbsb2* and *Cma1*. Interestingly, there was a similar increase in cells from VNMAA samples in cluster 4, but ontology searches of the genes involved in assigning cells to this cluster did not result in the identification of a likely cell type. These genes included those associated with ribosomal and actin proteins, however further analysis is required to better define and understand the function of this population. Although statistical analysis regarding cell type abundance was not possible due to only having two samples per

condition, graphical interpretations to quantify the number of cells for each of these cell types, as a percentage of total cells within that sample, supports the visual assessments made using the t-SNE plots (Figure 4.1.1C).

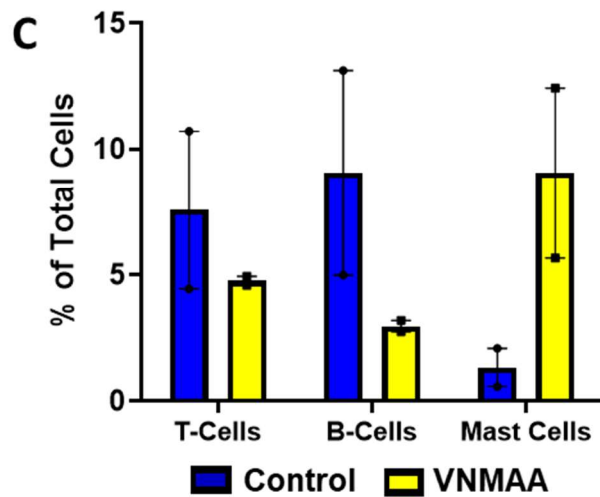
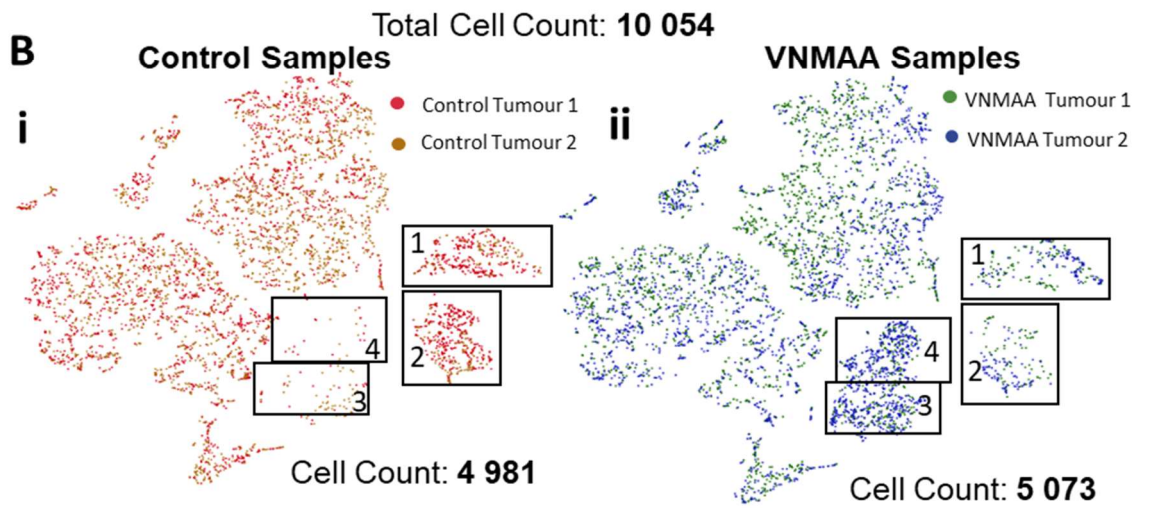
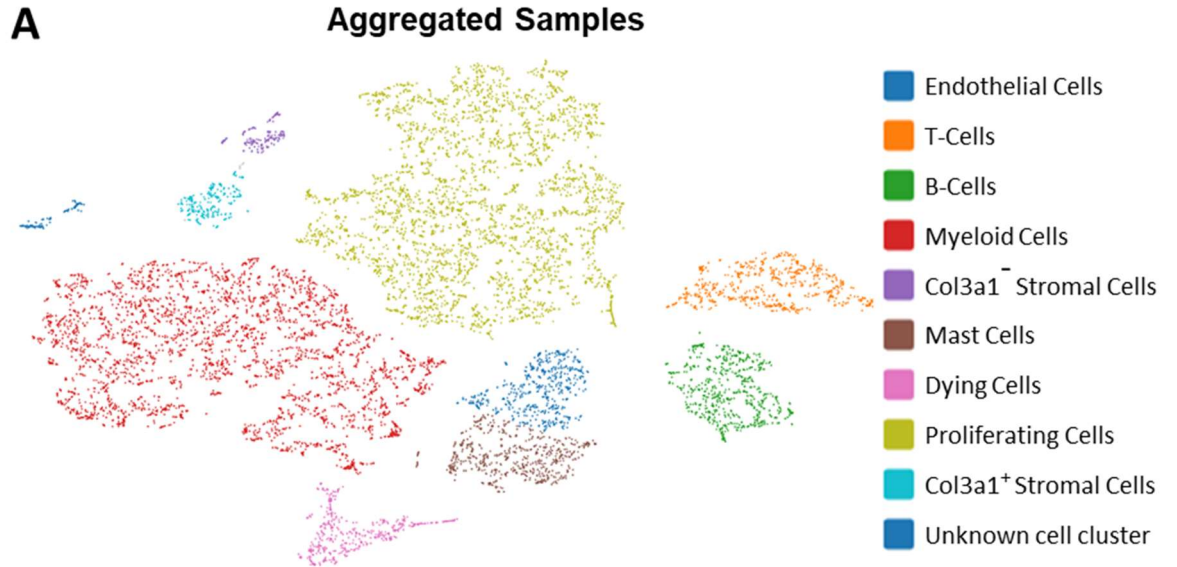


Figure 4.1.1. Preliminary analysis of tumour scRNA-seq outputs identified changes in the abundance of several cell types following VNMAA treatment. **A)** Assignment of cell types to clusters in the aggregated data t-SNE plot following in-software searches of known marker genes as well as gene ontology searches (DAVID and Panther) of the top 50 upregulated genes in each cluster relative to all other clusters. **B)** t-SNE clustering plots for combined tumour samples from animals treated with either **i)** a vehicle control or **ii)** VNMAA antibiotics and the cell clusters of interest identified through visual assessments of cluster densities: 1 – T-cells; 2 – B-cells; 3 – mast cells; 4 – unknown cell population. **C)** Bar graph of the mean (\pm SEM) abundances of the three cell type clusters identified as having different densities expressed as a percentage of the total cells per sample (n=2 tumours per condition).

4.1.2 Expert bioinformatic analysis highlights differences with Loupe Cell Browser analysis and identified increases in stromal gene signatures following VNMAA treatment.

The preliminary analysis of datasets using Loupe Cell Browser was limited to cell type identification based on upregulated gene expression relative to other cells and their clusters as well as visualisation of these clusters. Single cell transcriptomics can offer far more than simply cell identification and comparisons between conditions. Downstream analyses should offer insight into differential gene expression (DGE) within a cluster between conditions to identify changes in cellular activity of specific cell populations. Thus, bioinformatic expertise was sought from Matthew Madgwick of the Earlham Institute to support the more complex analyses of these data.

Following several quality control steps, including the removal of cells expressing high levels of mitochondrial genes which signal cells under stress and undergoing apoptosis, an improved dimension reduction algorithm was applied to the data, in place of t-SNE, in the form of uniform manifold approximation and projection (UMAP). Initial cluster assignments identified 21 clusters based upon gene expression of cells relative to all other cells (Supplementary Figure 4.1.2.1). Gene ontology searches of upregulated genes as well as searching marker gene expression in respective clusters aided in cluster identification and subsequent qualitative assessments of cell densities. When using Loupe Cell Browser, cell type assignments were limited to a total of 10 cell identities, including one unknown cluster and one identified as containing dying cells, from the original 17 clusters. Expert bioinformatic analysis assigned 14 cell types to the original 21 clusters (Figure 4.1.2). Similar to the observations made using Loupe Cell Browser, clusters identified as T-cells (cluster 1) and B-cells (cluster 2) showed reductions in cell density following VNMAA treatment. In contrast, a cluster containing cells with a stromal-associated transcriptome (cluster 3) appeared to be increased in density following VNMAA treatment. However, this analysis did not identify any of the clusters as having transcriptomes associated with an upregulation of the various mast cell genes presented in the t-SNE clustering from Loupe Cell Browser.

DGE analysis defined genes as being different in expression between conditions if the difference between the mean of the Log₂-fold expression values, from the two samples per condition, for a given gene was greater than or equal to a value of two. DGE analysis of each of the 14 clusters assigned cell types identified only two clusters where one or more genes were differentially expressed (Supplementary Figure 4.1.2.2). In the *C1qc* high macrophage cluster, expression of *Igk1* was significantly reduced in tumours from VNMAA treated animals compared to controls. In the cluster assigned as luminal cell 2, *Ltf* and *Mgp* expression was increased in tumours from VNMAA treated animals while *Sprr1a* expression was reduced.

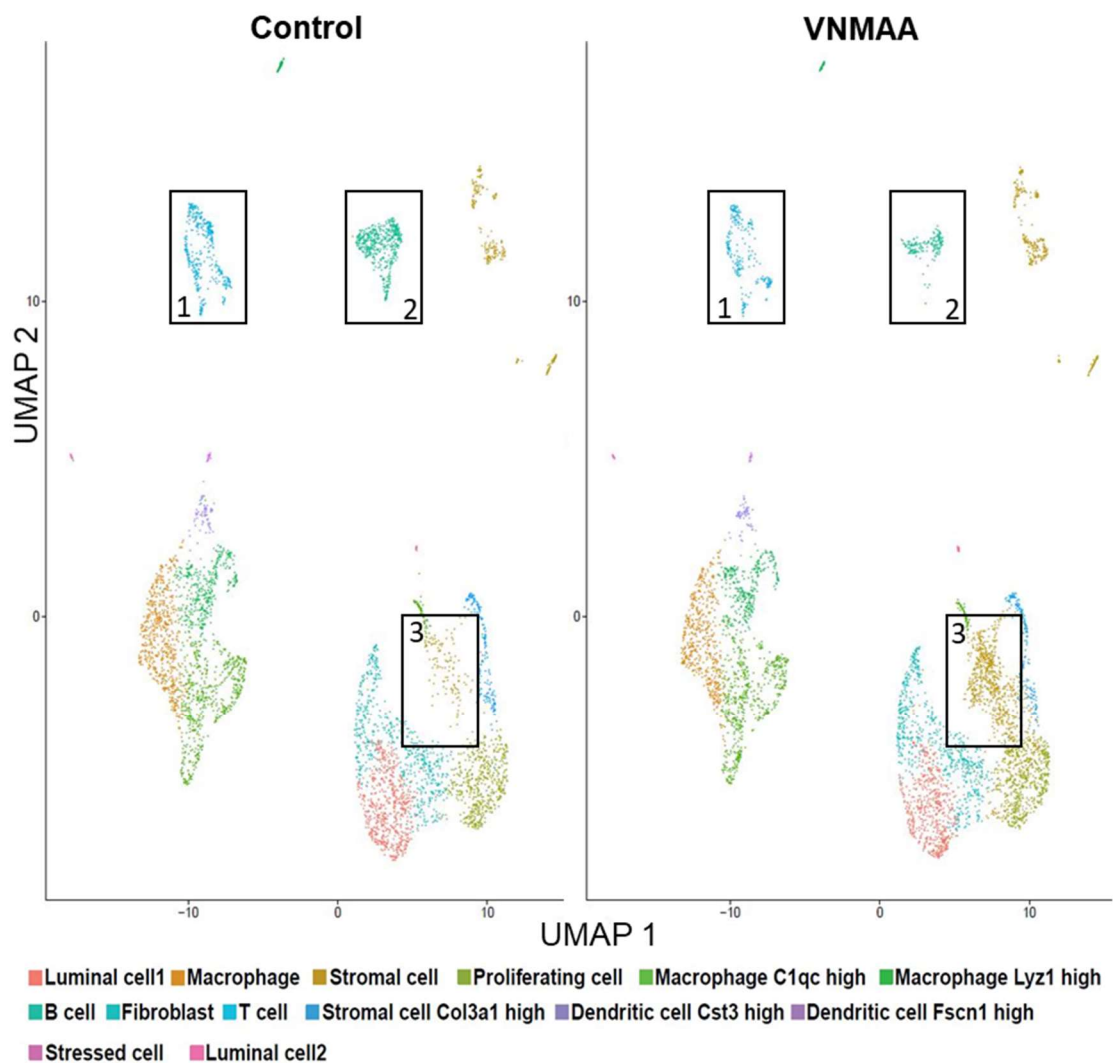


Figure 4.1.2. Bioinformatic analysis reveals an increase in the density of a cluster representing cells with a stromal-associated transcriptome. UMAP clustering of aggregated datasets from the four tumour samples sequenced. Different coloured clusters denote the 14 cell types identified from the original 21 clusters (see Supplementary Figure 4.1.2.1). T-cells (cluster 1), B-cells (cluster 2) and stromal cells (cluster 3) are indicated using rectangle boxes as they appear to have different cell densities between treatment conditions.

4.1.3 Deconvolution of historic whole tumour bulk RNA-sequencing data also identifies increases in stromal gene expression following VNMAA treatment.

Previous bulk RNA-sequencing of whole tumours from VNMAA treated animals had revealed several changes in gene expression associated with protein and lipid metabolism [570]. Since then, bioinformatic pipelines for the deconvolution of bulk RNA-seq data to identify cell types and estimate their abundance within a sample have been developed. These pipelines often rely on leveraging gene expression within known cell type clusters from scRNA-seq datasets [589,664]. Again, support from the Earlham Institute was sought to deconvolute the historical whole tumour bulk RNA-seq datasets. Subsequent analysis confirmed that stromal gene signatures were also elevated in these samples from VNMAA treated animals (Figure 4.1.3A) in a similar fashion to those observed in the scRNA-seq datasets (Figure 4.1.3B). However, no significant changes in T-cell or B-cell gene signatures between treatment conditions were observed in the deconvoluted samples.

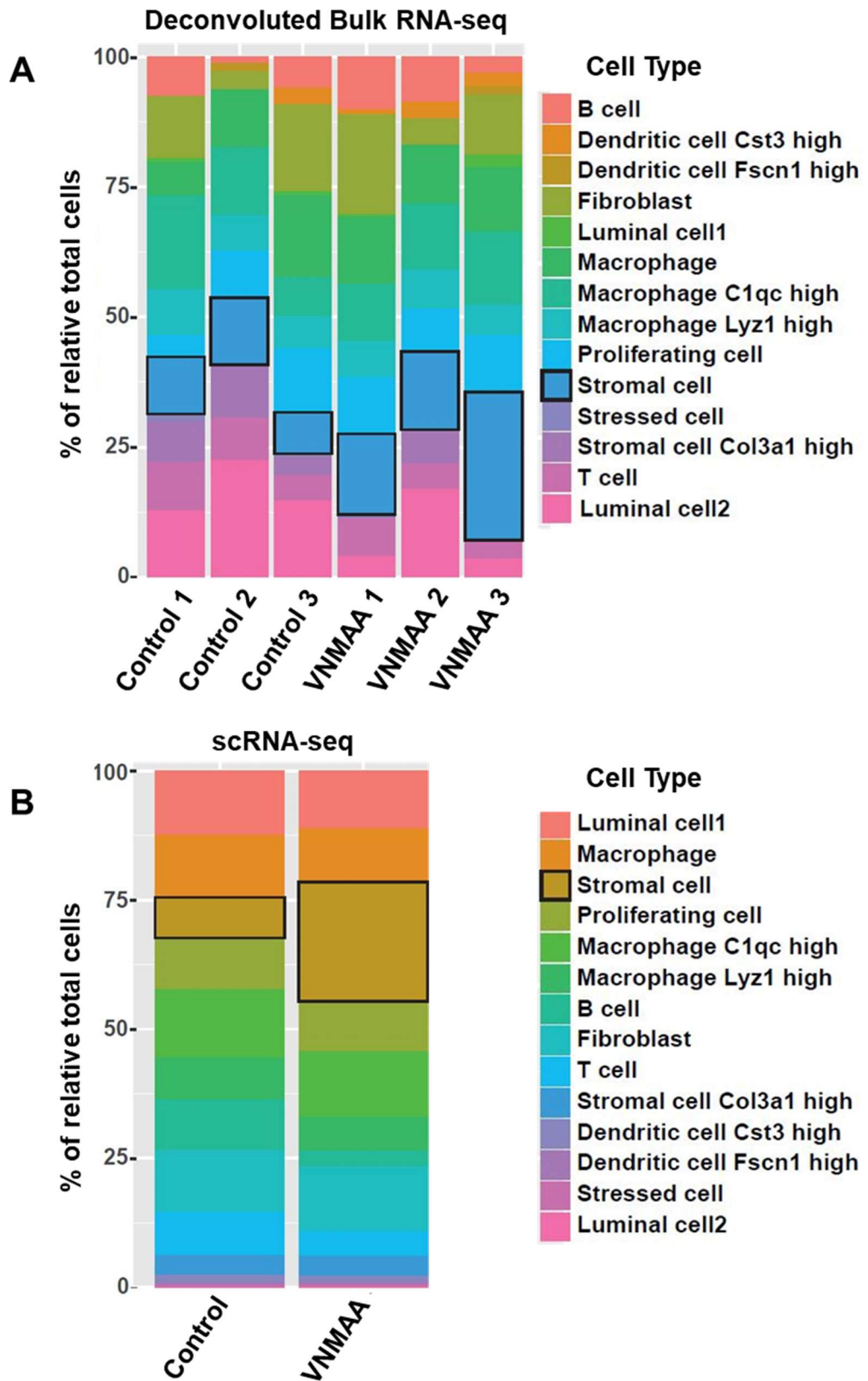


Figure 4.1.3. Deconvolution of historical bulk RNA-seq identifies a similar increase in gene expression associated with stromal cells following VNMAA treatment. A) Percent abundances of respective cell types relative to total number of cells per sample following deconvolution of historical bulk RNA-seq datasets (n=3 per tumours per condition). **B)** Percent abundances of cell types relative to total number of cells per treatment sequenced via scRNA-seq (pooled data from two samples per treatment).

4.2 Histological staining identifies the increased abundance of granular cells in tumours from antibiotic treated animals as mast cells.

To assess whether the increased expression of genes associated with tumour stroma following antibiotic treatment translated to increases in stromal density, collagen deposition within tumour sections was assessed using picosirius red staining and quantified using imageJ. This staining did identify evidence of an increase in collagen deposition in tumour sections from either VNMAA or cephalixin treated animals compared to controls (Figure 4.2A and B). However, while imaging tumour sections at higher magnifications, there appeared to be abundances of cells deemed to be granular in morphology within stromal areas of several tumour sections from VNMAA treated animals. After considering the lack of change in tumour infiltrating neutrophils following flow cytometry and the increased expression of mast cell specific genes in tumours from VNMAA treated animals observed during initial scRNA-seq analysis as well as consulting with collaborators in the U.S. (Melanie Rutkowski, University of Virginia), toluidine blue staining was undertaken on a tumour section cut sequentially to one stained with picosirius red and in which these granular cells had been observed.

Toluidine blue is a weakly hydrophilic cationic dye which, when bound to DNA and RNA, stains cells blue. However, when bound to glycosaminoglycans, it stains cells metachromatically purple [665]. The cytoplasmic granules present in mast cells contain high levels of heparin, a naturally occurring glycosaminoglycan [665,666]. Thus, tissue resident mast cells can be identified in the presence of a milieu of other cell types through toluidine blue staining. An overlay image of the sequential sections stained using picosirius red and toluidine blue was generated using an intra-tumoural landmark, in the form of a mammary duct within the stromal area, to ensure an accurate overlay. Overlay images confirmed the identity of these granular cells as mast cells due to the purple staining of intracellular mast cell granules (Figure 4.2C).

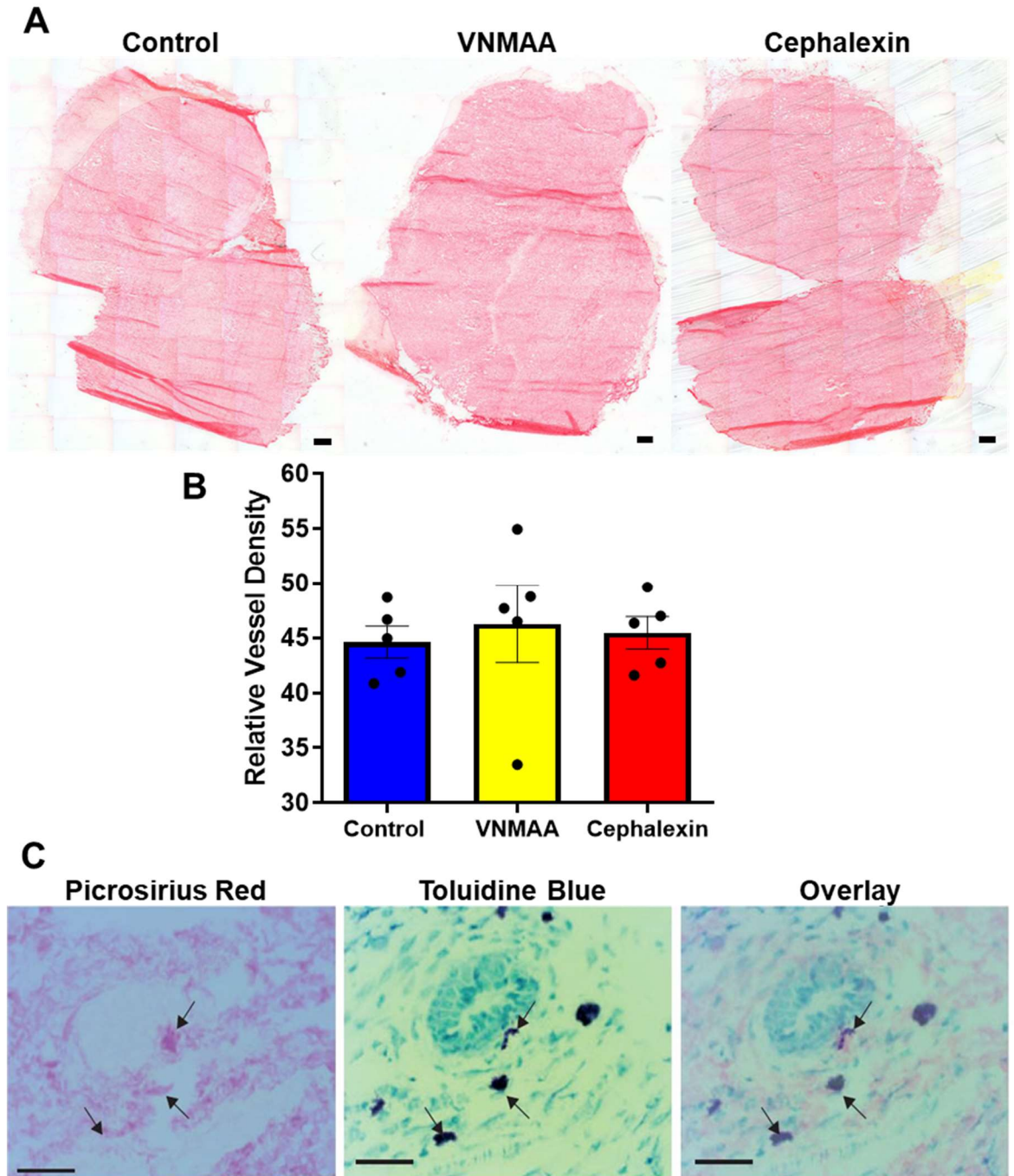


Figure 4.2. Picosirius red staining shows no changes in collagen deposition but aids in identifying mast cells as potentially increased in abundance in tumours from antibiotic treated animals. **A)** Representative tumour sections stained with picosirius red show collagen deposition, denoted by areas of intense red colouration, within tumour sections from animals treated with vehicle control, VNMAA or cephalixin. Scale bar = 100µm. **B)** Bar graph of the mean (\pm SEM) collagen deposition area as a percentage of total section area (N=1, n=5 animals per condition; Control Vs. VNMAA P=0.672, DBM=1.674, SEM=3.812; Control Vs. Cephalixin P=0.69, DBM=0.86, SEM=2.076). **C)** Overlay of picosirius red and toluidine blue images using histological landmarks from sequential tumour sections shows colocalization of granular cells (picosirius red) and mast cells (toluidine blue) in a tumour from a VNMAA treated animal. Scale bar = 100µm.

4.3 Mast cell densities are increased in several breast cancer models and following different antibiotic treatment regimens.

Mast cell biology is described in detail in Section 1.2.3. Briefly, these granulocytes are most well known for their role in allergen responses and inducing allergy related inflammation and, in severe cases, anaphylaxis [667]. Mast cells have a high affinity for binding IgE antibodies, produced by plasma cells [668–670]. IgE antibodies bind specific antigens, present on peptide or polysaccharide allergens, and trigger the activation of mast cells resulting in degranulation of cytoplasmic granules containing signalling and effector molecules, including histamine, heparin and tryptase, which promote inflammation, vasodilation and vascular permeability [201,671]. Additionally, mast cells have been linked to poor prognosis in several cancers including bladder, lung and prostate cancers [672–674]. While these cells are resident in normal breast tissue generally without causing health issues, their role in breast tumours is currently poorly defined. Several studies align mast cells with a pro-tumour and/or pro-metastatic influence while others suggest they may act protectively against breast cancer [675,676]. In either case, molecular subtype appears to play a role in the observed influences of these cells on the disease [676,677].

4.3.1 Flow cytometry of tumour resident mast cells does not show significant changes in mast cell abundance.

Mast cells can be identified from a heterogenous population by the cell surface expression of c-kit, a receptor tyrosine kinase which binds SCF and regulates haematopoietic pathways, and FCεR1α, a high affinity IgE receptor which binds the IgE antibodies that trigger mast cell degranulation [678–680]. Several attempts were made to identify mast cells in tumours via flow cytometry. Successful staining of these cells proved challenging, and several optimisation experiments were undertaken. Briefly, altering the strength of the collagenase digestion solution from a gentle collagenase IV-based solution to a stronger enzymatic digestion using a collagenase I solution (see section 2.18.2 for complete details) facilitated successful downstream isolation and staining of mast cells from tumours (Figure 4.3.1A). Unfortunately, the timing of this success was towards the end of the research period for this study and only one experiment was completed. Although statistically non-significant, this experiment suggested an increase in mast cell densities in tumours from both VNMAA and Cephalexin treated animals (Figure 4.3.1B). This author speculates that, had time allowed, additional experiments using flow cytometry would have confirmed a significant increase in mast cells abundance in both antibiotic treatment groups relative to controls.

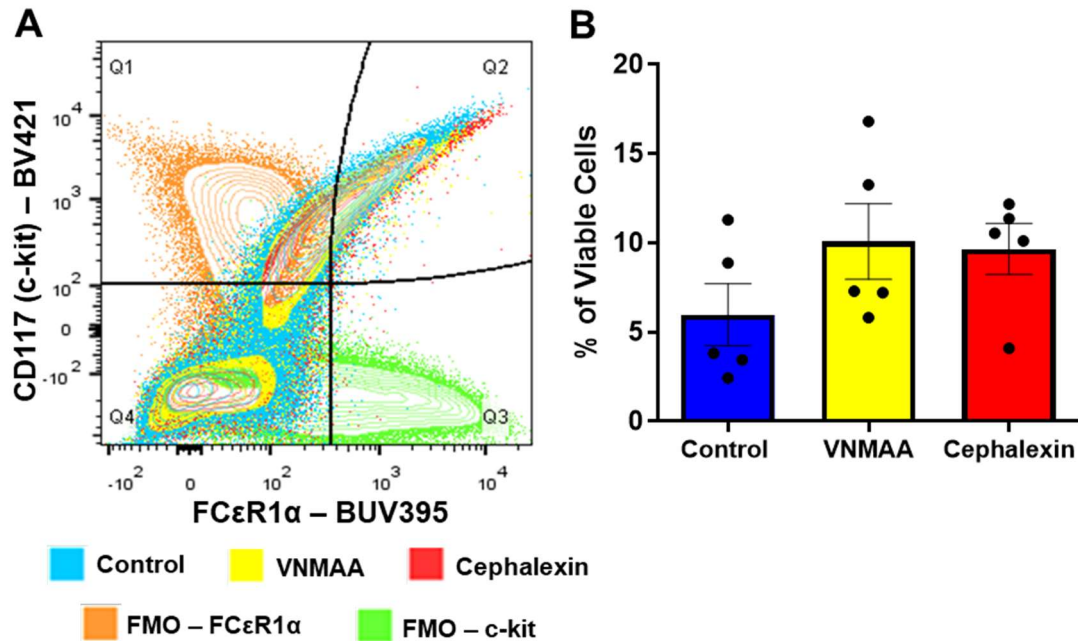


Figure 4.3.1. Flow cytometry of intra-tumoural mast cells does not show an increase in their cell abundance following antibiotic treatment. A) Dot plot of viable CD45+ leukocytes from representative samples as well as FMO controls for c-kit and FCεR1α gated according to the intensity of c-kit and FCεR1α staining. Cells in quadrant 2 (Q2) are positively stained for both of these markers and are considered mast cells. **B)** Bar graph of the mean (\pm SEM) number of intra-tumoural mast cells as a percentage of viable cells (N=1, n=5 animals per condition; Control Vs. VNMAA P=0.172, DBM=4.11, SEM=2.738; Control Vs. Cephalixin P=0.14, DBM=3.693, SEM=2.253).

4.3.2 Histological staining reveals mast cell densities are increased following VNMAA treatment.

Due to the challenges faced in quantifying mast cell number in tumours via flow cytometry, experiments were setup up so tumours from half the number of animals per group were subject to flow cytometry (as described above) while the other half were designated for histological toluidine blue staining which successfully and consistently identified mast cells within tumour sections (Figure 4.3.2A). Stained tumour sections were subject to mast cell counting and these counts made relative to section area (MC/mm^2) as a measure of tumour mast cell density. In animals induced with PyMT-BO1 tumours, both VNMAA and cephalixin treatments were associated with a significant increase in tumour mast cell density (Figure 4.3.2B and C). Additionally, in EO771 tumours from animals treated with VNMAA, mast cell density was also significantly increased (Figure 4.3.2D).

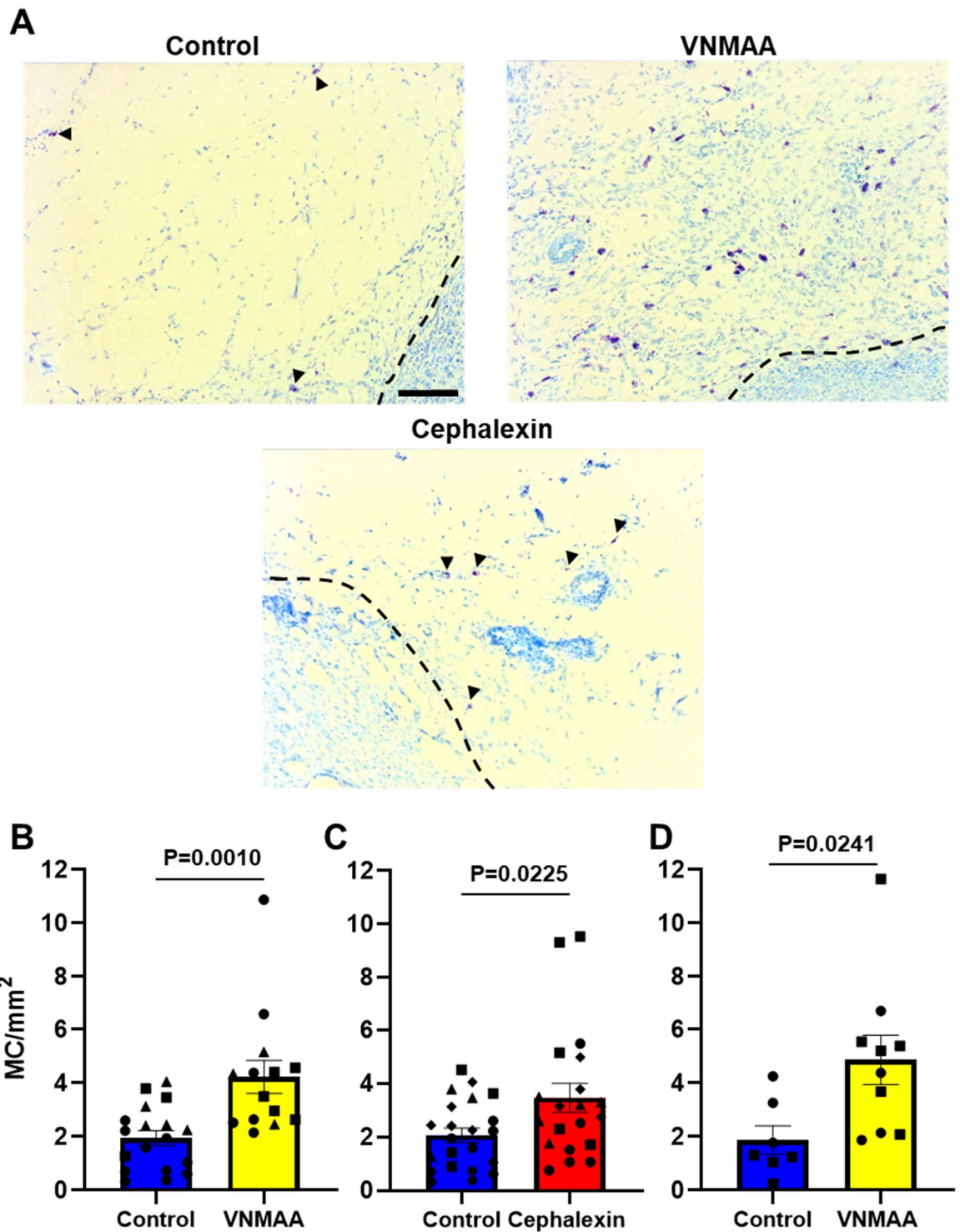


Figure 4.3.2. VNMAA antibiotic treatment is associated with increased tumour mast cell density in PyMT-BO1 and EO771 tumours. **A)** Mast cells (black arrow heads) appear purple following toluidine blue staining of tumours sections taken from vehicle control, VNMAA and cephalixin treated animals. Dashed lines denote tumour margins; Scale bar = 200 μ m. Bar graphs showing the mean (\pm SEM) mast cell densities, quantified as mast cell counts per tumour area (MC/mm²) in **B)** PyMT-BO1 tumours from VNMAA treated animals (N=3, n \geq 14animals per condition, P=0.001, DBM=2.287, SEM=0.625), **C)** PyMT-BO1 tumours from cephalixin treated animals (N=4, n \geq 20animals per condition, P=0.0225, DBM=1.408, SEM=0.593) and **D)** EO771 tumours from VNMAA treated animals (N=2, n \geq 7 animals per condition, P=0.0241, DBM=2.988, SEM=1.191) compared to respective vehicle treated controls.

4.3.3 International collaborators identify similar increases in mast cell densities in different models of breast cancer following different antibiotic treatment regimens.

As discussed in Section 1.1.4 and Section 3.4, the heterogenous nature of breast cancer means that physiological differences observed in tumours following specific treatment types are not uncommonly associated with one molecular subtype and not others. Furthermore, animals housed in different facilities are well known to harbour different microbiota profiles resulting in the potential for differences in gut microbial functional outputs in animals of the same genetic background between facilities [555,681]. Thus, the clinical relevance of the observations made in this study, regarding disease progression and mast cell density, would be strengthened further if similar observations were made in different breast cancer models, using different antibiotic treatment regimens in animals housed at different facilities. International collaborations with colleagues at the University of Virginia (Rutkowski Laboratory) and at the Fondazione IRCCS Istituto Nazionale di Tumori (Tagliabue laboratory) allowed for such an investigation. Following the results described in Section 4.3.2, collaborators were asked to assess mast cell density in tumour sections following antibiotic treatments. Members of the Rutkowski laboratory identified increased tumour mast cell densities in C57 BL/6 mice induced with a BRPKp110 luminal A-like breast cancer model following an antibiotic treatment regimen slightly different to the VNMAA treatment described here, in which amphotericin was replaced with gentamycin (VNMGA), administered every day for one week and followed by a four-day period to facilitate a microbiota recolonization prior to tumour induction (see Buchta Rosean *et al.* (2019) for a complete treatment methodology [569]) (Figure 4.3.3A). Similarly, the Tagliabue lab observed an increase in mast cell densities when using a spontaneous HER2-neu positive breast cancer model in animals treated with vancomycin only (Figure 4.3.3B).

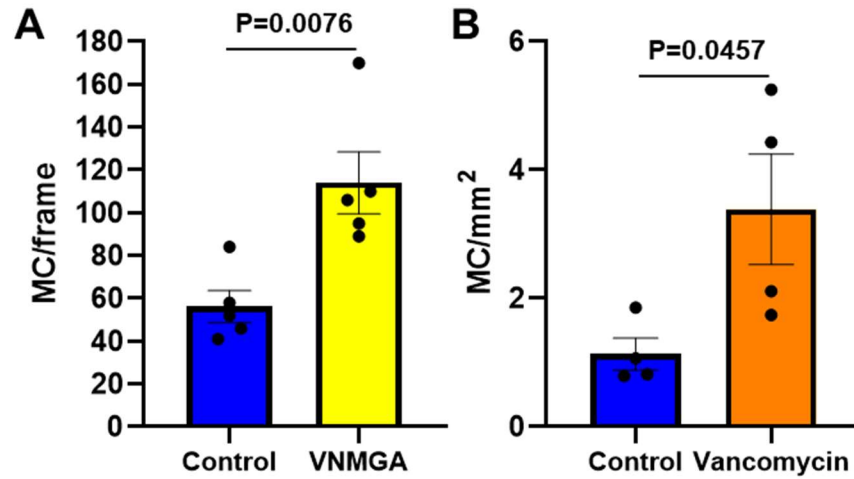


Figure 4.3.3. Mast cell densities are increased in different tumour models following different antibiotic treatments in animals housed at different facilities. A) Bar graph showing the mean (\pm SEM) mast cell counts per frame (MC/frame) in BRPKp110 tumours from animals treated with VNMGA antibiotics compared to controls (N=1, n=5 animals per condition, P=0.0076, DBM=57.8, SEM=16.33). **B)** Bar graph showing the mean (\pm SEM) mast cell density (MC/mm²) in HER2-neu spontaneous tumours from animals treated with vancomycin (N=1, n=4 animals per condition, P=0.0457, DBM=2.252, SEM=0.8957).

4.4 Increased tumour mast cell densities are not associated with an increase in serum IgE levels

Mast cell activation is governed by the binding of IgE immunoglobulins by FCεR1α receptors which facilitates crosslinking of these receptors and the resulting of chemokines and cytokines that trigger various biological pathways, including inflammation and angiogenesis [202]. IgE antibodies are produced by B-cells in response to cytokine signalling from TH2 T-cells following the exposure to particular antigens, termed allergens [202]. The gut is a common location of allergens associated with certain types of food. Thus, it was hypothesised that the antibiotic-induced perturbations of the gut microbiota may have resulted in the increased exposure of the immune system to these allergens, in turn promoting IgE production which may have been responsible for the increased number of mast cells observed in tumours from antibiotic treated animals. To assess systemic IgE levels, serum samples from PyMT-BO1 tumour bearing animals treated with either VNMAA or cephalixin were analysed by ELISA to ascertain IgE concentrations. This analysis did not identify any significant changes in serum IgE concentrations in either antibiotic treatment group compared to vehicle treated controls (Figure 4.4).

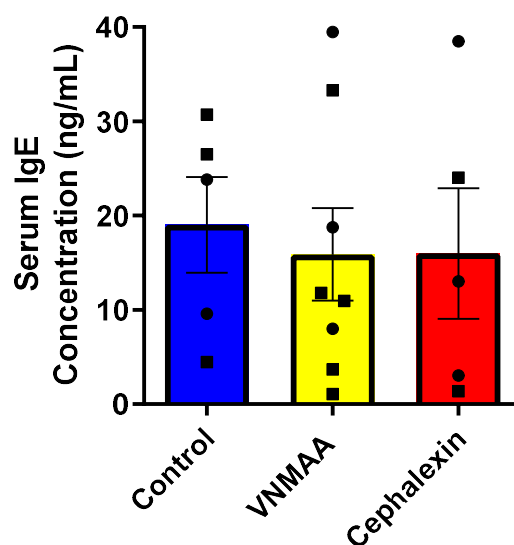


Figure 4.4. Serum IgE concentrations are not influenced by antibiotic treatment. Bar graph showing the mean (\pm SEM) IgE concentrations of serum samples obtained from PyMT-BO1 tumour bearing animals treated with either a vehicle control, VNMAA or cephalixin (N=2, n \geq 5 animals per condition; Control Vs. VNMAA P=0.68, DBM=-3.135, SEM=7.406; Control Vs. Cephalixin P=0.7338, DBM=-3.028, SEM=8.597).

4.5 Inhibition of mast cell degranulation reduces PyMT-BO1 tumour growth in VNMAA treated animals.

Collectively, an increase in mast cells has been observed in various breast cancer models, using a range of antibiotics and antibiotic regimens, across multiple “native” gut microbiotas (pertaining to animals housed in different facilities), correlating their involvement in breast cancer progression. However, these findings alone are not enough to reject the possibility that these observations are simply the result of disease progression rather than drivers of it. Therefore, inhibition of mast cell activity *in vivo* could allude to whether these cells are in fact involved in the microbiota dependent mechanism driving tumour growth following antibiotic treatment. Several drugs approved for use in humans are designed to inhibit the effects of mast cell derived mediators such as histamine, or inhibit mast cell activity altogether, for the purpose of preventing allergic responses. Cromolyn sodium (cromolyn) is one such drug and acts by preventing mast cells from degranulating, a process which results in the release of several proinflammatory signalling and effector molecules that often trigger immune responses that lead to allergic reactions and even anaphylaxis [201]. However, so far there has been no research investigating the effect of cromolyn on breast cancer progression.

Animal experiments were setup to incorporate the i.p. injection of cromolyn each day for the final five days of respective experiments into VNMAA treated animals harbouring PyMT-BO1 tumours for the purpose of inhibiting mast cell degranulation (Figure 4.5A). Animals treated with VNMAA + cromolyn exhibited significantly reduced tumour volumes compared to animals treated with VNMAA only or with vehicle control + cromolyn (Figure 4.5B). However, there was no change in tumour volume between animals treated with vehicle control compared to vehicle control + cromolyn.

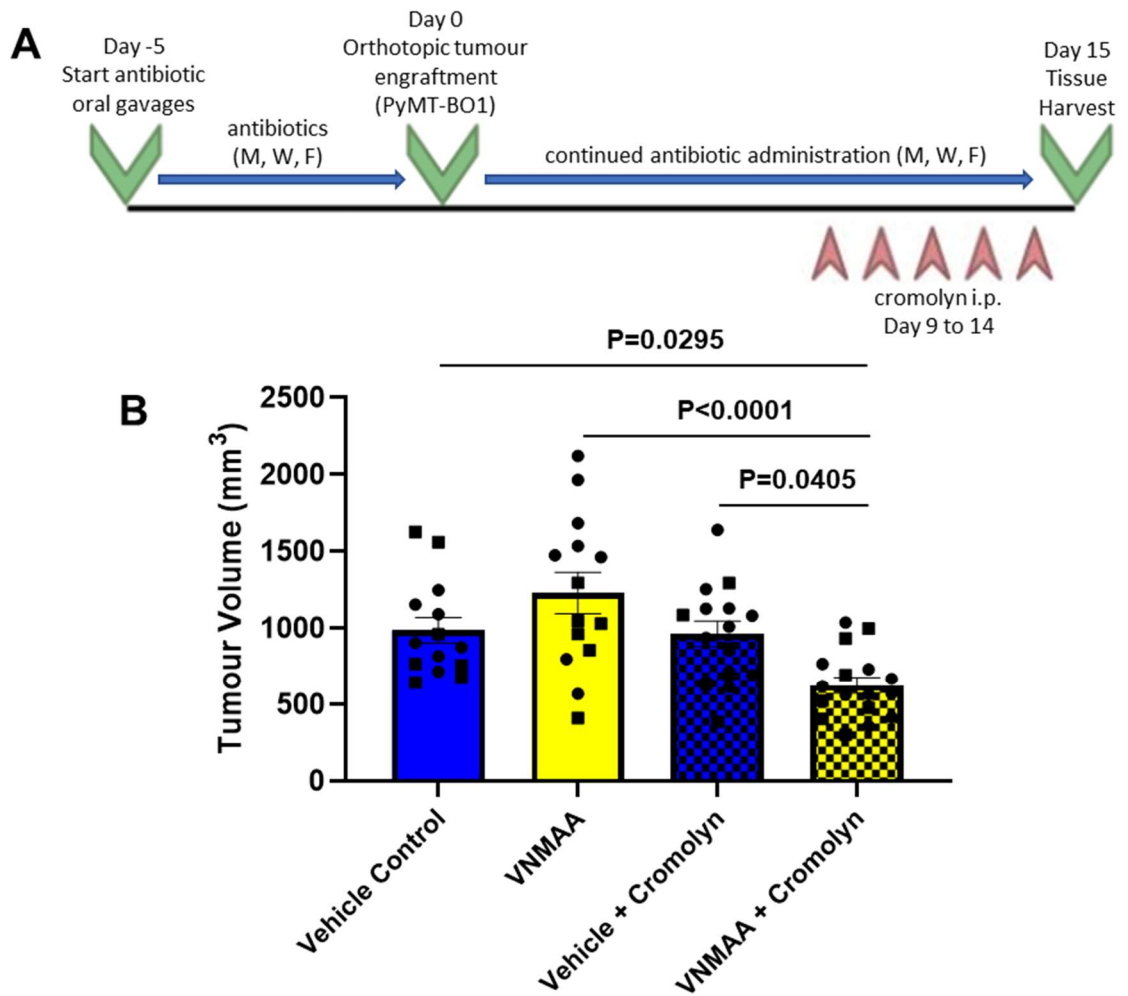


Figure 4.5. Inhibition of mast cell degranulation via cromolyn sodium i.p. injection rescues tumour growth in VNMAA treated animals but not in vehicle treated controls. A) Schematic of the VNMAA antibiotic treatment regimen. Antibiotic administration begins one week prior to PyMT-BO1 tumour induction (day 0) and continues for the duration of the experiment three times per week until experiment cessation on day 15 with the addition of cromolyn sodium administration from day 9 to 14 post tumour induction. **B)** Bar graphs showing the mean (\pm SEM) tumour volumes of PyMT-BO1 tumour volumes measured *ex situ* from vehicle control and VNMAA treated animals as well as those animals treated with the respective treatments with the addition of cromolyn sodium i.p. injections. Significantly different P-values are stated on the graph. Points of the same shape between conditions are from the same experiment (N) (N=2; $n \geq 14$ animals per condition; One-Way ANOVA $P=0.0002$; Tukey's multiple comparison tests with adjusted P-values: Vehicle Control Vs. VNMAA $P=0.263$, $\text{DBM}=-243.7$; Vehicle Control Vs. Vehicle + Cromolyn $P=0.9982$, $\text{DBM}=22.24$; Vehicle Control Vs. VNMAA + Cromolyn $P=0.0295$, $\text{DBM}=360.2$; VNMAA Vs. Vehicle + Cromolyn $P=0.1822$, $\text{DBM}=265.9$; VNMAA Vs. VNMAA + Cromolyn $P<0.0001$, $\text{DBM}=603.9$; Vehicle + Cromolyn Vs. VNMAA + Cromolyn $P=0.0405$, $\text{DBM}=337.9$).

4.6 Discussion

In many cancer studies, including breast cancer, the reporting of changes in tumour associated leukocyte populations is a regular observation when tumour progression is altered. It was surprising that low-level immune profiling of two different tumour models, which were significantly increased in size following one of two antibiotic treatments, did not find any changes in the major tumour associated leukocytes linked to disease progression. Thus, scRNA-seq was performed on PyMT-BO1 tumours from VNMAA treated animals to answer two questions. Firstly, were the immune cells present functionally different based on their gene expression profiles? Secondly, if tumour associated leukocytes were not behaving differently between treatment conditions, was it possible a rare cell type or cell types, that were not profiled during targeted flow cytometry approaches, were active in the mechanism driving tumour growth in antibiotic treated animals.

Due to funding limitations, sample numbers for scRNA-seq were limited to two per treatment condition. While this was sufficient for the purpose of investigating the differential expression of genes within specific clusters against those in the alternate treatment group, it meant that it would not be possible to statistically compare quantitative data such as the numbers of cells assigned to clusters between treatment conditions. Thus, observations of this nature would only infer possible effects on abundances of specific cell types and would require further investigation by alternate means to confirm any significance, in this case, using histology.

Two analyses methods were utilised when investigating differences in single cell transcriptomes following antibiotic treatment. The initial analysis utilised a new user-friendly software interface, called Loupe Cell Browser, which was developed for the purpose of giving users an overview assessment of raw data outputs from 10X Genomics sequencing platforms. This aided in identifying clusters and assigning cell types to them. Through this method, differences in cell density in respective clusters could be assessed but, as previously mentioned, due to low sample size these could not be statistically compared. Two clusters, identified as T-cells and B-cells, had reduced cell densities in tumours from VNMAA treated animals while gene expression profiles associated with mast cells defined another cluster which appeared to have increased cell densities in tumours from VNMAA treated animals compared to controls. At this point expert support was sought from the Earlham Institute who explained that Loupe Cell Browser lacked the QC and filtering steps required to more reliably assess transcriptomic data. One such step was the removal of cells in or entering apoptosis which were identified by high expression levels of mitochondrial genes, denoted by the official gene ID prefix "*mt-*". Following QC steps, dimension reduction (UMAP) and cell type identification, 14 cell types were identified, four more than the 10 identified via Loupe Cell Browser which had included one unknown cluster and one cluster identified as dying cells. Furthermore, the

resolution between similar cell types was improved. For example, classification of macrophage subsets based on increased *Lyz1* or *C1qc* expression. Additionally, this method facilitated DEG analysis comparing the expression of genes within each cluster between treatment conditions. Therefore, while results from Loupe Cell Browser were used to guide later investigations, the conclusions from scRNA-seq data were definitively drawn from the analysis performed in collaboration with the Earlham Institute.

DGE analysis of each of the 14 cell type clusters identified only four genes which had significantly different expression levels between tumour samples from vehicle control and VNMAA treated animals. In tumours from VNMAA treated animals compared to controls there was a reduction in *Igfc1* expression in the *C1qc* high macrophage cluster as well as was a reduction in *Spr1a* expression but increases in *Mgp* and *Ltf* expression in the luminal cell 2 cluster. While *Igfc1* is not currently linked to cancer progression, the other three DGEs have been. *Ltf* has been shown to be protective in renal, nasopharyngeal and gastric cancers while *Spr1a* has been linked with potentially poorer prognoses in progesterone receptor positive breast cancer [682–685], which the PyMT-BO1 model is. However, the direction of differential expression for these two genes in tumours from VNMAA treated animals does not fit with these associations. The only one of these four significant DGEs which might align with the pattern of increases in tumour growth following VNMAA treatment was the increase in *Mgp* expression. *Mgp* encodes matrix Gla protein (MGP), an ECM protein usually associated with calcium binding and the prevention of calcification in bone, heart and kidney tissues [686]. However, it has also been linked to the progression of colorectal cancer with one study describing increases in *Mgp* mRNA levels were associated with poorer prognoses in breast cancer patients, especially in those with hormone receptor negative cancers [686,687]. However, this was not supported by quantification of the actual amount of the MGP protein in breast tissues following protein translation. Further assessment of the expression and translation of this particular gene and its transcripts, respectively, may be useful in identifying possible drivers of tumour growth in this model.

In terms of the abundances of the various cell types identified, consistent reductions in the densities of T-cell and B-cell clusters were observed in both of the methods used to analyse the scRNA-seq data. A previous study using a spontaneous MMTV-PyMT mouse model deficient in B-cells showed tumour progression was unaffected by the lack of B-lymphocytes [688]. In the context of this study, which utilised an MMTV-PyMT derived tumour model, those results suggest B-cells are unlikely to be involved in driving tumour growth. In contrast, T-cells are heavily influential in the regulation of tumour success with both pro- and anti-tumour roles [689]. However, previous flow cytometry of both T- and B-cells found no significant changes in their abundances, including of T-cell subsets

(CD4+ and CD8+), in both PyMT-BO1 and EO771 tumours and following both VNMAA and cephalixin (PyMT-BO1 only) treatments. However, an increase in cell density in a cluster with gene signatures associated with stromal cells was observed in the samples from the VNMAA treated animals compared to controls. Thus, considering the lack of significant changes in differential gene expression within these three clusters between treatment conditions as well as the aforementioned immune flow cytometry results, it was decided that subsequent investigation should focus on the increase in stromal-associated cells as these had not been considered previously.

Histological analysis of collagen deposition did not identify differences in stromal density between treatment groups. However, it did aid in identifying the possible increase in abundance of granular cells in tumours from VNMAA treated animals, later identified as mast cells following toluidine blue staining. Flow cytometry of PyMT-BO1 tumours from VNMAA and cephalixin treated animals did not identify significant increases in tumour mast cell abundances compared to controls. However, from the one experiment successfully analysed, there was a clear trend suggesting increases in mast cells in both treatment groups. It is plausible that had time facilitated the repeating of flow cytometry experiments, mast cells may have been observed to be significantly increased in tumours from antibiotic treated animals via this methodology. As flowcytometry of mast cells had initially proven challenging, an alternate method of quantifying mast cell densities was sought. This was achieved through assessing mast cell counts per tumour section area (MC/mm²) following toluidine blue staining of tumour sections. This revealed increased abundances of mast cells in PyMT-BO1 tumours from both VNMAA and cephalixin treated animals as well as in EO771 tumours from VNMAA treated animals. After collaborative discussions, colleagues in the U.S. and Italy were asked to count mast cells in toluidine blue tumour sections from breast cancer models of a luminal A subtype treated with a cocktail of broad-spectrum antibiotics similar to VNMAA and a HER2-positive subtype treated with vancomycin. Both found similar increases in tumour mast cell abundances following these different antibiotic treatment regimens in the two alternate breast cancer tumour models.

Although these observations confirm antibiotic administrations result in increased mast cell densities in several breast tumour models, alone they are not enough to conclude that these cells are responsible for driving changes in tumour growth. IgE immunoglobulins are key regulators of mast cell activations and so serum IgE concentrations were measured in both VNMAA and cephalixin treated animals. These concentrations were not detected as being different in either antibiotic treatment group compared to those observed in controls, suggesting that an allergenic driver was unlikely to be causing the observed increases in mast cells in tumours from antibiotic treated animals. However, if mast cell function was inhibited in these models and a concurrent

reduction in tumour growth observed, this would suggest mast cells were playing a functional role in regulating the disease progression, likely in an IgE independent manner.

Cromolyn sodium, a mast cell stabiliser which inhibits degranulation of the cytoplasmic granules comprising proinflammatory signalling molecules, was administered to mice treated with either VNMAA or a vehicle control. Tumour volumes of these animals were compared to those from animals of the same antibiotic treatment groups but without receiving cromolyn doses. Animals receiving both VNMAA and cromolyn had final tumour volumes which were significantly reduced compared to all three other experimental arms (control only, control with cromolyn and VNMAA only). Cromolyn administration did not influence tumour growth in the vehicle control animals. These results point to two conclusions. Firstly, mast cells are indeed a functional member within the mechanism driving antibiotic-induced changes in breast cancer progression. Secondly, this mechanism is driven by a microbiota dependent pathway because only tumour growth in antibiotic treated animals was rescued following cromolyn administration while tumour growth in control animals was not influenced in the same way. Thus, it is likely that a perturbed microbiota promotes the pro-tumourigenic activity of tumour resident mast cells. The molecular interactions governing such activity remains to be elucidated.

In conclusion, scRNA-seq of tumours from VNMAA antibiotic treated animals identified reductions in B-cells and T-cells based on marker gene expression. It also identified an increase in cells with stromal gene expression profiles. Histological analysis of tumour sections did not find differences in tumour stromal density but did allude to increased abundances of granular cells in antibiotic treated animals, later confirmed to be mast cells through toluidine blue staining. Mast cell abundance was increased in several breast cancer tumour models following different antibiotic treatments in animals from three different facilities. To investigate whether these differences in mast cell abundance were causative or consequential of differences in tumour growth, cromolyn sodium, a mast cell stabiliser which inhibits mast cell function, was administered to tumour bearing mice receiving either VNMAA or a vehicle control. Cromolyn sodium was associated with a rescued tumour growth in VNMAA treated animals but not in vehicle treated control animals. Taken together these data suggest that antibiotics induce a perturbation of the gut microbiota which influences mast cell activity at a tumour level, ultimately promoting increased rates of tumour growth. Future studies will need to investigate the mechanistic pathways governing both the microbiota— mast cell interactions as well as the mast cell— tumour interactions.

These conclusions are not drawn without limitation. The single cell transcriptomics was undertaken using short-read technology. Such technology is suitable for generating a broad overview of

complex heterogenous tissues but resolution of cell types in particularly low abundance can be poor using short-read sequencing methods. Therefore, it is possible that one of the reasons mast cell differences were not carried forward to the analysis downstream of the QC stages is due to this limitation. Thus, should the opportunity arise, it may be useful to perform long-read based single cell transcriptomics to better assess possible differences in the abundances of cells generally present in very low abundances between antibiotic treatments as well as comparing differences in their gene expression profiles.

Additionally, although an effective mast cell stabilising agent in humans, there is some debate regarding the efficacy of cromolyn activity on mast cell stabilisation in mice [690]. However, there continues to be an array of murine based research utilising this drug and producing results consistent with successful stabilisation of mast cells [691–693]. Those studies are often further supported by the fact that the effects of cromolyn administration often mirror outcomes observed in mast cell deficient mice, suggesting its administration is indeed affecting mast cell function [694]. There has also been concerns raised regarding the length of time until functional onset of the drug in this study, because in humans time until onset is between two to six weeks after an oral administration [695]. However, the results presented in this study are themselves evidence that in mice where an i.p. injection is used to administer cromolyn, the functional activity of the drug is achieved during the five-day treatment based on the significant effect they have on the tumour model. Nonetheless, future testing of whether the observations made in C57 BL/6 wild-type mice translate over to mast cell deficient mouse models under the same conditions would go a long way in supporting the conclusions made in this study. There are already several models of mast cell deficient mice. The most common of these is the *Kit*^{W-sh/W-sh} model which carries a mutation in *Kit* gene encoding the c-KIT protein, one of the two major mast cell marker proteins [696]. More recently, models have been developed which use *Cre*-inducible mechanisms targeting mast cell protease genes and have been used successfully in several studies [697,698]. Unfortunately, these experiments were beyond the scope of this study, but future work hopes to utilise such models.

5 Antibiotic induced perturbations of the gut infer increased incidence and size of secondary breast cancer metastatic lesions in lung tissue

The progression of tumours often correlates with the spread of cancer cells from primary organs, in which a cancer originates, to secondary organs at distant sites in the body, a process termed metastasis. Metastasis can occur at any point after the establishment of a vascularised tumours but is generally considered to become more likely as tumour growth progresses. Unfortunately, metastasis is heavily linked to increased morbidity and mortality and once cancers progress to this stage, most are incurable, including breast cancer. Current treatments of metastatic disease aim to improve the length and quality of patients' lives, but it is estimated that around 90% of these patients succumb to their disease [699,700]. Thus, much of cancer research focusses on understanding the mechanisms behind metastasis and the therapeutic targets which may aid in preventing and treating it.

Metastasis occurs through several sequential steps which are all required for metastatic lesion outgrowth [701]. Firstly, primary cancer cells in the tumour need to transition from an epithelial morphology to a mesenchymal morphology where they become motile, a process which will be described in detail later in this section. Mesenchymal cancer cells break away from the primary tumour and intravasate into the blood vasculature or lymphatic system where they are transported to distant organs [702]. In the target organ they must extravasate into the tissue and avoid anti-cancer immune attack [703]. Finally, metastatic cells must initiate proliferation and maintain growth and vascularisation in order to form a tumour lesion [701].

Although the incidence of metastasis is heavily associated with mortality, the process by which it occurs is in fact extremely inefficient [700,703]. Once cancer cells manage to break away from a primary tumour, they must intravasate into either the vascular system or the lymphatic system where they face two major obstacles to their survival. Firstly, they need to resist the forces exerted on them by the flow rates of blood and lymph fluid as they move through the respective networks [704,705]. Secondly, they must avoid immune attack by circulating anticancer immune cells, such as cytotoxic T-cells and NK cells, which are capable of identifying cancer cells based on the presence or absence of specific antigen proteins which trigger cytotoxic activity that kill cancer cells before they reach a target organ [706,707]. For example the absence of MHC I on a cell surface promotes NK cell activation and targeted killing of cancer cells [708].

Although difficult to accurately quantify, research suggests that in some intravascular metastasis models, as little as 0.01 to 0.02% of CTCs successfully infiltrate target organs and form micro metastases [11,701,703,709]. Unlike cells in the primary tumour, cancer cells which enter

circulation are subjected to major forces exerted upon them by the flow rates of blood or lymph fluid which most cancer cells are often unprepared for. These forces are termed haemodynamic forces and the mechanism by which they affect cancer cells is called fluid shear stress (FSS) [710,711]. FSS is responsible for killing many cancer cells which make it into circulation [704]. Those that survive these forces, often through cytoskeletal mechano-adaptations which soften the outer cellular cortex [710], are termed CTCs and will travel through the vasculature to distant organs. However, unlike tumour cells within an established tumour microenvironment, these cells face increased exposure to anti-cancer immune cells without the protection of pre-established immune evasion mechanisms [706,707].

A major characteristic of malignant tumours is their ability to evade the components of the immune system which actively seek to kill cancer cells. In fact, immune evasion is one of the hallmarks of cancer [55]. Evasion can take place through direct methods, where cancer cells interact with cytotoxic cells directly in a manner which inhibits cytotoxic activity, or indirect methods, where cancer cells promote the activity of immunosuppressive cells that in turn prevent the anti-cancer activity of various effector cells. An example of a direct mechanism of immune evasion is the interaction between PD-1, on the surface of cytotoxic T-cells, with its ligand, PD-L1, on the cell surfaces of several cancer types [712–714]. The binding of these two proteins prevent the activity of cytotoxic T-cells and inhibits the release of their cytotoxic granzymes which would otherwise cause cancer cell death [714]. A secondary mechanism includes the recruitment of immunosuppressive cells, including MDSCs and T-reg cells, through production of chemoattractant molecular signals, which include the cytokines IL-10 and TGF- β [328,715,716]. IL-10 specifically has been implicated in the inhibition of antigen presentation by dendritic cells and MHCII+ macrophages which would otherwise evoke an anti-cancer immune response [717,718]. Another, more direct, immunosuppressive pathway involves the binding of CTLA4, on the surface of T-cells, to its ligands, namely B7.1 and B7.2, on the surface of antigen presenting cells which again triggers an inhibition of their ability to present antigens and as a result, the inability to activate effector cells such as cytotoxic T-cells [719]. However, these immune evasion escape mechanisms are largely reliant on an established immunogenic tumour microenvironment in which immunosuppressive chemotactic gradients can be maintained, environments which are not present in the circulatory system [720].

After surviving the haemodynamic stresses experienced during circulation as well as the potential of encounters with anti-cancer immune leukocytes in the peripheral blood, CTCs need to extravasate into the target organ tissue, where they become known as disseminated tumour cells (DTCs). Here tumour-derived cells enter a state of dormancy where proliferative activity is either

completely inhibited or kept to a minimum [721,722]. The reasons why these cells enter this quiescent state are largely undefined, however there is increasing evidence that interaction of DTCs with cytotoxic cells, including CD8+ T-cells cells, maintain cytostatic dormancy without killing the cancer cells [723,724]. Cancer cells can remain in a dormant state for long periods of time and are often unaffected by chemotherapies, which commonly aim to inhibit the proliferative activities of cancer cells [725]. Therefore, it is unfortunate that in many cancers, including breast cancer, patients who may be in remission experience the return of their disease years later in metastatic organs as dormant cancer cells “awaken” and begin to proliferate, forming metastatic lesions [723].

The PyMT-BO1 model employed in this study had been tagged with both GFP and firefly luciferase by the collaborators that supplied the cells (Weilbaeher laboratory, Washington University, St. Louis). These tags facilitate the identification of cancer cells which spread from primary tumours to organs and tissues at distant sites. The luciferase tag promotes the production of firefly luciferase, an enzyme which catalyses the oxidation of its substrate, luciferin, a reaction which generates luminescence. The GFP tag promotes the production of GFP, a cytoplasmic protein that when excited with light of wavelengths between 395 to 475nm, emits light at a wavelength of ~510nm. This dual tag system means both bioluminescent and fluorescent methods can be employed to track and identify cancer cells as they move away from the primary tumour. Additionally, the PyMT-BO1 model has been selectively developed according to its preference for metastasising to lung and, to a lesser extent, bone tissue. Thus, metastatic studies using this model can use targeted analysis of these tissues to quantify metastatic burden.

Following the same experimental workflow as described previously (see Figure 3.1A), primary PyMT-BO1 tumours, lungs, femur bones and blood were harvested from animals treated with either a vehicle control, VNMAA or cephalixin. The expression of epithelial to mesenchymal transition (EMT) markers, E-cadherin and vimentin, was assessed and western blot analysis of tumour lysates alluded to changes in the expression of these markers following antibiotic treatments at a timepoint of 18 days post tumour induction, suggesting antibiotic induced gut microbiota perturbations may promote dissemination of malignant cells from the primary tumour. Flow cytometric analysis of lungs and blood proved challenging and did not reliably identify PyMT-BO1 cells using the GFP and luciferase tags as markers of their cell status. However, *ex situ* bioluminescence imaging managed to identify metastatic cells in the lungs but not femur bones. The number of metastatic incidence was low within each of the three treatment groups but a Fisher’s exact test identified a significant increase in metastatic occurrence in animals from the cephalixin treatment group. However, from the experiments carried out there is not enough evidence to say one way or the other if VNMAA treatment is associated with increased risk of metastatic incidence, nor is there enough evidence

to suggest either if these treatments influence the size of lesions relative to the vehicle treated control group.

5.1 Epithelial to Mesenchymal Transition (EMT)

During early tumour development most cancer cells will take on an epithelial morphology, which promotes cell-to-cell adhesion and cellular immobility [726]. This is characterised by the presence of an intracellular apicobasal axis meaning organelles and other cellular components are organised asymmetrically within the cell to promote epithelial polarity which is responsible for cellular orientation within a tissue and ultimately tissue homeostasis [727]. Cellular adhesion is governed by membrane structures called adherens junctions. These structures express transmembrane proteins which bind extracellularly to identical proteins on the surface of neighbouring cells as well as interacting with intracellular scaffold proteins within the actin cytoskeleton to aid in maintaining cell structure [728]. E-cadherin is one of the major adherens junctions proteins responsible for maintaining cell-to-cell adherence and is a marker of an epithelial cellular morphology [729].

As tumours grow, cancer cells undergo a change in morphology from an epithelial state to a mesenchymal one in a process called EMT. Unlike epithelial cells, mesenchymal cells do not exhibit polarity but rather take on a spindle-like shape, resulting in the loss of an apicobasal axis. Additionally, these cells reduce the expression of adherens proteins, such as E-cadherin, responsible for cell-to-cell adhesion. Several studies have shown the reduction of E-cadherin specifically is due to the upregulation of transcription factors, namely Slug and Snail, which prevent the transcription of genes that encode E-cadherin [730]. Although its mechanism in regulating EMT is largely unknown, a major marker of a mesenchymal phenotype is vimentin, a filamentous protein positively correlated in expression with the increased activity of the Slug transcription factor [730]. These changes in cell morphology facilitate the mobility of cancer cells and enable them to translocate from primary tumours into the vasculature and ultimately make their way to distant organs.

Assessing the amounts of both E-cadherin and vimentin in tumour tissue can allude to the degree of EMT activity and in turn infer the extent of a tumour's metastatic invasiveness. Specifically, reductions in E-cadherin and increases in vimentin denote increased EMT activity and therefore the increased risk of cancer cell dissemination.

5.1.1 Immunostaining of EMT markers suggests a largely mesenchymal tumour dynamic in PyMT-BO1 tumours

Tumour sections from VNMAA and cephalixin treated animals were stained immunohistochemically for E-cadherin (Figure 5.1.1A) and immunofluorescently for vimentin (5.1.1B and C). Different staining techniques were employed due to the anti-vimentin immunohistochemical protocol not being successful after multiple attempts. Thus

immunofluorescence was used as an alternative and successfully identified areas of vimentin expression within the tumour sections. The PyMT-BO1 tumours were largely deficient of E-cadherin and across all tumours from all treatment groups, E-cadherin was only identified in epithelial mammary ducts and in structures which appeared similar to vasculature. Conversely, vimentin appeared ubiquitous throughout tumour tissues. However, qualitative assessments did not suggest differences in vimentin abundance between treatment groups.

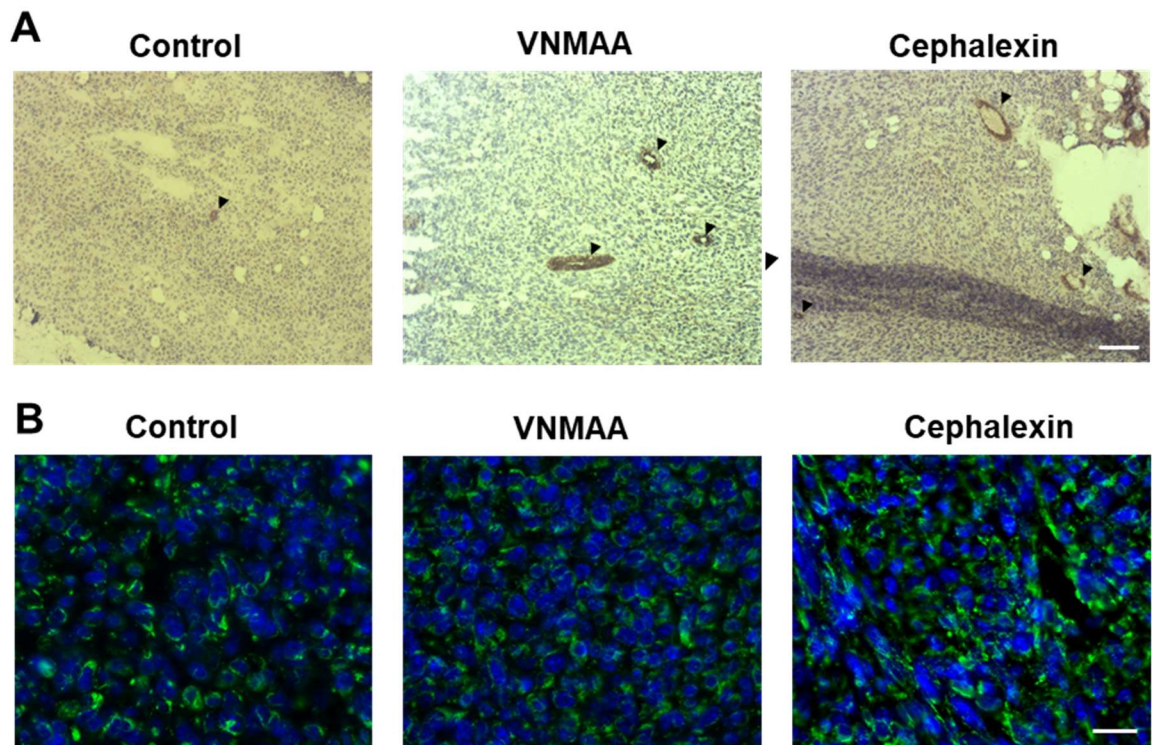


Figure 5.1.1. Immunostaining of tumour sections for the EMT markers E-cadherin and vimentin. A) Representative micrograph images of immunohistochemical staining of E-cadherin in tumour sections from animals treated with either a vehicle control, VNMAA or cephalixin. Scale bar = 100 μ m. **B)** Representative micrograph images of immunofluorescent staining of DAPI (blue) and vimentin (green) in tumour sections from animals treated with either a vehicle control, VNMAA or cephalixin. Scale bar = 20 μ m.

5.1.2 Western blot analysis supports histology and shows no differences in EMT markers between treatment conditions

Western blots were performed on tumours harvested 15 days post tumour induction from animal experiments which had employed both VNMAA and cephalixin treatments to better quantify the effect of antibiotic treatment on the downstream presence of E-cadherin and vimentin EMT markers in the PyMT-BO1 tumour model. Neither E-cadherin nor vimentin showed significant differences in their abundance following either antibiotic treatment based on densitometry analysis (Figure 5.1.2A, B, C and D).

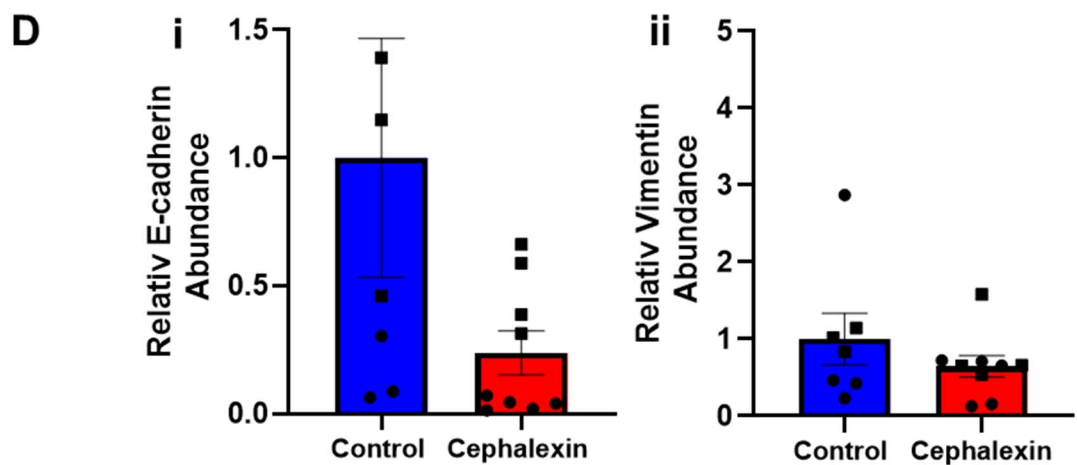
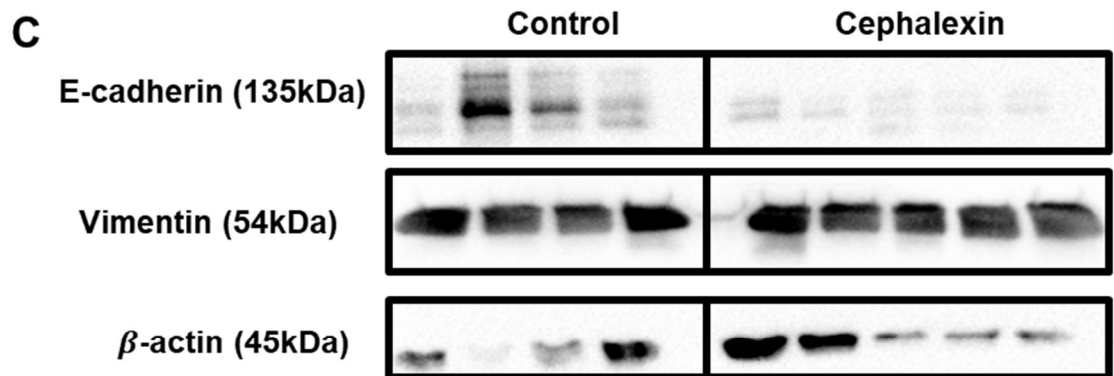
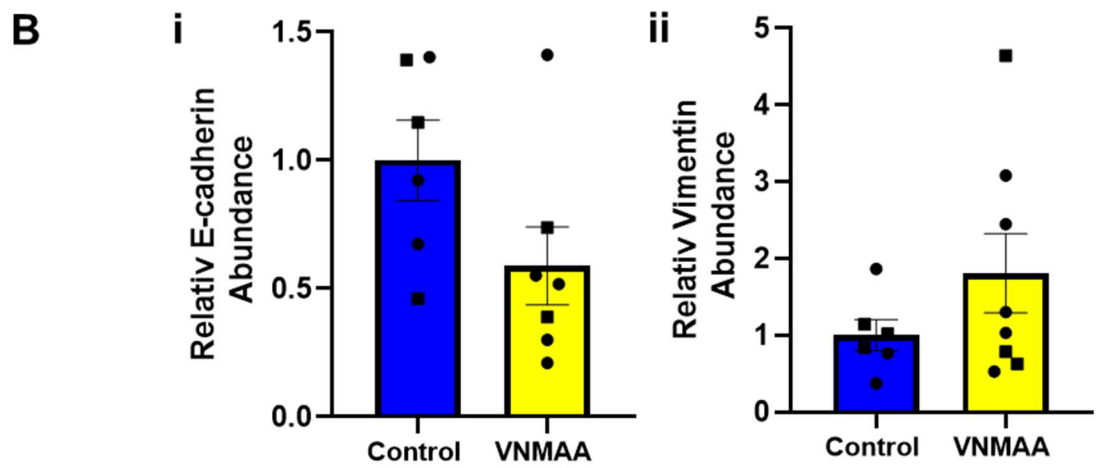
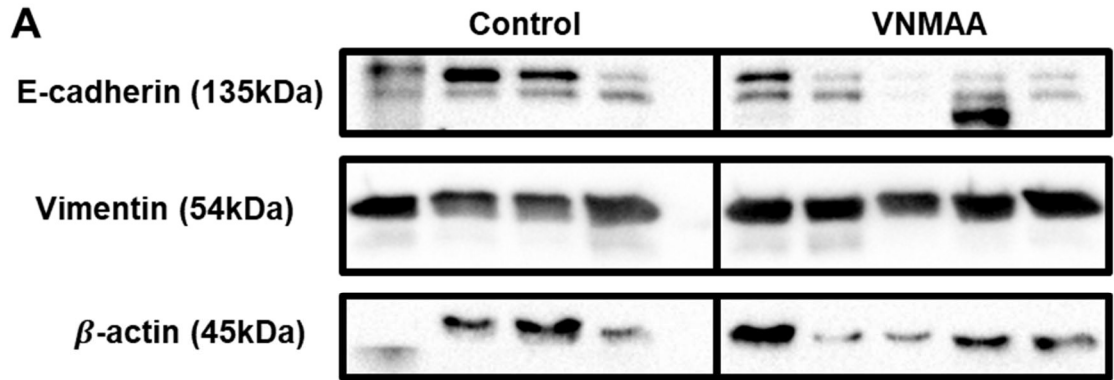


Figure 5.1.2. Western blot analysis of tumour lysates obtained 15 days post tumour induction from VNMAA and cephalixin treated animals for E-cadherin and vimentin alongside subsequent densitometry analysis. **A)** Representative western blot image of E-cadherin and vimentin abundance in whole tumour lysates (day 15 post tumour induction) from VNMAA treated animals, with β -actin as a loading control. **B)** Bar graphs of densitometry analysis performed on western blots showing the mean (\pm SEM) **i)** E-cadherin (N=2, n \geq 6 animals per condition, P=0.087, DBM=-0.412, SEM=0.219) and **ii)** vimentin (N=2, n \geq 6 animals per condition, P=0.224, DBM=-0.806, SEM=0.629) abundances in both vehicle control and VNMAA treatment groups relative to the mean value of vehicle controls. **C)** Representative western blot image of E-cadherin and vimentin abundance in whole tumour lysates (day 15 post tumour induction) from cephalixin treated animals, with β -actin as a loading control. **D)** Bar graphs of densitometry analysis performed on western blots showing the mean (\pm SEM) **i)** E-cadherin (N=2, n \geq 7 animals per condition, P=0.09, DBM=-0.763, SEM=0.419) and **ii)** vimentin (N=2, n \geq 7 animals per condition, P=0.306, DBM=-0.355, SEM=0.334) abundances in both vehicle control and cephalixin treatment groups relative to the mean value of vehicle controls.

5.1.3 Late-stage tumours do exhibit reductions in E-cadherin and increases in vimentin

Although the analysis performed in Section 5.1.2 did not highlight any significant changes in the amounts of the two EMT markers which were probed for, there appeared to be a general trend in samples from both VNMAA and cephalixin treatment groups suggesting E-cadherin was lower in abundance albeit not significant. To see if this observation may change to one of significance at a later timepoint, remaining tumour tissue from the single experiment that was harvested on day 18 post tumour induction was subject to western blot for the same EMT markers. While it did not appear that vimentin abundances changed in animals treated with VNMAA, a qualitative assessment of the western blot alluded to a significant loss of E-cadherin at this timepoint following treatment (Figure 5.1.3A). Densitometry was performed on bands for vimentin (Figure 5.1.3C) which confirmed no change in its abundance between treatment groups, but while clear bands were present for E-cadherin in control samples, there were no bands denoting E-cadherin presence in samples from the VNMAA treated animals. Therefore, it was not possible to perform densitometry to quantify differences in E-cadherin abundances between treatments. However, this clearly suggests at a later stage in tumour growth, VNMAA treatment is associated with a reduction of E-cadherin relative to vehicle controls. Additionally, while a qualitative observation suggests that E-cadherin was low in abundance in tumours from both control and cephalixin treated animals at the same timepoint (day 18) (Figure 5.1.3B), densitometry identified vimentin as being significantly increased in abundance relative to control samples supporting the hypothesis that antibiotics is promoting EMT (Figure 5.1.3D).

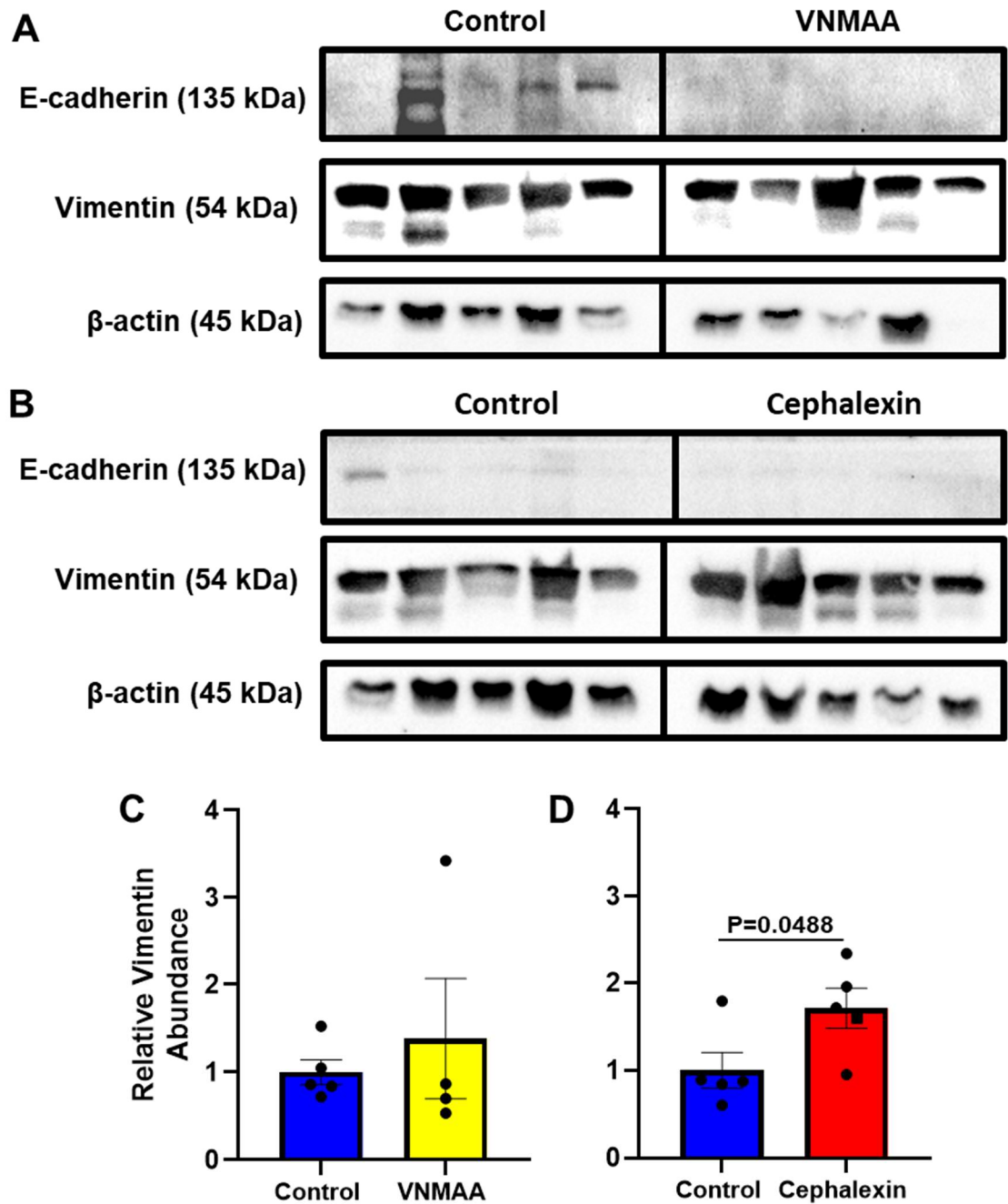


Figure 5.1.3. Western blot analysis of tumour lysates obtained 18 days post tumour induction from VNMAA and cephalalexin treated animals for E-cadherin and vimentin alongside subsequent densitometry analysis. Representative western blot images of E-cadherin and vimentin abundance in whole tumour lysates (day 18 post tumour induction) from **A**) VNMAA treated animals and **B**) cephalalexin treated animals alongside samples from vehicle treated control animals. β -actin was used as a loading control in both blots. **C**) Bar graph of densitometry analysis performed on the western blot in panel **A** showing the mean (\pm SEM) vimentin abundances in both vehicle control and VNMAA treatment groups relative to the mean value of vehicle controls (N=1, n=4, P=0.557, DBM=0.989, SEM=0.622). **D**) Bar graph of densitometry analysis performed on the western blot in panel **B** showing the mean (\pm SEM) vimentin abundances in both vehicle control and cephalalexin treatment groups relative to the mean value of vehicle controls (N=1, n=5, P=0.0488, DBM=0.712, SEM=0.307).

5.2 Treatment with cephalexin, but not VNMAA, significantly increases the incidence of PyMT-BO1 metastasis to the lungs during the relatively early stages in primary tumour development

Vascularisation of primary tumours is a major prognostic element when considering their metastatic potential [731]. Section 3.7 describes that PyMT-BO1 tumours were well vascularised by 15 days post tumour induction and Section 3.6 describes the highly proliferative state of tumours at the same timepoint, quantified by Ki67 staining. Therefore, this was deemed a suitable timepoint to begin investigating the incidence of metastasis, as well as the extent of said incidence, in animals harbouring PyMT-BO1 tumours and treated with antibiotics.

5.2.1 In situ imaging of mice to identify metastasis was unsuccessful

Often studies investigating the spread of cancer within an animal model will utilise *in situ* imaging techniques to identify both the locations to which the disease disseminates as well as the extent of said dissemination. Utilising the firefly luciferase tag status of the PyMT-BO1 cancer cells, this method was attempted. Once an experiment had reached its endpoint which was usually 15 days post tumour induction with the exception of the one experiment carried forward to day 18, animals were subject to an i.p. injection of *in vivo* grade luciferin substrate at a concentration of 2mg/150µl. Following an incubation period of five minutes, animals were anaesthetised, and bioluminescence imaging performed using the Bruker *in vivo* Xtreme instrument. This procedure was performed on two separate experiments concluding on day 15, but no metastatic signal was identified in any of the animals. To accommodate an increased period of time in which metastasis may grow to sizes that might emit a measurable signal, one experiment was carried to 18 days post tumour induction and imaged in the same way (Figure 5.2.1A). Again, there was no signal observed at this later timepoint. It was hypothesised that the high signal intensity generated by the primary tumour had resulted in the loss of smaller signals from micro metastases. Thus, an attempt was made to reduce the luminescence emission from the primary tumour to support the detection of potentially weaker signals elsewhere in the animals. This was done by placing aluminium bottle caps over the primary tumour site when animals were imaged (Figure 5.2.1B). However, although this managed to significantly dampen the luminescence signal from the primary tumour, there was still no evidence of metastasis in any other locations in any of the animals irrespective of treatment.

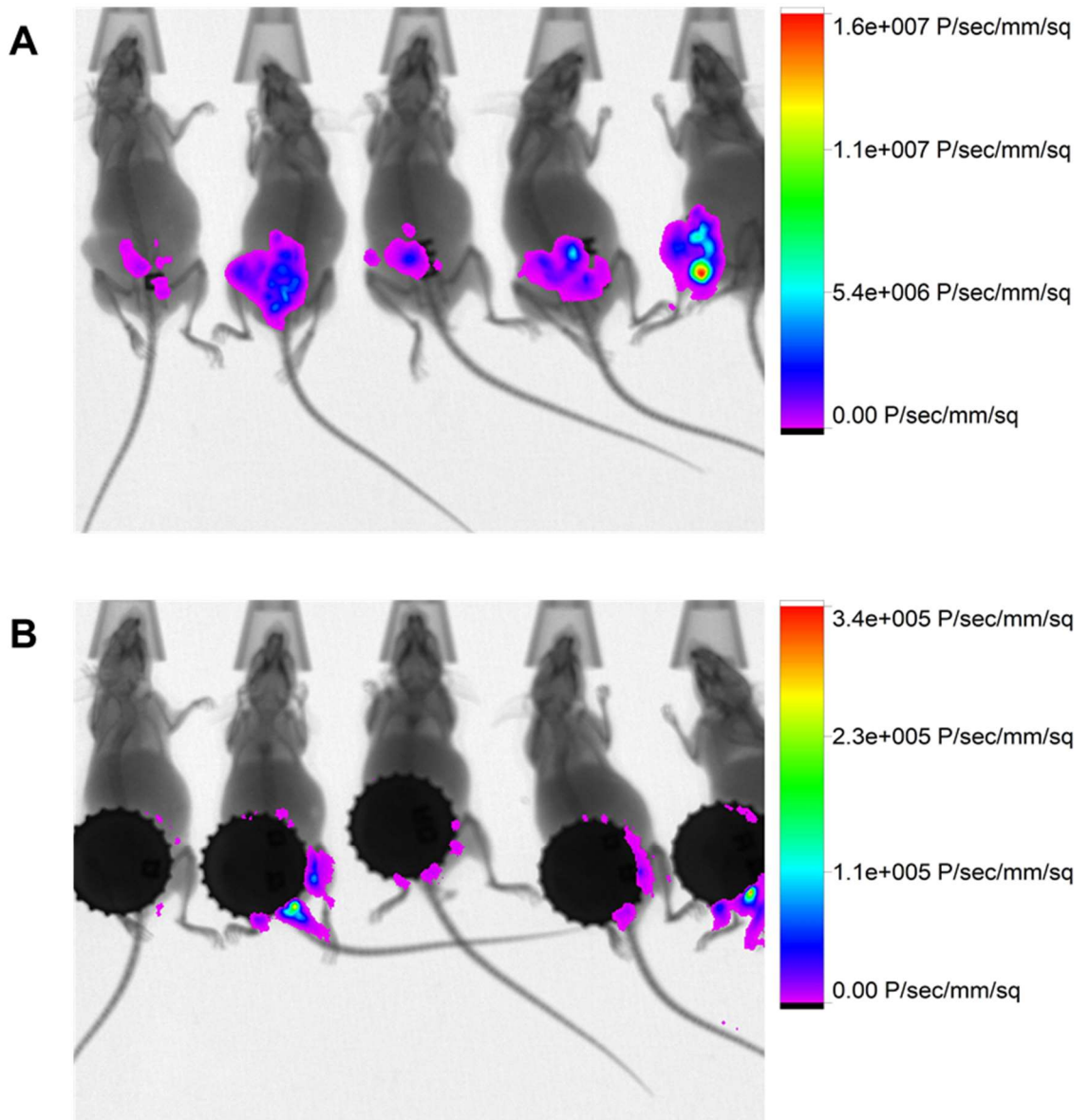


Figure 5.2.1. *In situ* bioluminescence imaging was unable to identify metastasis *in vivo*. **A)** Bioluminescence image of tumour bearing mice 18 days post tumour induction following i.p. luciferin injections. **B)** Bioluminescence image of the same animals in panel A but with tumours sites covered with aluminium bottle caps in an attempt to dampen signal emitted from primary tumours.

There were several hypotheses for why *in situ* imaging was unsuccessful in identifying overt metastasis. Firstly, it was possible that at the timepoints at which animals were imaged, metastases had not yet reached sizes large enough to generate a measurable signal. However, this seemed unlikely due to the known progression of this cancer model. The second possibility was that the black fur coat of C57 BL/6 mice, as well as other “obstacles”, such as the rib cage and surrounding organs, reduced the amount of emitted light that reached the detector to below measurable levels. In an attempt to overcome these obstacles, two subsequent methods were attempted to identify and quantify metastatic dissemination of PyMT-BO1 cells following antibiotic treatment. Flow

cytometry was undertaken on cultured blood and lung tissue isolated from animals at the endpoint of experiments and a method of *ex situ* imaging of lung and bone tissues was also performed.

5.2.2 Difficulties identifying circulating tumour cells and disseminated tumour cells due to low numbers in peripheral blood and digested lung tissue.

Due to the hypothesised reasons for *in situ* imaging being unable to identify the dissemination of cancer cells in the lung, flow cytometry was employed as an alternate method and was applied directly to blood and lung samples from antibiotic treated animals and vehicle treated controls. Mammalian cells are known to produce autofluorescence when excited by blue light and emit light in the green spectra [732]. In previous studies using PyMT-BO1 cells, autofluorescence had been noted when trying to separate populations using fluorophores that emit light in the green channel. Therefore, because it was expected that a relatively small proportion of the total events recorded from blood and bone samples would be PyMT-BO1 cells, it was possible that these might be lost in CD45- populations which produced autofluorescence in the same channel that was used to identify native GFP fluorescence, generating potentially false-positive data. To reduce this possibility, antibodies against both GFP (PE-Cy7 conjugate) and firefly luciferase (Alexa Fluor 647 conjugate) were used to stain cancer cells, and these were gated off of CD45- , native GFP+ populations (Supplementary Figure 5.2.2). This meant that to define a recorded event as a cancer cell it had to be positive for respective markers in three separate channels to ensure the utmost confidence in cancer cell identification.

Initial staining attempts proved challenging due to the nature of intracellular cytoplasmic staining and several experiments were unsuccessful in identifying PyMT-BO1 cells even in positive control samples from either cultured PyMT-BO1 cells or cells isolated from a primary tumour. However, by adjusting the fixation and permeabilization steps during the staining protocol, successful staining and identification was eventually achieved. Briefly, following staining with Live/Dead viability dye and extracellular staining of CD45, a 10 minute “soft fixation” using 2% PFA was introduced to the protocol prior to the use of a proprietary fixation/permeabilization buffer (eBioscience, 00-5523-00) and subsequent antibody staining. It was believed this adjustment prevented the leaking of the target proteins from the cytoplasm through permeabilised cell membrane as they were “semi-fixed” prior to membrane permeabilization. This hypothesis and protocol adjustment was derived from work done by Grupillo *et al.* (2011) who described improved staining using a similar method when staining fluorescently labelled cells for intranuclear proteins [733].

Blood samples were obtained via cardiac puncture at the endpoint of given experiments and red blood cells were removed, via a lysis buffer, followed by the selective culturing of cells for a period of one week to try and amplify the small numbers of PyMT-BO1 cells up to a measurable population size (see Section 2.17.2). Initial flow cytometric analysis suggested that while there was no difference in samples from cephalixin treated animals, the number of PyMT-BO1 cells was significantly increased in samples obtained from VNMAA treated animals compared to vehicle treated controls (Figure 5.2.2.1A). These populations were extremely rare and of the viable cells recorded, only between 0 and 1% of those fell into the final gate which defined a cell as being PyMT-BO1 (Figure 5.2.2.1B). However, although staining was confirmed as being successful based on the simultaneous staining of cultured PyMT-BO1 cells as a positive control and comparing these to FMO controls of the same cell type, after applying the stringent gating strategy already described, there were high numbers of events in the final gate of the negative control sample, far higher than any of the experimental samples, suggesting that noncancer cells were potentially being incorrectly identified as cancer cells (Figure 5.2.2.1A and C). Unfortunately, this result meant that the observations were largely unreliable. One explanation for observing cells in the final gate of the negative control sample might be if this sample was run after the positive control sample resulting in residual positive events passing through the cytometer during the collection of events for the negative control and potentially being recorded under the subsequent data collection for the negative control. Although care had been taken to avoid such an issue when running blood samples, when running lung samples, it was absolutely ensured that the negative control samples were run prior to any other samples including FMO controls. There appeared to be no change in lung infiltrating PyMT-BO1 cells between treatment conditions (Figure 5.2.2.2A). Again, the populations of cells classified as cancer cells were extremely small (0.02 to 0.08% of viable cells) (Figure 5.2.2.2B). Frustratingly though, even with further steps to avoid such a result and although staining was again shown to be successful based on positive controls and FMOs, cells from the negative control sample still made it into the final gate and at a higher proportion than any of the experimental samples (Figure 5.2.2.2A and C). Therefore, it was concluded that flow cytometry, like *in situ* bioluminescent imaging, had proven not suitable for measuring metastasis at this timepoint.

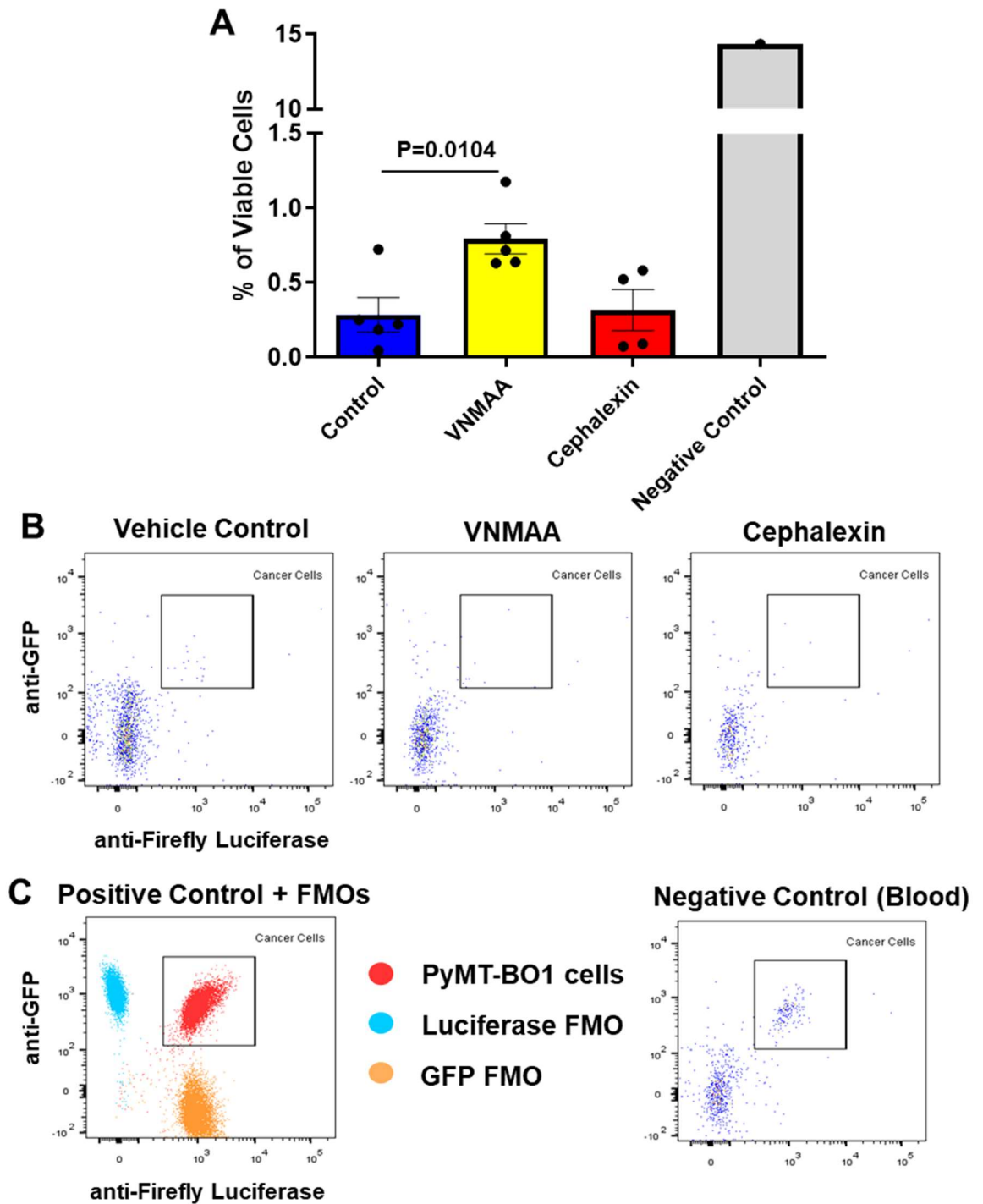


Figure 5.2.2.1 Flow cytometry was unable to reliably identify metastatic cells in blood samples of animals irrespective of treatment group. **A)** Bar graph showing the mean (\pm SEM) abundance of PyTM-BO1 cells as a percentage of viable cells in blood samples from vehicle control, VNMAA and cephalixin treated animals ($N=1$, $n \geq 4$ animals per condition; Control Vs. VNMAA $P=0.0104$, $DBM=0.509$, $SEM=0.153$; Control Vs. Cephalixin $P=0.862$, $DBM=0.032$, $SEM=0.177$). A negative control sample (lung cells from a non-tumour bearing animal) was run alongside experimental samples but produced false-positive results. **B)** Representative pseudocolour dot plots showing the events from blood samples which were gated as double positive for anti-GFP and anti-firefly luciferase staining from vehicle control, VNMAA and cephalixin treated animals. **C)** Dot plot showing successful staining of a positive control sample (cultured PyMT-BO1 cells) based on the lack of emission in respective channels of FMO controls as well as a pseudocolour dot plot showing the inclusion of cells in final gate in the negative control sample.

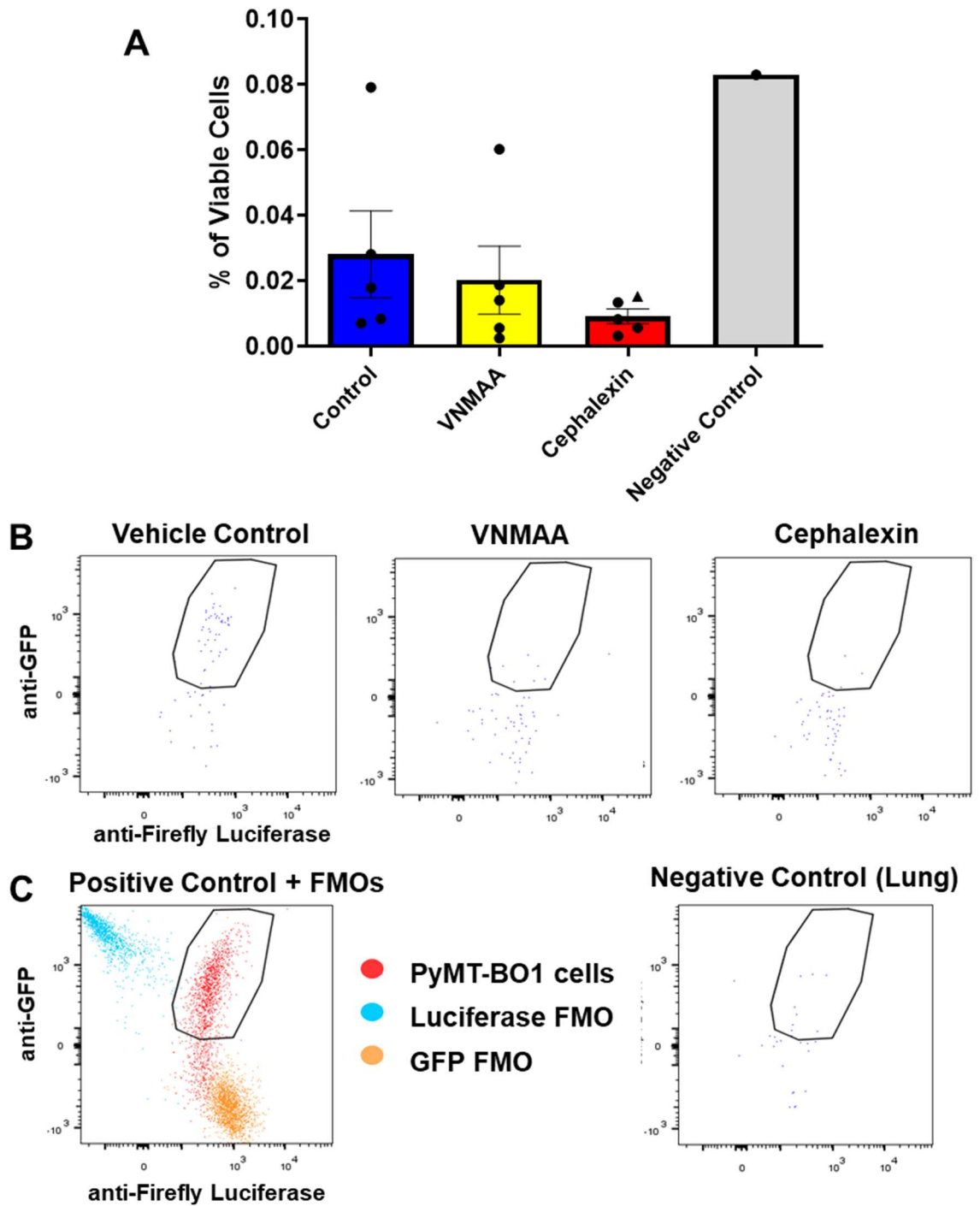


Figure 5.2.2.2 Flow cytometry was unable to reliably identify metastatic cells in lung samples of animals irrespective of treatment group. **A)** Bar graph showing the mean (\pm SEM) abundance of PyTM-BO1 cells as a percentage of viable cells in lung samples from vehicle control, VNMAA and cephalalexin treated animals ($N=1$, $n \geq 4$ animals per condition; Control Vs. VNMAA $P=0.652$, $DBM=0.-0.008$, $SEM=0.017$; Control Vs. Cephalalexin $P=0.197$, $DBM=0.-0.019$, $SEM=0.0.014$). A negative control sample (lung cells from a non-tumour bearing animal) was run alongside experimental samples but produced false-positive results. **B)** Representative pseudocolour dot plots showing the events from lung samples which were gated as double positive for anti-GFP and anti-firefly luciferase staining from vehicle control, VNMAA and cephalalexin treated animals. **C)** Dot plot showing successful staining of a positive control sample (cells isolated from a primary PyMT-BO1 tumour) based on the lack of emission in respective channels of FMO controls as well as a pseudocolour dot plot showing the inclusion of cells in final gate in the negative control sample.

5.2.3 *Ex situ* imaging of lungs identifies increased incidence of metastasis in antibiotic treated animals

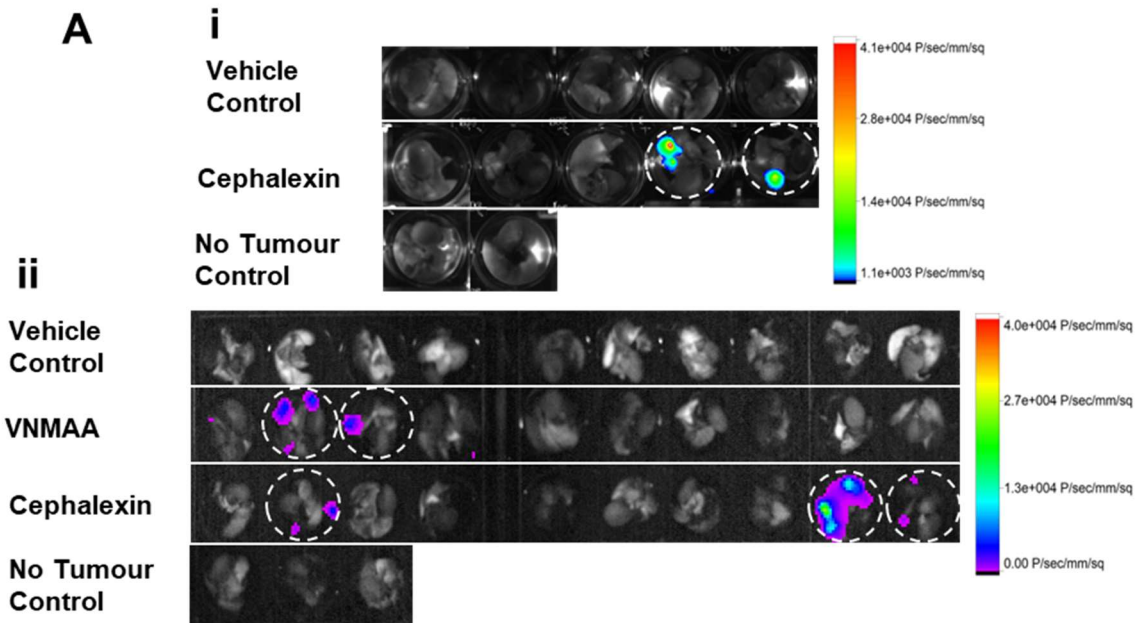
Neither *in situ* bioluminescence imaging nor flow cytometry identified metastasis using this model at this timepoint. However, it was understood that the PyMT-BO1 model had been employed successfully for this purpose by collaborators, namely the Weilbaecher laboratory at the University of Washington St. Louis, USA, and that the timepoint in question was an appropriate one, firstly because of experiences discussed with the same collaborators as well as the fact that the primary tumour was too large to facilitate further growth at day 15. Thus, in a final attempt to identify metastasis, lung and bone tissues were harvested and bathed in a weak solution of luciferin (300µg/ml) prior to *ex situ* bioluminescence imaging. This was a method which was novel in the Robinson laboratory and was based on the premise that it was expected to reduce the dampening of luminescent signal by the dark fur coats of the animals as well as increasing the availability of the luciferin substrate to PyMT-BO1 cells should they be present.

Tissues from each animal were placed in the luciferin bath at the same time to equilibrate exposure to the substrate and allowed to bathe for three minutes prior to imaging. An initial optimisation experiment was undertaken to ensure the success of the new method prior to scaling up to an experiment comprising what was expected to be an appropriate number of animals to compare metastatic incidence between treatment groups. The aims of these experiments were to firstly identify the incidence of metastasis and secondly to quantify the extent of metastatic burden according to the intensity of luminescence signal (photons/sec/mm²) generated by lungs or bones harbouring cancer cells. The PyMT-BO1 model is known to metastasise readily to the lungs, but metastasis to the bones is less common. The *ex situ* imaging method did not identify any metastatic signal in any of the 15 bones that were harvested from tumour bearing animals irrespective of treatment (Supplementary Figure 5.2.3). However, it worked well with lung tissues. Therefore, subsequent investigations focused only on lung tissue.

Using the overlay images produced by the Bruker Molecular Imaging Software (Figure 5.2.3Ai and ii), metastatic incidence was noted as either a positive (metastasis identified) or negative (metastasis not identified) result for each animal. Due to the overall small sample size and the fact that none of the 15 control samples exhibited metastasis at this stage, a Fisher's exact test was performed comparing the positive and negative results for vehicle control against VNMAA and separately for vehicle control against cephalixin treatment groups (Figure 5.2.3B). While the incidence of metastasis in VNMAA compared to control was not significantly increased, it was significantly increased in the lungs of cephalixin treated animals versus the vehicle control treated group.

Although no metastatic signal was identified in the lungs from vehicle control treated animals, quantification of metastatic burden in the lungs of antibiotic treated animals was carried out regardless. Regions of interest (ROI) were designated as the circumference of each well used to bathe the lungs in luciferin solution. Bioluminescence signal was quantified as the mean photons/sec/mm² for each ROI (mean photons/sec/mm²). Data from both experiments were collated following the normalisation of positive signal values against signals from the lungs of non-tumour bearing animals used as negative controls in each of the respective experiments (Figure 5.2.3C). While these data were visualised graphically alluding to larger metastatic lesions in antibiotic treatment groups, due to there being no cases of metastasis in control samples this cannot be confirmed via a statistical analysis.

As stated, when a tumour becomes vascularised, cancer cells are able to metastasize. As tumours grow, generally so to do the number of blood and lymphatic vessels within them [731]. The more vessels present within a tumour, the more “avenues” cancer cells have for intravasating into blood or lymph circulation and subsequently disseminating to distant organs. Additionally, tumour stroma is influential in promoting metastasis through its various microenvironmental components and is often associated with tumour growth [734,735]. Therefore, due to the low sample size obtained regarding metastatic incidence between these two experiments, to support the hypothesis that increased tumour size may be aligned with the incidence of metastasis, primary tumour volumes from the animals which exhibited metastasis were compared to the extent of their metastasis quantified as photons/sec/mm² (Figure 5.2.3D). A Spearman’s correlation analysis suggested that in these experiments, there was a weak positive correlation between tumour volume and metastatic burden based on a correlation coefficient of 0.32. However, this was not statistically significant ($P = 0.5$) and so there is not enough evidence to suggest larger primary tumour volumes result in increased metastatic incidence.



B

Treatment	Positive	Negative	Total	Fisher's Exact P-value analysed against Vehicle Control
Vehicle Control	0	15	15	
VNMAA	2	8	10	0.15
Cephalexin	5	10	15	0.0421

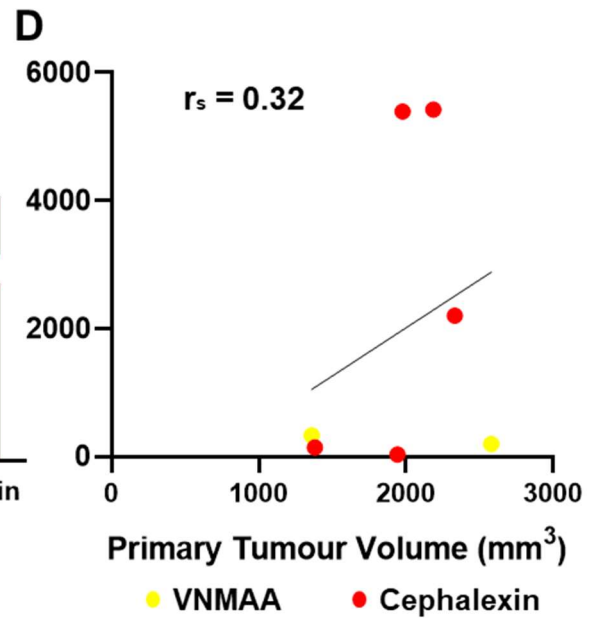
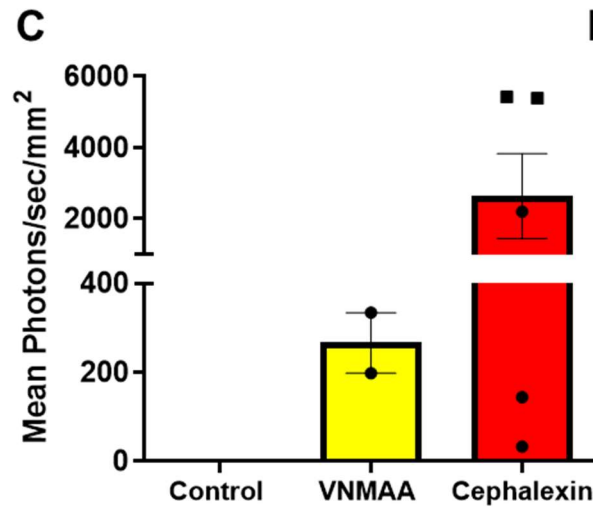


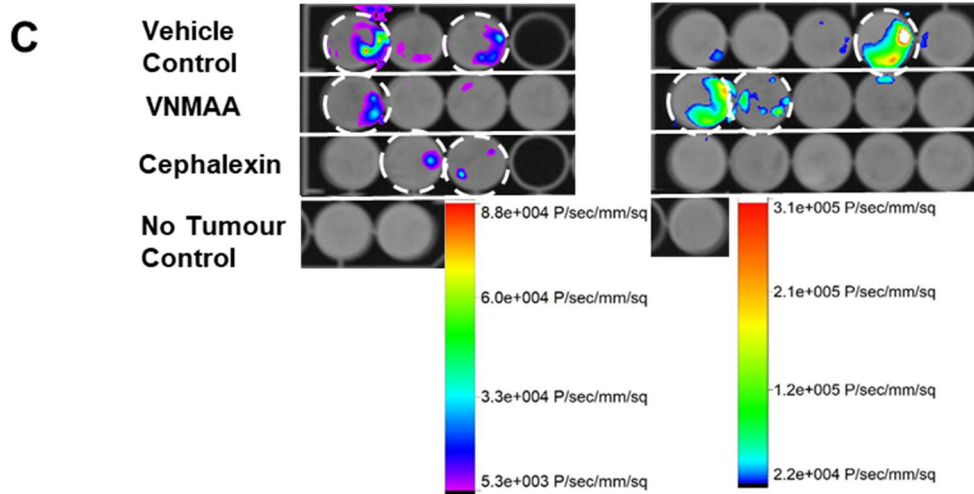
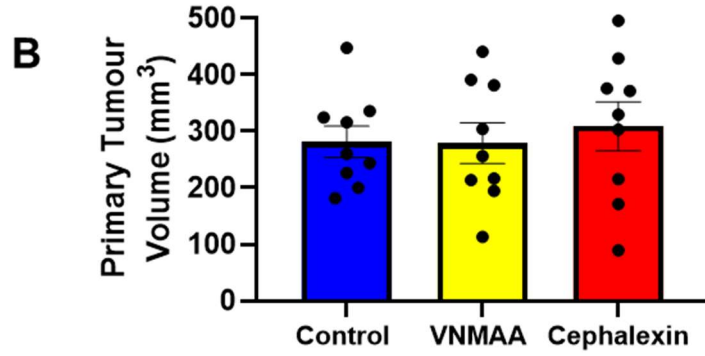
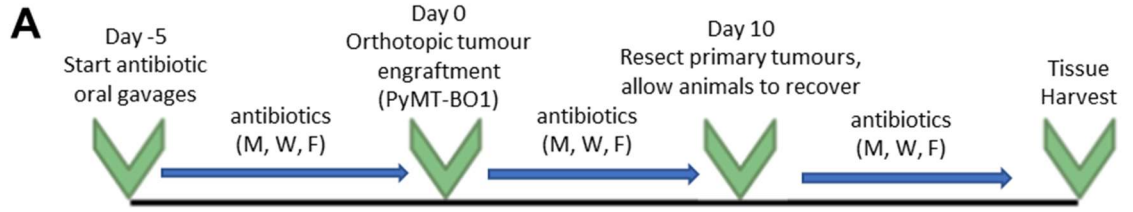
Figure 5.2.3. Metastatic incidence in the lungs appears increased in animals treated with antibiotics compared to vehicle treated controls. **A)** Bioluminescence images of lungs taken from PyMT-BO1 tumour bearing animals following respective antibiotic treatments bathed in luciferin solution (300 μ g/ml). Images are taken from two independent experiments (**i**: n=5 animals per condition and **ii**: n=10 animals per condition) with “no tumour controls” denoting lungs from non-tumour bearing animals for the purpose of downstream signal normalisation. Dashed circles aid in identifying samples positive for metastasis. **B)** Table showing the collated results from bioluminescence imaging for lung samples that were either positive (metastasis identified) or negative (no metastasis identified) for bioluminescent signal indicating metastasis. A Fisher’s exact test was performed on both VNMAA samples compared to vehicle controls and on cephalixin samples compared to vehicle controls. Calculated P-values are presented in the table. **C)** Bar graph showing the mean (\pm SEM) bioluminescence signal detected in average photons/sec/mm² from samples positive for metastasis. Points denote individual animals and points of different shapes denote different experiments (N=2, n \geq 2 animals per treatment condition). **D)** XY graph plotting tumour volume (mm³) against respective metastatic signal values (average photons/sec/mm²) showing no linear correlation between tumour size and the extent of metastatic burden irrespective of treatment, (Spearman’s correlation coefficient (r_s)=0.32; n=7 total samples).

5.3 At later stages of disease progression, there is no influence on the incidence or progression of metastasis following either antibiotic treatment

The data presented in Section 5.2.3 demonstrates that metastatic incidence and burden is increased in animals treated with cephalexin at day 15 post tumour induction. However, due to the low numbers of animals presenting with metastasis from each treatment group, it may be argued that the strength of these observations would be supported by bolstering the study size. Due to the numbers of animals that would be required to do so sufficiently and to uphold the “reduce” principle of the “three R’s” (replace, reduce and refine the use of animals in scientific research) [736], the experimental workflow was altered to include a resection element in which primary tumours were surgically removed and animals allowed to recover. Animals would then be monitored for signs of degrading health, such as cachexia and changes in behaviour, at which point they would be humanely euthanised (Figure 5.3A). This new workflow was expected to provide any dormant disseminated cancer cells with an increased period of time during which they might become active and proliferate to form micro metastasis which could then be identified by bioluminescence imaging at a later timepoint. This would aid in increasing the number of comparable metastatic incidences between treatment conditions without the need for using more animals to do so. Additionally, this workflow mimics more closely the disease progression pathway in breast cancer patients whereby lesions are often identified weeks or months after mastectomy or lumpectomy surgery to remove primary tumours, making the downstream observations more similar to clinical observations made in humans.

To avoid any potential bias in metastatic dissemination caused by larger primary tumours between groups, tumours were resected when they had reached palpable sizes and *in situ* measurements produced mean tumour volumes which were similar between treatment groups. For all animals this fell on day 10 post tumour induction (Figure 5.3B). Once tumours had been resected, incision sites were sutured closed and animals left to recover. Unfortunately, of the 30 animals making up the experimental cohort, five animals had to be humanely euthanised due to complications during resection surgery. Furthermore, although every effort was made to remove the primary tumours without leaving any residual tumour behind, by day 18 post tumour induction, just eight days after primary tumour resection, the majority of the animals had regrown tumours to palpable sizes along the incision line made during the resection surgery. As a result, the experiment had to be concluded to avoid unnecessary suffering to the animals. Regardless, downstream analysis was pursued, and lungs were harvested and subject *ex situ* bioluminescence imaging which identified several cases of metastasis in all three treatment groups (Figure 5.3C). Surprisingly, the incidence of metastasis in

lungs from the control cohort was the same as in the VNMAA treatment cohort and one more than the cephalixin treatment cohort, an observation that did not follow the hypothesis that antibiotic induce microbiota perturbations may drive increased metastatic incidence. However, similar to the analysis described in Section 5.2.3, a Fisher's exact test was carried out on these data from vehicle controls compared to VNMAA and cephalixin treatment groups respectively (Figure 5.3D) and in both cases confirmed no statistically significant differences in the incidence of metastasis between either antibiotic treatment group compared to vehicle treated controls. Metastatic burden was quantified, as described in Section 5.2.3, and identified that those lungs presenting with metastasis from the control cohort in fact had a greater mean photon emission, and thus a greater metastatic burden, than those lungs from both VNMAA and cephalixin treated cohorts. While again surprising, the differences in metastatic burden were not statistically significant between antibiotic treatment groups compared to vehicle treated controls in this resection experiment (Figure 5.3E).



D

Treatment	Positive	Negative	Total	Fisher's Exact P-value
				analysed against Vehicle Control
Vehicle Control	3	5	8	
VNMAA	3	6	9	1
Cephalixin	2	6	8	1

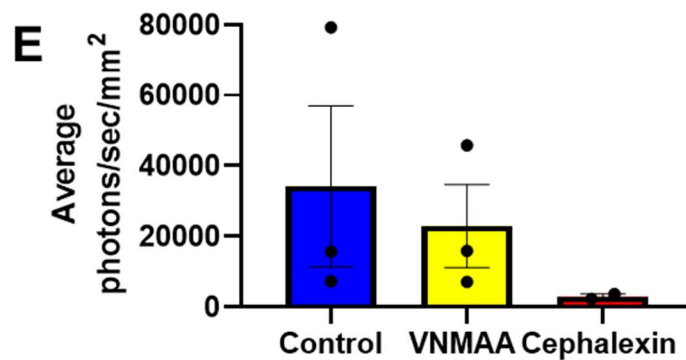


Figure 5.3. At later stages, metastasis is not influenced by antibiotic treatment. A) Schematic of adjusted experimental workflow to reflect primary tumour resection. Antibiotic administration and tumour induction was carried out as described in Section 2.4 until day 10 post tumour induction at which point primary tumours were resected under anaesthesia and animals allowed to recover. Antibiotic treatment (VNMAA) was then continued thrice weekly until experimental cessation which was determined by animal health during the experiment. **B)** Bar graph showing the mean (\pm SEM) primary tumour volumes at the point of resection on day 10 post tumour induction (N=1, n=10 animals per condition; Control Vs. VNMAA P=0.954, DBM=-2.663, SEM=45.37; Control Vs. Cephalexin P=0.602, DBM=27.28, SEM=51.25). **C)** Bioluminescence images of lungs taken from PyMT-BO1 tumour bearing animals on day 18 post tumour induction following respective antibiotic treatments (control n=8, VNMAA n=9, cephalixin n=8) bathed in luciferin solution (300 μ g/ml). Images are taken from the same experiment, but plates were imaged separately, “no tumour control” denotes lungs from non-tumour bearing animals for the purpose of downstream signal normalisation. Dashed circles aid in identifying samples positive for metastasis. **D)** Table showing the results from bioluminescence imaging for lung samples that were either positive (metastasis identified) or negative (no metastasis identified) for bioluminescent signal indicating metastasis. A Fisher’s exact test was performed on both VNMAA samples compared to vehicle controls and on cephalixin samples compared to vehicle controls. Calculated P-values are presented in the table. **E)** Bar graph showing the mean (\pm SEM) bioluminescence signal detected in average photons/sec/mm² from samples positive for metastasis. Points denote individual animals (N=1, n \geq 2 animals per treatment condition).

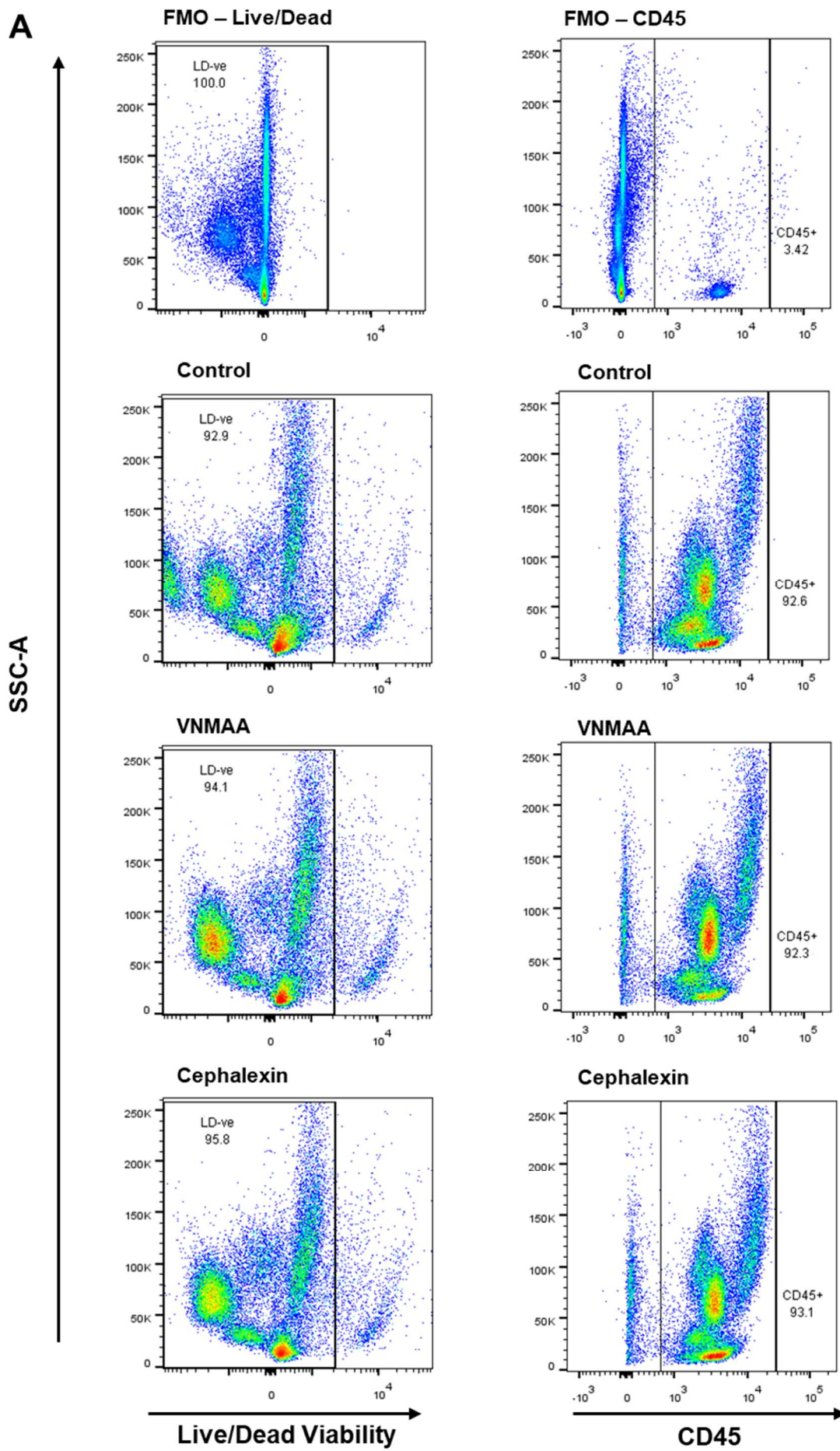
5.4 Immune activity in the lung following antibiotic treatment as an indication for metastatic invasion and secondary tumour initiation

The “Seed and Soil” hypothesis was first described by Stephen Paget in 1889 and inferred that the success of metastatic outgrowth relied upon the interaction between the disseminated cancer cells, the seeds, with the cellular and molecular environment of the metastatic target organ, the soil [737]. Although this theory has incurred some debate, it is largely still supported by the cancer research community of this era. When molecular signals which might normally be used to regulate tissue homeostasis in an organ are intercepted by dormant cancer cells, a change in cancer cell state occurs which turns the proliferative switch on and promotes the formation of micro metastases [725]. Similarly to the behaviours of cancer cells in the primary tumour, when this occurs DTCs start to shape a microenvironment which supports their proliferation and expansion by recruiting cell types to remodel the ECM, such as fibroblasts, and prevent anti-tumour immune activity, including T-reg cells, MDSCs and certain subsets of macrophages [11]. The abundances of anti-cancer T-cells, namely cytotoxic T-cells and Th1 T-cells, and natural killer cells are also observed to be reduced in tissues where metastases form [11].

5.4.1 *Antibiotics do not influence immune cell infiltration of lungs from tumour bearing mice*

To identify how antibiotic treatments influenced immune activity in the lung of tumour bearing animals, flow cytometry was undertaken to profile the immune populations associated with roles in regulating metastasis. As described in previous flow cytometry analyses, cell abundances were expressed as a percentage of viable cells. Unfortunately, the number of cells successfully passed through the flow cytometer were reduced, likely due to poor tissue digestion, and were between 35 000 to 55 000 events per sample. The percentage of leukocytes (CD45+ cells) were consistently around 90% of viable cells across all samples irrespective of antibiotic treatment. This was unusual as previous experience using the same protocol on tissues formed using the same tumour model usually result in leukocyte populations of around 70 to 80% of the viable cells isolated during tissue digestion [738]. However, respective FMO controls suggested staining and subsequent gating was appropriate (Figure 5.4.1A). Thus, this unusually high number of leukocytes relative to viable cells was likely due to the poor tissue digestion which resulted in successful isolation of leukocytes but poor isolation of other lung cell populations, such as alveolar epithelial cells. However, because all samples exhibited similar abundances of leukocytes relative to viable cells, comparisons between treatment groups, downstream analysis should not be affected by these unusually high percentage of viable cells. Therefore, investigation of possible differences in metastasis associated myeloid and lymphoid populations was carried forward. The myeloid populations profiled included granulocytic

and monocytic cells, several macrophage subsets including alveolar macrophages (AM), which are resident in the lung, as well as metastasis associated macrophages (MAM) and their progenitor cells (MAMPC) [739,740]. Gating strategies for these cell populations are presented in Supplementary Figure 5.4.1 and 5.4.2. There were no significant differences in any of the myeloid populations between either VNMAA or cephalixin treatment groups compared to control samples ($P > 0.05$; t-test), which surprisingly included what looks like a reduction in MAMs in both VNMAA and cephalixin groups (Figure 5.4.1B). Similarly, no significant observations were noted between treatment conditions regarding low level profiling of B-cell and T-cell populations (Figure 5.4.1C) ($P > 0.05$; t-test). Unfortunately, both Foxp3 and NK1.1 staining were unsuccessful in this experiment meaning T-regulatory and T-helper cell populations could not be distinguished nor could NK cells be identified.



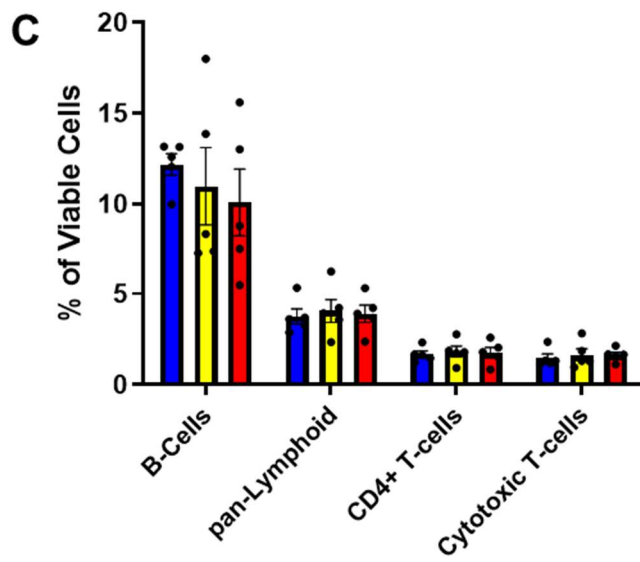
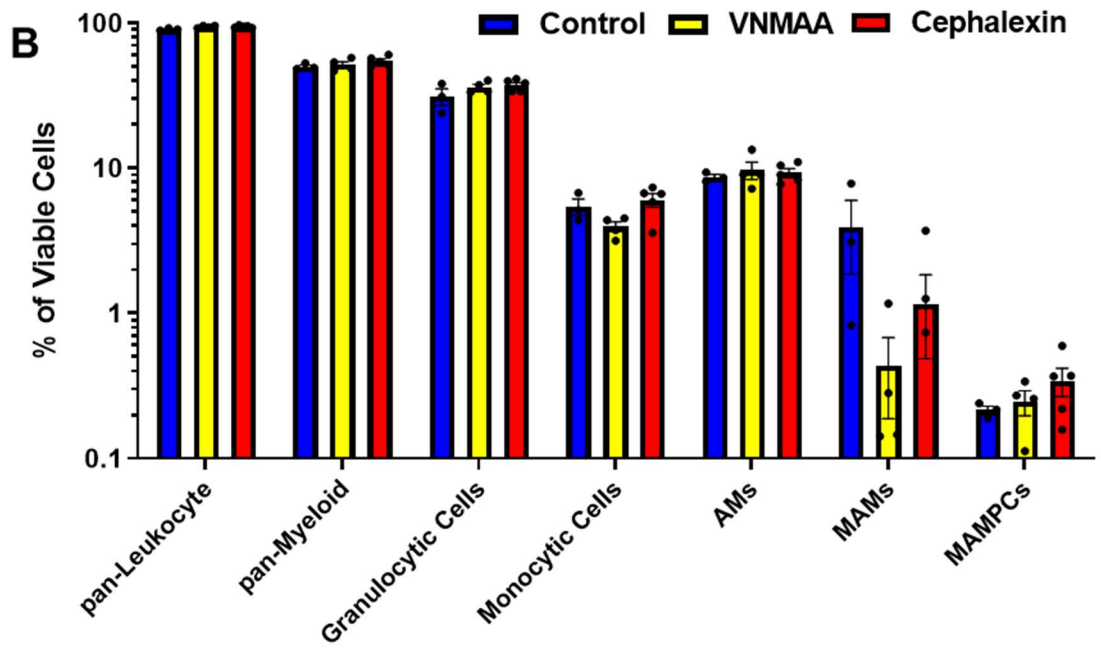


Figure 5.4.1. Antibiotic treatments do not influence immune populations in the lungs of tumour bearing animals. A) pseudocolour dot plots showing successful staining of viable and CD45+ cells from whole lungs with consistently high numbers of CD45+ cells across all three treatment groups. **B)** Grouped bar graphs of the mean (\pm SEM) percentage of viable cells for respective myeloid populations (N=1; n \geq 3 animals per condition), including pan-Leukocytes (Control Vs. VNMAA P=0.042, q=0.242; Control Vs. Cephalexin P=0.021, q=0.146), pan-Myeloid (Control Vs. VNMAA P=0.624, q=0.634; Control Vs. Cephalexin P=0.143, q=0.296), Granulocytic cells (Control Vs. VNMAA P=0.254, q=0.449; Control Vs. Cephalexin P=0.13, q=0.298), Monocytic cells (Control Vs. VNMAA P=0.086, q=0.242; Control Vs. Cephalexin P=0.57, q=0.575), Alveolar Macrophages (AMs) (Control Vs. VNMAA P=0.563, q=0.634; Control Vs. Cephalexin P=0.509, q=0.575), Metastasis Associated Macrophages (MAMs) (Control Vs. VNMAA P=0.103, q=0.242; Control Vs. Cephalexin P=0.167, q=0.296) and Metastasis Associated Macrophage Precursor Cells (MAMPCs) (Control Vs. VNMAA P=0.628, q=0.634; Control Vs. Cephalexin P=0.257, q=0.364). **C)** Grouped bar graphs of the mean (\pm SEM) percentage of viable cells for respective lymphoid populations (N=1; n=5 animals per condition), including B-cells (Control Vs. VNMAA P=0.599, q=0.705; Control Vs. Cephalexin P=0.31, q=0.831), pan-Lymphoid (Control Vs. VNMAA P=0.698, q=0.705; Control Vs. Cephalexin P=0.822, q=0.831), CD4+ cells (Control Vs. VNMAA P=0.668, q=0.705; Control Vs. Cephalexin P=0.799, q=0.831), Cytotoxic T-cells (Control Vs. VNMAA P=0.657, q=0.705; Control Vs. Cephalexin P=0.542, q=0.831).

5.4.2 Targeted analysis of pro-inflammatory cytokines does not highlight any changes in their abundance in lungs of tumour bearing mice following antibiotic treatment

In the absence of any obvious changes to immune populations in the lungs of antibiotic treated animals, cytokine profiling was undertaken to assess whether antibiotic treatments had influenced the molecular elements of the premetastatic microenvironment at this time point, 15 days post tumour induction, which may allude to whether any prospective differences in cytokine abundances may translate to differences in immune activity at a later stage. The MSD V-PLEX plate-based assay was employed to profile 10 cytokines associated with triggering inflammatory responses which might be associated with promoting a pro-metastatic microenvironment. This assay has the benefit of being very sensitive and can quantify cytokine concentrations to below 1pg/ml. For each sample, lung tissue was processed as per manufacturer's instruction and 100 μ g of total protein loaded per well with all samples analysed in duplicate. Downstream analysis, using multiple unpaired t-tests with a corrected FDR (q \leq 0.05), did not highlight any of the 10 cytokines as being significantly different in concentration between either VNMAA or cephalexin treated animals compared to controls (Figure 5.4.2).

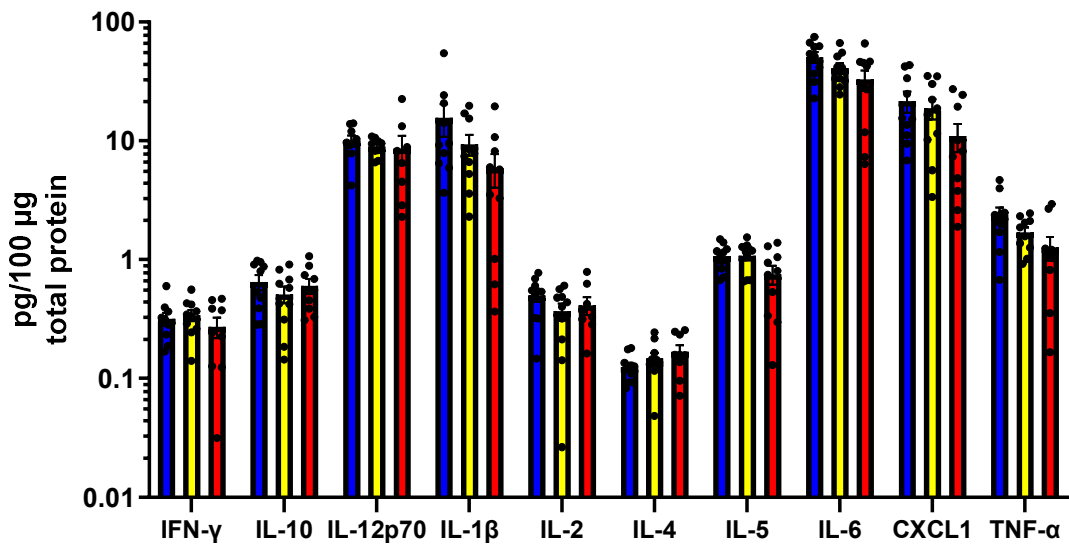


Figure 5.4.2. Cytokine production is not affected by antibiotic treatments in tumour bearing mice. Grouped bar graphs showing the mean (\pm SEM) concentrations, in pg/100 μ g of tissue, of 10 cytokines with known influences on inflammatory pathways, quantified using an MSD V-PLEX assay, from the lungs of animals treated with either a vehicle control, VNMAA or cephalixin and which bore PyMT-BO1 tumours (N=2, n \geq 8 animals per condition)). Cytokines include IFN- γ (Control vs. VNMAA P=0.682, q=765; Control Vs. Cephalixin P=0.486, q=0.614), IL-10 (Control vs. VNMAA P=0.268, q=0.451; Control Vs. Cephalixin P=0.706, q=0.713), IL-12p70 (Control vs. VNMAA P=0.326, q=0.47; Control Vs. Cephalixin P=0.56, q=0.628), IL-1 β (Control vs. VNMAA P=0.24, q=0.451; Control Vs. Cephalixin P=0.075, q=0.130), IL-2 (Control vs. VNMAA P=0.136, q=0.451; Control Vs. Cephalixin P=0.359, q=0.518), IL-4 (Control vs. VNMAA P=0.268, q=0.451; Control Vs. Cephalixin P=0.077, q=0.13), IL-5 (Control vs. VNMAA P=0.952, q=0.962; Control Vs. Cephalixin P=0.059, q=0.13), IL-6 (Control vs. VNMAA P=0.171, q=0.451; Control Vs. Cephalixin P=0.046, q=0.13), CXCL1 (Control vs. VNMAA P=0.636, q=0.765; Control Vs. Cephalixin P=0.057, q=0.13) and TNF α (Control vs. VNMAA P=0.125, q=0.451; Control Vs. Cephalixin P=0.032, q=0.13).

5.5 Discussion

The body of research describing the influences of the microbiota on cancer continues to grow exponentially and research of this nature with a focus on breast cancer specifically is beginning to gain traction among the scientific community. When breast cancer metastasizes to distant organs, the disease becomes incurable [741–743]. It is therefore imperative that influential components in the dissemination of cancer cells are identified, and their influences understood. To date, many studies investigating the link between the microbiota and breast cancer have generally focussed on the primary disease and the number of articles describing its influence on metastatic disease are relatively limited. Notably, one publication, by Buchta Rosean *et al.* (2019), performed experiments very similar to the ones undertaken in this study and identified that the administration of the robust VNMGA antibiotic cocktail was associated with increased metastasis of a luminal-A like breast cancer model (BRPKp110) to the lungs of C57 BL/6 mice [569].

Thus, the aims of this study were to build upon this small body of research through investigating whether an antibiotic induced perturbation of the gut microbiota, using either the VNMAA cocktail or cephalexin, would influence metastatic disease in a similar manner to that observed in the primary tumour using the luminal-B like PyMT-BO1 model. This model was derived from spontaneous MMTV-PyMT tumour cells which were selectively isolated from lung metastases, meaning they were highly metastatic. Additionally, the GFP and firefly luciferase tag status of these cells meant they should be easily tracked around the animal as they disseminate from the primary tumour to distant organs.

A major biological process in facilitating dissemination is EMT which sees cancer cells in the primary tumour change from an epithelial morphology, in which they adhere to neighbouring cells and form solid tissues, to a mesenchymal one, where these cell-to-cell connections are lost and cancer cells become motile as they pass through stroma and intravasate into circulation to be carried to distant organs. Reductions in the adhesion protein E-cadherin and increases in vimentin can be used to identify this process and are often used to investigate a tumour's metastatic potential [744,745]. Stromal density is associated with increased EMT. Therefore, due to the increase in stromal gene signatures in tumours from VNMAA treated animals identified through scRNA-seq (see Section 4.1.2), it was hypothesised that there may be a corresponding increase in EMT following antibiotic treatment. In tumours from all three treatment groups, immunostaining of E-cadherin revealed very few areas containing the adherence protein and these were limited to structures thought to be epithelial mammary ducts. Conversely, vimentin staining was ubiquitous in tumours from all three treatment groups. Although consistent with the highly metastatic nature of the model used, these observations initially did not suggest much difference in EMT between antibiotic treatments.

However, in an attempt to quantify these qualitative observations, western blots were performed on whole tumour lysates. At a timepoint of 15 days post tumour induction, densitometry analysis of western blots did not identify significant changes in either E-cadherin or vimentin in tumours from VNMAA or cephalixin treated animals relative to controls. However, at a later timepoint of 18 days post tumour induction, E-cadherin is clearly reduced in tumours from VNMAA treated animals to the point that semi-quantitative densitometry analysis could not be performed because while there were clear bands denoting the abundance of the adherence protein in control samples, there were none whatsoever in the VNMAA samples. Furthermore, although bands were quite faint, it appeared that in cephalixin samples a similar comparison could be made. Additionally, while vimentin was again unchanged in samples from the VNMAA treated cohort, densitometry suggested that it was significantly increased in samples from cephalixin treated animals relative to controls. These comparisons at two different timepoints suggest that as the primary tumour progresses, EMT progresses correlatively and because tumours from antibiotic treated animals grow more quickly than their control counterparts, EMT is likely occurring earlier than it is in control tumours, causing increased potential for the dissemination of cancer cells from the primary tumour and intravasation into the circulatory system.

Identifying both CTCs and DTCs proved troublesome and both *in situ* bioluminescence imaging and flow cytometry were not successful in identifying metastatic cells. However, through optimisation and collaboration one method was successfully employed. *Ex situ* bioluminescent imaging of lungs from PyMT-BO1 tumour bearing animals 15 days post tumour induction identified that out of 15 samples in the control groups from two experiments, there were no samples that presented with metastasis while there were 2 out of 10 samples with metastasis in the VNMAA treatment group and 5 out of 15 in the cephalixin treatment group. This result suggests that at this timepoint, both the antibiotic treatments increased the risk of metastatic incidence. Statistical analysis by means of a Fisher's exact test found that the differences in the metastatic incidence between the cephalixin and control groups was significant. However, the same test did not find the difference between VNMAA and the control group to be significantly increased. While the quantification of metastatic burden by photon emission suggests antibiotics may correlate to larger lesions, the incidence in the lungs was too few to statistically compare lesion size between groups. For example, the control arms from the two experiments imaged using the *ex situ* format had no incidence in any of the 15 lungs harvested and of the 10 lungs imaged from the VNMAA treated animals, only two produced a bioluminescent signal denoting metastasis.

Although at the day 15 timepoint primary tumours were large and vascularised and the metastatic cascade had clearly begun, the sample sizes for comparing metastatic burden were too small to

reliably infer an effect of antibiotic administration on overt metastasis. Therefore, a resection experiment was designed to facilitate time for lesions to grow to measurable sizes in lung and bone tissue. Primary tumours were resected at the same volumes across all treatment groups to avoid potential bias in cancer cell dissemination. Unfortunately, the aggressive nature of the PyMT-BO1 model meant that residual primary tumour cells grew back rapidly along the incision line made during the resection surgery and the experiment was terminated just 18 days post tumour induction as a result. Regardless, downstream analysis was carried out as planned and the results were somewhat conflicting with those observed at the earlier timepoint of day 15. While imaging of bones did not identify any metastasis in any of the samples from all three treatment groups, the number of samples presenting a metastatic signal by bioluminescent imaging of the lungs were similar between the three treatment groups. However, the surprising observation was that the quantification of metastatic burden suggested those lungs from the cephalexin treatment group which exhibited a metastatic signal had lesions smaller than those observed in both vehicle control and VNMAA treated animals. This was converse to the observation made at the day 15 timepoint.

While every attempt was made to robustly and reliably investigate the effect of antibiotics on overt metastasis to the target organs, the design of the experiments meant that the sample sizes of organs positive for metastases were simply too few to conclude with accuracy that antibiotic treatments influenced metastasis in the same or similar way to their effects on primary tumour progression. Future experimental design should consider the use of both spontaneous models, such as the MMTV-PyMT model, as well as the intravascular injection of cancer cells as a model of induced metastatic dissemination. These may aid in increasing the numbers of samples suitable for downstream analysis and therefore offer a robust and reliable dataset from which to draw conclusions.

The pre-metastatic microenvironment within secondary organs is key in the cascade of events which promotes the formation of metastases. Immune cells are major influencers shaping this microenvironment and are often prognostic markers in early tumour formation within secondary organs [11,746]. Chen *et al.* (2011) showed that macrophages promote breast cancer cell survival through direct interactions via VCAM-1 on the surface of cancer cells [746]. Gil-Bernabé *et al.* (2012) later identified a subset of macrophages within the lungs of tumour bearing mice, characterised by the expression of CD11b as opposed to CD11c expression seen in resident alveolar macrophages, were associated with promoting cancer cell extravasation and growth in lung tissue [747]. This subset was subsequently coined “metastasis associated macrophages” (MAMs) due to their involvement in promoting secondary tumour formation [747]. Dendritic cells can act both pro- and anti-tumourigenically depending on their activation status [748]. These antigen presenting cells

respond to cancer cell derived thymic stromal lymphopoietin (TSLP) which promotes the expression of OX40L that binds T-cells and stimulates the release of immunosuppressive cytokines such as IL-13, inhibiting cytotoxic activity and promoting tumour formation [749]. However, dendritic cells have been shown to support some chemotherapies, including oxaliplatin, as they respond to the release of high mobility group protein B1 (HMGB1) by dying cancer cells which binds TLR4 on their cell surface, promoting the presentation of antigens to T-cells, triggering T-cell activation and increasing intra-tumoural cytotoxic activity [748,750]. Additionally, immunosuppressive immune cells, predominantly T-reg cells and MDSCs, aid cancer cells in immune evasion by inhibiting the recruitment and activation of anti-cancer effector T cells, such as cytotoxic T cells, and NK cells which would otherwise identify cancer cells and release cytotoxic components, causing cancer cell death [746]. Therefore, profiling immune cells in the lungs may allude to the establishment of the pre-metastatic niche. High-level flow cytometry of myeloid populations, including several subsets of monocytic cells, including macrophages, and granulocytic cells, did not identify any significant changes in the abundances of myeloid-derived immune cells in the lungs of antibiotic animals treated with either VNMAA or cephalixin. Similarly, profiling of lymphocytes did not highlight any changes either. Therefore, it appears that neither VNMAA nor cephalixin was influencing the metastatic niche at this timepoint. Due to technical issues T-reg and NK cells were not assessed, and it may be beneficial for future research to profile those cell types specifically.

Cytokine profiling was undertaken in an effort to investigate whether pro-inflammatory pathways which may facilitate tumour establishment were beginning to take shape within the lungs and whether antibiotic treatment influenced the presence of those cytokines. Similarly to immune flow cytometry, there were no significant changes in any of the 10 cytokines associated with inflammatory influences in the lungs from VNMAA and cephalixin treated animals compared to controls suggesting that antibiotic treatments were again not exerting any effect on the pre-metastatic microenvironment in terms of influencing immune cell activation or suppression.

In conclusion, the results of this study provide some evidence to suggest that antibiotic treatments may promote the incidence and burden of breast cancer metastasis. It does not appear that those observations are correlated with associated changes in immune cell densities and immune signalling traditionally associated with driving metastasis. However, the sample sizes discussed here are far from large enough to reliably define the effect of antibiotic treatments on metastasis. Repeating these experiments, with larger numbers of animals and utilising the *ex situ* imaging method, would aid in improved statistical analysis between treatment groups. Preferentially though, utilising a spontaneous model or the intravenous induction of circulating tumour cells to by-pass overly aggressive orthotopic tumour growth during the establishment of metastatic lesions

should hopefully reduce the number of animals required to make reliable comparisons. These models and methods are now both being trialled in the Robinson lab and are showing initial signs of success for this purpose.

6 Live Biotherapeutic Products as microbiota regulators to rescue tumour progression in patients in dysbiosis

The inclusion of fermented foods in diets to promote human health has been common practice in many cultures from across the globe for millennia. While it is unlikely to have been known at the time of their conception, the major contributory components of these foods in promoting health was, and still is, the presence and activity of bacterial populations which carry out the process of fermentation [751]. Today, research around such foods has led to an era of the “-biotics”. “Antibiotics” has been a household word since Alexander Fleming first discovered penicillin in 1928 [752], but in today’s society, the terms “prebiotics” and “probiotics” are being increasingly discussed among clinicians, academics and the general public regarding the influences they infer on regulating local and systemic responses to disease [753].

Briefly, prebiotics refer to dietary components, predominantly plant-derived fibres, which when ingested offer suitable respiratory substrates to commensal members of the microbiota, facilitating their colonisation and growth within the gut and promoting the production of respiratory by-products, such as SCFAs [519,754]. These by-products are key regulators of an array of beneficial host cellular and metabolic processes. The Food and Agriculture Organization of the United Nations and the World Health Organization define probiotics as “live microorganisms that, when administered in adequate amounts, confer a health benefit on the host” [755]. Put simply, they are food stuffs which contain a defined composition of bacterial species with known health promoting influence within the gut, often consumed either within food, such as in yoghurts and kombucha, or as supplements in the form of tablets. Commercial pre- and pro-biotic products are significant drivers of a multibillion-pound industry promoting “gut-health” and large conglomerates, including companies like Nestlé, are involved in backing them [756]. However, while in principle these products should modulate the microbiota and consequently aid in regulating immune education, there are still relatively few studies which suitably define the cellular and molecular influences of the specific products on human health. Therefore, there are currently no probiotic products approved to be used in the treatment of specific diseases [757]. However, the number of pre-clinical studies using well defined bacterial species in quantified abundances to aid in the treatment of specific diseases is growing and the results look promising [757].

Early studies focussed on the influence of probiotic administration at a local level, with inflammatory diseases such as ulcerative colitis and Crohn’s disease featuring heavily in the literature between the 1990 and 2010. For example, Peran *et al.* (2005) described that the administration of *Lactobacillus salivarius* was associated with the amelioration of inflammation in

a TNBS model of rat ulcerative colitis and showed that TNF α , a pro-inflammatory cytokine, was reduced following the probiotic treatment [758]. Now, studies are linking the microbiota to diseases at sites distant to the gut. Many of these consider microbial intervention to aid in the treatment of various cancers alongside traditional treatments, such as chemo- and immunotherapies. One example is a publication by Vétizou *et al.* (2015) which showed that the administration of the known commensal *Bacteroides fragilis* improved the efficacy of ipilimumab, an anti-CTLA-4 monoclonal antibody immunotherapy which facilitates T-cell activation and tumour cell targeting by cytotoxic T-cells, in subcutaneous mouse models of both colon cancer (MC38 – murine colon carcinoma) and melanoma (RET melanoma model) [596].

These pre-clinical studies demonstrate the beneficial influences of novel and established probiotic species on regulating response to disease. Therefore, the advent of novel therapies involving probiotic bacteria to treat diseases in humans should be expected to follow suit. By design, these bacteria will be used within treatment pathways, either alone or in combination with traditional treatments, to target and treat specific diseases. As a result, they somewhat surpass the current definition of a probiotic as they are not simply conferring a general health benefit but are in fact being used a therapeutic. Thus, any bacterial candidate which was to become approved as a treatment is likely to be termed a “live biotherapeutic product” (LBP) to better reflect the difference between general health benefits conferred by various probiotic genera and the specific and targeted treatment applications of an LBP [759]. Unfortunately, there have so far been no examples of bacterial candidates which have progressed through clinical trials to become approved treatment options. However, there remains promise for the development of such therapeutics as several clinical trials involving probiotic bacteria are currently underway and pre-clinical research continues to identify prospective candidates [760–762].

In Section 3.8 the common loss of several bacterial species was observed in animals following both VNMAA and cephalexin treatment, concomitant with increased tumour volume relative to controls. Thus, to investigate whether supplementation with probiotic species may rescue the increased tumour growth associated with antibiotic administration, two live biotherapeutic approaches were trialled using the PyMT-BO1 model. The first was guided by the shotgun metagenomic sequencing, performed in Section 3.8, which identified *Faecalibaculum rodentium* as a potential protective member of the commensal microbiota in the context of regulating tumour growth. The second combined several bifidobacterial species which have previously been identified by the Hall Lab (Dr Lindsay Hall, Quadram Institute), as being important contributors in shaping a healthy gut microbiota in infants. Unfortunately, the latter cannot be further defined due to a pending patent and shall simply be referred to as “*Bif*” from here on in.

An altered experimental workflow was established to investigate whether these bacteria may be associated with reduction in primary tumour growth following antibiotic induced gut disturbances. Animals were switched from either a vehicle control or VNMAA antibiotic treatment to either *F. rodentium* or *Bif* supplementation following the induction of a PyMT-BO1 tumour. In both cases, when animals were switched from VNMAA to either *Bif* or *F. rodentium*, tumour volumes were significantly reduced relative to animals switched from VNMAA to a vehicle control. Histological assessment of mast cell densities was also undertaken but did not provide evidence suggesting that mast cell numbers become reduced following either of the bacterial treatments. However, there was no significant increases in mast cell densities between any of the four treatment groups either. Finally, combined immunofluorescence staining of the mast cell marker FCεR1α and terminal deoxynucleotidyl transferase dUTP nick end labelling, protocol used to identify apoptotic cells, suggested that in *Bif*-treated animals, FCεR1α-expressing cells appeared to be in a state of apoptosis while surrounding cells were not.

6.1 *Faecalibaculum rodentium* supplementation rescues PyMT-BO1 tumour growth in VNMAA treated animals

Aforementioned in Section 3.8, several species were identified as being commonly reduced following either VNMAA or cephalixin treatments via metagenomic sequencing. In an ideal study, each of these bacteria would be included in supplementation experiments where they might be administered to tumour bearing mice, both alone and in combination, with other commonly lost species to identify the effects of administration on tumour growth. Such experiments might also be performed with and without the administration of antibiotics to assess colonisation efficacy and whether their protective roles might be influenced by antibiotic treatments. Unfortunately, this would require an enormous number of animals in addition to having significant cost implications. Therefore, a more targeted approach was employed using literature searches to identify previously described anti-cancer influences and/or beneficial health effects associated with each of the 11 candidates identified via shotgun WGS, which included *Turicimonas muris*, *Faecalibaculum rodentium*, *Anaerotruncus* sp G3(2012), *Enterorhabdus caecimuris*, *Asaccharobacter celatus*, *Adlercreutzia equolifaciens*, *Lactobacillus reuteri*, *Lactobacillus taiwanensis*, *Lachnospiraceae bacterium 3(2)*, *Jeotgalicoccus halotolerans* and *Corynebacterium stationis*. Of these, there were few which appeared in the current body of research. Two of the candidates which did appear in the searches were from the established probiotic genera *Lactobacillus* and may have been an interesting pairing to trial in supplementation experiments. However, as stated in Section 3.10, neither of these species had so far been linked to influencing cancer of any type. More promising though was that *F. rodentium*, one of the 11 commonly reduced species (Figure 3.9C), had recently been shown to have a protective role against tumour establishment and progression in a mouse model of colorectal cancer [574]. Specifically, Zagato *et al.* (2020) demonstrated that in both an *Apc*^{min/+} spontaneous colorectal cancer model as well as in a mouse model with a humanised microbiota treated with AOM and dextran sulphate sodium (DSS) to induce inflammatory-associated colorectal cancer, *F. rodentium* was significantly reduced relative to healthy controls. Furthermore, when *F. rodentium*, or the spent media used to culture it, was supplemented to mice, tumour growth was significantly reduced. Subsequent analysis linked this role with bacterial-derived butyrate production which acted as a histone deacetylase inhibitor (HDACi), preventing the calcineurin dependent activation of the NFATc3 transcription factor which would otherwise facilitate tumour growth [574]. This was a novel observation and, therefore, an exciting avenue to pursue in this study. Thus, an experiment was designed to incorporate this species as an LBP in the treatment of the PyMT-BO1 model.

Animals were subject to either a vehicle control or VNMAA antibiotic treatment for a period of one week and, following tumour induction, were then switched to oral gavages of *F. rodentium* (*F. rod*) with the exception of one group which was switched from a VNMAA treatment to receiving vehicle control oral gavages (Figure 6.1A). An additional group was also maintained on vehicle control oral gavages for the full duration of the experiment as a base level control. At 15 days post tumour induction, tissues were harvested, measured and used for downstream analyses. In these experiments, a one-week administration of VNMAA prior to tumour induction was enough to result in a significant increase in primary tumour volumes relative to animals treated with vehicle controls at the point of cessation (Figure 6.1B), an interesting observation as experiments previously described in Section 3.1 had involved a longer VNMAA treatment regimen of three weeks. Thus, this result suggested even a short exposure to antibiotics results in increased tumour progression. However, the major observations of interest were that groups which initially received either the vehicle control or the VNMAA treatment but were subsequently switched to an *F. rod* treatment, i.e. vehicle to *F. rod* and VNMAA to *F. rod*, both had tumour volumes which were significantly reduced relative to the cohort of animals treated with VNMAA switched to a vehicle control (Figure 6.1B).

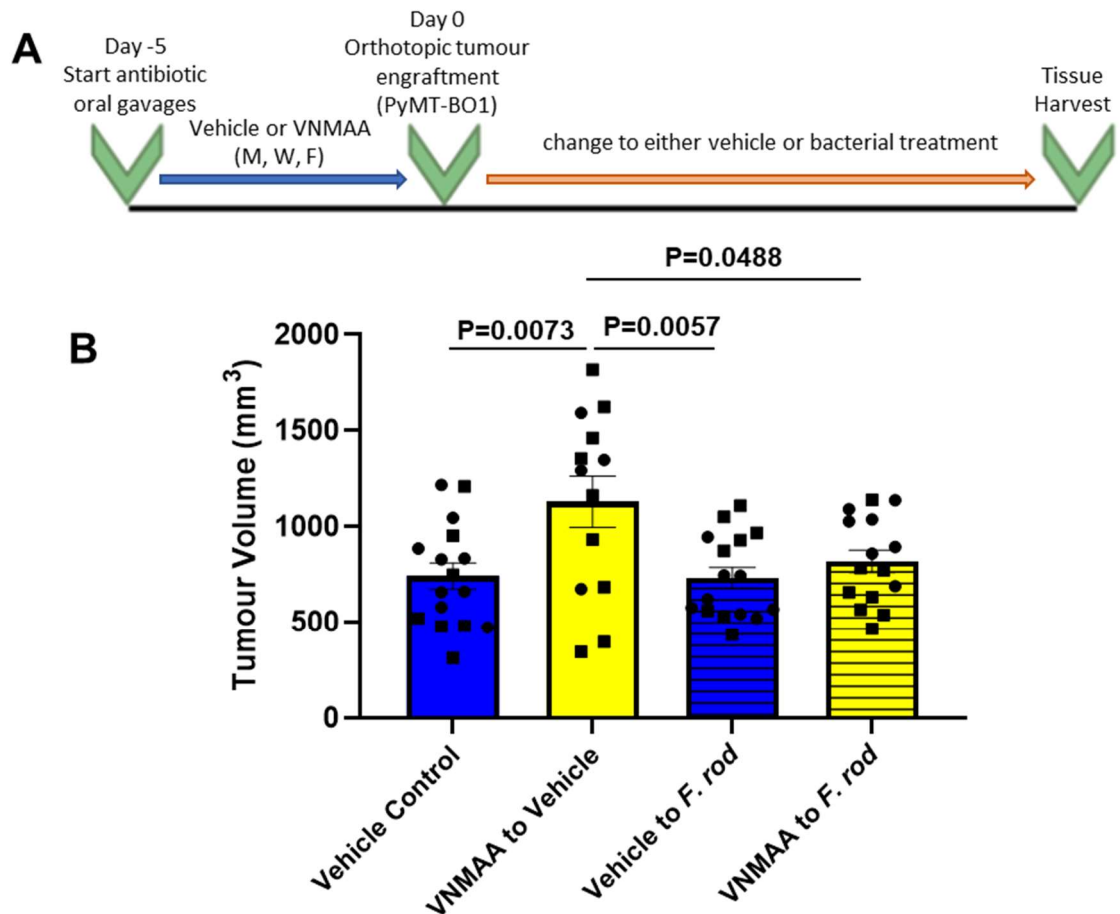


Figure 6.1. *F. rod* administration rescues PyMT-BO1 tumour growth compared to growth in animals treated with VNMAA. **A)** Schematic of treatment regimens for LBP experiments. Vehicle control or VNMAA treatment began one week prior to PyMT-BO1 tumour induction and was administered three times per week. After one week, tumours were orthotopically induced and treatment regimens switched to oral gavages containing live *F. rod* cultured as outline in section 5.2.2 and administered three times per week until experiment cessation 15 days post tumour induction. **B)** Bar graph depicting the mean tumour volumes (\pm SEM) measured *ex situ* (N=2, n \geq 13 animals per condition; One-Way ANOVA P=0.0037; Tukey's multiple comparison tests with adjusted P-values: Vehicle Control Vs. VNMAA to Vehicle P=0.0073, DBM=-387.0; Vehicle Control Vs. Vehicle to *F. rod* P=0.9997, DBM=10.03; Vehicle Control Vs. VNMAA to *F. rod* P=0.898, DBM=-77.04; VNMAA to Vehicle Vs. Vehicle to *F. rod* P=0.0057, DBM=397.0; VNMAA to Vehicle Vs. VNMAA to *F. rod* P=0.0488, DBM=309.9; Vehicle to *F. rod* Vs. VNMAA to *F. rod* P=0.86, DBM=-87.07). Significantly different P-values are stated on the graph. Points of the same shape between conditions are from the same experiment (N).

6.2 A proprietary cocktail of Bifidobacterial strains rescues PyMT-BO1 tumour growth in VNMAA treated animals in a similar fashion to *F. rod*

The protective role of *F. rod* was an exciting observation because it alluded to the potential of the anticancer action of LBPs in this model. However, from a clinical perspective it was only effective when compared to animals with an antibiotic induced perturbation of the gut microbiota suggesting it may only be useful in reducing the protumour action of a perturbed microbiota rather than being capable of slowing tumour progression in patients with a “healthy” microbiota. To some extent, it might be argued that this was a sensible outcome as *F. rod* contributes a large portion of the bacterial abundance in an established murine microbiota and was already present in mice treated with the vehicle control prior to tumour induction based on earlier metagenomic analysis. Therefore, it may be that administration in VNMAA treated animals simply brought the microbiota back to its original anti-tumour functional capacity without improving upon it. Thus, it was hypothesised that the introduction of probiotic bacteria which were not already resident in the gut, and which have been shown to influence cancers in other models, may further reduce tumour volume compared to both VNMAA treated animals and vehicle control animals. After reviewing the metagenomic data discussed in Section 3.8 and having intradepartmental discussions with Dr Lindsay Hall, who has significant expertise in studying the beneficial influences of bifidobacterial colonisation in the guts of pre-term infants, it was decided to pursue the supplementation of a combination of bifidobacterial species as an alternate LBP to *F. rod*. Dr Hall has previously isolated several bifidobacterial strains from healthy infants, which were not present in the faecal samples of pre-term infants, and it was decided that these should be trialled as an LBP cocktail in our breast cancer model for several reasons. Firstly, these were shown to improve morbidity in pre-term infants by reducing pathobiont colonisation demonstrating a positive influence on human health [415]. Secondly, several bifidobacterial species have been shown to slow tumour progression in immunogenic cancers, namely melanoma, and even support anti-cancer immunotherapies [555]. Thirdly and finally, should the isolates available to us successfully induce an anticancer response, there was scope to patent their use prior to any inclusion in clinical trials.

Animals were subject to the same treatment regimens described in Section 6.2 (see Figure 6.2A) with the exception that the oral gavages containing *F. rod* were substituted for one containing a cocktail of several probiotic bifidobacterial species (*Bif*). In this experiment, the one-week administration of VNMAA appeared to progress tumour volumes in the same way as observed previously though there was no statistically significant difference between vehicle treated control animals and VNMAA to vehicle treated animals. However, similarly to the observations made

following *F. rod* administration, animals on either vehicle or VNMAA treatments which were switched to the *Bif* showed significantly reduce tumour volumes compared to animals treated initially with VNMAA and switched to the vehicle (Figure 6.2). Finally, while it appeared that switching to *Bif* from either vehicle or VNMAA treatments reduced tumour volumes relative to vehicle treated controls, this was not a statistically significant reduction. Therefore, to ascertain whether *Bif* supplementation might influence tumour growth in the absence of an antibiotic treatment, further experimentation should be undertaken to reliably accept or reject such a hypothesis.

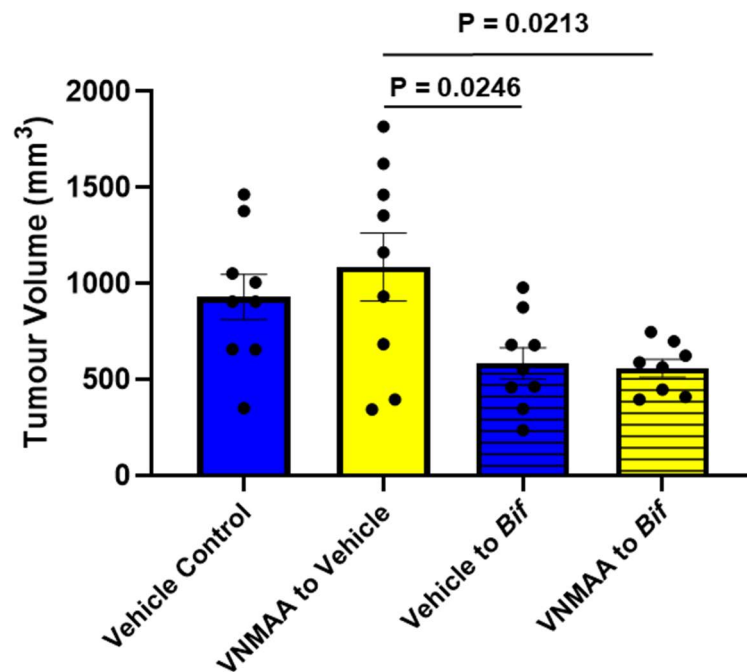


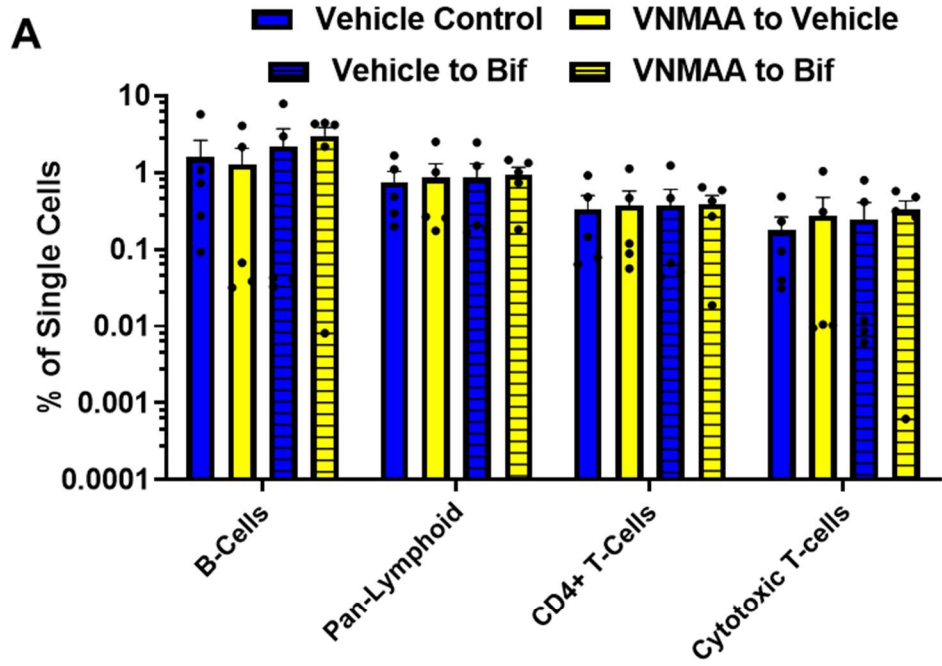
Figure 6.2. *Bif* administration rescues PyMT-BO1 tumour growth compared to growth in animals treated with VNMAA. Bar graph depicting the mean tumour volumes (\pm SEM) measured *ex situ* following respective *Bif* treatments (N=1, n \geq 8 animals per condition; One-Way ANOVA P=0.0077; Tukey's multiple comparison tests with adjusted P-values: Vehicle Control Vs. VNMAA to Vehicle P=0.784, DBM=-155.7; Vehicle Control Vs. Vehicle to *Bif* P=0.182, DBM=345.2; Vehicle Control Vs. VNMAA to *Bif* P=0.154, DBM=370.9; VNMAA to Vehicle Vs. Vehicle to *Bif* P=0.0246, DBM=500.9; VNMAA to Vehicle Vs. VNMAA to *Bif* P=0.0213, DBM=526.6; Vehicle to *Bif* Vs. VNMAA to *Bif* P=0.999, DBM=25.71). Significantly different P-values are stated on the graph.

6.3 No significant differences in lymphoid infiltration or mast cell density in tumours from *Bif* treated animals

Immune profiling of tumours from animals treated with either VNMAA or cephalixin for the full duration of the relevant experiments via flow cytometry did not identify any changes in either myeloid or lymphoid compartments compared to controls (see Section 3.4 and 3.5). However, bifidobacterial species are known to be immunogenic and elicit a variety of different responses depending on the species involved [763]. Many studies focussed on bifidobacterial influences on inflammatory diseases of the gut and largely demonstrate their ability to promote T-reg expansion and reduce the activity of pro-inflammatory immune cells via an IL-10 dependent mechanism [764–768]. However, several more recent studies investigating bifidobacterial effects at sites distant from the gut have demonstrated they have the potential to augment immune responses to promote anti-cancer activity. Of note is the study by Sivan *et al.* (2015) who demonstrated that, in a pre-clinical model of melanoma, administration of Bifidobacteria enriched the expression of several genes associated with T-cell activation in dendritic cells; many of these activated the anti-cancer activity of CD8+ T-cells. Subsequently, increased CD8+ T-cell accumulation was observed in melanoma tumours from animals treated with Bifidobacteria and those tumour volumes were reduced relative to control groups [555]. To assess if similar observations may be occurring in the model used in this study, flow cytometry was carried out on tumours from the *Bif* supplementation experiment to compare myeloid and lymphoid populations between control and treatment groups for signs of an immunogenic response which may have been associated with reduced tumour growth. Unfortunately, the myeloid panel failed all together and no data was obtained for those populations. Additionally, issues with the viability dye used and unsuccessful FoxP3 staining frustratingly meant that viable cells could not be distinguished from dead cells, nor could T-regulatory cells be distinguished from CD4+ T-cell populations. However, the data that was acquired did not identify any significant differences between treatment conditions in any of the profiled lymphoid populations ($P > 0.05$; t-test) (Figure 6.3A and Figure 6.3B).

In the experiments discussed in Section 4.3, mast cell densities were increased in tumours following VNMAA and cephalixin treatments and shown to have functional influences on tumour progression following antibiotic induced perturbations of the microbiota. Thus, it was hypothesised that the reductions in tumour volumes observed following LBP treatments may be associated with correlative decreases in mast cell densities in tumour sections. Toluidine blue staining and mast cell enumeration was carried out on tumour sections from both *F. rod* and *Bif* experiments in the same manner as was described previously. Interestingly, there were largely no significant changes in mast cell densities in *F. rod* (Figure 6.3C) or *Bif* (Figure 6.3D) experiments between any of the treatment

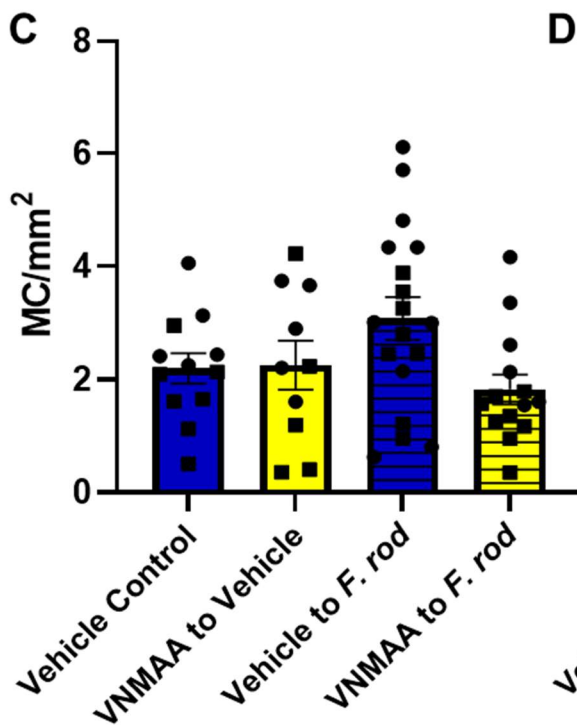
conditions, except for between Vehicle to *F. rod* and VNMAA to *F. rod* in which a one-way ANOVA test with a Tukey's multiple group comparison identified a significant reduction in mast cell densities in the latter group (Figure 6.3C).



B

Comparison	B-Cells		Pan-Lymphoid		CD4+ T-cells		Cytotoxic T-cells	
	Adjusted P-value	DBM	Adjusted P-value	DBM	Adjusted P-value	DBM	Adjusted P-value	DBM
Vehicle Control vs. VNMAA to Vehicle	0.982	0.317	1.000	-0.096	>0.999	-0.035	0.999	-0.098
Vehicle Control vs. Vehicle to <i>Bif</i>	0.888	-0.606	0.999	-0.097	>0.999	-0.036	1.000	-0.070
Vehicle Control vs. VNMAA to <i>Bif</i>	0.324	-1.441	0.996	-0.191	>0.999	-0.053	0.998	-0.149
VNMAA to Vehicle vs. Vehicle to <i>Bif</i>	0.691	-0.922	>0.999	-0.001	>0.999	-0.001	>0.999	0.028
VNMAA to Vehicle vs. VNMAA to <i>Bif</i>	0.166	-1.758	1.000	-0.095	>0.999	-0.018	>0.999	-0.052
Vehicle to <i>Bif</i> vs. VNMAA to <i>Bif</i>	0.753	-0.835	1.000	-0.093	>0.999	-0.017	1.000	-0.079

C



D

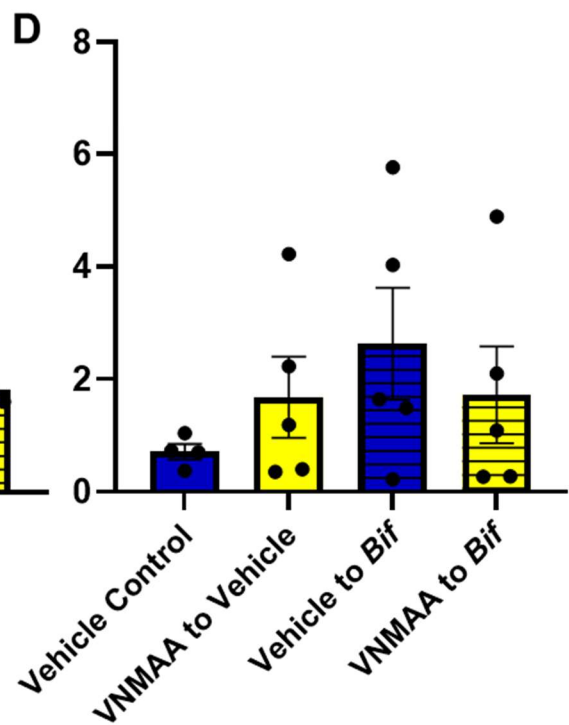


Figure 6.3. Tumour infiltrating lymphoid and mast cell populations are unaffected by *Bif* supplementation. **A)** Bar graphs showing mean (\pm SEM) abundances of tumour infiltrating lymphoid populations in PyMT-BO1 tumours harvested 15 days post tumour induction from animals treated with one of four treatments: vehicle control only, VNMAA to vehicle, vehicle to *Bif* or VNMAA to *Bif* (N=1, n=5 animal per condition). Abundances are presented as a percentage (%) of single cells. **B)** Table of results following a Two-Way ANOVA (Column Factor P=0.6391) with a Tukey's multiple comparison showing the adjusted P-values and difference between means (DBM) for each profiled immune cell type for each of the treatment groups. **C)** Bar graph depicting the mean mast cells per mm² (MC/mm²) (\pm SEM) in PyMT-BO1 tumours from animals treated with respective treatment regimens in the *F. rod* workflow described in Figure 6.1A (N=2, n \geq 10 animals per condition; One-Way ANOVA P=0.0535; Tukey's multiple comparison tests with adjusted P-values: Vehicle Control Vs. VNMAA to Vehicle P=0.0.996, DBM=-0.056; Vehicle Control Vs. Vehicle to *F. rod* P=0.269, DBM=-0.8844; Vehicle Control Vs. VNMAA to *F. rod* P=0.884, DBM=0.372; VNMAA to Vehicle Vs. Vehicle to *F. rod* P=0.374, DBM=-0.829; VNMAA to Vehicle Vs. VNMAA to *F. rod* P=0.854, DBM=0.428; Vehicle to *F. rod* Vs. VNMAA to *F. rod* P=0.0422, DBM=1.257). Points of the same shape between conditions are from the same experiment (N). **D)** Bar graph depicting the mean mast cells per mm² (MC/mm²) (\pm SEM) in PyMT-BO1 tumours from animals treated with respective treatment regimens in the *Bif* workflow described in Figure 6.1A (N=1, n \geq 4 animals per condition; One-Way ANOVA P=0.4621; Tukey's multiple comparison tests with adjusted P-values: Vehicle Control Vs. VNMAA to Vehicle P=0.839, DBM=-0.967; Vehicle Control Vs. Vehicle to *Bif* P=0.385, DBM=-1.915; Vehicle Control Vs. VNMAA to *Bif* P=0.8215, DBM=-1.01; VNMAA to Vehicle Vs. Vehicle to *Bif* P=0.823, DBM=-0.948; VNMAA to Vehicle Vs. VNMAA to *Bif* P>0.999, DBM=-0.043; Vehicle to *Bif* Vs. VNMAA to *Bif* P=0.8422, DBM=0.925).

6.4 *Bif* administration appears to promote apoptosis in FCεR1α-expressing cells

In both *F. rod* and *Bif* experiments the mast cell densities in tumours were unaffected by the administration of LBPs. Previous experiments using cromolyn sodium as a mast cell stabiliser demonstrated that inhibition of mast cell function rescued tumour growth in VNMAA treated animals. Therefore, it was hypothesised that while the administration of LBPs may not alter their numbers in tumours, they might inhibit the pro-tumour activity of mast cells in VNMAA treated animals. This would be a relatively complex and costly investigation to pursue with several options regarding employable methods. For example, mast cells could be isolated from tumours and RNA-seq performed on isolates from the various treatment regimens to identify changes in transcriptomes which could allude to differences in mast cell function. However, this was not a suitable undertaking at the time and so the literature was consulted to identify whether any previous links had been made between the effects of bacterial supplementation and changes in mast cell function or activity.

One study of relevance presented data showing that *Bifidobacterium longum* derived extracellular vesicles by mast cells in the intestine triggered mast cell apoptosis via a protein on the surface of the vesicles called extracellular solute-binding protein (ESPB) [769]. Thus, it was hypothesised that a similar influence may be exerted on tumour resident mast cells which may prevent them from functioning in a manner that would otherwise facilitate tumour growth, resulting in the observed reductions in tumour volume following LBP administration. To assess this, simultaneous immunofluorescence staining of mast cells using the mast cell marker FCεR1α, and terminal deoxynucleotidyl transferase dUTP nick end labelling (TUNEL), used to identify apoptotic cells, was performed on tumour sections from respective treatment arms of the *Bif* experiment.

FCεR1α is a receptor expressed on the surface of mast cells and binds IgE antibodies with high affinity. When two FCεR1α-IgE complexes bind an antigen, often in the form of an allergen, the receptors become cross linked and an intracellular signalling cascade is triggered which results in mast cell degranulation and the release of several types of proteases as well as other molecules, such as histamine, that promote inflammation [203]. It should be noted that this protein is not exclusive to mast cells. In humans, dendritic cells and basophils also express FCεR1α [770]. However, while mast cells are tissue resident, basophils are considered to be circulating cells which only tend to be found in connective tissues during the later stages of allergic response [191]. Additionally, while dendritic cells are known to play active roles within the tumour milieu in regulating cancer progression, in mice, they do not express FCεR1α as they do in humans [770]. It

is therefore highly likely that the cells identified in the results presented here using immunofluorescence staining of FCεR1α are indeed mast cells. However, in the interest of good scientific practice, in the absence of c-kit co-staining, the second marker used alongside FCεR1α to identify a cell as a mast cell, cells stained positive for FCεR1α will simply be referred to as FCεR1α-expressing cells with the implication being they are highly likely to be a mast cell.

Fluorescence microscopy of tumour sections stained for both FCεR1α and TUNEL from the *Bif* supplementation experiment showed that in *Bif* treated animals, the staining of FCεR1α coincided with TUNEL staining, while this was not the case in any of the tumour sections from animals who did not receive *Bif* treatments (Figure 6.4). This observation suggests it is plausible that LBP supplementation, in this case *Bif*, is preventing antibiotic induced pro-tumour activity of mast cells by inducing apoptosis in the FCεR1α-expressing cells.

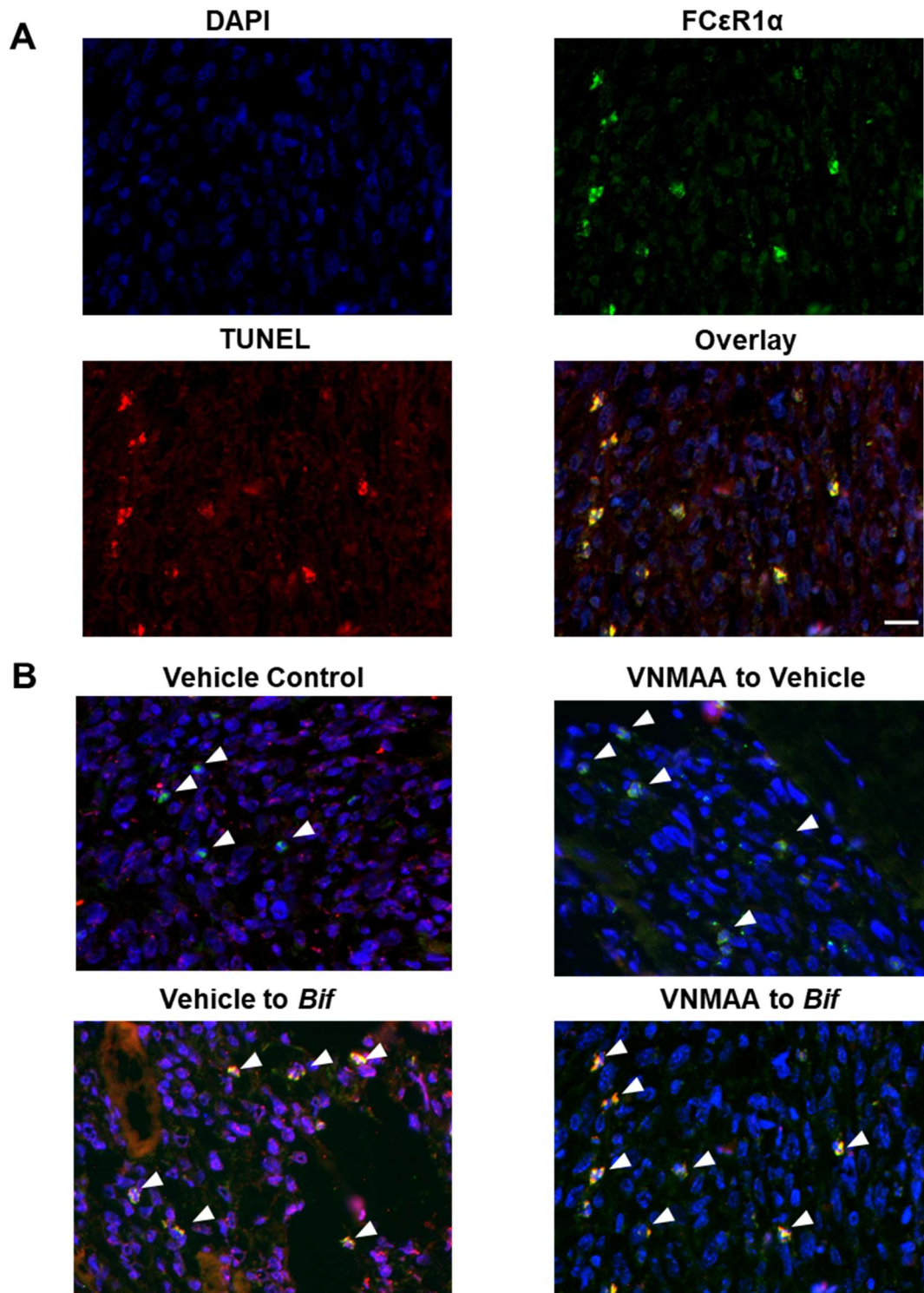


Figure 6.4. *Bif* supplementation is associated with apoptosis in FCεR1α-expressing cells in PyMT-BO1 tumours. **A)** Fluorescence micrographs showing DAPI stained cell nuclei (blue), immunostaining of FCεR1α (green) and TUNEL staining of apoptotic cells (red) as well as an overlay image showing colocalization of FCεR1α and TUNEL staining. **B)** Representative fluorescence overlay micrographs of FCεR1α and TUNEL staining in PyMT-BO1 tumours from animals treated with a vehicle control only, VNMAA followed by vehicle control, vehicle control followed by *Bif* or VNMAA followed by *Bif*. White arrowheads denote FCεR1α-expressing cells. Scale bar = 50µm.

6.5 Discussion

The concept of beneficial microbes is by no means new, and people around the world have consumed foods containing bacteria for millennia. However, the earliest known acknowledgement of the beneficial influences that bacteria are able to exert upon humans was described in 1903 by the immunologist, Elie Metchnikoff, when he observed that people in Bulgaria who consumed “soured milk” seemed to live longer lives than populations who did not [771,772]. Not long afterwards, in 1905, Stamen Grigorov identified the presence of lactic acid bacteria present in Bulgarian yogurt samples, specifically *Lactobacillus delbrueckii* subsp; *Bulgaricus*, and the concept of probiotics was born [773]. Today, the probiotics industry is worth billions of dollars and by 2023 its global value is expected to reach just shy of \$70 billion [774]. Although probiotics have so far been unable to cross the threshold from supplement to therapeutic, the vast number of pre-clinical research studies investigating their use as treatments, both alone and in combination with traditional therapeutics, against an array of diseases, including cancers, suggests there is still much promise for them to do so. Thus, considering the data presented in Section 3 of this thesis, which demonstrated that a perturbed microbiota drives increased primary tumour growth in two pre-clinical mouse models of breast cancer, it seemed logical to consider whether a supplementation of probiotic bacteria may rescue tumour growth in either, or both, animals treated with antibiotics or a vehicle control.

Metagenomic analysis of caecal samples identified several bacterial species which were commonly reduced between VNMAA and cephalixin treatment groups. Of these, *F. rod* was an interesting candidate due to its previously described anti-cancer influence in pre-clinical mouse models of colorectal cancers [574]. Thus, following a weeklong course of either vehicle control or VNMAA treatment, PyMT-BO1 tumours were induced and animals switched from these regimens to ones including *F. rod* administration. After 15 days post tumour induction, primary tumour volumes were significantly reduced in animals which received *F. rod* when compared to animals who started on a VNMAA treatment but were switched to vehicle control administration at the point of tumour induction. These observations demonstrate that aiding the microbiota in recovering from a perturbation may rescue negative influences of the initial disturbance. In clinic, many breast cancer patients are subject to prophylactic antibiotic treatment prior to chemotherapies or surgery. Therefore, there is a risk that a perturbed microbiota may promote outgrowth of any residual tumours following surgery and/or reduce the efficacy of chemotherapies. It may be beneficial that in cases where antibiotic administration is required, that probiotics be used to support microbiota recovery to reduce negative microbiota-associated influences on cancer. *F. rod* is a member of the murine microbiota but has a human homologue, *Holdemanella biformis* [574]. Based on the results

discussed here, it may be worthwhile trialling *H. biformis* treatment in a similar way in animals with a humanised microbiota to see if a similar rescue effect on tumours is observed.

The reduction in tumour volumes following *F. rod* treatment compared to antibiotic treated animals was promising in the context of reducing the detrimental effects of a perturbed microbiota by aiding it in its recovery. However, an improved outcome would be if an LBP could be used as an anti-cancer treatment regardless of prior antibiotic exposure. Shotgun metagenomics confirmed *F. rod* was resident in the gut microbiota prior to any treatments and so it is likely its influence is capped by its interactions with other commensals which may maintain its anticancer activity to levels seen in control animals. What then if an LBP species which was not originally resident in the gut was introduced at the point of tumour induction? Would a novel member in the system be better equipped to exert increased anti-cancer activity beyond that of an established microbiota? To test this hypothesis, a consortium of bifidobacterial species, currently protected under a pending patent application and shown to improve healthy development of the gut microbiota during the early stages of human life, were administered to animals at the point of tumour induction following a one week treatment of either a vehicle control or VNMAA treatment. As observed following *F. rod* administration, tumour volumes were significantly reduced in *Bif* treated groups compared to the VNMAA to vehicle group. However, a one-way ANOVA with Tukey's multigroup comparison found that tumour volumes in both *Bif* groups were not significantly reduced compared to the group which received only the vehicle treatment for the duration of the experiment. Therefore, based on the data presented here, there is not enough evidence to show that the administration of an LBP, previously resident or novel in nature, would reduce tumour growth in this breast cancer model when animals have not previously been exposed to antibiotics. It should be discussed though that this experiment was performed only once and although the number of animals were sufficient to draw statistical conclusions, it may benefit from being repeated as there is an obvious, albeit nonsignificant, reduction in tumour volumes in both *Bif* groups compared to the vehicle control group. Additionally, while analytically incorrect, when performing unpaired t-tests individually comparing each of the two *Bif* treatment cohorts to the vehicle control group, as opposed to the one-way ANOVA with Tukey's multigroup comparison which was appropriately employed, these reductions are significant in both cases ($P < 0.05$). While performing this analysis is not the correct statistical method based on the intergroup comparisons being made, it does suggest there may be a *Bif*-dependent tumour rescue independent of antibiotic treatment and supports the requirement for experimental repetition.

Bifidobacteria have been shown to elicit beneficial immunogenic responses to diseases in their hosts. In cancer studies these responses have generally involved improved activation and cytotoxic

activity of CD8+ cytotoxic T-cells [555,596,775,776]. Therefore, flowcytometry was employed to profile the immune landscape in tumours of *Bif* treated animals compared to vehicle controls. While the myeloid panel was unsuccessful, lymphoid profiling did not identify significant changes in either CD4+ T-cell or CD8+ Cytotoxic T-cell populations, nor were there differences in B-cell numbers between treatment groups. In addition, due to the increases in mast cell densities previously observed in tumours of larger volume from antibiotic treated animals compared to controls, mast cell enumeration was performed on tumours from both *F. rod* and *Bif* experiments. It was hypothesised that due to the rescue effect exhibited by LBP supplementation, mast cell densities may be reduced in relevant tumours. However, there were no significant changes in mast cell densities in tumours between any of the treatment groups from either LBP treatment regimen. It should also be noted that even between the vehicle control only group and the VNMAA to vehicle control group, there was not an increase in mast cell density in any of the experiments. However, this can likely be explained by the difference in treatment regimen compared to the experiment discussed in Section 4.3, where densities are significantly increased following antibiotic treatment, the antibiotic treatment is carried through for the duration of the experiment while in these LBP studies VNMAA is only administered up to the point of tumour induction (a one-week period) and then switched to a vehicle control while other groups are switched to relevant LBPs. Thus, the antibiotic administration period in LBP studies is reduced and this is likely to reduce the degree to which microbiota dependent mast cell programming and activity is influenced at the tumour level.

Section 3.2 presents evidence suggesting increased tumour growth of PyMT-BO1 tumours in antibiotic treated animals (Section 3.1) was promoted by the loss of symbiotic bacterial species in the gut microbiota following said antibiotic administration. Section 4.3 identified that tumours of increased volume from antibiotic treated animals were correlated with increased intra-tumoural mast cell densities and Section 4.4 showed that mast cell inhibition, by cromolyn sodium administration, rescued tumour growth in VNMAA treated animals. Therefore, although administration of LBPs did not reduce mast cell densities in tumours discussed in this Section, it was hypothesised that their administration may influence mast cell functionality within the tumour milieu in a manner that rescued tumour growth to below levels observed in antibiotic treated animals. A previous study had already identified that a bifidobacterial species, *B. longum*, released extracellular vesicles which interacted with mast cells and released several proteins that induced mast cell specific apoptosis [769]. Thus, to ascertain if a similar interaction was occurring following the *Bif* administration in this experiment, simultaneous TUNEL and FCεR1α staining was performed on tumour sections to identify mast cells in apoptosis. Microscopy analysis suggested that in samples from *Bif* treated animals, cells expressing FCεR1α were almost all apoptotic, while in

VNMAA or vehicle control groups, FCεR1α-expressing cells were not apoptotic based on negative TUNEL staining. This supports the hypothesis that LBPs, or at least *Bif*, reduce the activity of mast cells in tumours which may be associated with slowing primary tumour growth compared to those from animals treated with antibiotics and not an LBP.

The evidence presented in this chapter regarding how LBP administration rescues primary tumour growth is quite robust as the results are consistent across three experiments using two different LBP treatments. However, there are several limitations of the data discussed past that point. Flow cytometric profiling of immune populations was not performed on tumours from *F. rod* studies due to tumour tissue being required for separate analyses not discussed in this thesis. Furthermore, myeloid profiling was unsuccessful and lymphoid profiling lacked the lineage depth required to separate T-helper cells, which may act anti-tumourigenically, versus T-reg cells, which may benefit tumour progression. It was also mentioned above that the *Bif* experiment would benefit from repetition to more reliably conclude whether the LBP administration can influence tumour growth in the absence of antibiotic treatment in addition to better investigating the potential immune players involved. There is an array of future experimental options, particularly regarding the *Bif* cocktail of bacteria. Firstly, setting up a workflow where LBPs are administered prior to tumour induction may be an interesting avenue to pursue in the context of protecting from tumour initiation and/or slowing growth. Secondly, it would be interesting to individually test the strains that comprise the *Bif* cocktail to identify if they are capable of fulfilling a protective role on their own or if they require their generic peers. In addition to these experiments, there is an array of work that could be undertaken to profile the colonisation efficacy of these bacteria, through metagenomic sequencing, and their functional effects, possibly by metabolomic profiling of faeces or caecal contents in addition to metagenomic analysis. Such research may better allude to possible mechanisms behind the effect of LBPs on rescuing the tumour growth in this breast cancer model. Which leads on to the final suggestion, that these experiments be repeated in the alternative breast cancer models, such as the EO771 (basal-like) or BRPKp110 (Luminal A) models, to test their influences in other molecular subtypes of the disease.

Considering the limitations discussed above and the suggested requirement for further study regarding probiotic administrations, it is worth mentioning that since the conclusion of this author's time in the laboratory, other members in the Robinson group have begun to undertake such experiments. Building upon the results presented in this section, colleagues have very recently deconstructed the *Bif* cocktail and found that in several cases individual bifidobacterial strains exert an anti-tumour effect on both the PyMT-BO1 model used in the experiment presented in this thesis as well as when using the BRPKp110 model, the luminal-A like murine breast cancer model

described in section 4.3 and recently obtained from the Rutkowski laboratory as part of a collaborative project. While those colleagues are yet to further pursue the potential for mast cell involvement, they have identified other immunological changes which occur following bifidobacterial administration, namely an increase in CD8+ T-cell activation quantified by flow cytometry using staining of granzyme B, a cytotoxic serine protease enzyme released by cytotoxic T-cells to mediate apoptosis in cancer cells [777]. Thus, these recent experiments indeed support the many of conclusions drawn in this chapter.

7 Final Discussion and Future Perspectives

The understanding of the various roles the microbiota plays in regulating human health and response to disease has grown vastly over the past two decades and continues to do so. The influence it exerts on several cancers has highlighted its potential as a diagnostic, prognostic and therapeutic asset to clinicians in the management and treatment of malignant disease. However, until recently, the influence of the microbiota on breast cancers has been relatively poorly described. Thus, the research presented in this thesis aimed to investigate how manipulations of the microbiota, with a particular focus on antibiotic-induced gut perturbations, influenced the progression of the disease. To achieve this aim, several objectives were laid out at the outset of the research. Briefly, these included identifying: changes in tumour growth kinetics following administration of both a harsh cocktail of broad spectrum antibiotics (VNMAA) and a clinically relevant broad spectrum antibiotic (cephalexin) using animal model of the disease; cellular and molecular changes associated with changes in tumour growth; whether observations made at a primary tumour level may also influence metastatic progression of the disease and finally to see if the administration of commensal and probiotic bacterial species might prevent or reduce any negative tumour effects driven by antibiotics administration.

Initial investigations involved the administration of a cocktail of broad-spectrum antibiotics, the VNMAA cocktail, to induce a severe perturbation of the murine gut microbiota, eliminating almost all bacterial organisms within it. This resulted in the increased rate of primary tumour growth in both a luminal and basal-like orthotopic model of breast cancer. The question posed following these results was whether the increase in tumour growth was dependent on antibiotics directly or the deleterious effect they have on the gut microbiota. The lack of any increase in tumour growth following VNMAA administration to tumour-bearing germfree animals confirmed the latter.

Antibiotics are commonly used prophylactically as part of the treatment pathway for patients with breast cancer in order to prevent infection prior to surgery or during chemotherapy when the immune system is vulnerable. Therefore, to expand the clinical relevance of the experimental workflow employed here, the VNMAA treatment was substituted for cephalexin, a broad-spectrum cephalosporin antibiotic known to be used in breast cancer clinics. Again, tumour progression was increased as a result, emphasising the potential risks antibiotic administration may have on breast cancer progression in a clinical setting.

To ascertain the influence of both treatments at a microbiota level, shotgun metagenomic sequencing was performed on caecal samples. As stated, VNMAA treatment had a major deleterious effect on bacterial diversity while cephalexin was less aggressive in its influence. The

common loss of 11 species were identified between both treatment groups compared to controls and included two species of the probiotic genus *Lactobacillus* as well as *F. rod*, a bacterium previously linked to protective roles in animal models of colorectal cancer [574]. Additionally, ¹H NMR of caecal contents confirmed antibiotic administration altered the metabolite profiles of the gut. Although, cephalexin again appeared to have a lesser effect compared to VNMAA, and only three metabolites were significantly reduced in both treatment groups, none of which have so far been described in the literature as having any influence on cancer progression either locally or systemically.

Following metabolite profiling, focus shifted from the gut to the tumour. Most solid tumours are immunogenic and intra-tumoural immune profiles can allude to mechanisms behind tumour success. Cytotoxic T-cells, for example, are markers of a beneficial anti-tumour immune response while MDSCs are associated with immune evasion and promote tumour growth [689,717,778]. Targeted flow cytometric immune profiling of tumour samples from various experiments involving both antibiotic treatments and using both breast cancer models did not identify any significant changes in immune populations which are traditionally associated with affecting breast cancer tumour growth. This was particularly surprising based on observations made by Buchta Rosean *et al.* (2019) who described increases in tumour infiltrating myeloid cell populations in mice orthotopically induced with a luminal A model of breast cancer and treated with a similar cocktail of broad-spectrum antibiotics [569]. Thus, an untargeted single cell transcriptomics approach was applied to support a broader assessment of the cells present within the tumour milieu and their transcriptomic activity. There were largely no significant changes in gene expression within the various cell-type clusters between the two treatment conditions. However, this analysis did identify increases in the number of cells with a gene expression profile associated with tumour stromal cells in VNMAA treated animals, suggesting potential increases in stromal deposition following antibiotic treatment compared to controls.

Similarly, Buchta Rosean *et al.* (2019) described increases in collagen deposition in a luminal A murine tumour model, which denotes tumour stromal regions, following antibiotic treatment [569]. A result which supports the observation made here by single cell transcriptomic analysis regarding increases in stromal gene expression in VNMAA treated animals. Based on these two considerations, it was therefore surprising that subsequent histological analysis of actual collagen deposition in tumours from this study did not coincide with the increased expression of these stromal genes. However, early analysis of scRNA-seq data alluded to increased expression of several mast cell genes in tumours from VNMAA treated animals. Additionally, during histological analysis of collagen deposition, cells with a granular morphology were identified in stromal regions in

tumours from VNMAA treated animals. Thus, toluidine blue staining of tumours was performed, and downstream assessment identified mast cell densities being increased in tumours from VNMAA treated animals. In addition, collaborative projects with two independent colleagues working out of different animal facilities, using different tumour models and following different antibiotic treatment regimens also identified increased mast cell densities in their tumours, supporting the likely importance of these immune cells in tumour progression promoted by perturbations of the microbiota.

Mast cells are traditionally linked to atopic diseases and the altered development of the microbiota is linked to the presentation of several atopic diseases, including asthma and dermatitis [425,779]. Several studies have also described direct influences of the microbiota on mast cell activity, particularly regarding IBD [780]. However, research describing the activity and effects of mast cells in breast tumours is somewhat conflicting with an array of studies describing both pro- and anti-tumour influences, while others describe them as having no bearing on tumour progression and simply being “by-standers” within the tumour milieu [204,357,781–783]. Thus, in an attempt to show that increases in mast cell numbers were involved in driving tumour growth following antibiotic treatments, as opposed to simply being a result of it, their function was inhibited by means of administering the mast cell stabilizing agent, cromolyn. Cromolyn dependent inhibition of mast cell function rescued tumour growth in antibiotic treated animals but had no effect in control animals, suggesting their pro-tumorigenic influence at a tumour level was programmed by the antibiotic-induced perturbation of the gut microbiota. While mast cells have been independently linked to both the microbiota and breast cancer, the data presented in this thesis is novel and describes the first association connecting all three components in this manner. However, further *in vivo* studies are required to completely elucidate the mechanisms by which the microbiota triggers the pro-tumour activity of mast cells in this setting. Using mast cell deficient animal models may be a useful starting point in addition to transcriptomic approaches considering potential changes gene expression in mast cells isolated from antibiotic treated animals.

Much of the initial focus of this research was on primary tumour progression. However, it is when breast cancer reaches its metastatic stages that it becomes most morbid. Metastatic breast cancer remains incurable and improved understanding of the elements which promote or slow disease progression is imperative to reducing the currently high rates of its mortality [741,742]. Based on the influences the microbiota exerted on the primary tumour, it was hypothesised that a perturbed microbiota may similarly promote metastasis. EMT is largely considered a reliable marker of a tumour’s metastatic potential and there is already some evidence linking a disturbed microbiota to promoting this pathway [784]. Reductions in E-cadherin in samples from primary tumours taken

from VNMAA and cephalexin treated animals suggesting that EMT was increased. It was therefore likely that tumour cell dissemination is correlatively increased. In an attempt to ascertain if this actually translated to cancer cell dissemination, flow cytometry was undertaken on blood and lung tissues to measure cancer cell numbers in these tissues. Unfortunately, this proved difficult, and the results were unclear. Fortunately, bioluminescence imaging successfully identified metastatic spread to the lungs at both 15 days and 18 days post tumour induction. At day 15, it appeared that there was increased metastatic incidence in VNMAA and cephalexin treated animals, with the cephalexin group being significantly increased compared to controls based on a Fisher's exact test. Conversely, at day 18 there were no significant differences regarding the metastatic incidence. Based on these experiments, it became evident that, to reliably compare the effects of antibiotic-induced perturbations of the microbiota on overt metastasis, the numbers of animals required to gain a large enough dataset would be vast. That is not to say that such experiments are unjustified, simply that prior to such an undertaking, the methods available should be carefully considered to ensure the ethicality of the study cannot be questioned.

Although considered highly metastatic, the growth kinetics of the PyMT-BO1 model are such that primary tumours reach advanced stages at a relatively early timepoint. Thus, these tumours are often harvested or resected in a short timeframe, meaning the time between tumour induction and experimental end point is reduced and disseminated cancer cells have less time to form lesions which can be consistently observed and investigated. Therefore, one suggestion may be for future work to consider either tagging the EO771 model or obtaining an alternate reporter-tagged model. One such model may include the BRPKp110 luminal A orthotopic model described in the publication by Buchta Rosean *et al.* (2019) [569]. Their cell line carries a GFP tag and has a longer incubation time, approximately four weeks, before reaching limits of tumour volumes within ethical restrictions, almost double the time observed in the PyMT-BO1 model. Thus, during the final stages of the research presented here, a collaboration was established with the Rutkowski laboratory (University of Virginia) and the BRPKp110 line has since been obtained for use in future experiments within the Robinson laboratory.

As described above, the activity of the immune system can govern tumour success and progression. This also extends to tumour establishment at distant metastatic sites, in this case with a focus on the lung. Immune profiling of immune cells known to either prevent or promote lesion formation did not highlight any changes in cell numbers following antibiotic administration, of either cephalexin or VNMAA, compared to controls. Neither did profiling of inflammatory cytokines in lung tissue from the same treatment groups. Arguably, the lack of differences in immune activity between the treatment groups in the lungs is unsurprising when considering there were no changes

in the same immune populations profiled in the primary tumours either. Considering all the results presented regarding metastatic studies, further investigation is undoubtedly required to reliably assess the effects of antibiotic treatment on the establishment and progression of metastasis.

Several studies have shown the administration of probiotic bacteria can rescue tumour growth and improve the efficacy of traditional therapeutics. For example, Sivan *et al.* (2015) described how administration bifidobacterial species to murine models of melanoma reduced tumour growth to rates observed following an anti-PD-L1 immunotherapy and that combining these treatments nearly abolished tumour growth all together [555]. Similarly, Vétizou *et al.* (2016) described how *Bacteroides fragilis* administration improved the efficacy of an anti-CTLA-4 blockade in treatment of a murine fibrosarcoma [596]. As stated earlier, the metagenomic sequencing of DNA isolated from the caeca of VNMAA and cephalixin treated animals identified the common reduction of several species. Of these, *F. rod* was of particular interest due to Zagato *et al.* (2019) having described the protective role it offered against a murine colorectal cancer model [574]. Similarly to observations made by Zagato, administration of *F. rod* rescued PyMT-BO1 tumour growth in animals with a VNMAA-induced perturbation of the microbiota relative to animals that did not receive this LBP treatment. Additionally, *Bif*, a proprietary cocktail of bifidobacterial species, also rescued tumour growth in a similar fashion in animals with a perturbed microbiota. Although mast cell counts were not significantly reduced following either of these LBP treatments, staining of tumours from the *Bif* treated animals suggested such treatment may promote apoptosis in mast cells, based on FCεR1α expression coinciding with TUNEL staining in those animals, in turn reducing the pro-tumour influences of mast cells observed in previous antibiotic-only experiments. These early LBP experiments present promising and optimistic results regarding using the microbiota as therapeutic target, but there is still much research required in this area. Aims and objectives have already been outlined by this author's successors regarding such studies and their early results continue to build optimism around LBP use in treatment pathways against breast cancer.

In conclusion, the research presented here demonstrates the gut microbiota has an influence of breast cancer progression. More importantly, it shows that antibiotic induced perturbations of the microbiota promote tumour growth and strongly suggest that the use of antibiotics during the treatment of patients with breast cancer be done so with extreme caution. Additionally, it alludes to a possible mechanism involving mast cell activity promoting tumour growth in animals with a perturbed microbiota. While additional investigation is required to fully ascertain the effect of these perturbations on metastasis, the results so far suggest that, similar to primary tumours, antibiotics promote lesion outgrowth. Finally, there is some evidence to suggest that promoting a healthy

microbiota, through LBP administration, can rescue the increased tumour growth observed in animals with a perturbed microbiota.

In a broader context, the immediate impact of the research presented in this thesis is to highlight the clear link between the gut microbiota and breast cancer. However, the novel role of mast cells described here is expected to drive research to better understand the role of these cells in the context of the link between changes in the gut microbiota and breast cancer. These findings are expected to raise questions as to whether the presence and activity of Mast cells in breast tumours might be carry a prognostic potential. Furthermore, with additional investigation looking into the role of the microbiota in influencing mast cell activity at a tumour level, is their scope to target such a relationship to improve prognoses and response to current breast cancer therapies. Looking to the future, the latter results presented in this thesis offer hope regarding the potential for using LBP products to aid in breast cancer treatment. Although, significantly more pre-clinical work is required in this area before aspiring to move into human studies and clinical trials.

8 References

- [1] McKee, A.M., Kirkup, B.M., Madgwick, M., Fowler, W.J., Price, C.A., Dreger, S.A., et al. (2021) Antibiotic-induced disturbances of the gut microbiota result in accelerated breast tumor growth. *IScience*. 24 (9), 103012.
- [2] Javed, A. and Lteif, A. (2013) Development of the Human Breast. *Seminars in Plastic Surgery*. 27 (1), 5.
- [3] McKiernan, J.F. and Hull, D. (1981) Breast development in the newborn. *Archives of Disease in Childhood*. 56 (7), 525–529.
- [4] Jayasinghe, Y., Cha, R., Horn-Ommen, J., O'Brien, P., and Simmons, P.S. (2010) Establishment of Normative Data for the Amount of Breast Tissue Present in Healthy Children up to Two Years of Age. *Journal of Pediatric and Adolescent Gynecology*. 23 (5), 305–311.
- [5] Marshall, W.A. and Tanner, J.M. (1969) Variations in pattern of pubertal changes in girls. *Archives of Disease in Childhood*. 44 (235), 291–303.
- [6] Dimitrakakis, C. and Bondy, C. (2009) Androgens and the breast. *Breast Cancer Research*. 11 (5), 212.
- [7] Heber, D. (1998) A Review of the Department of Defense's Program for Breast Cancer Research. .
- [8] Morris, E.A. (2005) The Normal Breast. in: *Breast MRI*, Springer-Verlag, pp. 23–44.
- [9] Kothari, C., Diorio, C., and Durocher, F. (2020) The importance of breast adipose tissue in breast cancer. *International Journal of Molecular Sciences*. 21 (16), 1–33.
- [10] Tomasetti, C., Li, L., and Vogelstein, B. (2017) Stem cell divisions, somatic mutations, cancer etiology, and cancer prevention. *Science (New York, N.Y.)*. 355 (6331), 1330–1334.
- [11] Joyce, J.A. and Pollard, J.W. (2009) Microenvironmental regulation of metastasis. *Nature Reviews Cancer*. 9 (4), 239–252.
- [12] Vogelstein, B., Papadopoulos, N., Velculescu, V.E., Zhou, S., Diaz, L.A., and Kinzler, K.W. (2013) Cancer genome landscapes. *Science*. 340 (6127), 1546–1558.
- [13] Garraway, L.A. and Lander, E.S. (2013) Lessons from the cancer genome. *Cell*. 153 (1), 17–37.

- [14] Thomson, A.K., Heyworth, J.S., Girschik, J., Slevin, T., Saunders, C., and Fritschi, L. (2014) Beliefs and perceptions about the causes of breast cancer: A case-control study. *BMC Research Notes*. 7 (1), 1–8.
- [15] Zhu, Y., Wu, J., Zhang, C., Sun, S., Zhang, J., Liu, W., et al. (2016) BRCA mutations and survival in breast cancer: An updated systematic review and meta-analysis. *Oncotarget*. 7 (43), 70113–70127.
- [16] Pérez-Solis, M.A., Maya-Nuñez, G., Casas-González, P., Olivares, A., and Aguilar-Rojas, A. (2016) Effects of the lifestyle habits in breast cancer transcriptional regulation. *Cancer Cell International*. 16 (1), 7.
- [17] Bray, F., Ferlay, J., Soerjomataram, I., Siegel, R.L., Torre, L.A., and Jemal, A. (2018) Global cancer statistics 2018: GLOBOCAN estimates of incidence and mortality worldwide for 36 cancers in 185 countries. *CA: A Cancer Journal for Clinicians*. 68 (6), 394–424.
- [18] McGuire, A., Brown, J.A.L., Malone, C., McLaughlin, R., and Kerin, M.J. (2015) Effects of age on the detection and management of breast cancer. *Cancers*. 7 (2), 908–929.
- [19] Siegel, R., Ma, J., Zou, Z., and Jemal, A. (2014) Cancer statistics, 2014. *CA: A Cancer Journal for Clinicians*. 64 (1), 9–29.
- [20] Coleman, C. (2017) Early Detection and Screening for Breast Cancer. *Seminars in Oncology Nursing*. 33 (2), 141–155.
- [21] Ghoncheh, M., Pournamdar, Z., and Salehiniya, H. (2016) Incidence and mortality and epidemiology of breast cancer in the world. *Asian Pacific Journal of Cancer Prevention*. 17 (sup3), 43–46.
- [22] Sun, Y.S., Zhao, Z., Yang, Z.N., Xu, F., Lu, H.J., Zhu, Z.Y., et al. (2017) Risk factors and preventions of breast cancer. *International Journal of Biological Sciences*. 13 (11), 1387–1397.
- [23] Stein, C.J. and Colditz, G.A. (2004) Modifiable risk factors for cancer. *British Journal of Cancer*. 90 (2), 299–303.
- [24] Momenimovahed, Z. and Salehiniya, H. (2019) Epidemiological characteristics of and risk factors for breast cancer in the world. *Breast Cancer: Targets and Therapy*. 11 151–164.
- [25] Teng, N.M.Y., Price, C.A., McKee, A.M., Hall, L.J., and Robinson, S.D. (2021) Exploring the impact of gut microbiota and diet on breast cancer risk and progression. *International*

Journal of Cancer. 149 (3), 494–504.

- [26] Liu, Y., Nguyen, N., and Colditz, G.A. (2015) Links between alcohol consumption and breast cancer: A look at the evidence. *Women's Health*. 11 (1), 65–77.
- [27] Fournier, A., Berrino, F., Riboli, E., Avenel, V., and Clavel-Chapelon, F. (2005) Breast cancer risk in relation to different types of hormone replacement therapy in the E3N-EPIC cohort. *International Journal of Cancer*. 114 (3), 448–454.
- [28] Rossouw, J.E., Anderson, G.L., Prentice, R.L., LaCroix, A.Z., Kooperberg, C., Stefanick, M.L., et al. (2002) Risks and benefits of estrogen plus progestin in healthy postmenopausal women: Principal results from the women's health initiative randomized controlled trial. *Journal of the American Medical Association*. 288 (3), 321–333.
- [29] Anderson, G.L., Chlebowski, R.T., Rossouw, J.E., Rodabough, R.J., McTiernan, A., Margolis, K.L., et al. (2006) Prior hormone therapy and breast cancer risk in the Women's Health Initiative randomized trial of estrogen plus progestin. *Maturitas*. 55 (2), 103–115.
- [30] Del Pup, L., Codacci-Pisanelli, G., and Peccatori, F. (2019) Breast cancer risk of hormonal contraception: Counselling considering new evidence. *Critical Reviews in Oncology/Hematology*. 137 123–130.
- [31] Mørch, L.S., Skovlund, C.W., Hannaford, P.C., Iversen, L., Fielding, S., and Lidegaard, Ø. (2017) Contemporary Hormonal Contraception and the Risk of Breast Cancer. *New England Journal of Medicine*. 377 (23), 2228–2239.
- [32] Shah, N.R. and Wong, T. (2006) Current breast cancer risks of hormone replacement therapy in postmenopausal women. *Expert Opinion on Pharmacotherapy*. 7 (18), 2455–2463.
- [33] Saxe, G.A., Rock, C.L., Wicha, M.S., and Schottenfeld, D. (1999) Diet and risk for breast cancer recurrence and survival. *Breast Cancer Research and Treatment*. 53 (3), 241–253.
- [34] Lee, K., Kruper, L., Dieli-Conwright, C.M., and Mortimer, J.E. (2019) The Impact of Obesity on Breast Cancer Diagnosis and Treatment. *Current Oncology Reports*. 21 (5), 1–6.
- [35] Ecker, B.L., Lee, J.Y., Sterner, C.J., Solomon, A.C., Pant, D.K., Shen, F., et al. (2019) Impact of obesity on breast cancer recurrence and minimal residual disease. *Breast Cancer Research*. 21 (1), 1–16.
- [36] Barone, I., Giordano, C., Bonofiglio, D., Andò, S., and Catalano, S. (2020) The weight of

- obesity in breast cancer progression and metastasis: Clinical and molecular perspectives. *Seminars in Cancer Biology*. 60 274–284.
- [37] Liedtke, S., Schmidt, M.E., Vrieling, A., Lukanova, A., Becker, S., Kaaks, R., et al. (2012) Postmenopausal Sex hormones in relation to body fat distribution. *Obesity*. 20 (5), 1088–1095.
- [38] Picon-Ruiz, M., Morata-Tarifa, C., Valle-Goffin, J.J., Friedman, E.R., and Slingerland, J.M. (2017) Obesity and adverse breast cancer risk and outcome: Mechanistic insights and strategies for intervention. *CA: A Cancer Journal for Clinicians*. 67 (5), 378–397.
- [39] Blücher, C. and Stadler, S.C. (2017) Obesity and breast cancer: Current insights on the role of fatty acids and lipid metabolism in promoting breast cancer growth and progression. *Frontiers in Endocrinology*. 8 (OCT), 293.
- [40] Kamińska, M., Ciszewski, T., Łopacka-Szatan, K., Miotła, P., and Starostawska, E. (2015) Breast cancer risk factors. *Przegląd Menopauzalny*. 14 (3), 196–202.
- [41] Tchou, J. and Morrow, M. (2003) Available models for breast cancer risk assessment: How accurate are they? *Journal of the American College of Surgeons*. 197 (6), 1029–1035.
- [42] Spencer, C. (2019) The gut microbiome (GM) and immunotherapy response are influenced by host lifestyle factors. in: Am. Assoc. Cancer Res. Annu. Meet., Atlanta.
- [43] Alegre, M.M., Knowles, M.H., Robison, R.A., and O’Neill, K.L. (2013) Mechanics behind breast cancer prevention - focus on obesity, exercise and dietary fat. *Asian Pacific Journal of Cancer Prevention*. 14 (4), 2207–2212.
- [44] Harvie, M., Howell, A., and Evans, D.G. (2015) Can Diet and Lifestyle Prevent Breast Cancer: What Is the Evidence? *American Society of Clinical Oncology Educational Book*. (35), e66–e73.
- [45] Sung, H., Ferlay, J., Siegel, R.L., Laversanne, M., Soerjomataram, I., Jemal, A., et al. (2021) Global Cancer Statistics 2020: GLOBOCAN Estimates of Incidence and Mortality Worldwide for 36 Cancers in 185 Countries. *CA: A Cancer Journal for Clinicians*. 71 (3), 209–249.
- [46] Lei, S., Zheng, R., Zhang, S., Wang, S., Chen, R., Sun, K., et al. (2021) Global patterns of breast cancer incidence and mortality: A population-based cancer registry data analysis from 2000 to 2020. *Cancer Communications*.
- [47] Cardoso, F., Kyriakides, S., Ohno, S., Penault-Llorca, F., Poortmans, P., Rubio, I.T., et al.

- (2019) Early breast cancer: ESMO Clinical Practice Guidelines for diagnosis, treatment and follow-up. *Annals of Oncology*. 30 (8), 1194–1220.
- [48] Dafni, U., Tsourti, Z., and Alatsathianos, I. (2019) Breast cancer statistics in the european union: Incidence and survival across european countries. *Breast Care*. 14 (6), 344–353.
- [49] Shapira, N. (2017) The potential contribution of dietary factors to breast cancer prevention. *European Journal of Cancer Prevention*. 26 (5), 385–395.
- [50] Ziegler, R.G., Hoover, R.N., Pike, M.C., Hildesheim, A., Nomura, A.M.Y., West, D.W., et al. (1993) Migration patterns and breast cancer risk in Asian-American women. *Journal of the National Cancer Institute*. 85 (22), 1819–1827.
- [51] Simon, C.E. (2006) Breast Cancer Screening: Cultural Beliefs and Diverse Populations. *Health and Social Work*. 31 (1), 36–43.
- [52] Lukong, K.E., Ogunbolude, Y., and Kamdem, J.P. (2017) Breast cancer in Africa: prevalence, treatment options, herbal medicines, and socioeconomic determinants. *Breast Cancer Research and Treatment*. 166 (2), 351–365.
- [53] Sun, L., Legood, R., Dos-Santos-Silva, I., Gaiha, S.M., and Sadique, Z. (2018) Global treatment costs of breast cancer by stage: A systematic review. *PLoS ONE*. 13 (11), e0207993.
- [54] Hanahan, D. and Weinberg, R.A. (2000) The hallmarks of cancer. *Cell*. 100 (1), 57–70.
- [55] Hanahan, D. and Weinberg, R.A. (2011) Hallmarks of cancer: The next generation. *Cell*. 144 (5), 646–674.
- [56] Burke, H.B. (2004) Outcome prediction and the future of the TNM staging system. *Journal of the National Cancer Institute*. 96 (19), 1408–1409.
- [57] Greene, F.L. and Sobin, L.H. (2008) The Staging of Cancer: A Retrospective and Prospective Appraisal. *CA: A Cancer Journal for Clinicians*. 58 (3), 180–190.
- [58] Singletary, S.E. and Greene, F.L. (2003) Revision of breast cancer staging: The 6th edition of the TNM Classification. *Seminars in Surgical Oncology*. 21 (1), 53–59.
- [59] Cancer Research UK (2016) TNM staging for stomach cancer | Cancer Research UK. *Cancer Research UK*.
- [60] Singletary, S.E. and Connolly, J.L. (2006) Breast Cancer Staging: Working With the Sixth Edition of the AJCC Cancer Staging Manual. *CA: A Cancer Journal for Clinicians*. 56 (1), 37–

47.

- [61] Kennecke, H., Yerushalmi, R., Woods, R., Cheang, M.C.U., Voduc, D., Speers, C.H., et al. (2010) Metastatic behavior of breast cancer subtypes. *Journal of Clinical Oncology*. 28 (20), 3271–3277.
- [62] Kuperwasser, C., Dessain, S., Bierbaum, B.E., Garnet, D., Sperandio, K., Gauvin, G.P., et al. (2005) A Mouse Model of Human Breast Cancer Metastasis to Human Bone. *Cancer Research*. 65 (14), 6130–6138.
- [63] Gerber, B., Freund, M., and Reimer, T. (2010) Recurrent breast cancer: Treatment strategies for maintaining and prolonging good quality of life. *Deutsches Arzteblatt*. 107 (6), 85–91.
- [64] Koh, J. and Kim, M.J. (2019) Introduction of a new staging system of breast cancer for radiologists: An emphasis on the prognostic stage. *Korean Journal of Radiology*. 20 (1), 69–82.
- [65] Zhu, H. and Doğan, B.E. (2021) American Joint Committee on Cancer’s Staging System for Breast Cancer, Eighth Edition: Summary for Clinicians. *European Journal of Breast Health*. 17 (3), 234–238.
- [66] Syed, Y.Y. (2020) Oncotype DX Breast Recurrence Score®: A Review of its Use in Early-Stage Breast Cancer. *Molecular Diagnosis and Therapy*. 24 (5), 621–632.
- [67] Dian, D., Herold, H., Mylonas, I., Scholz, C., Janni, W., Sommer, H., et al. (2009) Survival analysis between patients with invasive ductal and invasive lobular breast cancer. *Archives of Gynecology and Obstetrics*. 279 (1), 23–28.
- [68] Chen, Z., Yang, J., Li, S., Lv, M., Shen, Y., Wang, B., et al. (2017) Invasive lobular carcinoma of the breast: A special histological type compared with invasive ductal carcinoma. *PLoS ONE*. 12 (9), e0182397.
- [69] Pape-Zambito, D., Jiang, Z., Wu, H., Devarajan, K., Slater, C.M., Cai, K.Q., et al. (2014) Identifying a highly-aggressive DCIS subgroup by studying intra-individual DCIS heterogeneity among invasive breast cancer patients. *PLoS ONE*. 9 (6),.
- [70] Gauthier, M.L., Berman, H.K., Miller, C., Kozakeiwicz, K., Chew, K., Moore, D., et al. (2007) Abrogated Response to Cellular Stress Identifies DCIS Associated with Subsequent Tumor Events and Defines Basal-like Breast Tumors. *Cancer Cell*. 12 (5), 479–491.
- [71] Yersal, O. and Barutca, S. (2014) Biological subtypes of breast cancer: Prognostic and

therapeutic implications. *World Journal of Clinical Oncology*. 5 (3), 412.

- [72] Dai, X., Li, T., Bai, Z., Yang, Y., Liu, X., Zhan, J., et al. (2015) Breast cancer intrinsic subtype classification, clinical use and future trends. *American Journal of Cancer Research*. 5 (10), 2929–2943.
- [73] Waks, A.G. and Winer, E.P. (2019) Breast Cancer Treatment: A Review. *JAMA*. 321 (3), 288–300.
- [74] Hess, R.A., Bunick, D., Lee, K.H., Bahr, J., Taylor, J.A., Korach, K.S., et al. (1997) A role for oestrogens in the male reproductive system. *Nature*. 390 (6659), 509–512.
- [75] Perry, R.J., Farquharson, C., and Ahmed, S.F. (2008) The role of sex steroids in controlling pubertal growth. *Clinical Endocrinology*. 68 (1), 4–15.
- [76] Hewitt, S.C. and Korach, K.S. (2000) Progesterone action and responses in the α ERKO mouse. *Steroids*. 65 (10–11), 551–557.
- [77] Leitman, D.C., Paruthiyil, S., Vivar, O.I., Saunier, E.F., Herber, C.B., Cohen, I., et al. (2010) Regulation of specific target genes and biological responses by estrogen receptor subtype agonists. *Current Opinion in Pharmacology*. 10 (6), 629–636.
- [78] Yaşar, P., Ayaz, G., User, S.D., Güpür, G., and Muyan, M. (2017) Molecular mechanism of estrogen–estrogen receptor signaling. *Reproductive Medicine and Biology*. 16 (1), 4–20.
- [79] Achinger-Kawecka, J., Valdes-Mora, F., Luu, P.L., Giles, K.A., Caldon, C.E., Qu, W., et al. (2020) Epigenetic reprogramming at estrogen-receptor binding sites alters 3D chromatin landscape in endocrine-resistant breast cancer. *Nature Communications*. 11 (1), 1–17.
- [80] Helguero, L.A., Faulds, M.H., Gustafsson, J.Å., and Haldosén, L.A. (2005) Estrogen receptors alfa (ER α) and beta (ER β) differentially regulate proliferation and apoptosis of the normal murine mammary epithelial cell line HC11. *Oncogene*. 24 (44), 6605–6616.
- [81] Duong, V., Licznar, A., Margueron, R., Bouille, N., Busson, M., Lacroix, M., et al. (2006) ER α and ER β expression and transcriptional activity are differentially regulated by HDAC inhibitors. *Oncogene*. 25 (12), 1799–1806.
- [82] Clemons, M. and Goss, P. (2001) Estrogen and the Risk of Breast Cancer. *New England Journal of Medicine*. 344 (4), 276–285.
- [83] Hua, H., Zhang, H., Kong, Q., and Jiang, Y. (2018) Mechanisms for estrogen receptor expression in human cancer 11 Medical and Health Sciences 1112 Oncology and

- Carcinogenesis 06 Biological Sciences 0604 Genetics. *Experimental Hematology and Oncology*. 7 (1), 1–11.
- [84] Katzenellenbogen, B.S. (2000) Mechanisms of action and cross-talk between estrogen receptor and progesterone receptor pathways. *Journal of the Society for Gynecologic Investigation*. 7 (1 Suppl), S33–S37.
- [85] Mohammed, H., Russell, I.A., Stark, R., Rueda, O.M., Hickey, T.E., Tarulli, G.A., et al. (2015) Progesterone receptor modulates ER α action in breast cancer. *Nature*. 523 (7560), 313–317.
- [86] Lange, C.A. and Yee, D. (2008) Progesterone and breast cancer. *Women's Health*. 4 (2), 151–162.
- [87] Mulac-Jericevic, B., Lydon, J.P., DeMayo, F.J., and Conneely, O.M. (2003) Defective mammary gland morphogenesis in mice lacking the progesterone receptor B isoform. *Proceedings of the National Academy of Sciences of the United States of America*. 100 (17), 9744–9749.
- [88] Mulac-Jericevic, B., Mullinax, R.A., DeMayo, F.J., Lydon, J.P., and Conneely, O.M. (2000) Subgroup of reproductive functions of progesterone mediated by progesterone receptor-B isoform. *Science*. 289 (5485), 1751–1754.
- [89] Wei, L.L., Norris, B.M., and Baker, C.J. (1997) An N-terminally truncated third progesterone receptor protein, PR(C), forms heterodimers with PR(B) but interferes in PR(B)-DNA binding. *Journal of Steroid Biochemistry and Molecular Biology*. 62 (4), 287–297.
- [90] Hsu, J.L. and Hung, M.C. (2016) The role of HER2, EGFR, and other receptor tyrosine kinases in breast cancer. *Cancer and Metastasis Reviews*. 35 (4), 575–588.
- [91] Roskoski, R. (2014) The ErbB/HER family of protein-tyrosine kinases and cancer. *Pharmacological Research*. 79 34–74.
- [92] Gee, J.M., Robertson, J.F., Gutteridge, E., Ellis, I.O., Pinder, S.E., Rubini, M., et al. (2005) Epidermal growth factor receptor/HER2/insulin-like growth factor receptor signalling and oestrogen receptor activity in clinical breast cancer. *Endocrine-Related Cancer*. 12 (Supplement_1), S99–S111.
- [93] Honarvar, H., Calce, E., Doti, N., Langella, E., Orlova, A., Buijs, J., et al. (2018) Evaluation of HER2-specific peptide ligand for its employment as radiolabeled imaging probe. *Scientific Reports*. 8 (1), 1–12.

- [94] Mitri, Z., Constantine, T., and O'Regan, R. (2012) The HER2 Receptor in Breast Cancer: Pathophysiology, Clinical Use, and New Advances in Therapy. *Chemotherapy Research and Practice*. 2012 1–7.
- [95] Kau, P., Nagaraja, G.M., Zheng, H., Gizachew, D., Galukande, M., Krishnan, S., et al. (2012) A mouse model for triple-negative breast cancer tumor-initiating cells (TNBC-TICs) exhibits similar aggressive phenotype to the human disease. *BMC Cancer*. 12 (1), 1–12.
- [96] Rakha, E.A., El-Sayed, M.E., Green, A.R., Lee, A.H.S., Robertson, J.F., and Ellis, I.O. (2007) Prognostic markers in triple-negative breast cancer. *Cancer*. 109 (1), 25–32.
- [97] Karaayvaz, M., Cristea, S., Gillespie, S.M., Patel, A.P., Mylvaganam, R., Luo, C.C., et al. (2018) Unravelling subclonal heterogeneity and aggressive disease states in TNBC through single-cell RNA-seq. *Nature Communications*. 9 (1), 1–10.
- [98] Li, L.T., Jiang, G., Chen, Q., and Zheng, J.N. (2015) Predict Ki67 is a promising molecular target in the diagnosis of cancer (Review). *Molecular Medicine Reports*. 11 (3), 1566–1572.
- [99] Scholzen, T. and Gerdes, J. (2000) The Ki-67 protein: From the known and the unknown. *Journal of Cellular Physiology*. 182 (3), 311–322.
- [100] Heng, B., Lim, C.K., Lovejoy, D.B., Bessedé, A., Gluch, L., and Guillemin, G.J. (2016) Understanding the role of the kynurenine pathway in human breast cancer immunobiology. *Oncotarget*. 7 (6), 6506–6520.
- [101] Fallahpour, S., Navaneelan, T., De, P., and Borgo, A. (2017) Breast cancer survival by molecular subtype: a population-based analysis of cancer registry data. *CMAJ Open*. 5 (3), E734–E739.
- [102] Akram, M., Iqbal, M., Daniyal, M., and Khan, A.U. (2017) Awareness and current knowledge of breast cancer. *Biological Research*. 50 (1), 1–23.
- [103] Gómez-Acebo, I., Dierssen-Sotos, T., Mirones, M., Pérez-Gómez, B., Guevara, M., Amiano, P., et al. (2021) Adequacy of early-stage breast cancer systemic adjuvant treatment to Saint Gallen-2013 statement: the MCC-Spain study. *Scientific Reports*. 11 (1), 5375.
- [104] Thompson, A.M. and Moulder-Thompson, S.L. (2012) Neoadjuvant treatment of breast cancer. *Annals of Oncology*. 23 (SUPPL. 10), x231–x236.
- [105] Fisher, B., Anderson, S., Redmond, C.K., Wolmark, N., Wickerham, D.L., and Cronin, W.M. (1995) Reanalysis and Results after 12 Years of Follow-up in a Randomized Clinical Trial

Comparing Total Mastectomy with Lumpectomy with or without Irradiation in the Treatment of Breast Cancer. *New England Journal of Medicine*. 333 (22), 1456–1461.

- [106] Paolucci, T., Bernetti, A., Bai, A. V., Segatori, L., Monti, M., Maggi, G., et al. (2021) The sequelae of mastectomy and quadrantectomy with respect to the reaching movement in breast cancer survivors: evidence for an integrated rehabilitation protocol during oncological care. *Supportive Care in Cancer*. 29 (2), 899–908.
- [107] Lieto, E., Auricchio, A., Erario, S., Sorbo, G. Del, and Cardella, F. (2021) Subcutaneous Quadrantectomy Is A Safe Procedure in Management of Early Stage Breast Cancer.
- [108] Vasileiadou, K., Kosmidis, C., Anthimidis, G., Miliaras, S., Kostopoulos, I., and Fahantidis, E. (2017) Cyanoacrylate Adhesive Reduces Seroma Production After Modified Radical Mastectomy or Quadrantectomy With Lymph Node Dissection—A Prospective Randomized Clinical Trial. *Clinical Breast Cancer*. 17 (8), 595–600.
- [109] Corradini, S., Reitz, D., Pazos, M., Schönecker, S., Braun, M., Harbeck, N., et al. (2019) Mastectomy or breast-conserving therapy for early breast cancer in real-life clinical practice: outcome comparison of 7565 cases. *Cancers*. 11 (2), 160.
- [110] Agha, R.A., Al Omran, Y., Wellstead, G., Sagoo, H., Barai, I., Rajmohan, S., et al. (2019) Systematic review of therapeutic nipple-sparing versus skin-sparing mastectomy. *BJS Open*. 3 (2), 135–145.
- [111] Welsh, J.L., Hoskin, T.L., Day, C.N., Thomas, A.S., Cogswell, J.A., Couch, F.J., et al. (2017) Clinical Decision-Making in Patients with Variant of Uncertain Significance in BRCA1 or BRCA2 Genes. *Annals of Surgical Oncology*. 24 (10), 3067–3072.
- [112] Yamauchi, H., Okawa, M., Yokoyama, S., Nakagawa, C., Yoshida, R., Suzuki, K., et al. (2018) High rate of occult cancer found in prophylactic mastectomy specimens despite thorough presurgical assessment with MRI and ultrasound: findings from the Hereditary Breast and Ovarian Cancer Registration 2016 in Japan. *Breast Cancer Research and Treatment*. 172 (3), 679–687.
- [113] Aquil, A., El kherchi, O., EL Azmaoui, N., Mouallif, M., Guerroumi, M., Benider, A., et al. (2021) Predictors of mental health disorders in women with breast and gynecological cancer after radical surgery: A cross-sectional study. *Annals of Medicine and Surgery*. 65 102278.
- [114] Derogatis, L.R. (2015) The Unique Impact of Breast and Gynecologic Cancers on Body Image and Sexual Identity in Women: A Reassessment. *Body Image, Self-Esteem, and Sexuality in*

Cancer Patients. 1–14.

- [115] Grizzi, G., Ghidini, M., Botticelli, A., Tomasello, G., Ghidini, A., Grossi, F., et al. (2020) Strategies for increasing the effectiveness of aromatase inhibitors in locally advanced breast cancer: An evidence-based review on current options. *Cancer Management and Research.* 12 675–686.
- [116] Sharma, D., Kumar, S., and Narasimhan, B. (2018) Estrogen alpha receptor antagonists for the treatment of breast cancer: A review. *Chemistry Central Journal.* 12 (1), 1–32.
- [117] Jaiyesimi, I.A., Buzdar, A.U., Decker, D.A., and Hortobagyi, G.N. (1995) Use of tamoxifen for breast cancer: Twenty-eight years later. *Journal of Clinical Oncology.* 13 (2), 513–529.
- [118] Shagufta and Ahmad, I. (2018) Tamoxifen a pioneering drug: An update on the therapeutic potential of tamoxifen derivatives. *European Journal of Medicinal Chemistry.* 143 515–531.
- [119] Davies, C., Pan, H., Godwin, J., Gray, R., Arriagada, R., Raina, V., et al. (2013) Long-term effects of continuing adjuvant tamoxifen to 10 years versus stopping at 5 years after diagnosis of oestrogen receptor-positive breast cancer: ATLAS, a randomised trial. *The Lancet.* 381 (9869), 805–816.
- [120] Moon, Z., Moss-Morris, R., Hunter, M.S., and Hughes, L.D. (2017) Understanding tamoxifen adherence in women with breast cancer: A qualitative study. *British Journal of Health Psychology.* 22 (4), 978–997.
- [121] Chumsri, S., Howes, T., Bao, T., Sabnis, G., and Brodie, A. (2011) Aromatase, aromatase inhibitors, and breast cancer. *The Journal of Steroid Biochemistry and Molecular Biology.* 125 (1–2), 13–22.
- [122] Assal, R. (2017) Cost Minimization Analysis of The Selective Aromatase Inhibitors; Anastrozole, Versus Letrozole and Exemestane for The Management of Breast Cancer From Patient Perspective in Egypt. *Value in Health.* 20 (9), A443.
- [123] De Placido, S., Gallo, C., De Laurentiis, M., Bisagni, G., Arpino, G., Sarobba, M.G., et al. (2018) Adjuvant anastrozole versus exemestane versus letrozole, upfront or after 2 years of tamoxifen, in endocrine-sensitive breast cancer (FATA-GIM3): a randomised, phase 3 trial. *The Lancet Oncology.* 19 (4), 474–485.
- [124] Fabian, C.J. (2007) The what, why and how of aromatase inhibitors: hormonal agents for treatment and prevention of breast cancer. *International Journal of Clinical Practice.* 61 (12), 2051.

- [125] Pistelli, M., Della Mora, A., Ballatore, Z., and Berardi, R. (2018) Aromatase inhibitors in premenopausal women with breast cancer: The state of the art and future prospects. *Current Oncology*. 25 (2), e168–e175.
- [126] Mates, M., Fletcher, G.G., Freedman, O.C., Eisen, A., Gandhi, S., Trudeau, M.E., et al. (2015) Systemic targeted therapy for HER2-positive early female breast cancer: A systematic review of the evidence for the 2014 cancer care Ontario systemic therapy guideline. *Current Oncology*. 22 (Suppl 1), S114–S122.
- [127] Bange, J., Zwick, E., and Ullrich, A. (2001) Molecular targets for breast cancer therapy and prevention. *Nature Medicine* 2001 7:5. 7 (5), 548–552.
- [128] Slamon, D.J., Leyland-Jones, B., Shak, S., Fuchs, H., Paton, V., Bajamonde, A., et al. (2001) Use of Chemotherapy plus a Monoclonal Antibody against HER2 for Metastatic Breast Cancer That Overexpresses HER2. *New England Journal of Medicine*. 344 (11), 783–792.
- [129] Ishii, K., Morii, N., and Yamashiro, H. (2019) Pertuzumab in the treatment of HER2-positive breast cancer: an evidence-based review of its safety, efficacy, and place in therapy. *Core Evidence*. Volume 14 51–70.
- [130] Xu, Z.Q., Zhang, Y., Li, N., Liu, P.J., Gao, L., Gao, X., et al. (2017) Efficacy and safety of lapatinib and trastuzumab for HER2-positive breast cancer: A systematic review and meta-analysis of randomised controlled trials. *BMJ Open*. 7 (3), e013053.
- [131] Gavilá, J., De La Haba, J., Bermejo, B., Rodríguez-Lescure, Antón, A., Ciruelos, E., et al. (2020) A retrospective, multicenter study of the efficacy of lapatinib plus trastuzumab in HER2-positive metastatic breast cancer patients previously treated with trastuzumab, lapatinib, or both: the Trastyvere study. *Clinical and Translational Oncology*. 22 (3), 420–428.
- [132] Lv, H., Yan, M., and Jiang, Z. (2021) Recent advances in the treatment of hormone receptor-positive/human epidermal growth factor 2-positive advanced breast cancer. *Therapeutic Advances in Medical Oncology*. 13 17588359211013326.
- [133] Kavanagh, E.L., Lindsay, S., Halasz, M., Gubbins, L.C., Weiner-Gorzal, K., Guang, M.H.Z., et al. (2017) Protein and chemotherapy profiling of extracellular vesicles harvested from therapeutic induced senescent triple negative breast cancer cells. *Oncogenesis*. 6 (10), e388–e388.
- [134] Khosravi-Shahi, P., Cabezón-Gutiérrez, L., and Custodio-Cabello, S. (2018) Metastatic triple negative breast cancer: Optimizing treatment options, new and emerging targeted

therapies. *Asia-Pacific Journal of Clinical Oncology*. 14 (1), 32–39.

- [135] Rossi, L., Biagioni, C., McCartney, A., Moretti, E., Pestrin, M., Sanna, G., et al. (2018) Platinum-based agent and fluorouracil in metastatic breast cancer: A retrospective monocentric study with a review of the literature. *Anticancer Research*. 38 (8), 4839–4845.
- [136] Zheng, R., Han, S., Duan, C., Chen, K., You, Z., Jia, J., et al. (2015) Role of taxane and anthracycline combination regimens in the management of advanced breast cancer a meta-analysis of randomized trials. *Medicine (United States)*. 94 (17), e803.
- [137] Schirmacher, V. (2019) From chemotherapy to biological therapy: A review of novel concepts to reduce the side effects of systemic cancer treatment (Review). *International Journal of Oncology*. 54 (2), 407–419.
- [138] Andreopoulou, E. and Sparano, J.A. (2013) Chemotherapy in patients with anthracycline and taxane-pretreated metastatic breast cancer: An overview. *Current Breast Cancer Reports*. 5 (1), 42–50.
- [139] Swain, S.M., Whaley, F.S., and Ewer, M.S. (2003) Congestive heart failure in patients treated with doxorubicin. *Cancer*. 97 (11), 2869–2879.
- [140] Gianfaldoni, S., Gianfaldoni, R., Wollina, U., Lotti, J., Tchernev, G., and Lotti, T. (2017) An overview on radiotherapy: From its history to its current applications in dermatology. *Open Access Macedonian Journal of Medical Sciences*. 5 (4 Special Issue GlobalDermatology), 521–525.
- [141] Flores-Balcázar, C.H., Flores-Luna, L., Villarreal-Garza, C., Mota-García, A., and Bargalló-Rocha, E. (2018) Impact of Delayed Adjuvant Radiotherapy in the Survival of Women with Breast Cancer. *Cureus*. 10 (7),.
- [142] Wang, J., Shi, M., Ling, R., Xia, Y., Luo, S., Fu, X., et al. (2011) Adjuvant chemotherapy and radiotherapy in triple-negative breast carcinoma: A prospective randomized controlled multi-center trial. *Radiotherapy and Oncology*. 100 (2), 200–204.
- [143] Ruland, J. (2011) Return to homeostasis: Downregulation of NF- κ B responses. *Nature Immunology*. 12 (8), 709–714.
- [144] Van Parijs, L. and Abbas, A.K. (1998) Homeostasis and self-tolerance in the immune system: Turning lymphocytes off. *Science*. 280 (5361), 243–248.
- [145] Chen, L., Deng, H., Cui, H., Fang, J., Zuo, Z., Deng, J., et al. (2018) Inflammatory responses

and inflammation-associated diseases in organs. *Oncotarget*. 9 (6), 7204.

- [146] Medzhitov, R. and Janeway C., J. (2000) Advances in immunology: Innate immunity. *New England Journal of Medicine*. 343 (5), 338–344.
- [147] Bonilla, F.A. and Oettgen, H.C. (2010) Adaptive immunity. *Journal of Allergy and Clinical Immunology*. 125 (2 SUPPL. 2), S33–S40.
- [148] Jagannathan-Bogdan, M. and Zon, L.I. (2013) Hematopoiesis. *Development (Cambridge)*. 140 (12), 2463–2467.
- [149] D’Andrea, A.D. (1994) Hematopoietic growth factors and the regulation of differentiative decisions. *Current Opinion in Cell Biology*. 6 (6), 804–808.
- [150] Robb, L. (2007) Cytokine receptors and hematopoietic differentiation. *Oncogene*. 26 (47), 6715–6723.
- [151] Stanley, E.R. (2009) Lineage Commitment: Cytokines Instruct, At Last! *Cell Stem Cell*. 5 (3), 234–236.
- [152] Iwasaki, H. and Akashi, K. (2007) Hematopoietic developmental pathways: On cellular basis. *Oncogene*. 26 (47), 6687–6696.
- [153] Evans, C.A., Pierce, A., Winter, S.A., Spooncer, E., Heyworth, C.M., and Whetton, A.D. (1999) Activation of Granulocyte-Macrophage Colony-Stimulating Factor and Interleukin-3 Receptor Subunits in a Multipotential Hematopoietic Progenitor Cell Line Leads to Differential Effects on Development. *Blood*. 94 (5), 1504–1514.
- [154] Grinenko, T., Eugster, A., Thielecke, L., Ramasz, B., Krüger, A., Dietz, S., et al. (2018) Hematopoietic stem cells can differentiate into restricted myeloid progenitors before cell division in mice. *Nature Communications* 2018 9:1. 9 (1), 1–10.
- [155] Noetzli, L.J., French, S.L., and Machlus, K.R. (2019) New Insights Into the Differentiation of Megakaryocytes From Hematopoietic Progenitors. *Arteriosclerosis, Thrombosis, and Vascular Biology*. 39 (7), 1288–1300.
- [156] Valent, P., Akin, C., Hartmann, K., Nilsson, G., Reiter, A., Hermine, O., et al. (2020) Mast cells as a unique hematopoietic lineage and cell system: From Paul Ehrlich’s visions to precision medicine concepts. *Theranostics*. 10 (23), 10743–10768.
- [157] Rennick, D., Hunte, B., Holland, G., and Thompson-Snipes, L.A. (1995) Cofactors are essential for stem cell factor-dependent growth and maturation of mast cell progenitors:

- Comparative effects of interleukin-3 (IL-3), IL-4, IL-10, and fibroblasts. *Blood*. 85 (1), 57–65.
- [158] Panopoulos, A.D. and Watowich, S.S. (2008) Granulocyte colony-stimulating factor: Molecular mechanisms of action during steady state and “emergency” hematopoiesis. *Cytokine*. 42 (3), 277–288.
- [159] Xu, M., Zhao, Z., Song, J., Lan, X., Lu, S., Chen, M., et al. (2017) Interactions between interleukin-6 and myeloid-derived suppressor cells drive the chemoresistant phenotype of hepatocellular cancer. *Experimental Cell Research*. 351 (2), 142–149.
- [160] Groth, C., Hu, X., Weber, R., Fleming, V., Altevogt, P., Utikal, J., et al. (2019) Immunosuppression mediated by myeloid-derived suppressor cells (MDSCs) during tumour progression. *British Journal of Cancer*. 120 (1), 16–25.
- [161] Poltorak, M.P. and Schraml, B.U. (2015) Fate mapping of dendritic cells. *Frontiers in Immunology*. 6 (MAY), 199.
- [162] Dias, S., Silva, H., Cumano, A., and Vieira, P. (2005) Interleukin-7 is necessary to maintain the B cell potential in common lymphoid progenitors. *Journal of Experimental Medicine*. 201 (6), 971–979.
- [163] Ranson, T., Vosshenrich, C.A.J., Corcuff, E., Richard, O., Müller, W., and Di Santo, J.P. (2003) IL-15 is an essential mediator of peripheral NK-cell homeostasis. *Blood*. 101 (12), 4887–4893.
- [164] Carson, W.E., Giri, J.G., Lindemann, M.J., Linett, M.L., Ahdieh, M., Paxton, R., et al. (1994) Interleukin (IL) 15 is a novel cytokine that activates human natural killer cells via components of the IL-2 receptor. *Journal of Experimental Medicine*. 180 (4), 1395–1403.
- [165] Karsunky, H., Merad, M., Cozzio, A., Weissman, I.L., and Manz, M.G. (2003) Flt3 ligand regulates dendritic cell development from Flt3+ lymphoid and myeloid-committed progenitors to Flt3+ dendritic cells in vivo. *Journal of Experimental Medicine*. 198 (2), 305–313.
- [166] Kondo, M., Scherer, D.C., Miyamoto, T., King, A.G., Akashi, K., Sugamura, K., et al. (2000) Cell-fate conversion of lymphoid-committed progenitors by instructive actions of cytokines. *Nature*. 407 (6802), 383–386.
- [167] Galeas-Pena, M., McLaughlin, N., and Pociask, D. (2019) The role of the innate immune system on pulmonary infections. *Biological Chemistry*. 400 (4), 443–456.
- [168] Kubelkova, K. and Macela, A. (2019) Innate Immune Recognition: An Issue More Complex

Than Expected. *Frontiers in Cellular and Infection Microbiology*. 9 241.

- [169] Mogensen, T.H. (2009) Pathogen recognition and inflammatory signaling in innate immune defenses. *Clinical Microbiology Reviews*. 22 (2), 240–273.
- [170] Brown, E.J. (1995) Phagocytosis. *BioEssays*. 17 (2), 109–117.
- [171] Gaudino, S.J. and Kumar, P. (2019) Cross-talk between antigen presenting cells and T cells impacts intestinal homeostasis, bacterial infections, and tumorigenesis. *Frontiers in Immunology*. 10 (MAR), 360.
- [172] van der Meer, J.W.M., Joosten, L.A.B., Riksen, N., and Netea, M.G. (2015) Trained immunity: A smart way to enhance innate immune defence. *Molecular Immunology*. 68 (1), 40–44.
- [173] Pardo, J., Aguilo, J.I., Anel, A., Martin, P., Joeckel, L., Borner, C., et al. (2009) The biology of cytotoxic cell granule exocytosis pathway: granzymes have evolved to induce cell death and inflammation. *Microbes and Infection*. 11 (4), 452–459.
- [174] Duffin, R., Leitch, A.E., Fox, S., Haslett, C., and Rossi, A.G. (2010) Targeting granulocyte apoptosis: Mechanisms, models, and therapies. *Immunological Reviews*. 236 (1), 28–40.
- [175] Franco, C.B., Chen, C.C., Drukker, M., Weissman, I.L., and Galli, S.J. (2010) Distinguishing Mast Cell and Granulocyte Differentiation at the Single-Cell Level. *Cell Stem Cell*. 6 (4), 361–368.
- [176] Döhrmann, S., Cole, J.N., and Nizet, V. (2016) Conquering Neutrophils. *PLoS Pathogens*. 12 (7), e1005682.
- [177] Gordon, S. (2016) Phagocytosis: An Immunobiologic Process. *Immunity*. 44 (3), 463–475.
- [178] Uribe-Querol, E. and Rosales, C. (2020) Phagocytosis: Our Current Understanding of a Universal Biological Process. *Frontiers in Immunology*. 11 1066.
- [179] Lacy, P. (2006) Mechanisms of Degranulation in Neutrophils. *Allergy, Asthma & Clinical Immunology*. 2 (3), 98.
- [180] Uhm, T.G., Kim, B.S., and Chung, Y. (2012) Eosinophil development, regulation of eosinophil-specific genes, and role of eosinophils in the pathogenesis of asthma. *Allergy, Asthma and Immunology Research*. 4 (2), 68–79.
- [181] Dombrowicz, D. and Capron, M. (2001) Eosinophils, allergy and parasites. *Current Opinion in Immunology*. 13 (6), 716–720.

- [182] MacGlashan, D.W. and Lichtenstein, L.M. (1980) The purification of human basophils. *Journal of Immunology (Baltimore, Md. : 1950)*. 124 (5), 2519–21.
- [183] Klion, A.D. and Nutman, T.B. (2004) The role of eosinophils in host defense against helminth parasites. *Journal of Allergy and Clinical Immunology*. 113 (1), 30–37.
- [184] Meeusen, E.N.T. and Balic, A. (2000) Do eosinophils have a role in the killing of helminth parasites? *Parasitology Today*. 16 (3), 95–101.
- [185] Ueki, S., Tokunaga, T., Fujieda, S., Honda, K., Hirokawa, M., Spencer, L.A., et al. (2016) Eosinophil ETosis and DNA Traps: a New Look at Eosinophilic Inflammation. *Current Allergy and Asthma Reports*. 16 (8), 1–8.
- [186] Rosenberg, H.F., Dyer, K.D., and Foster, P.S. (2013) Eosinophils: Changing perspectives in health and disease. *Nature Reviews Immunology*. 13 (1), 9–22.
- [187] Simon, H.U., Yousefi, S., Germic, N., Arnold, I.C., Haczku, A., Karaulov, A. V., et al. (2020) The Cellular Functions of Eosinophils: Collegium Internationale Allergologicum (CIA) Update 2020. *International Archives of Allergy and Immunology*. 181 (1), 11–23.
- [188] Melo, R.C.N. and Weller, P.F. (2010) Piecemeal degranulation in human eosinophils: A distinct secretion mechanism underlying inflammatory responses. *Histology and Histopathology*. 25 (10), 1341–1354.
- [189] Čelakovská, J. and Bukač, J. (2016) Eosinophils in patients suffering from atopic dermatitis and the relation to the occurrence of food allergy and other atopic diseases. *Food and Agricultural Immunology*. 27 (5), 700–710.
- [190] Al-Jahdali, H., Wali, S., Albanna, A.S., Allehebi, R., Al-Matar, H., Fattouh, M., et al. (2022) Prevalence of eosinophilic, atopic, and overlap phenotypes among patients with severe asthma in Saudi Arabia: a cross-sectional study. *BMC Pulmonary Medicine*. 22 (1), 67.
- [191] Stone, K.D., Prussin, C., and Metcalfe, D.D. (2010) IgE, mast cells, basophils, and eosinophils. *Journal of Allergy and Clinical Immunology*. 125 (2 SUPPL. 2), S73.
- [192] Franco, C.B., Chen, C.C., Drukker, M., Weissman, I.L., and Galli, S.J. (2010) Distinguishing Mast Cell and Granulocyte Differentiation at the Single-Cell Level. *Cell Stem Cell*. 6 (4), 361–368.
- [193] Min, B., Brown, M.A., and Legros, G. (2012) Understanding the roles of basophils: Breaking dawn. *Immunology*. 135 (3), 192–197.

- [194] Mukai, K., Tsai, M., Starkl, P., Marichal, T., and Galli, S.J. (2016) IgE and mast cells in host defense against parasites and venoms. *Seminars in Immunopathology*. 38 (5), 581–603.
- [195] Von Köckritz-Blickwede, M., Goldmann, O., Thulin, P., Heinemann, K., Norrby-Teglund, A., Rohde, M., et al. (2008) Phagocytosis-independent antimicrobial activity of mast cells by means of extracellular trap formation. *Blood*. 111 (6), 3070–3080.
- [196] Ahmed, A.A. (2018) Hematopoietic and Lymphoid Tissues. *Pathology Exam Review*. 365–401.
- [197] Crivellato, E., Travan, L., and Ribatti, D. (2010) Mast cells and basophils: A potential link in promoting angiogenesis during allergic inflammation. *International Archives of Allergy and Immunology*. 151 (2), 89–97.
- [198] Ashina, K., Tsubosaka, Y., Nakamura, T., Omori, K., Kobayashi, K., Hori, M., et al. (2015) Histamine Induces Vascular Hyperpermeability by Increasing Blood Flow and Endothelial Barrier Disruption In Vivo. *PLoS ONE*. 10 (7),.
- [199] Borriello, F., Iannone, R., and Marone, G. (2017) Histamine Release from Mast Cells and Basophils. *Handbook of Experimental Pharmacology*. 241 121–139.
- [200] White, M. V. (1990) The role of histamine in allergic diseases. *The Journal of Allergy and Clinical Immunology*. 86 (4 PART 2), 599–605.
- [201] Krystel-Whittemore, M., Dileepan, K.N., and Wood, J.G. (2016) Mast cell: A multi-functional master cell. *Frontiers in Immunology*. 6 (JAN), 620.
- [202] Janeway CA Jr, Travers P, Walport M, et al. (2001) The production of IgE - Immunobiology - NCBI Bookshelf.
- [203] Bax, H.J., Keeble, A.H., and Gould, H.J. (2012) Cytokinergic IgE action in mast cell activation. *Frontiers in Immunology*. 3 (AUG), 229.
- [204] Rajput, A.B., Turbin, D.A., Cheang, M.C., Voduc, D.K., Leung, S., Gelmon, K.A., et al. (2008) Stromal mast cells in invasive breast cancer are a marker of favourable prognosis: A study of 4,444 cases. *Breast Cancer Research and Treatment*. 107 (2), 249–257.
- [205] Varricchi, G., Raap, U., Rivellesse, F., Marone, G., and Gibbs, B.F. (2018) Human mast cells and basophils—How are they similar how are they different? *Immunological Reviews*. 282 (1), 8–34.
- [206] Marech, I., Ammendola, M., Leporini, C., Patruno, R., Luposella, M., Zizzo, N., et al. (2018)

- C-Kit receptor and tryptase expressing mast cells correlate with angiogenesis in breast cancer patients. *Oncotarget*. 9 (8), 7918–7927.
- [207] Vliagoftis, H., Worobec, A.S., and Metcalfe, D.D. (1997) The protooncogene c-kit and c-kit ligand in human disease. *Journal of Allergy and Clinical Immunology*. 100 (4), 435–440.
- [208] van Panhuys, N., Prout, M., Forbes, E., Min, B., Paul, W.E., and Le Gros, G. (2011) Basophils Are the Major Producers of IL-4 during Primary Helminth Infection. *The Journal of Immunology*. 186 (5), 2719–2728.
- [209] Italiani, P. and Boraschi, D. (2014) From monocytes to M1/M2 macrophages: Phenotypical vs. functional differentiation. *Frontiers in Immunology*. 5 (OCT), 514.
- [210] Parihar, A., Eubank, T.D., and Doseff, A.I. (2010) Monocytes and macrophages regulate immunity through dynamic networks of survival and cell death. *Journal of Innate Immunity*. 2 (3), 204–215.
- [211] Khare, S., Dorfleutner, A., Bryan, N.B., Yun, C., Radian, A.D., de Almeida, L., et al. (2012) An NLRP7-Containing Inflammasome Mediates Recognition of Microbial Lipopeptides in Human Macrophages. *Immunity*. 36 (3), 464–476.
- [212] Hughes, C.E., Benson, R.A., Bedaj, M., and Maffia, P. (2016) Antigen-presenting cells and antigen presentation in tertiary lymphoid organs. *Frontiers in Immunology*. 7 (NOV), 481.
- [213] Shi, C. and Pamer, E.G. (2011) Monocyte recruitment during infection and inflammation. *Nature Reviews Immunology*. 11 (11), 762–774.
- [214] Laskin, D.L., Sunil, V.R., Gardner, C.R., and Laskin, J.D. (2011) Macrophages and tissue injury: Agents of defense or destruction? *Annual Review of Pharmacology and Toxicology*. 51 267–288.
- [215] Chávez-Galán, L., Olleros, M.L., Vesin, D., and Garcia, I. (2015) Much more than M1 and M2 macrophages, there are also CD169+ and TCR+ macrophages. *Frontiers in Immunology*. 6 (MAY), 263.
- [216] Rath, M., Müller, I., Kropf, P., Closs, E.I., and Munder, M. (2014) Metabolism via arginase or nitric oxide synthase: Two competing arginine pathways in macrophages. *Frontiers in Immunology*. 5 (OCT), 532.
- [217] Alberts Bruce, Johnson Alexander, Lewis Julian, Raff Martin, Roberts Keith, and Walter Peter (2002) Helper T Cells and Lymphocyte Activation - Molecular Biology of the Cell - NCBI

Bookshelf. *Molecular Biology of the Cell*.

- [218] Mantovani, A., Schioppa, T., Porta, C., Allavena, P., and Sica, A. (2006) Role of tumor-associated macrophages in tumor progression and invasion. *Cancer and Metastasis Reviews*. 25 (3), 315–322.
- [219] Mantovani, A., Marchesi, F., Malesci, A., Laghi, L., and Allavena, P. (2017) Tumour-associated macrophages as treatment targets in oncology. *Nature Reviews Clinical Oncology*. 14 (7), 399–416.
- [220] Atri, C., Guerfali, F.Z., and Laouini, D. (2018) Role of human macrophage polarization in inflammation during infectious diseases. *International Journal of Molecular Sciences*. 19 (6),.
- [221] Yang, Z. and Ming, X.F. (2014) Functions of arginase isoforms in macrophage inflammatory responses: Impact on cardiovascular diseases and metabolic disorders. *Frontiers in Immunology*. 5 (OCT),.
- [222] Qi, L., Yu, H., Zhang, Y., Zhao, D., Lv, P., Zhong, Y., et al. (2016) IL-10 secreted by M2 macrophage promoted tumorigenesis through interaction with JAK2 in glioma. *Oncotarget*. 7 (44), 71673–71685.
- [223] Couper, K.N., Blount, D.G., and Riley, E.M. (2008) IL-10: The Master Regulator of Immunity to Infection. *The Journal of Immunology*. 180 (9), 5771–5777.
- [224] Iyer, S.S. and Cheng, G. (2012) Role of interleukin 10 transcriptional regulation in inflammation and autoimmune disease. *Critical Reviews in Immunology*. 32 (1), 23–63.
- [225] Xu, Z.J., Gu, Y., Wang, C.Z., Jin, Y., Wen, X.M., Ma, J.C., et al. (2020) The M2 macrophage marker CD206: a novel prognostic indicator for acute myeloid leukemia. *OncolImmunology*. 9 (1),.
- [226] Feinberg, H., Jégouzo, S.A.F., Lasanajak, Y., Smith, D.F., Drickamer, K., Weis, W.I., et al. (2021) Structural analysis of carbohydrate binding by the macrophage mannose receptor CD206. *Journal of Biological Chemistry*. 296.
- [227] van der Zande, H.J.P., Nitsche, D., Schlautmann, L., Guigas, B., and Burgdorf, S. (2021) The Mannose Receptor: From Endocytic Receptor and Biomarker to Regulator of (Meta)Inflammation. *Frontiers in Immunology*. 12 4274.
- [228] Chen, Y., Song, Y., Du, W., Gong, L., Chang, H., and Zou, Z. (2019) Tumor-associated macrophages: an accomplice in solid tumor progression. *Journal of Biomedical Science 2019*

26:1. 26 (1), 1–13.

- [229] Schraml, B.U. and Reis e Sousa, C. (2015) Defining dendritic cells. *Current Opinion in Immunology*. 32 13–20.
- [230] Gottschalk, C. and Kurts, C. (2015) The debate about dendritic cells and macrophages in the kidney. *Frontiers in Immunology*. 6 (SEP), 435.
- [231] Erwig, L.P., McPhillips, K.A., Wynes, M.W., Ivetic, A., Ridley, A.J., and Henson, P.M. (2006) Differential regulation of phagosome maturation in macrophages and dendritic cells mediated by Rho GTPases and ezrin-radixin-moesin (ERM) proteins. *Proceedings of the National Academy of Sciences of the United States of America*. 103 (34), 12825–12830.
- [232] Janeway, C.A. and Medzhitov, R. (2002) Innate immune recognition. *Annual Review of Immunology*. 20 197–216.
- [233] Savina, A. and Amigorena, S. (2007) Phagocytosis and antigen presentation in dendritic cells. *Immunological Reviews*. 219 (1), 143–156.
- [234] Wu, H., Li, X., Zhou, C., Yu, Q., Ge, S., Pan, Z., et al. (2021) Circulating mature dendritic cells homing to the thymus promote thymic epithelial cells involution via the Jagged1/Notch3 axis. *Cell Death Discovery*. 7 (1), 1–10.
- [235] Banchereau, J., Briere, F., Caux, C., Davoust, J., Lebecque, S., Liu, Y.J., et al. (2000) Immunobiology of dendritic cells. *Annual Review of Immunology*. 18 767–811.
- [236] Bruce Sundstrom, J. and Ansari, A. (1995) Comparative study of the role of professional versus semiprofessional or nonprofessional antigen presenting cells in the rejection of vascularized organ allografts. *Transplant Immunology*. 3 (4), 273–289.
- [237] Martín-Fontecha, A., Lanzavecchia, A., and Sallusto, F. (2009) Dendritic cell migration to peripheral lymph nodes. *Handbook of Experimental Pharmacology*. 188 (188), 31–49.
- [238] Lundberg, K., Rydnert, F., Greiff, L., and Lindstedt, M. (2014) Human blood dendritic cell subsets exhibit discriminative pattern recognition receptor profiles. *Immunology*. 142 (2), 279–288.
- [239] ten Broeke, T., Wubbolts, R., and Stoorvogel, W. (2013) MHC Class II Antigen Presentation by Dendritic Cells Regulated through Endosomal Sorting. *Cold Spring Harbor Perspectives in Biology*. 5 (12),.
- [240] Rahman, A., Tiwari, A., Narula, J., and Hickling, T. (2018) Importance of Feedback and

- Feedforward Loops to Adaptive Immune Response Modeling. *CPT: Pharmacometrics and Systems Pharmacology*. 7 (10), 621–628.
- [241] Lim, T.S., Goh, J.K.H., Mortellaro, A., Lim, C.T., Hämmerling, G.J., and Ricciardi-Castagnoli, P. (2012) CD80 and CD86 Differentially Regulate Mechanical Interactions of T-Cells with Antigen-Presenting Dendritic Cells and B-Cells. *PLoS ONE*. 7 (9), e45185.
- [242] Rudd, C.E., Taylor, A., and Schneider, H. (2009) CD28 and CTLA-4 coreceptor expression and signal transduction. *Immunological Reviews*. 229 (1), 12–26.
- [243] Hasegawa, H. and Matsumoto, T. (2018) Mechanisms of tolerance induction by dendritic cells in vivo. *Frontiers in Immunology*. 9 (FEB), 1.
- [244] Coquet, J.M., Ribot, J.C., Bąbala, N., Middendorp, S., van der Horst, G., Xiao, Y., et al. (2013) Epithelial and dendritic cells in the thymic medulla promote cd4+foxp3+ regulatory t cell development via the cd27-cd70 pathway. *Journal of Experimental Medicine*. 210 (4), 715–728.
- [245] Paul, S. and Lal, G. (2018) Development and Function of Natural Killer Cells and Its Importance in Cancer Immunotherapy. *Immunology: Immunotoxicology, Immunopathology, and Immunotherapy*. 1 (SEP), 117–140.
- [246] Paul, S. and Lal, G. (2017) The molecular mechanism of natural killer cells function and its importance in cancer immunotherapy. *Frontiers in Immunology*. 8 (SEP), 1124.
- [247] Vivier, E., Tomasello, E., Baratin, M., Walzer, T., and Ugolini, S. (2008) Functions of natural killer cells. *Nature Immunology*. 9 (5), 503–510.
- [248] Pegram, H.J., Andrews, D.M., Smyth, M.J., Darcy, P.K., and Kershaw, M.H. (2011) Activating and inhibitory receptors of natural killer cells. *Immunology and Cell Biology*. 89 (2), 216–224.
- [249] Chester, C., Fritsch, K., and Kohrt, H.E. (2015) Natural killer cell immunomodulation: Targeting activating, inhibitory, and co-stimulatory receptor signaling for cancer immunotherapy. *Frontiers in Immunology*. 6 (DEC), 601.
- [250] Krzewski, K. and Coligan, J.E. (2012) Human NK cell lytic granules and regulation of their exocytosis. *Frontiers in Immunology*. 3 (NOV), 335.
- [251] Voskoboinik, I., Whisstock, J.C., and Trapani, J.A. (2015) Perforin and granzymes: Function, dysfunction and human pathology. *Nature Reviews Immunology*. 15 (6), 388–400.
- [252] Osińska, I., Popko, K., and Demkow, U. (2014) Perforin: An important player in immune

- response. *Central European Journal of Immunology*. 39 (1), 109–115.
- [253] Trapani, J.A. (2001) Granzymes: a family of lymphocyte granule serine proteases. *Genome Biology*. 2 (12), reviews3014.1.
- [254] Goping, I.S., Barry, M., Liston, P., Sawchuk, T., Constantinescu, G., Michalak, K.M., et al. (2003) Granzyme B-Induced Apoptosis Requires Both Direct Caspase Activation and Relief of Caspase Inhibition. *Immunity*. 18 (3), 355–365.
- [255] Wu, C., Xue, Y., Wang, P., Lin, L., Liu, Q., Li, N., et al. (2014) IFN- γ Primes Macrophage Activation by Increasing Phosphatase and Tensin Homolog via Downregulation of miR-3473b. *The Journal of Immunology*. 193 (6), 3036–3044.
- [256] Arase, H., Arase, N., and Saito, T. (1996) Interferon γ production by natural killer (NK) cells and NK1.1+ T cells upon NKR-P1 cross-linking. *Journal of Experimental Medicine*. 183 (5), 2391–2396.
- [257] Belosevic, M., Davis, C.E., Meltzer, M.S., and Nacy, C.A. (1988) Regulation of activated macrophage antimicrobial activities: Identification of lymphokines that cooperate with IFN- γ for induction of resistance to infection. *Journal of Immunology*. 141 (3), 890–896.
- [258] Dzhagalov, I. and Phee, H. (2012) How to find your way through the thymus: A practical guide for aspiring T cells. *Cellular and Molecular Life Sciences*. 69 (5), 663–682.
- [259] Naparstek, Y., Holoshitz, J., Eisenstein, S., Reshef, T., Rappaport, S., Chemke, J., et al. (1982) Effector T lymphocyte line cells migrate to the thymus and persist there. *Nature*. 300 (5889), 262–264.
- [260] Vale, A.M. and Schroeder, H.W. (2010) Clinical consequences of defects in B-cell development. *Journal of Allergy and Clinical Immunology*. 125 (4), 778–787.
- [261] Twigg, H.L. (2005) Humoral immune defense (antibodies): Recent advances. *Proceedings of the American Thoracic Society*. 2 (5), 417–421.
- [262] Elgueta, R., De Vries, V.C., and Noelle, R.J. (2010) The immortality of humoral immunity. *Immunological Reviews*. 236 (1), 139–150.
- [263] Zlotoff, D.A. and Bhandoola, A. (2011) Hematopoietic progenitor migration to the adult thymus. *Annals of the New York Academy of Sciences*. 1217 (1), 122.
- [264] Sprent, J. (2005) Direct stimulation of naïve T cells by antigen-presenting cell vesicles. *Blood Cells, Molecules, and Diseases*. 35 (1), 17–20.

- [265] Tai, Y., Wang, Q., Korner, H., Zhang, L., and Wei, W. (2018) Molecular mechanisms of T cells activation by dendritic cells in autoimmune diseases. *Frontiers in Pharmacology*. 9 (JUN), 642.
- [266] Bevington, S.L., Cauchy, P., Withers, D.R., Lane, P.J.L., and Cockerill, P.N. (2017) T cell receptor and cytokine signaling can function at different stages to establish and maintain transcriptional memory and enable T helper cell differentiation. *Frontiers in Immunology*. 8 (MAR), 204.
- [267] Couture, A., Garnier, A., Docagne, F., Boyer, O., Vivien, D., Le-Mauff, B., et al. (2019) HLA-class II artificial antigen presenting cells in CD4⁺ T cell-based immunotherapy. *Frontiers in Immunology*. 10 (MAY), 1081.
- [268] Zhu, X. and Zhu, J. (2020) CD4 T helper cell subsets and related human immunological disorders. *International Journal of Molecular Sciences*. 21 (21), 1–26.
- [269] Lund, R.J., Chen, Z., Scheinin, J., and Lahesmaa, R. (2004) Early Target Genes of IL-12 and STAT4 Signaling in Th Cells. *The Journal of Immunology*. 172 (11), 6775–6782.
- [270] Park, W.R., Nakahira, M., Sugimoto, N., Bian, Y., Yashiro-Ohtani, Y., Zhou, X.Y., et al. (2004) A mechanism underlying STAT4-mediated up-regulation of IFN- γ induction in TCR-triggered T cells. *International Immunology*. 16 (2), 295–302.
- [271] Seif, F., Khoshmirasafa, M., Aazami, H., Mohsenzadegan, M., Sedighi, G., and Bahar, M. (2017) The role of JAK-STAT signaling pathway and its regulators in the fate of T helper cells. *Cell Communication and Signaling 2017 15:1*. 15 (1), 1–13.
- [272] Müller, E., Christopoulos, P.F., Halder, S., Lunde, A., Beraki, K., Speth, M., et al. (2017) Toll-like receptor ligands and interferon- γ synergize for induction of antitumor M1 macrophages. *Frontiers in Immunology*. 8 (OCT), 1383.
- [273] Huang, H., Hao, S., Li, F., Ye, Z., Yang, J., and Xiang, J. (2007) CD4⁺ Th1 cells promote CD8⁺ Tc1 cell survival, memory response, tumor localization and therapy by targeted delivery of interleukin 2 via acquired pMHC I complexes. *Immunology*. 120 (2), 148–159.
- [274] Fearon, E.R., Pardoll, D.M., Itaya, T., Golumbek, P., Levitsky, H.I., Simons, J.W., et al. (1990) Interleukin-2 production by tumor cells bypasses T helper function in the generation of an antitumor response. *Cell*. 60 (3), 397–403.
- [275] Paludan, S.R. (1998) Interleukin-4 and interferon- γ : The quintessence of a mutual antagonistic relationship. *Scandinavian Journal of Immunology*. 48 (5), 459–468.

- [276] Zhu, J., Guo, L., Min, B., Watson, C.J., Hu-Li, J., Young, H.A., et al. (2002) Growth factor independent-1 induced by IL-4 regulates Th2 cell proliferation. *Immunity*. 16 (5), 733–744.
- [277] Maier, E., Duschl, A., and Horejs-Hoeck, J. (2012) STAT6-dependent and -independent mechanisms in Th2 polarization. *European Journal of Immunology*. 42 (11), 2827–2833.
- [278] Junttila, I.S. (2018) Tuning the cytokine responses: An update on interleukin (IL)-4 and IL-13 receptor complexes. *Frontiers in Immunology*. 9 (JUN), 888.
- [279] Punnonen, J., Yssel, H., and De Vries, J.E. (1997) The relative contribution of IL-4 and IL-13 to human IgE synthesis induced by activated CD4+ or CD8+ T cells. *Journal of Allergy and Clinical Immunology*. 100 (6 Pt 1), 792–801.
- [280] Corren, J. (2011) Anti-interleukin-5 antibody therapy in asthma and allergies. *Current Opinion in Allergy and Clinical Immunology*. 11 (6), 565–570.
- [281] Qin, H., Wang, L., Feng, T., Elson, C.O., Niyongere, S.A., Lee, S.J., et al. (2009) TGF- β Promotes Th17 Cell Development through Inhibition of SOCS3. *The Journal of Immunology*. 183 (1), 97–105.
- [282] Waite, J.C. and Skokos, D. (2012) Th17 response and inflammatory autoimmune diseases. *International Journal of Inflammation*. 2012.
- [283] Zenobia, C. and Hajishengallis, G. (2015) Basic biology and role of interleukin-17 in immunity and inflammation. *Periodontology 2000*. 69 (1), 142–159.
- [284] Zelante, T., De Luca, A., D’Angelo, C., Moretti, S., and Romani, L. (2009) IL-17/Th17 in anti-fungal immunity: What’s new? *European Journal of Immunology*. 39 (3), 645–648.
- [285] Zambrano-Zaragoza, J.F., Romo-Martínez, E.J., Durán-Avelar, M.D.J., García-Magallanes, N., and Vibanco-Pérez, N. (2014) Th17 cells in autoimmune and infectious diseases. *International Journal of Inflammation*. 2014.
- [286] Kimura, A. and Kishimoto, T. (2010) IL-6: Regulator of Treg/Th17 balance. *European Journal of Immunology*. 40 (7), 1830–1835.
- [287] Veldhoen, M., Hocking, R.J., Atkins, C.J., Locksley, R.M., and Stockinger, B. (2006) TGF β in the context of an inflammatory cytokine milieu supports de novo differentiation of IL-17-producing T cells. *Immunity*. 24 (2), 179–189.
- [288] Mitra, S. and Leonard, W.J. (2018) Biology of IL-2 and its therapeutic modulation: Mechanisms and strategies. *Journal of Leukocyte Biology*. 103 (4), 643–655.

- [289] Ross, S.H. and Cantrell, D.A. (2018) Signaling and Function of Interleukin-2 in T Lymphocytes. *Annual Review of Immunology*. 36 411–433.
- [290] Ye, C., Brand, D., and Zheng, S.G. (2018) Targeting IL-2: an unexpected effect in treating immunological diseases. *Signal Transduction and Targeted Therapy*. 3 (1), 1–10.
- [291] Chinen, T., Kannan, A.K., Levine, A.G., Fan, X., Klein, U., Zheng, Y., et al. (2016) An essential role for the IL-2 receptor in T reg cell function. *Nature Immunology*. 17 (11), 1322–1333.
- [292] Pandiyan, P., Zheng, L., Ishihara, S., Reed, J., and Lenardo, M.J. (2007) CD4+CD25+Foxp3+ regulatory T cells induce cytokine deprivation-mediated apoptosis of effector CD4+ T cells. *Nature Immunology*. 8 (12), 1353–1362.
- [293] de la Rosa, M., Rutz, S., Dorninger, H., and Scheffold, A. (2004) Interleukin-2 is essential for CD4+CD25+ regulatory T cell function. *European Journal of Immunology*. 34 (9), 2480–2488.
- [294] Kim, C.H. (2009) FOXP3 and its role in the immune system. *Advances in Experimental Medicine and Biology*. 665 17–29.
- [295] Taylor, A., Verhagen, J., Blaser, K., Akdis, M., and Akdis, C.A. (2006) Mechanisms of immune suppression by interleukin-10 and transforming growth factor- β : The role of T regulatory cells. *Immunology*. 117 (4), 433–442.
- [296] Ng, T.H.S., Britton, G.J., Hill, E. V., Verhagen, J., Burton, B.R., and Wraith, D.C. (2013) Regulation of adaptive immunity; the role of interleukin-10. *Frontiers in Immunology*. 4 (MAY), 129.
- [297] Shouval, D.S., Ouahed, J., Biswas, A., Goettel, J.A., Horwitz, B.H., Klein, C., et al. (2014) Interleukin 10 receptor signaling: Master regulator of intestinal mucosal homeostasis in mice and humans. *Advances in Immunology*. 122 177–210.
- [298] Berlato, C., Cassatella, M.A., Kinjyo, I., Gatto, L., Yoshimura, A., and Bazzoni, F. (2002) Involvement of Suppressor of Cytokine Signaling-3 as a Mediator of the Inhibitory Effects of IL-10 on Lipopolysaccharide-Induced Macrophage Activation. *The Journal of Immunology*. 168 (12), 6404–6411.
- [299] Hutchins, A.P., Diez, D., and Miranda-Saavedra, D. (2013) The IL-10/STAT3-mediated anti-inflammatory response: Recent developments and future challenges. *Briefings in Functional Genomics*. 12 (6), 489–498.
- [300] Raskov, H., Orhan, A., Christensen, J.P., and Gögenur, I. (2021) Cytotoxic CD8+ T cells in

- cancer and cancer immunotherapy. *British Journal of Cancer*. 124 (2), 359–367.
- [301] Zhang, N. and Bevan, M.J. (2011) CD8+ T Cells: Foot Soldiers of the Immune System. *Immunity*. 35 (2), 161–168.
- [302] Rosenberg, J. and Huang, J. (2018) CD8+ T Cells and NK Cells: Parallel and Complementary Soldiers of Immunotherapy. *Current Opinion in Chemical Engineering*. 19 9.
- [303] Sigal, L.J. (2016) Activation of CD8 T Lymphocytes during Viral Infections. *Encyclopedia of Immunobiology*. 4 286.
- [304] Fuse, S., Obar, J.J., Bellfy, S., Leung, E.K., Zhang, W., and Usherwood, E.J. (2006) CD80 and CD86 Control Antiviral CD8 + T-Cell Function and Immune Surveillance of Murine Gammaherpesvirus 68 . *Journal of Virology*. 80 (18), 9159–9170.
- [305] Curtsinger, J.M., Johnson, C.M., and Mescher, M.F. (2003) CD8 T Cell Clonal Expansion and Development of Effector Function Require Prolonged Exposure to Antigen, Costimulation, and Signal 3 Cytokine. *The Journal of Immunology*. 171 (10), 5165–5171.
- [306] Davis, L.C., Morgan, A.J., Chen, J.L., Snead, C.M., Bloor-Young, D., Shenderov, E., et al. (2012) NAADP Activates two-pore channels on t cell cytolytic granules to stimulate exocytosis and killing. *Current Biology*. 22 (24), 2331–2337.
- [307] Liu, J., Ye, Y., and Cai, L. (2020) Supramolecular attack particle: the way cytotoxic T lymphocytes kill target cells. *Signal Transduction and Targeted Therapy*. 5 (1), 1–2.
- [308] Cartwright, A.N.R., Suo, S., Badrinath, S., Kumar, S., Melms, J., Luoma, A., et al. (2021) Immunosuppressive myeloid cells induce nitric oxide-dependent DNA damage and p53 pathway activation in CD8 β T cells. *Cancer Immunology Research*. 9 (4), 470–485.
- [309] Volpe, E., Sambucci, M., Battistini, L., and Borsellino, G. (2016) Fas-fas ligand: Checkpoint of t cell functions in multiple sclerosis. *Frontiers in Immunology*. 7 (SEP), 382.
- [310] Cooper, M.D. (2015) The early history of B cells. *Nature Reviews Immunology*. 15 (3), 191–197.
- [311] Lebien, T.W. and Tedder, T.F. (2008) B lymphocytes: How they develop and function. *Blood*. 112 (5), 1570–1580.
- [312] Janeway, C.A.J., Travers, P., and Walport, M. (2001) The generation of diversity in immunoglobulins. *Immunobiology: The Immune System in Health and Disease. 5th Edition*. 1–11.

- [313] Roth, D.B. (2014) V(D)J Recombination: Mechanism, Errors, and Fidelity. *Microbiology Spectrum*. 2 (6),.
- [314] Yam-Puc, J.C., Toellner, K.M., Zhang, L., and Zhang, Y. (2018) Role of B-cell receptors for B-cell development and antigen-induced differentiation. *F1000Research*. 7.
- [315] Hardy, R.R. and Hayakawa, K. (2001) B cell development pathways. *Annual Review of Immunology*. 19 595–621.
- [316] Woyach, J.A., Johnson, A.J., and Byrd, J.C. (2012) The B-cell receptor signaling pathway as a therapeutic target in CLL. *Blood*. 120 (6), 1175–1184.
- [317] Lanzavecchia, A. (1990) Receptor-mediated antigen uptake and its effect on antigen presentation to class II-restricted T lymphocytes. *Annual Review of Immunology*. 8 773–793.
- [318] Kim, Y.M., Pan, J.Y.J., Korbel, G.A., Peperzak, V., Boes, M., and Ploegh, H.L. (2006) Monovalent ligation of the B cell receptor induces receptor activation but fails to promote antigen presentation. *Proceedings of the National Academy of Sciences of the United States of America*. 103 (9), 3327–3332.
- [319] Quezada, S.A., Jarvinen, L.Z., Lind, E.F., and Noelle, R.J. (2004) CD40/CD154 interactions at the interface of tolerance and immunity. *Annual Review of Immunology*. 22 307–328.
- [320] Balagué, O. and Martínez, A. (2015) What is a plasmablast? A commentary to: “Plasmablastic lymphoma versus diffuse large B-cell lymphoma with plasmablastic differentiation: proposal for a novel diagnostic scoring system” by Sonja Catharina Boy et al., *J. Hematopathol* 2015. *Journal of Hematopathology* 2015 8:2. 8 (2), 51–52.
- [321] Gonzalez, H., Hagerling, C., and Werb, Z. (2018) Roles of the immune system in cancer: From tumor initiation to metastatic progression. *Genes and Development*. 32 (19–20), 1267–1284.
- [322] Balkwill, F. and Mantovani, A. (2001) Inflammation and cancer: Back to Virchow? *Lancet*. 357 (9255), 539–545.
- [323] Blankenstein, T., Coulie, P.G., Gilboa, E., and Jaffee, E.M. (2012) The determinants of tumour immunogenicity. *Nature Reviews Cancer*. 12 (4), 307–313.
- [324] Labani-Motlagh, A., Ashja-Mahdavi, M., and Loskog, A. (2020) The Tumor Microenvironment: A Milieu Hindering and Obstructing Antitumor Immune Responses. *Frontiers in Immunology*. 11 940.
- [325] Vitale, I., Manic, G., Coussens, L.M., Kroemer, G., and Galluzzi, L. (2019) Macrophages and

Metabolism in the Tumor Microenvironment. *Cell Metabolism*. 30 (1), 36–50.

- [326] Bates, J.P., Derakhshandeh, R., Jones, L., and Webb, T.J. (2018) Mechanisms of immune evasion in breast cancer. *BMC Cancer*. 18 (1), 1–14.
- [327] Lindau, D., Gielen, P., Kroesen, M., Wesseling, P., and Adema, G.J. (2013) The immunosuppressive tumour network: myeloid-derived suppressor cells, regulatory T cells and natural killer T cells. *Immunology*. 138 (2), 105.
- [328] Ohue, Y. and Nishikawa, H. (2019) Regulatory T (Treg) cells in cancer: Can Treg cells be a new therapeutic target? *Cancer Science*. 110 (7), 2080–2089.
- [329] Fridman, W.H., Pagès, F., Sautès-Fridman, C., and Galon, J. (2012) The immune contexture in human tumours: impact on clinical outcome. *Nature Reviews. Cancer*. 12 (4), 298–306.
- [330] Bates, G.J., Fox, S.B., Han, C., Leek, R.D., Garcia, J.F., Harris, A.L., et al. (2006) Quantification of regulatory T cells enables the identification of high-risk breast cancer patients and those at risk of late relapse. *Journal of Clinical Oncology*. 24 (34), 5373–5380.
- [331] Sheikhpour, E., Noorbakhsh, P., Foroughi, E., Farahnak, S., Nasiri, R., and Neamatzadeh, H. (2017) A survey on the role of interleukin-10 in breast cancer: A narrative. *Reports of Biochemistry and Molecular Biology*. 7 (1), 30–37.
- [332] Hubo, M., Trinschek, B., Kryczanowsky, F., Tuettenberg, A., Steinbrink, K., and Jonuleit, H. (2013) Costimulatory molecules on immunogenic versus tolerogenic human dendritic cells. *Frontiers in Immunology*. 4 (APR), 82.
- [333] Dennis, K.L., Blatner, N.R., Gounari, F., and Khazaie, K. (2013) Current status of interleukin-10 and regulatory T-cells in cancer. *Current Opinion in Oncology*. 25 (6), 637–645.
- [334] Romano, M., Fanelli, G., Albany, C.J., Giganti, G., and Lombardi, G. (2019) Past, present, and future of regulatory T cell therapy in transplantation and autoimmunity. *Frontiers in Immunology*. 10 (JAN), 43.
- [335] Walker, L.S.K. (2013) Treg and CTLA-4: Two intertwining pathways to immune tolerance. *Journal of Autoimmunity*. 45 (100), 49.
- [336] Zhao, S., Zhang, L., Xiang, S., Hu, Y., Wu, Z., and Shen, J. (2022) Gnawing Between Cells and Cells in the Immune System: Friend or Foe? A Review of Trogocytosis. *Frontiers in Immunology*. 13 239.
- [337] Tekguc, M., Wing, J.B., Osaki, M., Long, J., and Sakaguchi, S. (2021) Treg-expressed CTLA-4

- depletes CD80/CD86 by trogocytosis, releasing free PD-L1 on antigen-presenting cells. *Proceedings of the National Academy of Sciences of the United States of America*. 118 (30),.
- [338] Veglia, F., Sanseviero, E., and Gabrilovich, D.I. (2021) Myeloid-derived suppressor cells in the era of increasing myeloid cell diversity. *Nature Reviews Immunology* 21:8. 21 (8), 485–498.
- [339] Talmadge, J.E. and Gabrilovich, D.I. (2013) History of myeloid-derived suppressor cells. *Nature Reviews Cancer*. 13 (10), 739–752.
- [340] Law, A.M.K., Valdes-Mora, F., and Gallego-Ortega, D. (2020) Myeloid-Derived Suppressor Cells as a Therapeutic Target for Cancer. *Cells*. 9 (3),.
- [341] Casbon, A.J., Reynau, D., Park, C., Khu, E., Gan, D.D., Schepers, K., et al. (2015) Invasive breast cancer reprograms early myeloid differentiation in the bone marrow to generate immunosuppressive neutrophils. *Proceedings of the National Academy of Sciences of the United States of America*. 112 (6), E566–E575.
- [342] Ferrer, G., Jung, B., Chiu, P.Y., Aslam, R., Palacios, F., Mazzarello, A.N., et al. (2021) Myeloid-derived suppressor cell subtypes differentially influence T-cell function, T-helper subset differentiation, and clinical course in CLL. *Leukemia* 2021 35:11. 35 (11), 3163–3175.
- [343] De Cicco, P., Ercolano, G., and Ianaro, A. (2020) The New Era of Cancer Immunotherapy: Targeting Myeloid-Derived Suppressor Cells to Overcome Immune Evasion. *Frontiers in Immunology*. 11 1680.
- [344] Pan, Y., Yu, Y., Wang, X., and Zhang, T. (2020) Tumor-Associated Macrophages in Tumor Immunity. *Frontiers in Immunology*. 11 3151.
- [345] Van Dyken, S.J. and Locksley, R.M. (2013) Interleukin-4-and interleukin-13-mediated alternatively activated macrophages: Roles in homeostasis and disease. *Annual Review of Immunology*. 31 317–343.
- [346] Jayasingam, S.D., Citartan, M., Thang, T.H., Mat Zin, A.A., Ang, K.C., and Ch'ng, E.S. (2020) Evaluating the Polarization of Tumor-Associated Macrophages Into M1 and M2 Phenotypes in Human Cancer Tissue: Technicalities and Challenges in Routine Clinical Practice. *Frontiers in Oncology*. 9.
- [347] Ma, X., Gao, Y., Chen, Y., Liu, J., Yang, C., Bao, C., et al. (2021) M2-type macrophages induce tregs generation by activating the $\text{tgf-}\beta$ /smad signalling pathway to promote colorectal cancer development. *OncoTargets and Therapy*. 14 5391–5402.

- [348] Zuazo-Gatzelu, I. and Casanovas, O. (2018) Unraveling the role of angiogenesis in cancer ecosystems. *Frontiers in Oncology*. 8 (JUL), 248.
- [349] Lin, L., Chen, Y.S., Yao, Y.D., Chen, J.Q., Chen, J.N., Huang, S.Y., et al. (2015) CCL18 from tumor-associated macrophages promotes angiogenesis in breast cancer. *Oncotarget*. 6 (33), 34758.
- [350] Liu, T., Han, C., Wang, S., Fang, P., Ma, Z., Xu, L., et al. (2019) Cancer-associated fibroblasts: An emerging target of anti-cancer immunotherapy. *Journal of Hematology and Oncology*. 12 (1), 1–15.
- [351] Wu, H.J., Hao, M., Yeo, S.K., and Guan, J.L. (2020) FAK signaling in cancer-associated fibroblasts promotes breast cancer cell migration and metastasis by exosomal miRNAs-mediated intercellular communication. *Oncogene*. 39 (12), 2539–2549.
- [352] Chen, Y., Zhang, S., Wang, Q., and Zhang, X. (2017) Tumor-recruited M2 macrophages promote gastric and breast cancer metastasis via M2 macrophage-secreted CHI3L1 protein. *Journal of Hematology and Oncology*. 10 (1), 1–13.
- [353] Fujisawa, T., Joshi, B.H., and Puri, R.K. (2012) IL-13 regulates cancer invasion and metastasis through IL-13R α 2 via ERK/AP-1 pathway in mouse model of human ovarian cancer. *International Journal of Cancer*. 131 (2), 344–356.
- [354] Maciel, T.T., Moura, I.C., and Hermine, O. (2015) The role of mast cells in cancers. *F1000Prime Reports*. 7.
- [355] Nonomura, N., Takayama, H., Nishimura, K., Oka, D., Nakai, Y., Shiba, M., et al. (2007) Decreased number of mast cells infiltrating into needle biopsy specimens leads to a better prognosis of prostate cancer. *British Journal of Cancer*. 97 (7), 952–956.
- [356] Strouch, M.J., Cheon, E.C., Salabat, M.R., Krantz, S.B., Gounaris, E., Melstrom, L.G., et al. (2010) Crosstalk between mast cells and pancreatic cancer cells contributes to pancreatic tumor progression. *Clinical Cancer Research*. 16 (8), 2257–2265.
- [357] Ribatti, D., Annese, T., and Tamma, R. (2021) Controversial role of mast cells in breast cancer tumor progression and angiogenesis. *Clinical Breast Cancer*. 21 (6), 486–491.
- [358] Galli, S.J., Tsai, M., Wershil, B.K., Tama, S.Y., and Costa, J.J. (1995) Regulation of mouse and human mast cell development, survival and function by stem cell factor, the ligand for the c-kit receptor. *International Archives of Allergy and Immunology*. 107 (1–3), 51–53.

- [359] Huang, B., Lei, Z., Zhang, G.M., Li, D., Song, C., Li, B., et al. (2008) SCF-mediated mast cell infiltration and activation exacerbate the inflammation and immunosuppression in tumor microenvironment. *Blood*. 112 (4), 1269–1279.
- [360] Saleem, S.J., Martin, R.K., Morales, J.K., Sturgill, J.L., Gibb, D.R., Graham, L., et al. (2012) Mast cells critically augment myeloid derived suppressor cell activity. *Journal of Immunology (Baltimore, Md. : 1950)*. 189 (2), 511.
- [361] Yang, Z., Zhang, B., Li, D., Lv, M., Huang, C., Shen, G.X., et al. (2010) Mast cells mobilize myeloid-derived suppressor cells and Treg cells in tumor microenvironment via IL-17 pathway in murine hepatocarcinoma model. *PLoS ONE*. 5 (1), e8922.
- [362] Cheon, E.C., Khazaie, K., Khan, M.W., Strouch, M.J., Krantz, S.B., Phillips, J., et al. (2011) Mast cell 5-lipoxygenase activity promotes intestinal polyposis in APC Δ 468 mice. *Cancer Research*. 71 (5), 1627–1636.
- [363] Aponte-López, A., Fuentes-Pananá, E.M., Cortes-Muñoz, D., and Muñoz-Cruz, S. (2018) Mast Cell, the Neglected Member of the Tumor Microenvironment: Role in Breast Cancer. *Journal of Immunology Research*. 2018 1–11.
- [364] Meng Xiang, Yiping Gu, Fengdi Zhao, Hong Lu, Sifeng Chen, L.Y. (2010) Mast cell tryptase promotes breast cancer migration and invasion. *Oncology Reports*. 23 (3),.
- [365] Jezierska, A. and Motyl, T. (2009) Matrix metalloproteinase-2 involvement in breast cancer progression: A mini-review. *Medical Science Monitor*. 15 (2), RA32-40.
- [366] He, L., Zhu, Z., Chen, S., Wang, Y., and Gu, H. (2016) Mammary tumor growth and metastasis are reduced in c-Kit mutant Sash mice. *Cancer Medicine*. 5 (6), 1292–1297.
- [367] Uzhachenko, R. V. and Shanker, A. (2019) CD8+ T lymphocyte and NK cell network: Circuitry in the cytotoxic domain of immunity. *Frontiers in Immunology*. 10 (AUG), 1906.
- [368] Brennan, A.J., Chia, J., Browne, K.A., Ciccone, A., Ellis, S., Lopez, J.A., et al. (2011) Protection from Endogenous Perforin: Glycans and the C Terminus Regulate Exocytic Trafficking in Cytotoxic Lymphocytes. *Immunity*. 34 (6), 879–892.
- [369] Kabanova, A., Zurli, V., and Baldari, C.T. (2018) Signals controlling lytic granule polarization at the cytotoxic immune synapse. *Frontiers in Immunology*. 9 (FEB), 307.
- [370] Topham, N.J. and Hewitt, E.W. (2009) Natural killer cell cytotoxicity: How do they pull the trigger? *Immunology*. 128 (1), 7–15.

- [371] Sconocchia, G., Eppenberger, S., Spagnoli, G.C., Tornillo, L., Drosner, R., Caratelli, S., et al. (2014) Nk cells and T cells cooperate during the clinical course of colorectal cancer. *Onc Immunology*. 3 (8), 1–6.
- [372] Ascierto, M.L., Idowu, M.O., Zhao, Y., Khalak, H., Payne, K.K., Wang, X.Y., et al. (2013) Molecular signatures mostly associated with NK cells are predictive of relapse free survival in breast cancer patients. *Journal of Translational Medicine*. 11 (1), 1–11.
- [373] Pasero, C., Gravis, G., Granjeaud, S., Guerin, M., Thomassin-Piana, J., Rocchi, P., et al. (2015) Highly effective NK cells are associated with good prognosis in patients with metastatic prostate cancer. *Oncotarget*. 6 (16), 14360–14373.
- [374] Henriksen, J.R., Donskov, F., Waldstrøm, M., Jakobsen, A., Hjortkjaer, M., Petersen, C.B., et al. (2020) Favorable prognostic impact of Natural Killer cells and T cells in high-grade serous ovarian carcinoma. *Acta Oncologica*. 59 (6), 652–659.
- [375] Wilgenhof, S., Corthals, J., Heirman, C., Van Baren, N., Lucas, S., Kvistborg, P., et al. (2016) Phase II Study of Autologous Monocyte-Derived mRNA Electroporated Dendritic Cells (TriMixDC-MEL) Plus Ipilimumab in Patients With Pretreated Advanced Melanoma. *Journal of Clinical Oncology : Official Journal of the American Society of Clinical Oncology*. 34 (12), 1330–1338.
- [376] Liao, L.M., Ashkan, K., Tran, D.D., Campian, J.L., Trusheim, J.E., Cobbs, C.S., et al. (2018) First results on survival from a large Phase 3 clinical trial of an autologous dendritic cell vaccine in newly diagnosed glioblastoma. *Journal of Translational Medicine*. 16 (1), 1.
- [377] Aminin, D. and Wang, Y.M. (2021) Macrophages as a “weapon” in anticancer cellular immunotherapy. *The Kaohsiung Journal of Medical Sciences*. 37 (9), 749–758.
- [378] Liu, J., Geng, X., Hou, J., and Wu, G. (2021) New insights into M1/M2 macrophages: key modulators in cancer progression. *Cancer Cell International*. 21 (1), 1–7.
- [379] Mills, C.D. and Ley, K. (2014) M1 and M2 Macrophages: The Chicken and the Egg of Immunity. *Journal of Innate Immunity*. 6 (6), 716.
- [380] Guerriero, J.L. (2019) Macrophages: Their Untold Story in T Cell Activation and Function. *International Review of Cell and Molecular Biology*. 342 73–93.
- [381] Haabeth, O.A.W., Lorvik, K.B., Hammarström, C., Donaldson, I.M., Haraldsen, G., Bogen, B., et al. (2011) Inflammation driven by tumour-specific Th1 cells protects against B-cell cancer. *Nature Communications* 2011 2:1. 2 (1), 1–12.

- [382] Jorgovanovic, D., Song, M., Wang, L., and Zhang, Y. (2020) Roles of IFN- γ in tumor progression and regression: a review. *Biomarker Research* 2020 8:1. 8 (1), 1–16.
- [383] Klimp, A.H., De Vries, E.G.E., Scherphof, G.L., and Daemen, T. (2002) A potential role of macrophage activation in the treatment of cancer. *Critical Reviews in Oncology/Hematology*. 44 (2), 143–161.
- [384] Kennel, K.B. and Greten, F.R. (2021) Immune cell - produced ROS and their impact on tumor growth and metastasis. *Redox Biology*. 42 101891.
- [385] Liou, G.Y. and Storz, P. (2010) Reactive oxygen species in cancer. *Free Radical Research*. 44 (5), 479–496.
- [386] He, X. and Xu, C. (2020) Immune checkpoint signaling and cancer immunotherapy. *Cell Research* 2020 30:8. 30 (8), 660–669.
- [387] Gattinoni, L., Ranganathan, A., Surman, D.R., Palmer, D.C., Antony, P.A., Theoret, M.R., et al. (2006) CTLA-4 dysregulation of self/tumor-reactive CD8+ T-cell function is CD4+ T-cell dependent. *Blood*. 108 (12), 3818.
- [388] Han, Y., Liu, D., and Li, L. (2020) PD-1/PD-L1 pathway: current researches in cancer. *American Journal of Cancer Research*. 10 (3), 727–742.
- [389] Salmaninejad, A., Khoramshahi, V., Azani, A., Soltaninejad, E., Aslani, S., Zamani, M.R., et al. (2018) PD-1 and cancer: molecular mechanisms and polymorphisms. *Immunogenetics*. 70 (2), 73–86.
- [390] Zhang, Y. and Zhang, Z. (2020) The history and advances in cancer immunotherapy: understanding the characteristics of tumor-infiltrating immune cells and their therapeutic implications. *Cellular and Molecular Immunology*. 17 (8), 807–821.
- [391] Leach, D.R., Krummel, M.F., and Allison, J.P. (1996) Enhancement of antitumor immunity by CTLA-4 blockade. *Science*. 271 (5256), 1734–1736.
- [392] Hodi, F.S., O'Day, S.J., McDermott, D.F., Weber, R.W., Sosman, J.A., Haanen, J.B., et al. (2010) Improved survival with ipilimumab in patients with metastatic melanoma. *The New England Journal of Medicine*. 363 (8), 711–723.
- [393] Seidel, J.A., Otsuka, A., and Kabashima, K. (2018) Anti-PD-1 and Anti-CTLA-4 Therapies in Cancer: Mechanisms of Action, Efficacy, and Limitations. *Frontiers in Oncology*. 8 (MAR), 86.
- [394] Ledford, H. (2011) Melanoma drug wins US approval. *Nature*. 471 (7340), 561.

- [395] Larkin, J., Chiarion-Sileni, V., Gonzalez, R., Grob, J.J., Cowey, C.L., Lao, C.D., et al. (2015) Combined Nivolumab and Ipilimumab or Monotherapy in Untreated Melanoma. *New England Journal of Medicine*. 373 (1), 23–34.
- [396] Denkert, C. (2014) The immunogenicity of breast cancer-molecular subtypes matter. *Annals of Oncology*. 25 (8), 1453–1455.
- [397] Zhao, J. and Huang, J. (2020) Breast cancer immunology and immunotherapy: Targeting the programmed cell death protein-1/programmed cell death protein ligand-1. *Chinese Medical Journal*. 133 (7), 853–862.
- [398] Castagnoli, L., Cancila, V., Cordoba-Romero, S.L., Faraci, S., Talarico, G., Belmonte, B., et al. (2019) WNT signaling modulates PD-L1 expression in the stem cell compartment of triple-negative breast cancer. *Oncogene*. 38 (21), 4047–4060.
- [399] Vikas, P., Borcherdig, N., and Zhang, W. (2018) The clinical promise of immunotherapy in triple-negative breast cancer. *Cancer Management and Research*. 10 6823–6833.
- [400] Kwapisz, D. (2021) Pembrolizumab and atezolizumab in triple-negative breast cancer. *Cancer Immunology, Immunotherapy*. 70 (3), 607–617.
- [401] Schmid, P., Cortes, J., Pusztai, L., McArthur, H., Kümmel, S., Bergh, J., et al. (2020) Pembrolizumab for Early Triple-Negative Breast Cancer. *New England Journal of Medicine*. 382 (9), 810–821.
- [402] Sender, R., Fuchs, S., and Milo, R. (2016) Revised Estimates for the Number of Human and Bacteria Cells in the Body. *PLOS Biology*. 14 (8), e1002533.
- [403] Hillman, E.T., Lu, H., Yao, T., and Nakatsu, C.H. (2017) Microbial Ecology along the Gastrointestinal Tract. *Microbes and Environments*. 32 (4), 300–313.
- [404] Tremaroli, V. and Bäckhed, F. (2012) Functional interactions between the gut microbiota and host metabolism. *Nature*. 489 (7415), 242–249.
- [405] Noh, C.-K., Kim, B.S., Hong, G., Cheong, J.Y., and Lee, K.J. (2018) Effects of the Administration of Probiotics on Fecal Microbiota Diversity and Composition in Healthy Individuals. *Journal of Neurogastroenterology and Motility*. 24 (3), 452–459.
- [406] Kau, A.L., Ahern, P.P., Griffin, N.W., Goodman, A.L., and Gordon, J.I. (2011) Human nutrition, the gut microbiome and the immune system. *Nature*. 474 (7351), 327–36.
- [407] Aagaard, K., Petrosino, J., Keitel, W., Watson, M., Katancik, J., Garcia, N., et al. (2013) The

Human Microbiome Project strategy for comprehensive sampling of the human microbiome and why it matters. *FASEB Journal*. 27 (3), 1012–1022.

- [408] Stinson, L.F., Boyce, M.C., Payne, M.S., and Keelan, J.A. (2019) The not-so-sterile womb: Evidence that the human fetus is exposed to bacteria prior to birth. *Frontiers in Microbiology*. 10 (JUN), 1124.
- [409] Aagaard, K., Ma, J., Antony, K.M., Ganu, R., Petrosino, J., and Versalovic, J. (2014) The placenta harbors a unique microbiome. *Science Translational Medicine*. 6 (237),.
- [410] Aagaard, K., Riehle, K., Ma, J., Segata, N., Mistretta, T.A., Coarfa, C., et al. (2012) A metagenomic approach to characterization of the vaginal microbiome signature in pregnancy. *PLoS ONE*. 7 (6),.
- [411] Dunn, A.B., Jordan, S., Baker, B.J., and Carlson, N.S. (2017) The Maternal Infant Microbiome: Considerations for Labor and Birth. *MCN The American Journal of Maternal/Child Nursing*. 42 (6), 318–325.
- [412] Wang, J. and Lin, L. (2021) Early-life gut microbiota development from maternal vertical transmission. *Gynecology and Obstetrics Clinical Medicine*. 1 (2), 79–82.
- [413] Martin, R., Nauta, A.J., Ben Amor, K., Knippels, L.M.J., Knol, J., and Garssen, J. (2010) Early life: Gut microbiota and immune development in infancy. *Beneficial Microbes*. 1 (4), 367–382.
- [414] Rodríguez, J.M., Murphy, K., Stanton, C., Ross, R.P., Kober, O.I., Juge, N., et al. (2015) The composition of the gut microbiota throughout life, with an emphasis on early life. *Microbial Ecology in Health & Disease*. 26 (0),.
- [415] Alcon-Giner, C., Dalby, M.J., Caim, S., Ketskemety, J., Shaw, A., Sim, K., et al. (2020) Microbiota Supplementation with Bifidobacterium and Lactobacillus Modifies the Preterm Infant Gut Microbiota and Metabolome: An Observational Study. *Cell Reports Medicine*. 1 (5), 100077.
- [416] Koenig, J.E., Spor, A., Scalfone, N., Fricker, A.D., Stombaugh, J., Knight, R., et al. (2011) Succession of microbial consortia in the developing infant gut microbiome. *Proceedings of the National Academy of Sciences of the United States of America*. 108 (SUPPL. 1), 4578–4585.
- [417] Sela, D.A., Chapman, J., Adeuya, A., Kim, J.H., Chen, F., Whitehead, T.R., et al. (2008) The genome sequence of *Bifidobacterium longum* subsp. *infantis* reveals adaptations for milk

utilization within the infant microbiome. *Proceedings of the National Academy of Sciences of the United States of America*. 105 (48), 18964–18969.

- [418] Yatsunencko, T., Rey, F.E., Manary, M.J., Trehan, I., Dominguez-Bello, M.G., Contreras, M., et al. (2012) Human gut microbiome viewed across age and geography. *Nature*. 486 (7402), 222–227.
- [419] Palmer, C., Bik, E.M., DiGiulio, D.B., Relman, D.A., and Brown, P.O. (2007) Development of the human infant intestinal microbiota. *PLoS Biology*. 5 (7), 1556–1573.
- [420] Shen, X., Wang, M., Zhang, X., He, M., Li, M., Cheng, G., et al. (2019) Dynamic construction of gut microbiota may influence allergic diseases of infants in Southwest China. *BMC Microbiology*. 19 (1), 1–13.
- [421] Dominguez-Bello, M.G., Costello, E.K., Contreras, M., Magris, M., Hidalgo, G., Fierer, N., et al. (2010) Delivery mode shapes the acquisition and structure of the initial microbiota across multiple body habitats in newborns. *Proceedings of the National Academy of Sciences of the United States of America*. 107 (26), 11971–11975.
- [422] Romano-Keeler, J. and Weitkamp, J.H. (2015) Maternal influences on fetal microbial colonization and immune development. *Pediatric Research*. 77 (1), 189–195.
- [423] Eck, A., Rutten, N.B.M.M., Singendonk, M.M.J., Rijkers, G.T., Savelkoul, P.H.M., Meijssen, C.B., et al. (2020) Neonatal microbiota development and the effect of early life antibiotics are determined by two distinct settler types. *PLoS ONE*. 15 (2),.
- [424] Laubereau, B., Filipiak-Pittroff, B., Von Berg, A., Grübl, A., Reinhardt, D., Wichmann, H.E., et al. (2004) Caesarean section and gastrointestinal symptoms, atopic dermatitis, and sensitisation during the first year of life. *Archives of Disease in Childhood*. 89 (11), 993–997.
- [425] Van Nimwegen, F.A., Penders, J., Stobberingh, E.E., Postma, D.S., Koppelman, G.H., Kerkhof, M., et al. (2011) Mode and place of delivery, gastrointestinal microbiota, and their influence on asthma and atopy. *Journal of Allergy and Clinical Immunology*. 128 (5), 948-955.e3.
- [426] Abrahamsson, T.R., Jakobsson, H.E., Andersson, A.F., Björkstén, B., Engstrand, L., and Jenmalm, M.C. (2014) Low gut microbiota diversity in early infancy precedes asthma at school age. *Clinical and Experimental Allergy*. 44 (6), 842–850.
- [427] Mosca, A., Leclerc, M., and Hugot, J.P. (2016) Gut microbiota diversity and human diseases: Should we reintroduce key predators in our ecosystem? *Frontiers in Microbiology*. 7 (MAR), 455.

- [428] Kriss, M., Hazleton, K.Z., Nusbacher, N.M., Martin, C.G., and Lozupone, C.A. (2018) Low diversity gut microbiota dysbiosis: drivers, functional implications and recovery. *Current Opinion in Microbiology*. 44 34–40.
- [429] Eckburg, P.B., Bik, E.M., Bernstein, C.N., Purdom, E., Dethlefsen, L., Sargent, M., et al. (2005) Diversity of the human intestinal microbial flora. *Science (New York, N.Y.)*. 308 (5728), 1635–8.
- [430] Engelbrektson, A., Kunin, V., Wrighton, K.C., Zvenigorodsky, N., Chen, F., Ochman, H., et al. (2010) Experimental factors affecting PCR-based estimates of microbial species richness and evenness. *The ISME Journal*. 4 (5), 642–647.
- [431] Cox, M.J., Cookson, W.O.C.M., and Moffatt, M.F. (2013) Sequencing the human microbiome in health and disease. *Human Molecular Genetics*. 22 (R1), R88–R94.
- [432] Magne, F., Gotteland, M., Gauthier, L., Zazueta, A., Pessoa, S., Navarrete, P., et al. (2020) The firmicutes/bacteroidetes ratio: A relevant marker of gut dysbiosis in obese patients? *Nutrients*. 12 (5), 1474.
- [433] Rios-Covian, D., Salazar, N., Gueimonde, M., and de los Reyes-Gavilan, C.G. (2017) Shaping the metabolism of intestinal Bacteroides population through diet to improve human health. *Frontiers in Microbiology*. 8 (MAR), 376.
- [434] Stojanov, S., Berlec, A., and Štrukelj, B. (2020) The influence of probiotics on the firmicutes/bacteroidetes ratio in the treatment of obesity and inflammatory bowel disease. *Microorganisms*. 8 (11), 1–16.
- [435] Koliada, A., Syzenko, G., Moseiko, V., Budovska, L., Puchkov, K., Perederiy, V., et al. (2017) Association between body mass index and Firmicutes/Bacteroidetes ratio in an adult Ukrainian population. *BMC Microbiology*. 17 (1),.
- [436] Sokol, H., Seksik, P., Furet, J.P., Firmesse, O., Nion-Larmurier, I., Beaugerie, L., et al. (2009) Low counts of faecalibacterium prausnitzii in colitis microbiota. *Inflammatory Bowel Diseases*. 15 (8), 1183–1189.
- [437] Candela, M., Biagi, E., Maccaferri, S., Turrone, S., and Brigidi, P. (2012) Intestinal microbiota is a plastic factor responding to environmental changes. *Trends in Microbiology*. 20 (8), 385–391.
- [438] Wen, L. and Duffy, A. (2017) Factors Influencing the Gut Microbiota, Inflammation, and Type 2 Diabetes. *The Journal of Nutrition*. 147 (7), 1468S-1475S.

- [439] Ursell, L.K., Clemente, J.C., Rideout, J.R., Gevers, D., Caporaso, J.G., and Knight, R. (2012) The interpersonal and intrapersonal diversity of human-associated microbiota in key body sites. *Journal of Allergy and Clinical Immunology*. 129 (5), 1204–1208.
- [440] Sommer, F., Anderson, J.M., Bharti, R., Raes, J., and Rosenstiel, P. (2017) The resilience of the intestinal microbiota influences health and disease. *Nature Reviews Microbiology*. 15 (10), 630–638.
- [441] Spellberg, B. (2008) Dr. William H. Stewart: Mistaken or maligned? *Clinical Infectious Diseases*. 47 (2), 294.
- [442] Ventola, C.L. (2015) The Antibiotic Resistance Crisis: Part 1: Causes and Threats. *Pharmacy and Therapeutics*. 40 (4), 277.
- [443] McNulty, C.A.M., Collin, S.M., Cooper, E., Lecky, D.M., and Butler, C.C. (2019) Public understanding and use of antibiotics in England: Findings from a household survey in 2017. *BMJ Open*. 9 (10), e030845.
- [444] Bakhit, M., Del Mar, C., Gibson, E., and Hoffmann, T. (2019) Exploring patients' understanding of antibiotic resistance and how this may influence attitudes towards antibiotic use for acute respiratory infections: A qualitative study in Australian general practice. *BMJ Open*. 9 (3), e026735.
- [445] Zhang, S., Chen, D.C., and Chen, L.M. (2019) Facing a new challenge: The adverse effects of antibiotics on gut microbiota and host immunity. *Chinese Medical Journal*. 132 (10), 1135–1138.
- [446] Dudek-Wicher, R.K., Junka, A., and Bartoszewicz, M. (2018) The influence of antibiotics and dietary components on gut microbiota. *Przegląd Gastroenterologiczny*. 13 (2), 85–92.
- [447] Qian, X., Yanagi, K., Kane, A. V., Alden, N., Lei, M., Snyderman, D.R., et al. (2020) Ridinilazole, a narrow spectrum antibiotic for treatment of *Clostridioides difficile* infection, enhances preservation of microbiota-dependent bile acids. *American Journal of Physiology - Gastrointestinal and Liver Physiology*. 319 (2), G227–G237.
- [448] Letten, A.D., Baumgartner, M., Pfrunder-Cardozo, K.R., Levine, J.M., and Hall, A.R. (2021) Human-associated microbiota suppress invading bacteria even under disruption by antibiotics. *ISME Journal*. 15 (9), 2809–2812.
- [449] Melander, R.J., Zurawski, D. V., and Melander, C. (2018) Narrow-spectrum antibacterial agents. *MedChemComm*. 9 (1), 12–21.

- [450] Grada, A. and Bunick, C.G. (2021) Spectrum of Antibiotic Activity and Its Relevance to the Microbiome. *JAMA Network Open*. 4 (4), e215357–e215357.
- [451] Peng, C., Zhang, T., Ortiz-Ortiz, D.N., Vishwakarma, A., Barton, H.A., and Joy, A. (2019) Modification of narrow-spectrum peptidomimetic polyurethanes with fatty acid chains confers broad-spectrum antibacterial activity. *Polymer International*. 68 (7), 1255–1262.
- [452] Cotter, P.D., Stanton, C., Ross, R.P., and Hill, C. (2012) The Impact of Antibiotics on the Gut Microbiota as Revealed by High Throughput DNA Sequencing. *Discovery Medicine*. 13 (70), 193–199.
- [453] Langdon, A., Crook, N., and Dantas, G. (2016) The effects of antibiotics on the microbiome throughout development and alternative approaches for therapeutic modulation. *Genome Medicine*. 8 (1),.
- [454] Lee, S.E., Lim, J.Y., Ryu, D. Bin, Kim, T.W., Park, S.S., Jeon, Y.W., et al. (2019) Alteration of the Intestinal Microbiota by Broad-Spectrum Antibiotic Use Correlates with the Occurrence of Intestinal Graft-versus-Host Disease. *Biology of Blood and Marrow Transplantation*. 25 (10), 1933–1943.
- [455] Louie, T.J., Emery, J., Krulicki, W., Byrne, B., and Mah, M. (2009) OPT-80 Eliminates *Clostridium difficile* and Is Sparing of *Bacteroides* Species during Treatment of *C. difficile* Infection. *Antimicrobial Agents and Chemotherapy*. 53 (1), 261.
- [456] Zhanel, G.G., Walkty, A.J., and Karlowsky, J.A. (2015) Fidaxomicin: A Novel Agent for the Treatment of *Clostridium difficile* Infection. *Canadian Journal of Infectious Diseases and Medical Microbiology*. 26 (6), 305–312.
- [457] Crook, D.W., Sarah Walker, A., Kean, Y., Weiss, K., Cornely, O.A., Miller, M.A., et al. (2012) Fidaxomicin versus vancomycin for *clostridium difficile* infection: Meta-analysis of pivotal randomized controlled trials. *Clinical Infectious Diseases*. 55 (SUPPL.2), S93–S103.
- [458] Rescigno, M. (2014) Intestinal microbiota and its effects on the immune system. *Cellular Microbiology*. 16 (7), 1004–1013.
- [459] Makki, K., Deehan, E.C., Walter, J., and Bäckhed, F. (2018) The Impact of Dietary Fiber on Gut Microbiota in Host Health and Disease. *Cell Host and Microbe*. 23 (6), 705–715.
- [460] Zmora, N., Suez, J., and Elinav, E. (2018) You are what you eat: diet, health and the gut microbiota. *Nature Reviews Gastroenterology & Hepatology* 2018 16:1. 16 (1), 35–56.

- [461] Buret, A.G., Motta, J.P., Allain, T., Ferraz, J., and Wallace, J.L. (2019) Pathobiont release from dysbiotic gut microbiota biofilms in intestinal inflammatory diseases: A role for iron? 06 Biological Sciences 0605 Microbiology. *Journal of Biomedical Science*. 26 (1), 1–14.
- [462] Hyoju, S.K., Zaborin, A., Keskey, R., Sharma, A., Arnold, W., Van Den Berg, F., et al. (2019) Mice fed an obesogenic western diet, administered antibiotics, and subjected to a sterile surgical procedure develop lethal septicemia with multidrug-resistant pathobionts. *MBio*. 10 (4),.
- [463] Soares, F.S., Amaral, F.C., Silva, N.L.C., Valente, M.R., Santos, L.K.R., Yamashiro, L.H., et al. (2017) Antibiotic-induced pathobiont dissemination accelerates mortality in severe experimental pancreatitis. *Frontiers in Immunology*. 8 (DEC), 1890.
- [464] Tuohy, K.M., Probert, H.M., Smejkal, C.W., and Gibson, G.R. (2003) Using probiotics and prebiotics to improve gut health. *Drug Discovery Today*. 8 (15), 692–700.
- [465] Rolhion, N. and Chassaing, B. (2016) When pathogenic bacteria meet the intestinal microbiota. *Philosophical Transactions of the Royal Society B: Biological Sciences*. 371 (1707),.
- [466] Garcia-Gutierrez, E., Mayer, M.J., Cotter, P.D., and Narbad, A. (2019) Gut microbiota as a source of novel antimicrobials. *Gut Microbes*. 10 (1), 1–21.
- [467] Kamada, N., Chen, G.Y., Inohara, N., and Núñez, G. (2013) Control of pathogens and pathobionts by the gut microbiota. *Nature Immunology*. 14 (7), 685–690.
- [468] Corr, S.C., Li, Y., Riedel, C.U., O’Toole, P.W., Hill, C., and Gahan, C.G.M. (2007) Bacteriocin production as a mechanism for the antiinfective activity of *Lactobacillus salivarius* UCC118. *Proceedings of the National Academy of Sciences of the United States of America*. 104 (18), 7617–7621.
- [469] Cai, Y., Folkerts, J., Folkerts, G., Maurer, M., and Braber, S. (2020) Microbiota-dependent and -independent effects of dietary fibre on human health. *British Journal of Pharmacology*. 177 (6), 1363–1381.
- [470] Lu, Z., Xu, Z., Shen, Z., Tian, Y., and Shen, H. (2021) Corrigendum: Dietary Energy Level Promotes Rumen Microbial Protein Synthesis by Improving the Energy Productivity of the Ruminal Microbiome (Front. Microbiol, (2019), 10, (847), 10.3389/fmicb.2019.00847). *Frontiers in Microbiology*. 12 (APR), 847.
- [471] Gao, H., Shu, Q., Chen, J., Fan, K., Xu, P., Zhou, Q., et al. (2019) Antibiotic Exposure Has Sex-

Dependent Effects on the Gut Microbiota and Metabolism of Short-Chain Fatty Acids and Amino Acids in Mice. *MSystems*. 4 (4),.

- [472] Silva, Y.P., Bernardi, A., and Frozza, R.L. (2020) The Role of Short-Chain Fatty Acids From Gut Microbiota in Gut-Brain Communication. *Frontiers in Endocrinology*. 0 25.
- [473] Cummings, J.H., Pomare, E.W., Branch, H.W.J., Naylor, C.P.E., and MacFarlane, G.T. (1987) Short chain fatty acids in human large intestine, portal, hepatic and venous blood. *Gut*. 28 (10), 1221–1227.
- [474] Visekruna, A. and Luu, M. (2021) The Role of Short-Chain Fatty Acids and Bile Acids in Intestinal and Liver Function, Inflammation, and Carcinogenesis. *Frontiers in Cell and Developmental Biology*. 9 2030.
- [475] Zhang, S., Zhao, J., Xie, F., He, H., Johnston, L.J., Dai, X., et al. (2021) Dietary fiber-derived short-chain fatty acids: A potential therapeutic target to alleviate obesity-related nonalcoholic fatty liver disease. *Obesity Reviews*. 22 (11), e13316.
- [476] den Besten, G., Lange, K., Havinga, R., van Dijk, T.H., Gerding, A., van Eunen, K., et al. (2013) Gut-derived short-chain fatty acids are vividly assimilated into host carbohydrates and lipids. *American Journal of Physiology. Gastrointestinal and Liver Physiology*. 305 (12),.
- [477] Mollica, M.P., Raso, G.M., Cavaliere, G., Trinchese, G., De Filippo, C., Aceto, S., et al. (2017) Butyrate regulates liver mitochondrial function, efficiency, and dynamics in insulin-resistant obese mice. *Diabetes*. 66 (5), 1405–1418.
- [478] Vrieze, A., Van Nood, E., Holleman, F., Salojärvi, J., Kootte, R.S., Bartelsman, J.F.W.M., et al. (2012) Transfer of intestinal microbiota from lean donors increases insulin sensitivity in individuals with metabolic syndrome. *Gastroenterology*. 143 (4), 913-916.e7.
- [479] De Winter, B.Y., van den Wijngaard, R.M., and de Jonge, W.J. (2012) Intestinal mast cells in gut inflammation and motility disturbances. *Biochimica et Biophysica Acta - Molecular Basis of Disease*. 1822 (1), 66–73.
- [480] Varol, C., Zigmond, E., and Jung, S. (2010) Securing the immune tightrope: Mononuclear phagocytes in the intestinal lamina propria. *Nature Reviews Immunology*. 10 (6), 415–426.
- [481] Okumura, R. and Takeda, K. (2016) Maintenance of gut homeostasis by the mucosal immune system. *Proceedings of the Japan Academy Series B: Physical and Biological Sciences*. 92 (9), 423–435.

- [482] Natividad, J.M.M. and Verdu, E.F. (2013) Modulation of intestinal barrier by intestinal microbiota: Pathological and therapeutic implications. *Pharmacological Research*. 69 (1), 42–51.
- [483] Ali, A., Tan, H.Y., and Kaiko, G.E. (2020) Role of the Intestinal Epithelium and Its Interaction With the Microbiota in Food Allergy. *Frontiers in Immunology*. 11 3222.
- [484] Roda, G., Sartini, A., Zambon, E., Calafiore, A., Marocchi, M., Caponi, A., et al. (2010) Intestinal epithelial cells in inflammatory bowel diseases. *World Journal of Gastroenterology*. 16 (34), 4264–4271.
- [485] Burgueño, J.F. and Abreu, M.T. (2020) Epithelial Toll-like receptors and their role in gut homeostasis and disease. *Nature Reviews Gastroenterology and Hepatology*. 17 (5), 263–278.
- [486] Cianci, R., Pagliari, D., Piccirillo, C.A., Fritz, J.H., and Gambassi, G. (2018) The microbiota and immune system crosstalk in health and disease. *Mediators of Inflammation*. 2018.
- [487] Chen, J. and Vitetta, L. (2020) The role of butyrate in attenuating pathobiont-induced hyperinflammation. *Immune Network*. 20 (2),.
- [488] Caricilli, A.M. (2014) Intestinal barrier: A gentlemen’s agreement between microbiota and immunity. *World Journal of Gastrointestinal Pathophysiology*. 5 (1), 18.
- [489] Cong, Y., Feng, T., Fujihashi, K., Schoeb, T.R., and Elson, C.O. (2009) A dominant, coordinated T regulatory cell-IgA response to the intestinal microbiota. *Proceedings of the National Academy of Sciences of the United States of America*. 106 (46), 19256–19261.
- [490] Lathrop, S.K., Bloom, S.M., Rao, S.M., Nutsch, K., Lio, C.W., Santacruz, N., et al. (2011) Peripheral education of the immune system by colonic commensal microbiota. *Nature*. 478 (7368), 250–254.
- [491] Cushing, K., Alvarado, D.M., and Ciorba, M.A. (2015) Butyrate and mucosal inflammation: New scientific evidence supports clinical observation. *Clinical and Translational Gastroenterology*. 6 (8), e108.
- [492] Dang, G., Wu, W., Zhang, H., and Everaert, N. (2021) A new paradigm for a new simple chemical: butyrate & immune regulation. *Food & Function*.
- [493] Mazmanian, S.K., Round, J.L., and Kasper, D.L. (2008) A microbial symbiosis factor prevents intestinal inflammatory disease. *Nature*. 453 (7195), 620–625.

- [494] Hazem, S.H., Hamed, M.F., Saad, M.A.A., and Gameil, N.M. (2018) Comparison of lactate and β -hydroxybutyrate in the treatment of concanavalin-A induced hepatitis. *International Immunopharmacology*. 61 376–384.
- [495] Pan, P., Oshima, K., Huang, Y.W., Agle, K.A., Drobyski, W.R., Chen, X., et al. (2018) Loss of FFAR2 promotes colon cancer by epigenetic dysregulation of inflammation suppressors. *International Journal of Cancer*. 143 (4), 886–896.
- [496] Watanabe, S., Alexander, M., Misharin, A. V., and Budinger, G.R.S. (2019) The role of macrophages in the resolution of inflammation. *Journal of Clinical Investigation*. 129 (7), 2619–2628.
- [497] Lührs, H., Gerke, T., Müller, J.G., Melcher, R., Schaubert, J., Boxberger, F., et al. (2002) Butyrate inhibits NF- κ B activation in lamina propria macrophages of patients with ulcerative colitis. *Scandinavian Journal of Gastroenterology*. 37 (4), 458–466.
- [498] Park, J.W., Kim, H.Y., Kim, M.G., Jeong, S., Yun, C.H., and Han, S.H. (2019) Short-chain fatty acids inhibit staphylococcal lipoprotein-induced nitric oxide production in murine macrophages. *Immune Network*. 19 (2),.
- [499] Li, H., Jiang, T., Li, M.Q., Zheng, X.L., and Zhao, G.J. (2018) Transcriptional regulation of macrophages polarization by microRNAs. *Frontiers in Immunology*. 9 (MAY), 1175.
- [500] Elvers, K.T., Wilson, V.J., Hammond, A., Duncan, L., Huntley, A.L., Hay, A.D., et al. (2020) Antibiotic-induced changes in the human gut microbiota for the most commonly prescribed antibiotics in primary care in the UK: a systematic review. *BMJ Open*. 10 (9), e035677.
- [501] Ramirez, J., Guarner, F., Bustos Fernandez, L., Maruy, A., Sdepanian, V.L., and Cohen, H. (2020) Antibiotics as Major Disruptors of Gut Microbiota. *Frontiers in Cellular and Infection Microbiology*. 10 731.
- [502] Walker, A.W. and Lawley, T.D. (2013) Therapeutic modulation of intestinal dysbiosis. *Pharmacological Research*. 69 (1), 75–86.
- [503] Wu, N., Yang, X., Zhang, R., Li, J., Xiao, X., Hu, Y., et al. (2013) Dysbiosis Signature of Fecal Microbiota in Colorectal Cancer Patients. *Microbial Ecology*. 66 (2), 462–470.
- [504] Gagnière, J., Raisch, J., Veziat, J., Barnich, N., Bonnet, R., Buc, E., et al. (2016) Gut microbiota imbalance and colorectal cancer. *World Journal of Gastroenterology*. 22 (2), 501–18.

- [505] Tian, H., Ge, X., Nie, Y., Yang, L., Ding, C., McFarland, L. V., et al. (2017) Fecal microbiota transplantation in patients with slow-transit constipation: A randomized, clinical trial. *PLOS ONE*. 12 (2), e0171308.
- [506] Rani, R.A., Ali, R.A.R., and Lee, Y.Y. (2016) Irritable bowel syndrome and inflammatory bowel disease overlap syndrome: pieces of the puzzle are falling into place. *Intestinal Research*. 14 (4), 297.
- [507] Honda, K. and Littman, D.R. (2012) The Microbiome in Infectious Disease and Inflammation. *Annual Review of Immunology*. 30 (1), 759–795.
- [508] Morgan, X.C., Reyes, J.A., Ward, D. V, Sokol, H., Shah, S.A., Xavier, R.J., et al. (2012) Dysfunction of the intestinal microbiome in inflammatory bowel disease and treatment. *Genome Biology*. 13 (9), R79.
- [509] Ni, J., Wu, G.D., Albenberg, L., and Tomov, V.T. (2017) Gut microbiota and IBD: causation or correlation? *Nature Reviews Gastroenterology & Hepatology*. 14 (10), 573.
- [510] Shaw, S.Y., Blanchard, J.F., and Bernstein, C.N. (2010) Association Between the Use of Antibiotics in the First Year of Life and Pediatric Inflammatory Bowel Disease. *American Journal of Gastroenterology*. 105 (12), 2687–2692.
- [511] Ananthakrishnan, A.N. (2015) Epidemiology and risk factors for IBD. *Nature Reviews Gastroenterology & Hepatology*. 12 (4), 205–217.
- [512] Zaylaa, M., Al Kassaa, I., Alard, J., Peucelle, V., Boutillier, D., Desramaut, J., et al. (2018) Probiotics in IBD: Combining in vitro and in vivo models for selecting strains with both anti-inflammatory potential as well as a capacity to restore the gut epithelial barrier. *Journal of Functional Foods*. 47 304–315.
- [513] Guandalini, S. and Sansotta, N. (2019) Probiotics in the Treatment of Inflammatory Bowel Disease. in: Springer, New York, NY, pp. 1–7.
- [514] Aragon, G., Graham, D.B., Borum, M., and Doman, D.B. (2010) Probiotic therapy for irritable bowel syndrome. *Gastroenterology and Hepatology*. 6 (1), 39–44.
- [515] Whorwell, P.J., Altringer, L., Morel, J., Bond, Y., Charbonneau, D., O’Mahony, L., et al. (2006) Efficacy of an encapsulated probiotic *Bifidobacterium infantis* 35624 in women with irritable bowel syndrome. *American Journal of Gastroenterology*. 101 (7), 1581–1590.
- [516] Brenner, D.M., Moeller, M.J., Chey, W.D., and Schoenfeld, P.S. (2009) The utility of

- probiotics in the treatment of irritable bowel syndrome: A systematic review. *American Journal of Gastroenterology*. 104 (4), 1033–1049.
- [517] Lee, B.J. and Bak, Y.T. (2011) Irritable bowel syndrome, gut microbiota and probiotics. *Journal of Neurogastroenterology and Motility*. 17 (3), 252–266.
- [518] O’Mahony, L., Mccarthy, J., Kelly, P., Hurley, G., Luo, F., Chen, K., et al. (2005) Lactobacillus and Bifidobacterium in irritable bowel syndrome: Symptom responses and relationship to cytokine profiles. *Gastroenterology*. 128 (3), 541–551.
- [519] Collins, S., Reid, G., Collins, S., and Reid, G. (2016) Distant Site Effects of Ingested Prebiotics. *Nutrients*. 8 (9), 523.
- [520] Zitvogel, L., Ayyoub, M., Routy, B., and Kroemer, G. (2016) Microbiome and Anticancer Immunosurveillance. *Cell*. 165 (2), 276–287.
- [521] Reid, G., Abrahamsson, T., Bailey, M., Bindels, L.B., Bubnov, R., Ganguli, K., et al. (2017) How do probiotics and prebiotics function at distant sites? *Beneficial Microbes*. 8 (4), 521–533.
- [522] Huang, Y.J. and Boushey, H.A. (2015) The microbiome in asthma. *Journal of Allergy and Clinical Immunology*. 135 (1), 25–30.
- [523] Riiser, A. (2015) The human microbiome, asthma, and allergy. *Allergy, Asthma & Clinical Immunology*. 11 (1), 35.
- [524] Sevelsted, A., Stokholm, J., and Bisgaard, H. (2016) Risk of Asthma from Cesarean Delivery Depends on Membrane Rupture. *The Journal of Pediatrics*. 171 38-42.e4.
- [525] Madan, J.C., Hoen, A.G., Lundgren, S.N., Farzan, S.F., Cottingham, K.L., Morrison, H.G., et al. (2016) Association of Cesarean Delivery and Formula Supplementation With the Intestinal Microbiome of 6-Week-Old Infants. *JAMA Pediatrics*. 170 (3), 212.
- [526] Holt, P.G. and Sly, P.D. (2007) Prevention of allergic respiratory disease in infants: current aspects and future perspectives. *Current Opinion in Allergy and Clinical Immunology*. 7 (6), 547–555.
- [527] Deo, S.S., Mistry, K.J., Kakade, A.M., and Niphadkar, P. V. (2010) Role played by Th2 type cytokines in IgE mediated allergy and asthma. *Lung India*. 27 (2), 66–71.
- [528] Kalliomäki, M., Salminen, S., Arvilommi, H., Kero, P., Koskinen, P., and Isolauri, E. (2001) Probiotics in primary prevention of atopic disease: a randomised placebo-controlled trial. *The Lancet*. 357 (9262), 1076–1079.

- [529] Elazab, N., Mendy, A., Gasana, J., Vieira, E.R., Quizon, A., and Forno, E. (2013) Probiotic administration in early life, atopy, and asthma: a meta-analysis of clinical trials. *Pediatrics*. 132 (3), e666-76.
- [530] Senga, S.S. and Grose, R.P. (2021) Hallmarks of cancer—the new testament. *Open Biology*. 11 (1),.
- [531] Polk, D.B. and Peek, R.M. (2010) Helicobacter pylori: gastric cancer and beyond. *Nature Reviews Cancer*. 10 (6), 403–414.
- [532] Herbst, A., Jurinovic, V., Krebs, S., Thieme, S.E., Blum, H., Göke, B., et al. (2014) Comprehensive analysis of β -catenin target genes in colorectal carcinoma cell lines with deregulated Wnt/ β -catenin signaling. *BMC Genomics*. 15 (1), 74.
- [533] Sears, C.L. and Garrett, W.S. (2014) Microbes, Microbiota, and Colon Cancer. *Cell Host & Microbe*. 15 (3), 317–328.
- [534] Wu, S., Morin, P.J., Maouyo, D., and Sears, C.L. (2003) Bacteroides fragilis enterotoxin induces c-Myc expression and cellular proliferation. *Gastroenterology*. 124 (2), 392–400.
- [535] Castellarin, M., Warren, R.L., Freeman, J.D., Dreolini, L., Krzywinski, M., Strauss, J., et al. (2012) Fusobacterium nucleatum infection is prevalent in human colorectal carcinoma. *Genome Research*. 22 (2), 299–306.
- [536] Yu, T.C., Guo, F., Yu, Y., Sun, T., Ma, D., Han, J., et al. (2017) Fusobacterium nucleatum Promotes Chemoresistance to Colorectal Cancer by Modulating Autophagy. *Cell*. 170 (3), 548-563.e16.
- [537] Ghazalpour, A., Cespedes, I., Bennett, B.J., and Allayee, H. (2016) Expanding role of gut microbiota in lipid metabolism. *Current Opinion in Lipidology*. 27 (2), 141–7.
- [538] Koh, A., De Vadder, F., Kovatcheva-Datchary, P., and Bäckhed, F. (2016) From Dietary Fiber to Host Physiology: Short-Chain Fatty Acids as Key Bacterial Metabolites. *Cell*. 165 (6), 1332–1345.
- [539] Rowland, I., Gibson, G., Heinken, A., Scott, K., Swann, J., Thiele, I., et al. (2018) Gut microbiota functions: metabolism of nutrients and other food components. *European Journal of Nutrition*. 57 (1), 1–24.
- [540] Louis, P., Hold, G.L., and Flint, H.J. (2014) The gut microbiota, bacterial metabolites and colorectal cancer. *Nature Reviews Microbiology*. 12 (10), 661–672.

- [541] Geirnaert, A., Calatayud, M., Grootaert, C., Laukens, D., Devriese, S., Smagghe, G., et al. (2017) Butyrate-producing bacteria supplemented in vitro to Crohn's disease patient microbiota increased butyrate production and enhanced intestinal epithelial barrier integrity. *Scientific Reports*. 7 (1), 11450.
- [542] Hinnebusch, B.F., Meng, S., Wu, J.T., Archer, S.Y., and Hodin, R.A. (2002) The Effects of Short-Chain Fatty Acids on Human Colon Cancer Cell Phenotype Are Associated with Histone Hyperacetylation. *The Journal of Nutrition*. 132 (5), 1012–1017.
- [543] Salimi, V., Shahsavari, Z., Safizadeh, B., Hosseini, A., Khademian, N., and Tavakoli-Yaraki, M. (2017) Sodium butyrate promotes apoptosis in breast cancer cells through reactive oxygen species (ROS) formation and mitochondrial impairment. *Lipids in Health and Disease*. 16 (1),.
- [544] Wu, X., Wu, Y., He, L., Wu, L., Wang, X., and Liu, Z. (2018) Effects of the intestinal microbial metabolite butyrate on the development of colorectal cancer. *Journal of Cancer*. 9 (14), 2510.
- [545] Davie, J.R. (2003) Inhibition of Histone Deacetylase Activity by Butyrate. *The Journal of Nutrition*. 133 (7), 2485S-2493S.
- [546] Thangaraju, M., Cresci, G.A., Liu, K., Ananth, S., Gnanaprakasam, J.P., Browning, D.D., et al. (2009) GPFM 09A is a G-protein-coupled receptor for the bacterial fermentation product butyrate and functions as a tumor suppressor in colon. *Cancer Research*. 69 (7), 2826–2832.
- [547] Raman, M., Ambalam, P., Kondepudi, K.K., Pithva, S., Kothari, C., Patel, A.T., et al. (2013) Potential of probiotics, prebiotics and synbiotics for management of colorectal cancer. *Gut Microbes*. 4 (3), 181–192.
- [548] Jacouton, E., Chain, F., Sokol, H., Langella, P., and Bermúdez-Humarán, L.G. (2017) Probiotic Strain *Lactobacillus casei* BL23 Prevents Colitis-Associated Colorectal Cancer. *Frontiers in Immunology*. 8 1553.
- [549] Mendes, M.C.S., Paulino, D.S., Brambilla, S.R., Camargo, J.A., Persinoti, G.F., and Carnevali, J.B.C. (2018) Microbiota modification by probiotic supplementation reduces colitis associated colon cancer in mice. *World Journal of Gastroenterology*. 24 (18), 1995.
- [550] Mousavi Jam, S.A., Talebi, M., Alipour, B., and Khosroushahi, A.Y. (2021) The therapeutic effect of potentially probiotic *Lactobacillus paracasei* on dimethylhydrazine induced colorectal cancer in rats. *Food Bioscience*. 41 101097.
- [551] Chang, C.W., Liu, C.Y., Lee, H.C., Huang, Y.H., Li, L.H., Chiau, J.S.C., et al. (2018) *Lactobacillus*

casei Variety rhamnosus probiotic preventively attenuates 5-Fluorouracil/Oxaliplatin-induced intestinal injury in a syngeneic colorectal cancer model. *Frontiers in Microbiology*. 9 (MAY), 983.

- [552] Zaharuddin, L., Mokhtar, N.M., Muhammad Nawawi, K.N., and Raja Ali, R.A. (2019) A randomized double-blind placebo-controlled trial of probiotics in post-surgical colorectal cancer. *BMC Gastroenterology*. 19 (1), 131.
- [553] Rajagopala, S. V, Vashee, S., Oldfield, L.M., Suzuki, Y., Venter, J.C., Telenti, A., et al. (2017) The human microbiome and cancer. *Cancer Prevention Research*. 10 (4), 226–234.
- [554] Zitvogel, L. and Kroemer, G. (2012) Targeting PD-1/PD-L1 interactions for cancer immunotherapy. *Oncotarget*. 1 (8), 1223–1225.
- [555] Sivan, A., Corrales, L., Hubert, N., Williams, J.B., Aquino-Michaels, K., Earley, Z.M., et al. (2015) Commensal Bifidobacterium promotes antitumor immunity and facilitates anti-PD-L1 efficacy. *Science*. 350 (6264), 1084–1089.
- [556] Tanoue, T., Morita, S., Plichta, D.R., Skelly, A.N., Suda, W., Sugiura, Y., et al. (2019) A defined commensal consortium elicits CD8 T cells and anti-cancer immunity. *Nature*. 565 (7741), 600–605.
- [557] Gruenbacher, G. and Thurnher, M. (2017) Mevalonate metabolism in immuno-oncology. *Frontiers in Immunology*. 8 (DEC), 1714.
- [558] Taplitz, R.A., Kennedy, E.B., Bow, E.J., Crews, J., Gleason, C., Langston, A.A., et al. (2018) Antimicrobial prophylaxis for adult patients with cancer-related immunosuppression: ASCO and IDSA clinical practice guideline update. *Journal of Clinical Oncology*. 36 (30), 3043–3054.
- [559] Gulluoglu, B.M., Guler, S.A., Ugurlu, M.U., and Culha, G. (2013) Efficacy of prophylactic antibiotic administration for breast cancer surgery in overweight or obese patients: A randomized controlled trial. *Annals of Surgery*. 257 (1), 37–43.
- [560] Pinato, D.J., Howlett, S., Ottaviani, D., Urus, H., Patel, A., Mineo, T., et al. (2019) Association of prior antibiotic treatment with survival and response to immune checkpoint inhibitor therapy in patients with cancer. *JAMA Oncology*. 5 (12), 1774–1778.
- [561] Rao, V.P., Poutahidis, T., Ge, Z., Nambiar, P.R., Boussahmain, C., Wang, Y.Y., et al. (2006) Innate immune inflammatory response against enteric bacteria *Helicobacter hepaticus* induces mammary adenocarcinoma in mice. *Cancer Research*. 66 (15), 7395–7400.

- [562] Rao, V.P., Poutahidis, T., Fox, J.G., and Erdman, S.E. (2007) Breast cancer: Should gastrointestinal bacteria be on our radar screen? *Cancer Research*. 67 (3), 847–850.
- [563] Chen, H.P., Zhao, Y.T., and Zhao, T.C. (2015) Histone deacetylases and mechanisms of regulation of gene expression. *Critical Reviews in Oncogenesis*. 20 (1–2), 35–47.
- [564] Berni Canani, R., Di Costanzo, M., and Leone, L. (2012) The epigenetic effects of butyrate: Potential therapeutic implications for clinical practice. *Clinical Epigenetics*. 4 (1), 4.
- [565] Myzak, M. and Dashwood, R. (2006) Histone Deacetylases as Targets for Dietary Cancer Preventive Agents: Lessons Learned with Butyrate, Diallyl Disulfide, and Sulforaphane. *Current Drug Targets*. 7 (4), 443–452.
- [566] Kovács, T., Mikó, E., Vida, A., Sebő, É., Toth, J., Csonka, T., et al. (2019) Cadaverine, a metabolite of the microbiome, reduces breast cancer aggressiveness through trace amino acid receptors. *Scientific Reports*. 9 (1), 1–14.
- [567] Kilkinen, A., Rissanen, H., Klaukka, T., Pukkala, E., Heliövaara, M., Huovinen, P., et al. (2008) Antibiotic use predicts an increased risk of cancer. *International Journal of Cancer*. 123 (9), 2152–2155.
- [568] Boursi, B., Mamtani, R., Haynes, K., and Yang, Y.X. (2015) Recurrent antibiotic exposure may promote cancer formation-Another step in understanding the role of the human microbiota? *European Journal of Cancer*. 51 (17), 2655–2664.
- [569] Buchta Rosean, C.B., Bostic, R.R., Ferey, J.C.M., Feng, T.-Y., Azar, F.N., Tung, K.S., et al. (2019) Pre-existing commensal dysbiosis is a host-intrinsic regulator of tissue inflammation and tumor cell dissemination in hormone receptor-positive breast cancer. *Cancer Research*. canres.3464.2018.
- [570] Kirkup, B.M. (2019) Understanding how the host gut microbiota influences distant immunological niches, University of East Anglia, 2019.
- [571] Wang, Z. and Dong, C. (2019) Gluconeogenesis in Cancer: Function and Regulation of PEPCK, FBPase, and G6Pase. *Trends in Cancer*. 5 (1), 30–45.
- [572] Fernald, K. and Kurokawa, M. (2013) Evading apoptosis in cancer. *Trends in Cell Biology*. 23 (12), 620–633.
- [573] Arshad, F.-A., Mehmood, R., Hussain, S., Annus Khan, M., and Khan, M.S. (2018) Lactobacilli as Probiotics and their Isolation from Different Sources. *British Journal of Research*. 05 (03),

43.

- [574] Zagato, E., Pozzi, C., Bertocchi, A., Schioppa, T., Saccheri, F., Guglietta, S., et al. (2020) Endogenous murine microbiota member *Faecalibaculum rodentium* and its human homologue protect from intestinal tumour growth. *Nature Microbiology*. 5 (3), 511–524.
- [575] Tomayko, M.M. and Reynolds, C.P. (1989) Determination of subcutaneous tumor size in athymic (nude) mice. *Cancer Chemotherapy and Pharmacology*. 24 (3), 148–154.
- [576] Castagnoli, L., Iezzi, M., Ghedini, G.C., Ciravolo, V., Marzano, G., Lamolinara, A., et al. (2014) Activated d16HER2 homodimers and src kinase mediate optimal efficacy for trastuzumab. *Cancer Research*. 74 (21), 6248–6259.
- [577] Marchini, C., Gabrielli, F., Iezzi, M., Zenobi, S., Montani, M., Pietrella, L., et al. (2011) The human splice variant δ 16HER2 induces rapid tumor onset in a reporter transgenic mouse. *PLoS ONE*. 6 (4), e18727.
- [578] Schindelin, J., Arganda-Carreras, I., Frise, E., Kaynig, V., Longair, M., Pietzsch, T., et al. (2012) Fiji: an open-source platform for biological-image analysis. *Nature Methods* 2012 9:7. 9 (7), 676–682.
- [579] Wood, D.E., Lu, J., and Langmead, B. (2019) Improved metagenomic analysis with Kraken 2. *Genome Biology*. 20 (1), 1–13.
- [580] Chen, S., Zhou, Y., Chen, Y., and Gu, J. (2018) Fastp: An ultra-fast all-in-one FASTQ preprocessor. *Bioinformatics*. 34 (17), i884–i890.
- [581] Segata, N., Waldron, L., Ballarini, A., Narasimhan, V., Jousson, O., and Huttenhower, C. (2012) Metagenomic microbial community profiling using unique clade-specific marker genes. *Nature Methods*. 9 (8), 811.
- [582] Buchfink, B., Xie, C., and Huson, D.H. (2014) Fast and sensitive protein alignment using DIAMOND. *Nature Methods* 2014 12:1. 12 (1), 59–60.
- [583] Dennis, G., Sherman, B.T., Hosack, D.A., Yang, J., Gao, W., Lane, H.C., et al. (2003) DAVID: Database for Annotation, Visualization, and Integrated Discovery. *Genome Biology*. 4 (5), 1–11.
- [584] Mi, H., Muruganujan, A., Casagrande, J.T., and Thomas, P.D. (2013) Large-scale gene function analysis with the panther classification system. *Nature Protocols*. 8 (8), 1551–1566.
- [585] Stuart, T., Butler, A., Hoffman, P., Hafemeister, C., Papalexi, E., Mauck, W.M., et al. (2019)

Comprehensive Integration of Single-Cell Data. *Cell*. 177 (7), 1888-1902.e21.

- [586] Schaum, N., Karkanas, J., Neff, N.F., May, A.P., Quake, S.R., Wyss-Coray, T., et al. (2018) Single-cell transcriptomics of 20 mouse organs creates a Tabula Muris. *Nature*. 562 (7727), 367–372.
- [587] Han, X., Wang, R., Zhou, Y., Fei, L., Sun, H., Lai, S., et al. (2018) Mapping the Mouse Cell Atlas by Microwell-Seq. *Cell*. 172 (5), 1091-1107.e17.
- [588] Wagner, J., Rapsomaniki, M.A., Chevrier, S., Anzeneder, T., Langwieder, C., Dykgers, A., et al. (2019) A Single-Cell Atlas of the Tumor and Immune Ecosystem of Human Breast Cancer. *Cell*. 177 (5), 1330-1345.e18.
- [589] Jew, B., Alvarez, M., Rahmani, E., Miao, Z., Ko, A., Garske, K.M., et al. (2020) Accurate estimation of cell composition in bulk expression through robust integration of single-cell information. *Nature Communications*. 11 (1), 1–11.
- [590] Sarkaria, J.N., Galanis, E., Wu, W., Dietz, A.B., Kaufmann, T.J., Gustafson, M.P., et al. (2010) Combination of Temsirolimus (CCI-779) with Chemoradiation in Newly Diagnosed Glioblastoma Multiforme (GBM) (NCCTG trial N027D) Is Associated with Increased Infectious Risks. *Clinical Cancer Research*. 16 (22), 5573–5580.
- [591] Bow, E.J. (1998) Infection risk and cancer chemotherapy: The impact of the chemotherapeutic regimen in patients with lymphoma and solid tissue malignancies. *Journal of Antimicrobial Chemotherapy*. 41 (SUPPL. D), 1–5.
- [592] Crawford, J., Dale, D.C., and Lyman, G.H. (2004) Chemotherapy-induced neutropenia. *Cancer*. 100 (2), 228–237.
- [593] Edwards, B.L., Stukenborg, G.J., Brenin, D.R., and Schroen, A.T. (2014) Use of Prophylactic Postoperative Antibiotics During Surgical Drain Presence Following Mastectomy. *Annals of Surgical Oncology*. 21 (10), 3249–3255.
- [594] Maxson, T. and Mitchell, D.A. (2016) Targeted Treatment for Bacterial Infections: Prospects for Pathogen-Specific Antibiotics Coupled with Rapid Diagnostics. *Tetrahedron*. 72 (25), 3609.
- [595] Ranganathan, K., Sears, E.D., Zhong, L., Chung, T.T., Chung, K.C., Kozlow, J.H., et al. (2018) Antibiotic prophylaxis after immediate breast reconstruction: The reality of its efficacy. *Plastic and Reconstructive Surgery*. 141 (4), 865–877.

- [596] Vétizou, M., Pitt, J.M., Daillère, R., Lepage, P., Waldschmitt, N., Flament, C., et al. (2015) Anticancer immunotherapy by CTLA-4 blockade relies on the gut microbiota. *Science*. 350 (6264), 1079–1084.
- [597] Gopalakrishnan, V., Spencer, C.N., Nezi, L., Reuben, A., Andrews, M.C., Karpinets, T. V, et al. (2018) Gut microbiome modulates response to anti-PD-1 immunotherapy in melanoma patients. *Science (New York, N.Y.)*. 359 (6371), 97–103.
- [598] Routy, B., Le Chatelier, E., Derosa, L., Duong, C.P.M., Alou, M.T., Daillère, R., et al. (2018) Gut microbiome influences efficacy of PD-1-based immunotherapy against epithelial tumors. *Science*. 359 (6371), 91–97.
- [599] Ács, B., Zámbo, V., Vízkeleti, L., Szász, A.M., Madaras, L., Szentmártoni, G., et al. (2017) Ki-67 as a controversial predictive and prognostic marker in breast cancer patients treated with neoadjuvant chemotherapy. *Diagnostic Pathology*. 12 (1), 20.
- [600] Crowley, L.C., Marfell, B.J., Scott, A.P., and Waterhouse, N.J. (2016) Quantitation of apoptosis and necrosis by annexin V binding, propidium iodide uptake, and flow cytometry. *Cold Spring Harbor Protocols*. 2016 (11), 953–957.
- [601] Yi, P. and Li, L.J. (2012) The germfree murine animal: An important animal model for research on the relationship between gut microbiota and the host. *Veterinary Microbiology*. 157 (1–2), 1–7.
- [602] Al-Asmakh, M.F. (2015) Use of Germ-Free Animal Models in Microbiota-Related Research. *Journal of Microbiology and Biotechnology*. 25 (10), 1583–1588.
- [603] Sugiura, K. and Stock, C.C. (1952) Studies in a tumor spectrum. I. Comparison of the action of methylbis(2-chloroethyl)amine and 3-bis(2-chloroethyl)aminomethyl-4-methoxymethyl-5-hydroxy-6-methylpyridine on the growth of a variety of mouse and rat tumors. *Cancer*. 5 (2), 382–402.
- [604] Johnstone, C.N., Smith, Y.E., Cao, Y., Burrows, A.D., Cross, R.S.N., Ling, X., et al. (2015) Functional and molecular characterisation of EO771.LMB tumours, a new C57BL/6-mouse-derived model of spontaneously metastatic mammary cancer. *DMM Disease Models and Mechanisms*. 8 (3), 237–251.
- [605] Bailey, A., Walker, A., Hadley, A., and Geraint James, D. (1970) Cephalixin-a new oral antibiotic. *Postgraduate Medical Journal*. 46 (533), 157–158.
- [606] Nishida, N., Yano, H., Nishida, T., Kamura, T., and Kojiro, M. (2006) Angiogenesis in Cancer.

Vascular Health and Risk Management. 2 (3), 213.

- [607] Ellison, T.S., Atkinson, S.J., Steri, V., Kirkup, B.M., Preedy, M.E.J., Johnson, R.T., et al. (2015) Suppression of β 3-integrin in mice triggers a neuropilin-1-dependent change in focal adhesion remodelling that can be targeted to block pathological angiogenesis. *Disease Models & Mechanisms*. 8 (9), 1105–1119.
- [608] Uzzan, B., Nicolas, P., Cucherat, M., and Perret, G.-Y. (2004) Microvessel Density as a Prognostic Factor in Women with Breast Cancer. *Cancer Research*. 64 (9), 2941–2955.
- [609] Hasan, J., Byers, R., and Jayson, G.C. (2002) Intra-tumoural microvessel density in human solid tumours. *British Journal of Cancer*. 86 (10), 1566.
- [610] Ranjan, R., Rani, A., Metwally, A., McGee, H.S., and Perkins, D.L. (2016) Analysis of the microbiome: Advantages of whole genome shotgun versus 16S amplicon sequencing. *Biochemical and Biophysical Research Communications*. 469 (4), 967–977.
- [611] Hong, Y.H., Nishimura, Y., Hishikawa, D., Tsuzuki, H., Miyahara, H., Gotoh, C., et al. (2005) Acetate and propionate short chain fatty acids stimulate adipogenesis via GPCR43. *Endocrinology*. 146 (12), 5092–5099.
- [612] Pingitore, A., Chambers, E.S., Hill, T., Maldonado, I.R., Liu, B., Bewick, G., et al. (2017) The diet-derived short chain fatty acid propionate improves beta-cell function in humans and stimulates insulin secretion from human islets in vitro. *Diabetes, Obesity and Metabolism*. 19 (2), 257–265.
- [613] Morrison, D.J. and Preston, T. (2016) Formation of short chain fatty acids by the gut microbiota and their impact on human metabolism. *Gut Microbes*. 7 (3), 189.
- [614] Becattini, S., Taur, Y., and Pamer, E.G. (2016) Antibiotic-Induced Changes in the Intestinal Microbiota and Disease. *Trends in Molecular Medicine*. 22 (6), 458–478.
- [615] Aminov, R.I. (2010) A brief history of the antibiotic era: lessons learned and challenges for the future. *Frontiers in Microbiology*. 1 134.
- [616] Valdes, A.M., Walter, J., Segal, E., and Spector, T.D. (2018) Role of the gut microbiota in nutrition and health. *BMJ (Online)*. 361 36–44.
- [617] Shreiner, A.B., Kao, J.Y., and Young, V.B. (2015) The gut microbiome in health and in disease. *Current Opinion in Gastroenterology*. 31 (1), 69–75.
- [618] Sun, L., Zhang, X., Zhang, Y., Zheng, K., Xiang, Q., Chen, N., et al. (2019) Antibiotic-Induced

- Disruption of Gut Microbiota Alters Local Metabolomes and Immune Responses. *Frontiers in Cellular and Infection Microbiology*. 0 (APR), 99.
- [619] Wang, B., Yao, M., Lv, L., Ling, Z., and Li, L. (2017) The Human Microbiota in Health and Disease. *Engineering*. 3 (1), 71–82.
- [620] J, T., C, M., M, P., AN, T., CR, M., and L, M. (2014) The role of short-chain fatty acids in health and disease. *Advances in Immunology*. 121 91–119.
- [621] Littman, D.R. and Pamer, E.G. (2011) Role of the commensal microbiota in normal and pathogenic host immune responses. *Cell Host and Microbe*. 10 (4), 311–323.
- [622] Dik, V.K., van Oijen, M.G.H., Smeets, H.M., and Siersema, P.D. (2016) Frequent Use of Antibiotics Is Associated with Colorectal Cancer Risk: Results of a Nested Case–Control Study. *Digestive Diseases and Sciences*. 61 (1), 255–264.
- [623] Yuan, Y., Jiang, Y.-C., Sun, C.-K., and Chen, Q.-M. (2016) Role of the tumor microenvironment in tumor progression and the clinical applications (Review). *Oncology Reports*. 35 (5), 2499–2515.
- [624] Renner, K., Singer, K., Koehl, G.E., Geissler, E.K., Peter, K., Siska, P.J., et al. (2017) Metabolic Hallmarks of Tumor and Immune Cells in the Tumor Microenvironment. *Frontiers in Immunology*. 0 (MAR), 248.
- [625] Albin, A., Bruno, A., Noonan, D.M., and Mortara, L. (2018) Contribution to tumor angiogenesis from innate immune cells within the tumor microenvironment: Implications for immunotherapy. *Frontiers in Immunology*. 9 (APR), 527.
- [626] Whiteside, T. (2008) The tumor microenvironment and its role in promoting tumor growth. *Oncogene*. 27 (45), 5904.
- [627] Ding, S., Chen, X., and Shen, K. (2020) Single-cell RNA sequencing in breast cancer: Understanding tumor heterogeneity and paving roads to individualized therapy. *Cancer Communications*. 40 (8), 329–344.
- [628] González-Silva, L., Quevedo, L., and Varela, I. (2020) Tumor Functional Heterogeneity Unraveled by scRNA-seq Technologies. *Trends in Cancer*. 6 (1), 13–19.
- [629] Wu, H., Xie, S., Miao, J., Li, Y., Wang, Z., Wang, M., et al. (2020) *Lactobacillus reuteri* maintains intestinal epithelial regeneration and repairs damaged intestinal mucosa. *Gut Microbes*. 11 (4), 997–1014.

- [630] Schepper, J.D., Collins, F.L., Rios-Arce, N.D., Raehtz, S., Schaefer, L., Gardinier, J.D., et al. (2019) Probiotic *Lactobacillus reuteri* Prevents Postantibiotic Bone Loss by Reducing Intestinal Dysbiosis and Preventing Barrier Disruption. *Journal of Bone and Mineral Research*. 34 (4), 681–698.
- [631] Pessione, E. (2012) Lactic acid bacteria contribution to gut microbiota complexity: lights and shadows. *Frontiers in Cellular and Infection Microbiology*. 2 86.
- [632] Hassan, M.U., Nayab, H., Rehman, T.U., Williamson, M.P., Haq, K.U., Shafi, N., et al. (2020) Characterisation of Bacteriocins Produced by *Lactobacillus* spp. Isolated from the Traditional Pakistani Yoghurt and Their Antimicrobial Activity against Common Foodborne Pathogens. *BioMed Research International*. 2020.
- [633] Pridmore, R.D., Pittet, A.-C., Praplan, F., and Cavadini, C. (2008) Hydrogen peroxide production by *Lactobacillus johnsonii* NCC 533 and its role in anti-Salmonella activity. *FEMS Microbiology Letters*. 283 (2), 210–215.
- [634] Ruiz-Palacios, G., Guerrero, M.L., Hilty, M., Dohnalek, M., Newton, P., Calva, J.J., et al. (1996) Feeding of a Probiotic for the Prevention of Community-Acquired Diarrhea in Young Mexican Children † 1089. *Pediatric Research*. 39 (4), 184–184.
- [635] Schreck Bird, A., Gregory, P.J., Jalloh, M.A., Risoldi Cochrane, Z., and Hein, D.J. (2017) Probiotics for the Treatment of Infantile Colic: A Systematic Review. *Journal of Pharmacy Practice*. 30 (3), 366–374.
- [636] Athalye-Jape, G., Rao, S., and Patole, S. (2016) *Lactobacillus reuteri* DSM 17938 as a Probiotic for Preterm Neonates. *Journal of Parenteral and Enteral Nutrition*. 40 (6), 783–794.
- [637] Chen, S.-M., Chieng, W.-W., Huang, S.-W., Hsu, L.-J., and Jan, M.-S. (2020) The synergistic tumor growth-inhibitory effect of probiotic *Lactobacillus* on transgenic mouse model of pancreatic cancer treated with gemcitabine. *Scientific Reports 2020 10:1*. 10 (1), 1–12.
- [638] Zhuo, Q., Yu, B., Zhou, J., Zhang, J., Zhang, R., Xie, J., et al. (2019) Lysates of *Lactobacillus acidophilus* combined with CTLA-4-blocking antibodies enhance antitumor immunity in a mouse colon cancer model. *Scientific Reports 2019 9:1*. 9 (1), 1–12.
- [639] Jahanshahi, M., Maleki Dana, P., Badehnoosh, B., Asemi, Z., Hallajzadeh, J., Mansournia, M.A., et al. (2020) Anti-tumor activities of probiotics in cervical cancer. *Journal of Ovarian Research*. 13 (1),.
- [640] Nilsson, A.G., Sundh, D., Bäckhed, F., and Lorentzon, M. (2018) *Lactobacillus reuteri* reduces

- bone loss in older women with low bone mineral density: a randomized, placebo-controlled, double-blind, clinical trial. *Journal of Internal Medicine*. 284 (3), 307–317.
- [641] Oliphant, K. and Allen-Vercoe, E. (2019) Macronutrient metabolism by the human gut microbiome: major fermentation by-products and their impact on host health. *Microbiome* 2019 7:1. 7 (1), 1–15.
- [642] Zhao, J., Hu, J., and Ma, X. (2021) Sodium caprylate improves intestinal mucosal barrier function and antioxidant capacity by altering gut microbial metabolism. *Food & Function*.
- [643] Mihaylova, M.M. and Shaw, R.J. (2011) The AMPK signalling pathway coordinates cell growth, autophagy and metabolism. *Nature Cell Biology*. 13 (9), 1016–1023.
- [644] Nicolas, G.R. and Chang, P. V. (2019) Deciphering the Chemical Lexicon of Host–Gut Microbiota Interactions. *Trends in Pharmacological Sciences*. 40 (6), 430–445.
- [645] Schroeder, B.O. and Bäckhed, F. (2016) Signals from the gut microbiota to distant organs in physiology and disease. *Nature Medicine*. 22 (10), 1079–1089.
- [646] Guo, C.J., Allen, B.M., Hiam, K.J., Dodd, D., van Treuren, W., Higginbottom, S., et al. (2019) Depletion of microbiome-derived molecules in the host using *Clostridium* genetics. *Science*. 366 (6471),.
- [647] Gall, G. Le, Noor, S.O., Ridgway, K., Scovell, L., Jamieson, C., Johnson, I.T., et al. (2011) Metabolomics of Fecal Extracts Detects Altered Metabolic Activity of Gut Microbiota in Ulcerative Colitis and Irritable Bowel Syndrome. *Journal of Proteome Research*. 10 (9), 4208–4218.
- [648] Pryde, S.E., Duncan, S.H., Hold, G.L., Stewart, C.S., and Flint, H.J. (2002) The microbiology of butyrate formation in the human colon. *FEMS Microbiology Letters*. 217 (2), 133–139.
- [649] Keating, A. (2006) Mesenchymal stromal cells. *Current Opinion in Hematology*. 13 (6), 419–425.
- [650] Hu, M. and Polyak, K. (2008) Molecular characterisation of the tumour microenvironment in breast cancer. *European Journal of Cancer*. 44 (18), 2760–2765.
- [651] Eiro, N., Gonzalez, L.O., Fraile, M., Cid, S., Schneider, J., and Vizoso, F.J. (2019) Breast cancer tumor stroma: Cellular components, phenotypic heterogeneity, intercellular communication, prognostic implications and therapeutic opportunities. *Cancers*. 11 (5), 1–26.

- [652] Carmeliet, P. (2005) VEGF as a key mediator of angiogenesis in cancer. *Oncology*. 69 (SUPPL. 3), 4–10.
- [653] Facciabene, A., Motz, G.T., and Coukos, G. (2012) T-Regulatory cells: Key players in tumor immune escape and angiogenesis. *Cancer Research*. 72 (9), 2162–2171.
- [654] Facciabene, A., Peng, X., Hagemann, I.S., Balint, K., Barchetti, A., Wang, L.-P., et al. (2011) Tumour hypoxia promotes tolerance and angiogenesis via CCL28 and Treg cells. *Nature* 2011 475:7355. 475 (7355), 226–230.
- [655] Liao, D., Luo, Y., Markowitz, D., Xiang, R., and Reisfeld, R.A. (2009) Cancer associated fibroblasts promote tumor growth and metastasis by modulating the tumor immune microenvironment in a 4T1 murine breast cancer model. *PLoS ONE*. 4 (11), e7965.
- [656] Ren, G., Liu, Y., Zhao, X., Zhang, J., Zheng, B., Yuan, Z.R., et al. (2014) Tumor resident mesenchymal stromal cells endow naïve stromal cells with tumor-promoting properties. *Oncogene*. 33 (30), 4016–4020.
- [657] Mao, Y., Keller, E.T., Garfield, D.H., Shen, K., and Wang, J. (2013) Stromal cells in tumor microenvironment and breast cancer. *Cancer and Metastasis Reviews*. 32 (1–2), 303–315.
- [658] Rowan, B.G., Gimble, J.M., Sheng, M., Anbalagan, M., Jones, R.K., Frazier, T.P., et al. (2014) Human adipose tissue-derived stromal/stem cells promote migration and early metastasis of triple negative breast cancer xenografts. *PLoS ONE*. 9 (2),.
- [659] Yu, P.F., Huang, Y., Han, Y.Y., Lin, L.Y., Sun, W.H., Rabson, A.B., et al. (2017) TNF α -activated mesenchymal stromal cells promote breast cancer metastasis by recruiting CXCR2+ neutrophils. *Oncogene*. 36 (4), 482–490.
- [660] Kester, L. and van Oudenaarden, A. (2018) Single-Cell Transcriptomics Meets Lineage Tracing. *Cell Stem Cell*. 23 (2), 166–179.
- [661] Levitin, H.M., Yuan, J., and Sims, P.A. (2018) Single-Cell Transcriptomic Analysis of Tumor Heterogeneity. *Trends in Cancer*. 4 (4), 264–268.
- [662] Haber, A.L., Biton, M., Rogel, N., Herbst, R.H., Shekhar, K., Smillie, C., et al. (2017) A single-cell survey of the small intestinal epithelium. *Nature*. 551 (7680), 333–339.
- [663] Fan, J., Slowikowski, K., and Zhang, F. (2020) Single-cell transcriptomics in cancer: computational challenges and opportunities. *Experimental and Molecular Medicine*. 52 (9), 1452–1465.

- [664] Sun, X., Sun, S., and Yang, S. (2019) An Efficient and Flexible Method for Deconvoluting Bulk RNA-Seq Data with Single-Cell RNA-Seq Data. *Cells* 2019, Vol. 8, Page 1161. 8 (10), 1161.
- [665] Ribatti, D. (2018) The Staining of Mast Cells: A Historical Overview. *International Archives of Allergy and Immunology*. 176 (1), 55–60.
- [666] da Silva, E.Z.M., Jamur, M.C., and Oliver, C. (2014) Mast Cell Function: A New Vision of an Old Cell. *Journal of Histochemistry and Cytochemistry*. 62 (10), 698–738.
- [667] Moon, T.C., Dean Befus, A., and Kulka, M. (2014) Mast cell mediators: Their differential release and the secretory pathways involved. *Frontiers in Immunology*. 5 (NOV),.
- [668] Rivera, J., Fierro, N.A., Olivera, A., and Suzuki, R. (2008) Chapter 3 New Insights on Mast Cell Activation via the High Affinity Receptor for IgE. *Advances in Immunology*. 98 85–120.
- [669] Asai, K., Kitauro, J., Kawakami, Y., Yamagata, N., Tsai, M., Carbone, D.P., et al. (2001) Regulation of mast cell survival by IgE. *Immunity*. 14 (6), 791–800.
- [670] Amin, K. (2012) The role of mast cells in allergic inflammation. *Respiratory Medicine*. 106 (1), 9–14.
- [671] Crompton, R., Clifton, V.L., Bisits, A.T., Read, M.A., Smith, R., and Wright, I.M.R. (2003) Corticotropin-Releasing Hormone Causes Vasodilation in Human Skin via Mast Cell-Dependent Pathways. *Journal of Clinical Endocrinology and Metabolism*. 88 (11), 5427–5432.
- [672] Rao, Q., Chen, Y., Yeh, C.R., Ding, J., Li, L., Chang, C., et al. (2016) Recruited mast cells in the tumor microenvironment enhance bladder cancer metastasis via modulation of ER β /CCL2/CCR2 EMT/MMP9 signals. *Oncotarget*. 7 (7), 7842–7855.
- [673] Li, L., Dang, Q., Xie, H., Yang, Z., He, D., Liang, L., et al. (2016) Correction: Infiltrating mast cells enhance prostate cancer invasion via altering LncRNA-HOTAIR/PRC2-androgen receptor (AR)-MMP9 signals and increased stem/progenitor cell population [Oncotarget. 2015; 6(16):14179-14190]. doi: 10.18632/oncotarget.3651. *Oncotarget*. 7 (50), 83828.
- [674] Öhrvik, H., Grujic, M., Waern, I., Gustafson, A.M., Ernst, N., Roers, A., et al. (2016) Mast cells promote melanoma colonization of lungs. *Oncotarget*. 7 (42), 68990–69001.
- [675] Glajcar, A., Szpor, J., Pacek, A., Tyrak, K.E., Chan, F., Streb, J., et al. (2017) The relationship between breast cancer molecular subtypes and mast cell populations in tumor microenvironment. *Virchows Archiv*. 470 (5), 505–515.

- [676] Carpenco, E., Ceaușu, R.A., Cimpean, A.M., Gaje, P.N., Șaptefrați, L., Fulga, V., et al. (2019) Mast cells as an indicator and prognostic marker in molecular subtypes of breast cancer. *In Vivo*. 33 (3), 743–748.
- [677] Sang, J., Yi, D., Tang, X., Zhang, Y., and Huang, T. (2016) The associations between mast cell infiltration, clinical features and molecular types of invasive breast cancer. *Oncotarget*. 7 (49), 81661–81669.
- [678] Kritikou, Depuydt, de Vries, Mulder, Govaert, Smit, et al. (2019) Flow Cytometry-Based Characterization of Mast Cells in Human Atherosclerosis. *Cells*. 8 (4), 334.
- [679] Galli, S.J., Tsai, M., and Wershil, B.K. (1993) The c-kit receptor, stem cell factor, and mast cells: What each is teaching us about the others. *American Journal of Pathology*. 142 (4), 965–974.
- [680] Pang, J., Taylor, G.R., Munroe, D.G., Ishaque, A., Fung-Leung, W.P., Lau, C.Y., et al. (1993) Characterization of the gene for the human high affinity IgE receptor (FcεRI) α-chain. *The Journal of Immunology (1950)*. 151 (11), 6166–6174.
- [681] Ivanov, I.I., Atarashi, K., Manel, N., Brodie, E.L., Shima, T., Karaoz, U., et al. (2009) Induction of Intestinal Th17 Cells by Segmented Filamentous Bacteria. *Cell*. 139 (3), 485–498.
- [682] Deng, M., Zhang, W., Tang, H., Ye, Q., Liao, Q., Zhou, Y., et al. (2013) Lactotransferrin acts as a tumor suppressor in nasopharyngeal carcinoma by repressing AKT through multiple mechanisms. *Oncogene*. 32 (36), 4273–4283.
- [683] Chiu, I.J., Hsu, Y.H., Chang, J.S., Yang, J.C., Chiu, H.W., and Lin, Y.F. (2020) Lactotransferrin downregulation drives the metastatic progression in clear cell renal cell carcinoma. *Cancers*. 12 (4),.
- [684] Luo, G., Zhou, Y., Yi, W., and Yi, H. (2015) Lactotransferrin expression is downregulated and affects the mitogen-activated protein kinase pathway in gastric cancer. *Oncology Letters*. 9 (5), 2409–2413.
- [685] Chen, G., Li, G., Luo, M., Wei, X., Wang, D., Zhang, H., et al. (2015) Clinical significance of SPRR1A expression in progesterone receptor-positive breast cancer. *Tumor Biology*. 36 (4), 2601–2605.
- [686] Li, X., Wei, R., Wang, M., Ma, L., Zhang, Z., Chen, L., et al. (2020) MGP Promotes Colon Cancer Proliferation by Activating the NF-κB Pathway through Upregulation of the Calcium Signaling Pathway. *Molecular Therapy - Oncolytics*. 17 371–383.

- [687] Yoshimura, K., Takeuchi, K., Nagasaki, K., Ogishima, S., Tanaka, H., Iwase, T., et al. (2009) Prognostic value of matrix Gla protein in breast cancer. *Molecular Medicine Reports*. 2 (4), 549–553.
- [688] DeNardo, D.G., Barreto, J.B., Andreu, P., Vasquez, L., Tawfik, D., Kolhatkar, N., et al. (2009) CD4+ T Cells Regulate Pulmonary Metastasis of Mammary Carcinomas by Enhancing Protumor Properties of Macrophages. *Cancer Cell*. 16 (2), 91–102.
- [689] Gisterek, I., Frydecka, I., Światoniowski, G., Fidler, S., and Kornafel, J. (2008) Tumour-infiltrating CD4 and CD8 T lymphocytes in breast cancer. *Reports of Practical Oncology and Radiotherapy*. 13 (4), 206–209.
- [690] Oka, T., Kalesnikoff, J., Starkl, P., Tsai, M., and Galli, S.J. (2012) Evidence questioning cromolyns effectiveness and selectivity as a mast cell stabilizer in mice. *Laboratory Investigation*. 92 (10), 1472–1482.
- [691] Gan, X., Liu, D., Ge, M., Luo, C., Gao, W., and Hei, Z. (2013) Treatment of mice with cromolyn sodium after reperfusion, but not prior to ischemia, attenuates small intestinal ischemia-reperfusion injury. *Molecular Medicine Reports*. 8 (3), 928–934.
- [692] Gan, P.Y., O’Sullivan, K.M., Ooi, J.D., Alikhan, M.A., Odobasic, D., Summers, S.A., et al. (2016) Mast cell stabilization ameliorates autoimmune anti-myeloperoxidase glomerulonephritis. *Journal of the American Society of Nephrology*. 27 (5), 1321–1333.
- [693] Vincent, L., Lapointe, C., Lo, M., Gagnon, H., Pejler, G., Takai, S., et al. (2021) Mast cell degranulation increases mouse mast cell protease 4-Dependent vasopressor responses to big Endothelin-1 but Not Angiotensin I. *Journal of Pharmacology and Experimental Therapeutics*. 376 (2), 213–221.
- [694] Zhang, X., Dong, H., Wang, F., and Zhang, J. (2020) Mast Cell Deficiency Protects Mice from Surgery-Induced Neuroinflammation. *Mediators of Inflammation*. 2020.
- [695] Bernstein, I.L. (1985) Cromolyn sodium. *Chest*. 87 (1 SUPPL.), 68S-73S.
- [696] Michel, A., Schüler, A., Friedrich, P., Döner, F., Bopp, T., Radsak, M., et al. (2013) Mast Cell-deficient Kit W-sh “Sash” Mutant Mice Display Aberrant Myelopoiesis Leading to the Accumulation of Splenocytes That Act as Myeloid-Derived Suppressor Cells . *The Journal of Immunology*. 190 (11), 5534–5544.
- [697] Dudeck, A., Dudeck, J., Scholten, J., Petzold, A., Surianarayanan, S., Köhler, A., et al. (2011) Mast Cells Are Key Promoters of Contact Allergy that Mediate the Adjuvant Effects of

- Haptens. *Immunity*. 34 (6), 973–984.
- [698] Feyerabend, T.B., Weiser, A., Tietz, A., Stassen, M., Harris, N., Kopf, M., et al. (2011) Cre-mediated cell ablation contests mast cell contribution in models of antibody- and T cell-mediated autoimmunity. *Immunity*. 35 (5), 832–844.
- [699] Leone, K., Poggiana, C., and Zamarchi, R. (2018) The Interplay between Circulating Tumor Cells and the Immune System: From Immune Escape to Cancer Immunotherapy. *Diagnostics*. 8 (3), 59.
- [700] Valastyan, S. and Weinberg, R.A. (2011) Tumor metastasis: Molecular insights and evolving paradigms. *Cell*. 147 (2), 275–292.
- [701] Chambers, A.F., Groom, A.C., and MacDonald, I.C. (2002) Dissemination and growth of cancer cells in metastatic sites. *Nature Reviews Cancer*. 2 (8), 563–572.
- [702] Banyard, J. and Bielenberg, D.R. (2015) The role of EMT and MET in cancer dissemination. *Connective Tissue Research*. 56 (5), 403–413.
- [703] Luzzi, K.J., MacDonald, I.C., Schmidt, E.E., Kerkvliet, N., Morris, V.L., Chambers, A.F., et al. (1998) Multistep nature of metastatic inefficiency: Dormancy of solitary cells after successful extravasation and limited survival of early micrometastases. *American Journal of Pathology*. 153 (3), 865–873.
- [704] Fan, R., Emery, T., Zhang, Y., Xia, Y., Sun, J., and Wan, J. (2016) Circulatory shear flow alters the viability and proliferation of circulating colon cancer cells. *Scientific Reports*. 6.
- [705] Montagner, M. and Dupont, S. (2020) Mechanical Forces as Determinants of Disseminated Metastatic Cell Fate. *Cells*. 9 (1),.
- [706] Dianat-Moghadam, H., Mahari, A., Heidarifard, M., Parnianfard, N., Pourmousavi-Kh, L., Rahbarghazi, R., et al. (2021) NK cells-directed therapies target circulating tumor cells and metastasis. *Cancer Letters*. 497 41–53.
- [707] Krijgsman, D., de Vries, N.L., Skovbo, A., Andersen, M.N., Swets, M., Bastiaannet, E., et al. (2019) Characterization of circulating T-, NK-, and NKT cell subsets in patients with colorectal cancer: the peripheral blood immune cell profile. *Cancer Immunology, Immunotherapy*. 68 (6), 1011–1024.
- [708] Lanier, L.L. and Phillips, J.H. (1996) Inhibitory MHC class I receptors on NK cells and T cells. *Immunology Today*. 17 (2), 86–91.

- [709] Peng, L., Zhang, Y., and Wang, Z. (2021) Immune responses against disseminated tumor cells. *Cancers*. 13 (11), 2515.
- [710] Moose, D.L., Krog, B.L., Kim, T.H., Zhao, L., Williams-Perez, S., Burke, G., et al. (2020) Cancer Cells Resist Mechanical Destruction in Circulation via RhoA/Actomyosin-Dependent Mechano-Adaptation. *Cell Reports*. 30 (11), 3864-3874.e6.
- [711] Huang, Q., Hu, X., He, W., Zhao, Y., Hao, S., Wu, Q., et al. (2018) Fluid shear stress and tumor metastasis. *American Journal of Cancer Research*. 8 (5), 763–777.
- [712] Planes-Laine, G., Rochigneux, P., Bertucci, F., Chrétien, A.S., Viens, P., Sabatier, R., et al. (2019) PD-1/PD-L1 targeting in breast cancer: The first clinical evidences are emerging. a literature review. *Cancers*. 11 (7), 1033.
- [713] Schütz, F., Stefanovic, S., Mayer, L., Von Au, A., Domschke, C., and Sohn, C. (2017) PD-1/PD-L1 Pathway in Breast Cancer. *Oncology Research and Treatment*. 40 (5), 294–297.
- [714] Dermani, F.K., Samadi, P., Rahmani, G., Kohlan, A.K., and Najafi, R. (2019) PD-1/PD-L1 immune checkpoint: Potential target for cancer therapy. *Journal of Cellular Physiology*. 234 (2), 1313–1325.
- [715] Li, C., Jiang, P., Wei, S., Xu, X., and Wang, J. (2020) Regulatory T cells in tumor microenvironment: new mechanisms, potential therapeutic strategies and future prospects. *Molecular Cancer* 2020 19:1. 19 (1), 1–23.
- [716] Rong, L., Li, R., Li, S., and Luo, R. (2016) Immunosuppression of breast cancer cells mediated by transforming growth factor- β in exosomes from cancer cells. *Oncology Letters*. 11 (1), 500–504.
- [717] Ostrand-Rosenberg, S., Sinha, P., Beury, D.W., and Clements, V.K. (2012) Cross-talk between myeloid-derived suppressor cells (MDSC), macrophages, and dendritic cells enhances tumor-induced immune suppression. *Seminars in Cancer Biology*. 22 (4), 275–281.
- [718] Mittal, S.K. and Roche, P.A. (2015) Suppression of antigen presentation by IL-10. *Current Opinion in Immunology*. 34 22–27.
- [719] Peggs, K.S., Quezada, S.A., Korman, A.J., and Allison, J.P. (2006) Principles and use of anti-CTLA4 antibody in human cancer immunotherapy. *Current Opinion in Immunology*. 18 (2), 206–213.
- [720] Gasser, S., Lim, L.H.K., and Cheung, F.S.G. (2017) The role of the tumour microenvironment

- in immunotherapy. *Endocrine-Related Cancer*. 24 (12), T283–T295.
- [721] Yeh, A.C. and Ramaswamy, S. (2015) Mechanisms of cancer cell dormancy-another hallmark of cancer? *Cancer Research*. 75 (23), 5014–5022.
- [722] Osisami, M. and Keller, E. (2013) Mechanisms of Metastatic Tumor Dormancy. *Journal of Clinical Medicine*. 2 (3), 136–150.
- [723] Park, S.Y. and Nam, J.S. (2020) The force awakens: metastatic dormant cancer cells. *Experimental and Molecular Medicine*. 52 (4), 569–581.
- [724] Eyles, J., Puaux, A.L., Wang, X., Toh, B., Prakash, C., Hong, M., et al. (2010) Tumor cells disseminate early, but immunosurveillance limits metastatic outgrowth, in a mouse model of melanoma. *Journal of Clinical Investigation*. 120 (6), 2030–2039.
- [725] Neophytou, C.M., Kyriakou, T.C., and Papageorgis, P. (2019) Mechanisms of metastatic tumor dormancy and implications for cancer therapy. *International Journal of Molecular Sciences*. 20 (24),.
- [726] Coradini, D., Casarsa, C., and Oriana, S. (2011) Epithelial cell polarity and tumorigenesis: New perspectives for cancer detection and treatment. *Acta Pharmacologica Sinica*. 32 (5), 552–564.
- [727] Dow, L.E. and Humbert, P.O. (2007) Polarity Regulators and the Control of Epithelial Architecture, Cell Migration, and Tumorigenesis. *International Review of Cytology*. 262 253–302.
- [728] Niessen, C.M. (2007) Tight junctions/adherens junctions: Basic structure and function. *Journal of Investigative Dermatology*. 127 (11), 2525–2532.
- [729] Coopman, P. and Djiane, A. (2016) Adherens Junction and E-Cadherin complex regulation by epithelial polarity. *Cellular and Molecular Life Sciences*. 73 (18), 3535–3553.
- [730] Vuoriluoto, K., Haugen, H., Kiviluoto, S., Mpindi, J.P., Nevo, J., Gjerdrum, C., et al. (2011) Vimentin regulates EMT induction by Slug and oncogenic H-Ras and migration by governing Axl expression in breast cancer. *Oncogene*. 30 (12), 1436–1448.
- [731] Westenend, P.J., Meurs, C.J.C., and Damhuis, R.A.M. (2005) Tumour size and vascular invasion predict distant metastasis in stage I cancer. Grade distinguishes early and late metastasis. *Journal of Clinical Pathology*. 58 (2), 196–201.
- [732] Mosiman, V.L., Patterson, B.K., Canterero, L., and Goolsby, C.L. (1997) Reducing cellular

- autofluorescence in flow cytometry: An in situ method. *Communications in Clinical Cytometry*. 30 (3), 151–156.
- [733] Grupillo, M., Lakomy, R., Geng, X., Styche, A., Rudert, W.A., Trucco, M., et al. (2011) An improved intracellular staining protocol for efficient detection of nuclear proteins in YFP-expressing cells. *BioTechniques*. 51 (6), 417–420.
- [734] Horimoto, Y., Polanska, U.M., Takahashi, Y., and Orimo, A. (2012) Emerging roles of the tumor-associated stroma in promoting tumor metastasis. *Cell Adhesion and Migration*. 6 (3), 193–203.
- [735] Khamis, Z.I., Sahab, Z.J., and Sang, Q.-X.A. (2012) Active Roles of Tumor Stroma in Breast Cancer Metastasis. *International Journal of Breast Cancer*. 2012 1–10.
- [736] NC3Rs (2020) The 3Rs | NC3Rs. *National Centre for the Replacement Refinement & Reduction of Animals in Research*.
- [737] Paget, S. (1889) the Distribution of Secondary Growths in Cancer of the Breast. *The Lancet*. 133 (3421), 571–573.
- [738] Barletta, K.E., Cagnina, R.E., Wallace, K.L., Ramos, S.I., Mehrad, B., and Linden, J. (2012) Leukocyte compartments in the mouse lung: Distinguishing between marginated, interstitial, and alveolar cells in response to injury. *Journal of Immunological Methods*. 375 (1–2), 100–110.
- [739] Kitamura, T., Doughty-Shenton, D., Cassetta, L., Frangkogianni, S., Brownlie, D., Kato, Y., et al. (2018) Monocytes differentiate to immune suppressive precursors of metastasis-associated macrophages in mouse models of metastatic breast cancer. *Frontiers in Immunology*. 8 (JAN), 17.
- [740] Bronte, V., Brandau, S., Chen, S.H., Colombo, M.P., Frey, A.B., Greten, T.F., et al. (2016) Recommendations for myeloid-derived suppressor cell nomenclature and characterization standards. *Nature Communications*. 7 (1), 1–10.
- [741] Cristofanilli, M., Thomas Budd, G., Ellis Baylor, M.J., Reuben, J.M., Hayes, D.F., Thomas Budd, G., et al. (2005) Circulating tumor cells: A novel prognostic factor for newly diagnosed metastatic breast cancer. *Journal of Clinical Oncology*. 23 (7), 1420–1430.
- [742] Jolly, T., Williams, G.R., Jones, E., and Muss, H.B. (2012) Treatment of metastatic breast cancer in women aged 65 years and older. *Women's Health*. 8 (4), 455–471.

- [743] Shibasaki, S., Jotoku, H., Watanabe, K., and Takahashi, M. (2011) Does primary tumor resection improve outcomes for patients with incurable advanced breast cancer? *Breast*. 20 (6), 543–547.
- [744] Liu, T., Zhang, X., Shang, M., Zhang, Y., Xia, B., Niu, M., et al. (2013) Dysregulated expression of Slug, vimentin, and E-cadherin correlates with poor clinical outcome in patients with basal-like breast cancer. *Journal of Surgical Oncology*. 107 (2), 188–194.
- [745] Elzamy, S., Badri, N., Padilla, O., Dwivedi, A.K., Alvarado, L.A., Hamilton, M., et al. (2018) Epithelial-Mesenchymal Transition Markers in Breast Cancer and Pathological Response after Neoadjuvant Chemotherapy. *Breast Cancer: Basic and Clinical Research*. 12 1178223418788074.
- [746] Kitamura, T., Qian, B.Z., and Pollard, J.W. (2015) Immune cell promotion of metastasis. *Nature Reviews Immunology*. 15 (2), 73–86.
- [747] Gil-Bernabé, A.M., Ferjančič, Š., Tlalka, M., Zhao, L., Allen, P.D., Im, J.H., et al. (2012) Recruitment of monocytes/macrophages by tissue factor-mediated coagulation is essential for metastatic cell survival and premetastatic niche establishment in mice. *Blood*. 119 (13), 3164–3175.
- [748] Palucka, K., Coussens, L.M., and O’Shaughnessy, J. (2013) Dendritic cells, inflammation, and breast cancer. *Cancer Journal (United States)*. 19 (6), 511–516.
- [749] Pedroza-Gonzalez, A., Xu, K., Wu, T.C., Asford, C., Tindle, S., Marches, F., et al. (2011) Thymic stromal lymphopoietin fosters human breast tumor growth by promoting type 2 inflammation. *Journal of Experimental Medicine*. 208 (3), 479–490.
- [750] Kroemer, G., Galluzzi, L., Kepp, O., and Zitvogel, L. (2013) Immunogenic cell death in cancer therapy. *Annual Review of Immunology*. 31 51–72.
- [751] Paul Ross, R., Morgan, S., and Hill, C. (2002) Preservation and fermentation: Past, present and future. *International Journal of Food Microbiology*. 79 (1–2), 3–16.
- [752] Geddes, A. (2008) 80th Anniversary of the discovery of penicillin. An appreciation of Sir Alexander Fleming. *International Journal of Antimicrobial Agents*. 32 (5), 373.
- [753] Cunningham, M., Azcarate-Peril, M.A., Barnard, A., Benoit, V., Grimaldi, R., Guyonnet, D., et al. (2021) Shaping the Future of Probiotics and Prebiotics. *Trends in Microbiology*. 29 (8), 667–685.

- [754] Davani-Davari, D., Negahdaripour, M., Karimzadeh, I., Seifan, M., Mohkam, M., Masoumi, S.J., et al. (2019) Prebiotics: Definition, types, sources, mechanisms, and clinical applications. *Foods*. 8 (3),.
- [755] Hill, C., Guarner, F., Reid, G., Gibson, G.R., Merenstein, D.J., Pot, B., et al. (2014) Expert consensus document: The international scientific association for probiotics and prebiotics consensus statement on the scope and appropriate use of the term probiotic. *Nature Reviews Gastroenterology and Hepatology*. 11 (8), 506–514.
- [756] de Simone, C. (2019) The Unregulated Probiotic Market. *Clinical Gastroenterology and Hepatology*. 17 (5), 809–817.
- [757] Aggarwal, N., Breedon, A.M.E., Davis, C.M., Hwang, I.Y., and Chang, M.W. (2020) Engineering probiotics for therapeutic applications: recent examples and translational outlook. *Current Opinion in Biotechnology*. 65 171–179.
- [758] Peran, L., Camuesco, D., Comalada, M., Nieto, A., Concha, A., Diaz-Ropero, M.P., et al. (2005) Preventative effects of a probiotic, *Lactobacillus salivarius* ssp. *salivarius*, in the TNBS model of rats colitis. *World Journal of Gastroenterology*. 11 (33), 5185–5192.
- [759] Martín, R. and Langella, P. (2019) Emerging health concepts in the probiotics field: Streamlining the definitions. *Frontiers in Microbiology*. 10 (MAY),.
- [760] Pharma, 4D (2020) A Study for Efficacy and Safety of Live Biotherapeutic MRx4DP0004 to Treat COVID-19 - Full Text View - [ClinicalTrials.gov](https://clinicaltrials.gov).
- [761] ActoGeniX (2008) A Phase 2a Study to Evaluate the Safety, Tolerability, Pharmacodynamics and Efficacy of AG011 in Ulcerative Colitis - Full Text View - . [ClinicalTrials.Gov](https://clinicaltrials.gov).
- [762] Pharma, 4D (n.d.) Live Biotherapeutic Product MRx0518 and Pembrolizumab Combination Study in Solid Tumors - Full Text View - [ClinicalTrials.gov](https://clinicaltrials.gov).
- [763] Ruiz, L., Delgado, S., Ruas-Madiedo, P., Sánchez, B., and Margolles, A. (2017) Bifidobacteria and their molecular communication with the immune system. *Frontiers in Microbiology*. 8 (DEC), 2345.
- [764] Jeon, S.G., Kayama, H., Ueda, Y., Takahashi, T., Asahara, T., Tsuji, H., et al. (2012) Probiotic *Bifidobacterium breve* induces IL-10-producing Tr1 cells in the colon. *PLoS Pathogens*. 8 (5), e1002714.
- [765] Yu, R., Zuo, F., Ma, H., and Chen, S. (2019) Exopolysaccharide-producing bifidobacterium

- adolescentis strains with similar adhesion property induce differential regulation of inflammatory immune response in Treg/Th17 axis of DSS-colitis mice. *Nutrients*. 11 (4), 782.
- [766] Sun, S., Luo, L., Liang, W., Yin, Q., Guo, J., Rush, A.M., et al. (2020) Bifidobacterium alters the gut microbiota and modulates the functional metabolism of T regulatory cells in the context of immune checkpoint blockade. *Proceedings of the National Academy of Sciences of the United States of America*. 117 (44), 27509–27515.
- [767] López, P., González-Rodríguez, I., Gueimonde, M., Margolles, A., and Suárez, A. (2011) Immune response to Bifidobacterium bifidum strains support Treg/Th17 plasticity. *PLoS ONE*. 6 (9), e24776.
- [768] López, P., González-Rodríguez, I., Sánchez, B., Gueimonde, M., Margolles, A., and Suárez, A. (2012) Treg-inducing membrane vesicles from Bifidobacterium bifidum LMG13195 as potential adjuvants in immunotherapy. *Vaccine*. 30 (5), 825–829.
- [769] Kim, J.H., Jeun, E.J., Hong, C.P., Kim, S.H., Jang, M.S., Lee, E.J., et al. (2016) Extracellular vesicle-derived protein from Bifidobacterium longum alleviates food allergy through mast cell suppression. *Journal of Allergy and Clinical Immunology*. 137 (2), 507-516.e8.
- [770] Shin, J.S. and Greer, A.M. (2015) The role of FcεRI expressed in dendritic cells and monocytes. *Cellular and Molecular Life Sciences*. 72 (12), 2349–2360.
- [771] Podolsky, S.H. (2012) Metchnikoff and the microbiome. *The Lancet*. 380 (9856), 1810–1811.
- [772] Mackowiak, P.A. (2013) Recycling Metchnikoff: Probiotics, the intestinal microbiome and the quest for long life. *Frontiers in Public Health*. 1 (NOV),.
- [773] McFarland, L. V. (2015) From yaks to yogurt: The history, development, and current use of probiotics. *Clinical Infectious Diseases*. 60 (suppl_2), S85–S90.
- [774] Khoruts, A., Hoffmann, D.E., and Britton, R.A. (2020) Probiotics: Promise, Evidence, and Hope. *Gastroenterology*. 159 (2), 409–413.
- [775] Rong, Y., Dong, Z., Hong, Z., Jin, Y., Zhang, W., Zhang, B., et al. (2017) Reactivity toward Bifidobacterium longum and Enterococcus hirae demonstrate robust CD8+ T cell response and better prognosis in HBV-related hepatocellular carcinoma. *Experimental Cell Research*. 358 (2), 352–359.
- [776] Lee, J.W., Shin, J.G., Kim, E.H., Kang, H.E., Yim, I.B., Kim, J.Y., et al. (2004) Immunomodulatory and antitumor effects in vivo by the cytoplasmic fraction of

Lactobacillus casei and Bifidobacterium longum. *Journal of Veterinary Science (Suwon-Si, Korea)*. 5 (1), 41–48.

- [777] Krepela (2010) Granzyme B-induced apoptosis in cancer cells and its regulation (Review). *International Journal of Oncology*. 37 (6),.
- [778] Thiele Orberg, E., Fan, H., Tam, A.J., Dejea, C.M., Destefano Shields, C.E., Wu, S., et al. (2017) The myeloid immune signature of enterotoxigenic *Bacteroides fragilis*-induced murine colon tumorigenesis. *Mucosal Immunology*. 10 (2), 421–433.
- [779] Penders, J., Thijs, C., Van Den Brandt, P.A., Kummeling, I., Snijders, B., Stelma, F., et al. (2007) Gut microbiota composition and development of atopic manifestations in infancy: The KOALA birth cohort study. *Gut*. 56 (5), 661–667.
- [780] De Zuani, M., Dal Secco, C., and Frossi, B. (2018) Mast cells at the crossroads of microbiota and IBD. *European Journal of Immunology*. 48 (12), 1929–1937.
- [781] Dabiri, S., Huntsman, D., Makretsov, N., Cheang, M., Gilks, B., Badjik, C., et al. (2004) The presence of stromal mast cells identifies a subset of invasive breast cancers with a favorable prognosis. *Modern Pathology: An Official Journal of the United States and Canadian Academy of Pathology, Inc.* 17 (6), 690–695.
- [782] Varricchi, G., Galdiero, M.R., Loffredo, S., Marone, G., Iannone, R., Marone, G., et al. (2017) Are mast cells MASTers in cancer? *Frontiers in Immunology*. 8 (APR), 424.
- [783] Mangia, A., Malfettone, A., Rossi, R., Paradiso, A., Ranieri, G., Simone, G., et al. (2011) Tissue remodelling in breast cancer: human mast cell tryptase as an initiator of myofibroblast differentiation. *Histopathology*. 58 (7), 1096–1106.
- [784] Vergara, D., Simeone, P., Damato, M., Maffia, M., Lanuti, P., and Trerotola, M. (2019) The Cancer Microbiota: EMT and Inflammation as Shared Molecular Mechanisms Associated with Plasticity and Progression. *Journal of Oncology*. 2019.

9 Abbreviations

¹ H-Nuclear Magnetic Resonance	¹ HNMR
2,4,6-trinitrobenzene sulfonic acid	TNBS
5-fluorouracil	5-FU
adenosine monophosphate	AMP
adenosine monophosphate activated protein kinase	AMPK
adenosine triphosphate	ATP
allophycocyanin	APC
alternatively activated macrophage	M2
alveolar macrophages	AM
analysis of variance	ANOVA
antigen binding fragments	Fab
antigen presenting cell	APC
aorta-gonad-mesonephros	AGM
azoxymethane	AOM
B-cell receptors	BCR
body mass index	BMI
bovine serum albumin	BSA
carboxyfluorescein diacetate succinimidyl ester	CFSE
CD40-ligand	CD40L
chemokine CC motif ligand	CCL
chitinase 3-like protein 1	CHI3L1
circulating tumour cell	CTC
classically activated macrophage	M1
cluster differentiation protein	CD
colony forming units	CFU
colorectal cancer	CRC
common lymphoid progenitor	CLP
conventional dendritic cell	cDC
cytotoxic T-lymphocyte associated protein 4	CTLA4
damage-associated molecular pattern	DAMP
dendritic cell	DC
deoxyuridine triphosphate	dUTP
dextran sulphate sodium	DSS
difference between means	DBM
differential gene expression	DGE
disseminated tumour cells	DTC
ductal carcinoma <i>in situ</i>	DCIS
D'ibacco's Modified Eagle Medium	DMEM
enzyme-linked immunosorbent assay	ELISA
Enzyme-linked Immunosorbent Assay	ELISA
epidermal growth factor receptors	EGFR
epithelial cadherin	E-cadherin
epithelial to mesenchymal transition	EMT
Ethylenediaminetetraacetic acid	EDTA

extracellular matrix	ECM
extracellular solute-binding protein	ESPB
<i>Faecalibaculum rodentium</i>	F. rod
false discovery rate	FDR
Fas-ligand	FasL
Firmicutes to Bacteroidetes ratio	F/B ratio
fluid shear stress	FSS
fluorescence minus one	FMO
FMS-like tyrosine kinase 3 ligand	FLT3L
foetal bovine serum	FBS
Food and Drug Administration	FDA
forkhead box P3	FoxP3
fragment crystallizable	Fc
gastrointestinal	GI
gene ontology	GO
G-protein coupled receptors	GPCR
granulocyte colony-stimulating factor	G-CSF
granulocyte-macrophage colony-stimulating factor	GM-CSF
granulocytic myeloid-derived suppressor cells	gMDSC
green fluorescent protein	GFP
haematopoietic stem cells	HSC
Hanks' buffered Salt Solution	HBSS
histone deacetylase	HDAC
histone deacetylase inhibitors	HDACi
hormone replacement therapies	HRT
horseradish peroxidase	HRP
human epidermal growth factor receptor	HER
human umbilical vascular endothelial cells	HUVEC
inflammatory bowel disease	IBD
interferon γ	IFN- γ
interleukin	IL
intraperitoneal	i.p.
irritable bowel syndrome	IBS
Janus kinase	JAK
killer Ig-like receptors	KIRs
Kruppel-like factor	KLF
<i>Lactobacillus casei</i> variety <i>rhamnosus</i>	Lcr35
lipopolysaccharides	LPS
live biotherapeutic product	LBP
lymphocyte antigen 6	Ly6
macrophage colony-stimulating factor	M-CSF
macrophage progenitor cells	MAMPC
major histocompatibility complex	MHC
major histocompatibility complex class I	MHC-I
major histocompatibility complex class II	MHC-II
mammary fat pad	MFP

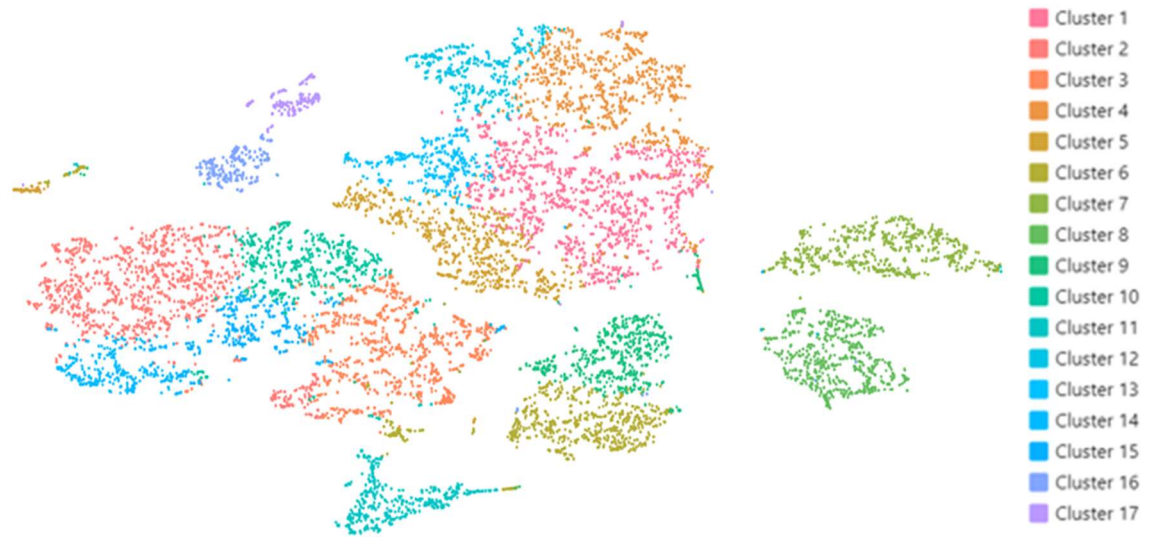
mast cell per mm ²	MC/mm ²
matrix Gla protein	MGP
matrix metalloproteinase	MMP
matrix metalloproteinase	MMP
median fluorescence intensity	MFI
Metastasis associated macrophages	MAM
methanol	MeOH
mitogen-activated protein kinase	MAPK
monocytic myeloid-derived suppressor cells	mMDSC
myeloid derived suppressor cell	MDSC
myeloid-derived suppressor cell	MDSC
natural killer	NK
nitric oxide	NO
nitric oxide synthase 2	NOS2
nuclear factor κ B	NF-κB
oestrogen receptor	ER
optical density	OD
over night	o/n
parts per million	ppm
passive faecal microbiota transplants	pFMT
pathogen-associated molecular pattern	PAMP
pattern recognition receptor	PRR
PBS 0.1% Tween-20	PBST
penicillin/streptomycin	Pen/Strep
Peptone Yeast Glucose	PYG
peripheral blood mononuclear cells	PBMCS
phosphate buffered saline	PBS
plasmacytoid dendritic cell	pDC
polymerase chain reaction	PCR
Principal components analysis	PCA
progesterone receptor	PR
programmed cell death ligand-1	PD-L1
programmed cell death protein-1	PD-1
proprietary Bifidobacterial cocktail	<i>Bif</i>
reactive oxygen species	ROS
red blood cell	RBC
Regions of interest	ROI
relative centrifugal force	rcf
resident macrophages	RMAC
ribonucleic acid	RNA
room temperature	RT
short-chain fatty acids	SCFA
signal transducer and activator of transcription	STAT
single cell	sc
single cell RNA sequencing	scRNA-seq
Sodium Dodecyl Sulfate	SDS

specified pathogen free	SPF
standard error from mean	SEM
stem cell factor	SCF
stem-cell factor	SCF
suppressor of cytokine signalling	SOCS
T-cell receptors	TCR
t-distributed stochastic neighbour embedding	t-SNE
terminal deoxynucleotidyl transferase	TdT
terminal deoxynucleotidyl transferase dUTP nick end labelling	TUNEL
Th	T-helper
Th1	T-helper 1
Th17	T-helper 17
Th2	T-helper 2
toll-like receptor	TLR
transforming growth factor β	TGF β
T-regulatory	T-reg
tumour necrosis factor α	TNF α
tumour-node-metastasis	TNM
uniform manifold approximation and projection	UMAP
unique molecular identifier	UMI
United Kingdom	UK
United States of America	USA
vancomycin, neomycin, metronidazole, amphotericin-B and ampicillin	VNMAA
vancomycin, neomycin, metronidazole, gentamycin and ampicillin	VNMGA
variable diversity joining	V(D)J
vascular endothelial growth factor	VEGF
vascular endothelial growth factor	VEGF
whole genome sequencing	WGS

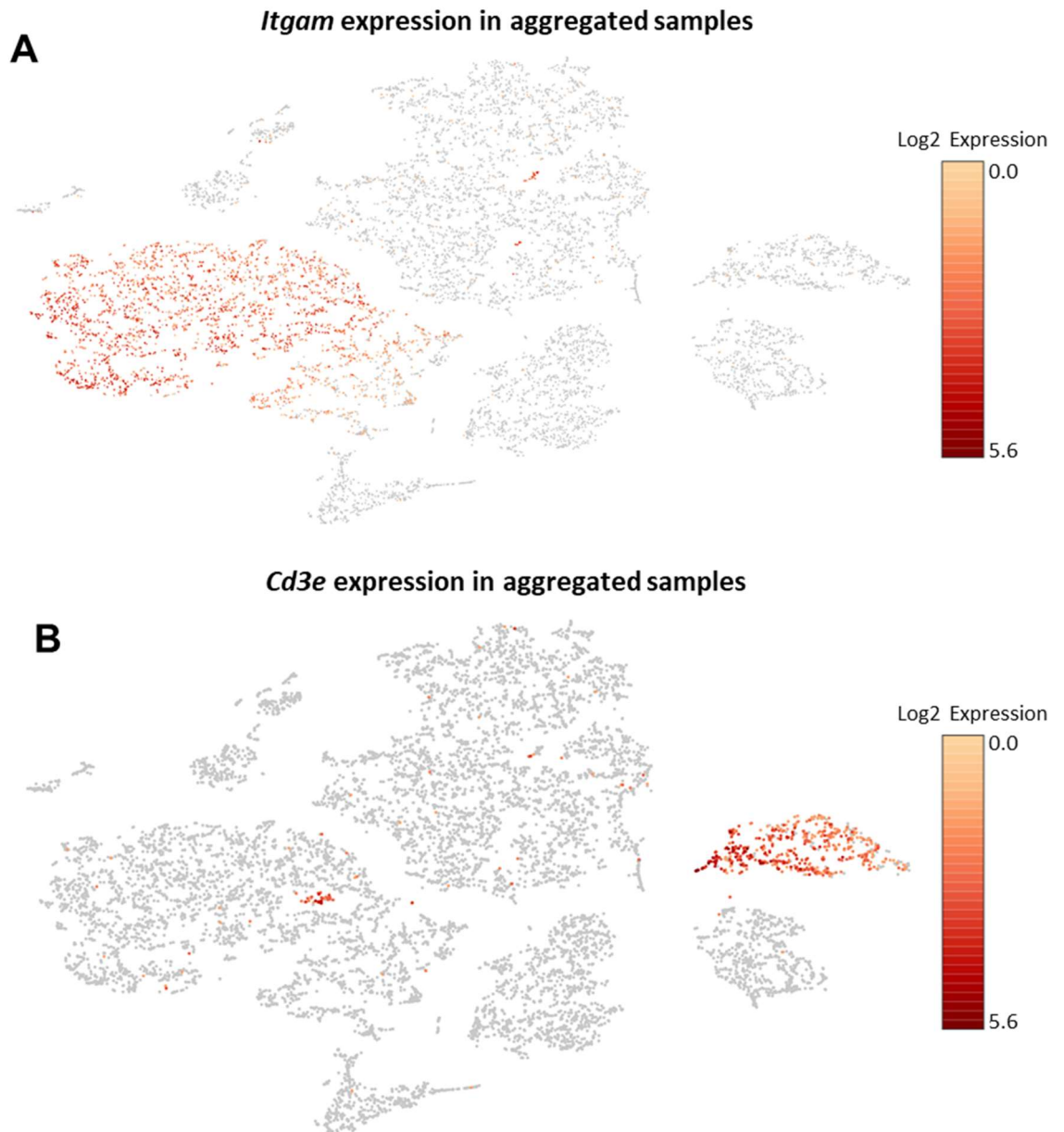
10 Supplementary Figures

Metabolite	Control Vs. VNMAA		Control Vs. Cephalixin		Difference between DBM for each analysis
	P-value	DBM	P-value	DBM	
Ornithine	0.036	1.922	0.996	0.060	1.862
Choline	0.044	7.717	0.951	-0.896	8.613
Dimethylamine	0.046	0.301	0.863	-0.060	0.362
Putrescine	0.027	1.622	0.995	-0.055	1.677
Maltose	0.019	-43.681	0.983	-2.477	-41.205
Glutamine	0.008	-17.085	0.215	-8.646	-8.440
Deoxyuridine	0.100	-0.651	0.005	-1.231	0.579
Tryptophan	0.003	-3.396	0.268	-1.392	-2.004
Caprylate	0.008	2.669	0.011	2.669	0.000
Urocanate	0.017	0.443	0.687	-0.119	0.562
Arabinose	0.282	4.637	0.040	-8.648	13.285
Leucine	0.003	-43.409	0.085	-24.721	-18.688
ABX system like citrate	0.037	10.404	0.252	-6.482	16.885
deoxy cytidine monoP	1.000	0.000	0.006	-40.475	40.475
Taurine	0.008	69.189	0.782	-13.174	82.364
Valine	0.002	-34.650	0.197	-14.644	-20.006
Isoleucine	0.001	-24.226	0.139	-10.713	-13.513
Stachyose	0.003	-615.030	1.000	0.000	-615.030
Niacinamide	0.003	-1.154	1.000	0.000	-1.154
2-Oxoisocaproate	0.002	1.764	0.979	-0.081	1.846
3-Hydroxyphenylacetate	0.004	0.737	0.433	-0.242	0.980
Fumarate	0.001	1.720	1.000	0.009	1.711
Trimethylamine	0.001	10.916	0.999	0.089	10.827
5-Aminopentanoate	0.000	9.343	0.057	4.588	4.756
Glutamate	0.000	102.995	0.381	26.141	76.854
Methylsuccinate	0.003	2.862	0.243	-1.211	4.073
Valerate	0.001	12.729	0.868	-1.345	14.074
2'-Deoxyadenosine	1.000	0.000	0.001	-6.385	6.385
Deoxythymidine triP	0.954	0.088	0.000	-1.741	1.829
Glucose	0.010	92.218	0.013	-94.442	186.660
Alanine	0.000	-62.108	0.457	-12.347	-49.760
Ribose	0.002	19.493	0.062	-11.815	31.308
Tyramine	0.000	2.250	0.593	0.359	1.892
3-Phenylpropionate	0.000	2.565	0.645	-0.428	2.993
Raffinose	0.000	-1412.536	1.000	0.000	-1412.536
Methylamine	0.002	1.074	0.039	-0.693	1.766
Sucrose	0.000	-62.514	0.991	-1.113	-61.400
Aspartate	0.000	-20.694	0.796	-1.760	-18.934
Pyruvate	0.000	33.878	0.961	-1.193	35.071
adenosine monoP	0.000	1.111	0.000	1.111	0.000
Hypoxanthine	0.000	17.842	0.871	1.107	16.734
Uracil	0.000	17.911	0.962	-0.596	18.507
2-methylbutyrate	0.000	2.380	0.003	1.064	1.316
Butyrate	0.000	288.828	0.178	-65.850	354.678
Xanthine	0.000	9.807	0.031	-3.693	13.500
Glucose-1-phosphate	0.000	-23.361	1.000	0.000	-23.361
Asparagine	0.000	-30.541	0.234	-4.809	-25.732
Nicotinate	0.000	9.926	0.306	1.105	8.821
Propionate	0.000	132.396	0.305	11.731	120.665
Acetate	0.000	725.850	0.122	-87.565	813.414

Supplementary Figure 3.9. Table showing output from 2-way ANOVA using Qlucore Omics Explorer with a pre-set q-value of ≥ 0.05 for multiple comparisons. Table present the significant P-values for comparisons between Control and VNMAA as well as Control and Cephalexin treatment groups and the difference between means (DBM) between the relevant groups. The difference between the DBMs highlight the similarity in the means between the treatment cohort comparisons. This aids in identifying metabolites which were reduced in both VNMAA and Cephalexin treatment cohorts relative to the control.



Supplementary Figure 4.1.1.1. Initial clustering of aggregated data by Loupe Cell Browser. The cells from the aggregated scRNA-seq datasets for tumour samples from both vehicle control and VNMAA treated animals was assigned to one 17 clusters using a t-SNE dimension reduction plot.



Supplementary Figure 4.1.1.2. Examples of marker gene searched to aid in cell type identification. The in-software search function in Loupe Cell Browser was used to search known marker genes to aid in identifying the cell types comprising each cluster. **A)** Expression of *Itgam* identifies a group of cells with a myeloid lineage. **B)** *Cd3e* expression identifies a group of cells with a lymphoid lineage.

Top 50 Upregulated Genes

Cluster 1	Cluster 2	Cluster 3	Cluster 4	Cluster 5	Cluster 6	Cluster 7
<i>Clu</i>	<i>Fcna</i>	<i>Napsa</i>	<i>Hist1h2ap</i>	<i>Cdh15</i>	<i>Mcpt2</i>	<i>Trbc2</i>
<i>Klk8</i>	<i>Folr2</i>	<i>Chil3</i>	<i>Ube2c</i>	<i>Cp</i>	<i>Iglc1</i>	<i>Trac</i>
<i>Bmp7</i>	<i>F13a1</i>	<i>Ccl17</i>	<i>Pimreg</i>	<i>Ibsp</i>	<i>Tpsb2</i>	<i>Cd3g</i>
<i>Krt18</i>	<i>Cbr2</i>	<i>Plac8</i>	<i>Pbk</i>	<i>Wisp2</i>	<i>Iglv1</i>	<i>Cd3d</i>
<i>Krt8</i>	<i>Stab1</i>	<i>Ltb4r1</i>	<i>Ccna2</i>	<i>Egfl7</i>	<i>Slpi</i>	<i>Cd3e</i>
<i>Prl2c3</i>	<i>Hpgds</i>	<i>Ramp3</i>	<i>Ccnb1</i>	<i>Plvap</i>	<i>Mcpt4</i>	<i>Lck</i>
<i>Perp</i>	<i>Npl</i>	<i>Mcemp1</i>	<i>Cdc20</i>	<i>Ddit4l</i>	<i>Cma1</i>	<i>Ms4a4b</i>
2200002D01Rik	<i>Ms4a7</i>	<i>S100a9</i>	<i>Birc5</i>	<i>Sparcl1</i>	<i>Ighg1</i>	<i>Lat</i>
<i>Lamc2</i>	<i>Selenop</i>	<i>S100a8</i>	<i>Aurkb</i>	<i>Fabp4</i>	<i>Igkv3-11</i>	<i>Cd28</i>
<i>Sfn</i>	<i>Fcrls</i>	<i>Ifitm6</i>	<i>Tubb4b</i>	<i>Dmp1</i>	<i>Mcpt1</i>	<i>Skap1</i>
<i>Padi4</i>	<i>Gas6</i>	<i>Ly6c2</i>	<i>Rrm2</i>	<i>Plpp3</i>	<i>Mzb1</i>	<i>Icos</i>
<i>Msln</i>	<i>Mrc1</i>	<i>F10</i>	<i>Plk1</i>	<i>Pdgfrb</i>	<i>Egfl7</i>	<i>Gimap3</i>
<i>Gm4610</i>	<i>Nxpe5</i>	<i>Ms4a4c</i>	<i>H2afx</i>	<i>Spry1</i>	<i>Jchain</i>	<i>Cd2</i>
<i>Ramp1</i>	<i>Frm4b</i>	<i>Clec4e</i>	<i>Cdk1</i>	<i>Sema5a</i>	<i>Mir6236</i>	<i>Itk</i>
<i>Add2</i>	<i>Maf</i>	<i>Ccr7</i>	<i>Cdca8</i>	<i>Tgfb2</i>	<i>Pecam1</i>	<i>Rit1</i>
<i>Tinag1l</i>	G530011O06Rik	<i>Il1r2</i>	<i>Racgap1</i>	<i>Col6a1</i>	<i>Rb1cc1</i>	<i>Cd247</i>
<i>Anxa8</i>	<i>Ccl12</i>	<i>Cytip</i>	<i>Kif20a</i>	<i>Pecam1</i>	<i>Cops5</i>	<i>Lef1</i>
<i>Dynap</i>	<i>Lyve1</i>	<i>Klrd1</i>	<i>Pclaf</i>	<i>Nrep</i>	<i>Arfgef1</i>	<i>Nkg7</i>
<i>Qrfp</i>	<i>Ccl8</i>	<i>H2-Eb1</i>	<i>Tk1</i>	<i>Jup</i>	<i>Mcm3</i>	<i>Cd8b1</i>
<i>Cda</i>	<i>Tnfaip8l2</i>	<i>Plbd1</i>	<i>Tpx2</i>	<i>Gadd45a</i>	<i>Gm28437</i>	<i>Satb1</i>
<i>Tmprss11e</i>	<i>Cela1</i>	<i>Nr4a3</i>	<i>Prc1</i>	<i>Igfbp7</i>	<i>Phf3</i>	<i>Cd5</i>
<i>Aldh2</i>	<i>P2ry6</i>	<i>Il1b</i>	<i>Tubb6</i>	<i>Cd34</i>	<i>Dst</i>	<i>Sh2d2a</i>
<i>Upp1</i>	<i>Rab3il1</i>	<i>H2-Aa</i>	<i>Tacc3</i>	<i>Camk2n1</i>	<i>Plekhh2</i>	<i>Ltb</i>
<i>Apol9b</i>	<i>Fcgr2b</i>	<i>Osm</i>	<i>Spc25</i>	<i>Nupr1</i>	<i>Arid5a</i>	<i>Dapl1</i>
<i>Ggct</i>	<i>Apoe</i>	<i>H2-Ab1</i>	<i>Hmmr</i>	<i>Slc20a1</i>	<i>Lman2l</i>	<i>Cd27</i>
<i>Hspb1</i>	<i>Wfdc17</i>	<i>Cxcl2</i>	<i>Cenpf</i>	<i>Mgp</i>	<i>Actr1b</i>	<i>Cd8a</i>
<i>Angptl4</i>	<i>C3ar1</i>	<i>Srgn</i>	<i>Top2a</i>	<i>Gpc1</i>	<i>Zap70</i>	<i>Txk</i>
<i>Acsbg1</i>	<i>Adgre1</i>	<i>Alox5ap</i>	<i>Cks2</i>	<i>Sdc2</i>	<i>Txndc9</i>	<i>Sh2d1a</i>
<i>Car9</i>	<i>Sirpa</i>	<i>Pmaip1</i>	<i>Spc24</i>	<i>Id3</i>	<i>Map4k4</i>	<i>Tox</i>
<i>Serpinb6a</i>	<i>Ccl7</i>	<i>Clec4d</i>	<i>Sgol2a</i>	<i>Ednra</i>	<i>Il1r1</i>	<i>Gimap6</i>
<i>Htra1</i>	<i>Lair1</i>	<i>H2-DMb2</i>	<i>Cdca3</i>	<i>Ly6c1</i>	<i>Tpp2</i>	<i>Ctla4</i>
<i>Eno3</i>	<i>Fcgrt</i>	<i>Cd74</i>	<i>Ccnb2</i>	<i>Adamts2</i>	<i>Cavin2</i>	<i>Zap70</i>
<i>Serpinb2</i>	<i>Mpeg1</i>	<i>B3gnt5</i>	<i>Nusap1</i>	<i>Fbn1</i>	<i>Myo1b</i>	<i>Nsg2</i>
<i>Cpe</i>	<i>Cd93</i>	<i>G0s2</i>	<i>Anln</i>	<i>Klf9</i>	<i>Gls</i>	<i>Tnfrsf4</i>
<i>Cystm1</i>	<i>Pf4</i>	<i>Pid1</i>	<i>Tubb3</i>	<i>Pik3ip1</i>	<i>Pgap1</i>	<i>Cd6</i>
<i>Anxa2</i>	<i>Cebpa</i>	<i>Gm45153</i>	<i>Diaph3</i>	<i>Grem1</i>	<i>Sf3b1</i>	<i>Il2rb</i>
<i>Cited2</i>	<i>Itga9</i>	<i>Ccr2</i>	<i>Ncapg</i>	<i>Col6a2</i>	<i>Sgol2a</i>	<i>Tnfrsf18</i>
<i>Mgst3</i>	<i>C1qc</i>	<i>Myo1g</i>	<i>Cenpe</i>	<i>Tcp11l2</i>	<i>Bzw1</i>	<i>Prkcq</i>
<i>S100a16</i>	<i>Trem2</i>	<i>Cd14</i>	<i>Smc2</i>	<i>Pla2g7</i>	<i>Clk1</i>	<i>Ptprcap</i>
<i>Tns4</i>	<i>Abcc3</i>	<i>Pkib</i>	<i>Tuba1c</i>	<i>Unc5b</i>	<i>Cflar</i>	<i>AC140209.1</i>
<i>Antxr2</i>	<i>Tifab</i>	<i>Gpr132</i>	<i>Asf1b</i>	<i>Med24</i>	<i>Nop58</i>	<i>Gimap4</i>
<i>Atg9b</i>	<i>Cd84</i>	<i>P2ry10</i>	<i>Kif23</i>	<i>Rbp1</i>	<i>Bmpr2</i>	<i>Ctsw</i>
<i>Crip2</i>	<i>C1qa</i>	<i>Bcl2a1d</i>	<i>Ckap2l</i>	<i>Plat</i>	<i>Nbeal1</i>	<i>Grap2</i>
<i>S100a10</i>	<i>Msr1</i>	<i>Rnase6</i>	<i>Cit</i>	<i>Fgfr1</i>	<i>Raph1</i>	<i>Izumo1r</i>
<i>Gfpt2</i>	<i>Csf1r</i>	<i>Slfn1</i>	<i>Tuba1a</i>	<i>Heg1</i>	<i>Nrp2</i>	<i>Themis</i>
<i>Hist1h2bc</i>	<i>Ccr1</i>	<i>Btg2</i>	<i>Cks1b</i>	<i>Rnf125</i>	<i>Klf7</i>	<i>Gimap1</i>
<i>Igfbp4</i>	<i>Gdf15</i>	<i>Nr4a1</i>	<i>Cenpw</i>	<i>Col4a1</i>	<i>Ikzf2</i>	<i>Gimap7</i>
<i>Hspb8</i>	<i>Fam213b</i>	<i>Cd7</i>	<i>Kif20b</i>	<i>Gng11</i>	<i>Atic</i>	<i>C230085N15Rik</i>
<i>S100a6</i>	<i>Slc7a8</i>	<i>Clec7a</i>	<i>H1fx</i>	<i>Fam43a</i>	<i>Igfbp5</i>	<i>Tespa1</i>
<i>Spns2</i>	<i>Ms4a6d</i>	<i>Thbs1</i>	<i>Tyms</i>	<i>Pxdn</i>	<i>Tmbim1</i>	<i>Tcf7</i>

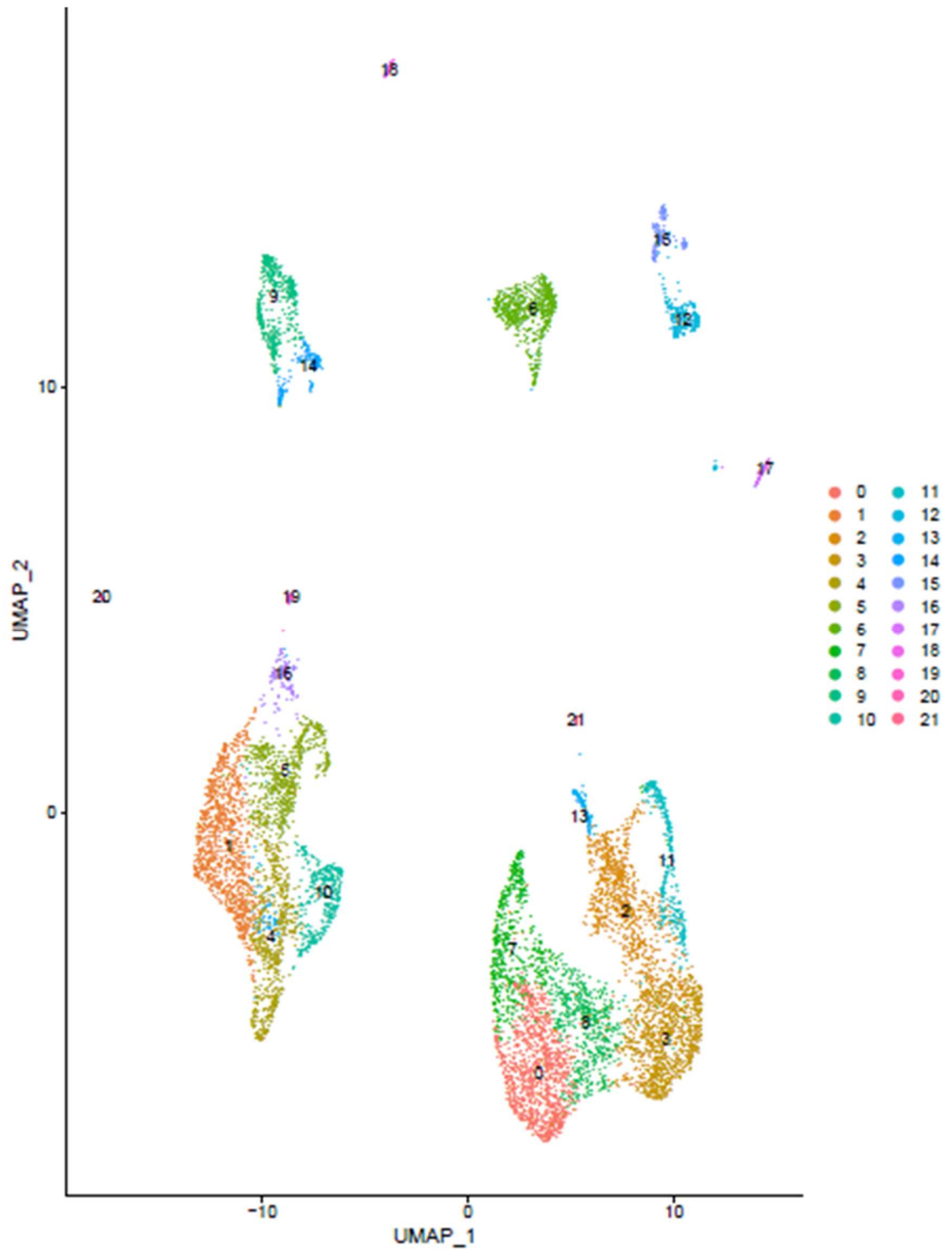
Top 50 Upregulated Genes

Cluster 8	Cluster 9	Cluster 10	Cluster 11	Cluster 12	Cluster 13	Cluster 14
<i>Fcmmr</i>	<i>Snhg6</i>	<i>Slc7a11</i>	<i>mt-Nd3</i>	<i>Cenpf</i>	<i>Tmprss11e</i>	<i>Ptpn7</i>
<i>Cd79a</i>	<i>Rpl7</i>	<i>Ccl24</i>	<i>mt-Cytb</i>	<i>Anln</i>	<i>Lamc2</i>	<i>Cbr2</i>
<i>Ighd</i>	<i>Eloc</i>	<i>Il1a</i>	<i>mt-Nd4</i>	<i>Kif11</i>	<i>Jag1</i>	<i>Stab1</i>
<i>Igll3</i>	<i>Gm28437</i>	<i>Mmp12</i>	<i>mt-Nd2</i>	<i>Top2a</i>	<i>Tns4</i>	<i>Ccl2</i>
<i>Igll2</i>	<i>Cox5b</i>	<i>Adamdec1</i>	<i>mt-Atp6</i>	<i>Cenpe</i>	<i>Spaca6</i>	<i>Fcrls</i>
<i>Ms4a1</i>	<i>Actr1b</i>	<i>Nlrp3</i>	<i>mt-Nd1</i>	<i>Kif20b</i>	<i>Padi4</i>	<i>Rab3il1</i>
<i>Fcer2a</i>	<i>Mrpl30</i>	<i>Mmp13</i>	<i>mt-Co3</i>	<i>Prc1</i>	<i>Qrpf</i>	<i>Dok2</i>
<i>Igkc</i>	<i>Pdcl3</i>	<i>Hilpda</i>	<i>mt-Co2</i>	<i>Mki67</i>	<i>Bmp7</i>	<i>Clec5a</i>
<i>Ighm</i>	<i>Rpl31</i>	<i>Ifitm1</i>	<i>mt-Rnr1</i>	<i>Kn11</i>	<i>Btc</i>	<i>Ccl12</i>
<i>Cd79b</i>	<i>Cavin2</i>	<i>Il1b</i>	<i>mt-Co1</i>	<i>Sgol2a</i>	<i>Gm14636</i>	<i>C5ar1</i>
<i>Ly6d</i>	<i>Hspd1</i>	<i>Cxcl2</i>	<i>mt-Atp8</i>	<i>Kif15</i>	<i>Ogt</i>	<i>P2ry6</i>
<i>Cd19</i>	<i>Hspe1</i>	<i>Cxcl1</i>	<i>mt-Nd4l</i>	<i>Gm42047</i>	<i>Nptx1</i>	<i>Slamf9</i>
<i>Tnfrsf13c</i>	<i>Sgol2a</i>	<i>Nrg1</i>	<i>mt-Nd5</i>	<i>Kif23</i>	<i>Atg9b</i>	<i>Olfm1</i>
<i>Mzb1</i>	<i>Bzw1</i>	<i>Ccrl2</i>	<i>mt-Rnr2</i>	<i>Ncapg</i>	<i>Asap2</i>	<i>Ccl7</i>
<i>Pax5</i>	<i>Sumo1</i>	<i>Itgax</i>	<i>Gm28437</i>	<i>Diaph3</i>	<i>Add2</i>	<i>Cfp</i>
<i>H2-Ob</i>	<i>Eef1b2</i>	<i>Il1r2</i>	<i>mt-Nd6</i>	<i>Cit</i>	<i>Car9</i>	<i>Inpp5d</i>
<i>Fcrla</i>	<i>Rpl10a-ps1</i>	<i>Nr4a3</i>	<i>Mir6236</i>	<i>Hmmr</i>	<i>Prl2c3</i>	<i>Mrc1</i>
<i>Cr2</i>	<i>Atic</i>	<i>Cd14</i>	<i>Lars2</i>	<i>Smc2</i>	<i>Arhgap6</i>	<i>Gm43305</i>
<i>Bank1</i>	<i>Rpl37a</i>	<i>Csf2rb</i>	<i>Zap70</i>	<i>Ulbp1</i>	<i>Peak1</i>	<i>Pf4</i>
<i>Gm31243</i>	<i>Tuba4a</i>	<i>Cd83</i>	<i>Icos</i>	<i>Plk4</i>	<i>Cadm1</i>	<i>Al662270</i>
<i>Vpreb3</i>	<i>Ncl</i>	<i>Clec7a</i>	<i>Gm38365</i>	<i>Smc4</i>	<i>Itpr3</i>	<i>Clec4a2</i>
<i>Pou2af1</i>	<i>Ptma</i>	<i>Rgs1</i>	<i>Sned1</i>	<i>Ube2c</i>	<i>Ahnak</i>	<i>Pycard</i>
<i>Cd37</i>	<i>Ndufa10</i>	<i>Pde4b</i>	<i>Pdcd1</i>	<i>Nusap1</i>	<i>Tnik</i>	<i>Elmo1</i>
<i>Bcl11a</i>	<i>Cops9</i>	<i>Ocstamp</i>	<i>Fcmmr</i>	<i>Tpx2</i>	<i>Sox9</i>	<i>Adgre1</i>
<i>Gm30211</i>	<i>Sned1</i>	<i>Thbs1</i>	<i>Prelp</i>	<i>Ncapd2</i>	<i>Ccdc88c</i>	<i>Dock2</i>
<i>Gm8369</i>	<i>Bok</i>	<i>Cd74</i>	<i>E330020D12Rik</i>	<i>E2f8</i>	<i>Myof</i>	<i>Ms4a6c</i>
<i>Spib</i>	<i>Dtymk</i>	<i>Fcgr4</i>	<i>Dnm3os</i>	<i>Rad18</i>	<i>Afap1</i>	<i>Alox5ap</i>
<i>Cxcr5</i>	<i>Pdcd1</i>	<i>Trf</i>	<i>Sell</i>	<i>Ccnb1</i>	<i>Man1a</i>	<i>Slc7a8</i>
<i>BE692007</i>	<i>Pam</i>	<i>Jaml</i>	<i>Rcsd1</i>	<i>Incenp</i>	<i>Acsbg1</i>	<i>Lyl1</i>
<i>Siglecg</i>	<i>Kdsr</i>	<i>Gpr132</i>	<i>lfi206</i>	<i>Cep192</i>	<i>Rapgef3</i>	<i>F13a1</i>
<i>H2-Oa</i>	<i>Dbi</i>	<i>Slc15a3</i>	<i>lfi214</i>	<i>Dbf4</i>	<i>Gpr149</i>	<i>Wdfy4</i>
<i>Ikzf3</i>	<i>Snrpe</i>	<i>Il1rn</i>	<i>lfi209</i>	<i>Pbk</i>	<i>Lgr6</i>	<i>Myo1f</i>
<i>Blk</i>	<i>Adipor1</i>	<i>H2-DMb1</i>	<i>Grem2</i>	<i>Ckap2l</i>	<i>Perp</i>	<i>Msr1</i>
<i>Srpk3</i>	<i>Timm17a</i>	<i>H2-Ab1</i>	<i>Kif26b</i>	<i>Cdk1</i>	<i>Slco2a1</i>	<i>C1qc</i>
<i>Gm42870</i>	<i>Csrp1</i>	<i>Cd274</i>	<i>Gm37033</i>	<i>Atad2</i>	<i>Dock9</i>	<i>Maf</i>
<i>Fcrl1</i>	<i>Tnnt2</i>	<i>H2-Aa</i>	<i>G0s2</i>	<i>Ckap5</i>	<i>Utrn</i>	<i>Nrros</i>
<i>Cd22</i>	<i>Glrx2</i>	<i>Mgl2</i>	<i>Cr2</i>	<i>Pimreg</i>	<i>Cep170</i>	<i>Fam105a</i>
<i>Btla</i>	<i>Uchl5</i>	<i>Trem1</i>	<i>Prkcq</i>	<i>Hjurp</i>	<i>Kdm5b</i>	<i>Folr2</i>
<i>Ptprcap</i>	<i>Mrps14</i>	<i>Tspan13</i>	<i>Egfl7</i>	<i>Cks2</i>	<i>Nfat5</i>	<i>Rassf4</i>
<i>Gm4759</i>	<i>Cacybp</i>	<i>Lag3</i>	<i>Sh2d1a</i>	<i>Aurkb</i>	<i>Ghr</i>	<i>Fcgr1</i>
<i>Cd55</i>	<i>Gas5</i>	<i>Zmynd15</i>	<i>Srpk3</i>	<i>Birc5</i>	<i>Pthlh</i>	<i>Syce2</i>
<i>Ebf1</i>	<i>Prdx6</i>	<i>Arl5c</i>	<i>Xist</i>	<i>Cdca8</i>	<i>Clu</i>	<i>C1qb</i>
<i>Stap1</i>	<i>Dnm3os</i>	<i>Prdm1</i>	<i>Srpx2</i>	<i>Kif20a</i>	<i>Cd44</i>	<i>Ccr2</i>
<i>H2-DMb2</i>	<i>Mgst3</i>	<i>H2-Eb1</i>	<i>Fcrl1</i>	<i>Topbp1</i>	<i>Frm4a</i>	<i>Cyth4</i>
<i>Hvcn1</i>	<i>Rgs5</i>	<i>Malt1</i>	<i>Sh2d2a</i>	<i>Racgap1</i>	<i>Pbx1</i>	<i>Hcls1</i>
<i>5830444F18Rik</i>	<i>Ddr2</i>	<i>Nfil3</i>	<i>Fam189b</i>	<i>Ccna2</i>	<i>Mllt3</i>	<i>Ntpcr</i>
<i>Gpr18</i>	<i>Ndufs2</i>	<i>Mmp9</i>	<i>S100a8</i>	<i>Plk1</i>	<i>Tfap2a</i>	<i>C1qa</i>
<i>Sell</i>	<i>Ufc1</i>	<i>Plxdc2</i>	<i>S100a9</i>	<i>Btc</i>	<i>Slc25a37</i>	<i>Tifab</i>
<i>Satb1</i>	<i>Tagln2</i>	<i>Crem</i>	<i>Gm15472</i>	<i>Spc25</i>	<i>Cpe</i>	<i>Pid1</i>
<i>Clec2i</i>	<i>Fh1</i>	<i>Cxcl16</i>	<i>Gm31243</i>	<i>Spc24</i>	<i>Flt1</i>	<i>Cd180</i>

Top 50 Upregulated Genes

Cluster 15	Cluster 16	Cluster 17
<i>Ccr2</i>	<i>Meg3</i>	<i>Sulf1</i>
<i>F10</i>	<i>Col1a2</i>	<i>Col3a1</i>
<i>Arg1</i>	<i>Mfap5</i>	<i>Col5a2</i>
<i>Ltb4r1</i>	<i>Col5a2</i>	<i>Col6a3</i>
<i>Mcemp1</i>	<i>Col1a1</i>	<i>Prrx1</i>
<i>Pygl</i>	<i>Postn</i>	<i>Serping1</i>
<i>Acp5</i>	<i>Rian</i>	<i>Fibin</i>
<i>Bcl2a1a</i>	<i>Fibin</i>	<i>Cpxm1</i>
<i>Cfp</i>	<i>Lox</i>	<i>Postn</i>
<i>H2-DMb1</i>	<i>Col15a1</i>	<i>Mfap2</i>
<i>Sirpb1c</i>	<i>Lrrc15</i>	<i>Col1a2</i>
<i>Alox5ap</i>	<i>Thy1</i>	<i>Mfap5</i>
<i>Bcl2a1d</i>	<i>Crabp1</i>	<i>Dcn</i>
<i>Clec5a</i>	<i>Col3a1</i>	<i>Lum</i>
<i>Napsa</i>	<i>Col6a3</i>	<i>Mmp2</i>
<i>Ncf4</i>	<i>Col12a1</i>	<i>Thy1</i>
<i>H2-Ab1</i>	<i>Cthrc1</i>	<i>Tagln</i>
<i>Cyp4f18</i>	<i>Mmp23</i>	<i>Col12a1</i>
<i>Mgl2</i>	<i>Pla1a</i>	<i>Mfap4</i>
<i>Tgfb1</i>	<i>Lum</i>	<i>Col1a1</i>
<i>Ucp2</i>	<i>Ccdc80</i>	<i>Meg3</i>
<i>Ccl6</i>	<i>Rarres2</i>	<i>Cthrc1</i>
<i>Ifi30</i>	<i>Tagln</i>	<i>Lrrc15</i>
<i>Olfm1</i>	<i>Col27a1</i>	<i>Pla1a</i>
<i>Plbd1</i>	<i>Spon1</i>	<i>Ccdc80</i>
<i>Lyz2</i>	<i>Rcn3</i>	<i>Lox</i>
<i>Scimp</i>	<i>Tmem45a</i>	<i>Pcsk5</i>
<i>Pilra</i>	<i>Dcn</i>	<i>Col15a1</i>
<i>H2-Eb1</i>	<i>Aspn</i>	<i>Loxl2</i>
<i>Csf2ra</i>	<i>Mfap4</i>	<i>Cygb</i>
<i>Pycard</i>	<i>Svep1</i>	<i>Nid1</i>
<i>Ccl9</i>	<i>Dnm3os</i>	<i>Crlf1</i>
<i>Fgr</i>	<i>Cpxm1</i>	<i>Cpxm2</i>
<i>Slamf9</i>	<i>Prrx1</i>	<i>Aspn</i>
<i>Bcl2a1b</i>	<i>Nfatc4</i>	<i>Dpt</i>
<i>Hcls1</i>	<i>Cpxm2</i>	<i>Ndufa4l2</i>
<i>Coro1a</i>	<i>Gpx7</i>	<i>Fkbp10</i>
<i>Cd74</i>	<i>Pcsk5</i>	<i>Rarres2</i>
<i>Emilin2</i>	<i>Acta2</i>	<i>Itm2a</i>
<i>Dok2</i>	<i>Fxyd6</i>	<i>Tmem45a</i>
<i>Cd52</i>	<i>Eln</i>	<i>Fndc1</i>
<i>Pid1</i>	<i>Sfrp1</i>	<i>Abi3bp</i>
<i>H2-Aa</i>	<i>Col6a2</i>	<i>Slit3</i>
<i>Clec4a2</i>	<i>Crispld2</i>	<i>C1s1</i>
<i>Itgb2</i>	<i>Gm38211</i>	<i>Spon1</i>
<i>Itgam</i>	<i>Serping1</i>	<i>Ccl11</i>
<i>Pld4</i>	<i>Fkbp10</i>	<i>Svep1</i>
<i>Hck</i>	<i>Grem2</i>	<i>Islr</i>
<i>Ctss</i>	<i>Dcl1</i>	<i>Cdh11</i>
<i>Slc11a1</i>	<i>Crlf1</i>	<i>Lrrc17</i>

Supplementary Figure 4.1.1.3 Upregulated genes defining respective cell clusters. Table showing the top 50 most highly expressed genes in each cluster relative to all other clusters which were subsequently used in GO searches to identify the cell types comprising each cluster.



Supplementary Figure 4.1.2.1. UMAP clustering of aggregated scRNA-seq data sets for cells from control and VNMAA tumour samples. Bioinformatic analysis assigned all cells sequenced to one of 21 clusters using UMAP dimension reduction based on gene expression relative to other cells.

Macrophages				C1qc Macrophages			
Gene ID	Control	VNMAA	Differential Expression	Gene ID	Control	VNMAA	Differential Expression
<i>Ccl24</i>	3.03	1.86	1.17	<i>Igk1</i>	2.00	0.00	2.00
<i>Rps28</i>	2.17	2.83	0.66	<i>Ighg1</i>	1.80	0.00	1.80
<i>Mmp13</i>	2.27	1.72	0.55	<i>S100a9</i>	1.11	0.00	1.11
<i>Mmp9</i>	2.24	1.71	0.53	<i>Ccl8</i>	2.06	1.02	1.04
<i>Ifitm1</i>	3.53	3.00	0.53	<i>S100a8</i>	0.97	0.01	0.96
<i>Mmp12</i>	2.02	1.53	0.49	<i>Spp1</i>	2.52	3.20	0.69
<i>Ifitm3</i>	2.89	2.40	0.49	<i>Rps28</i>	1.97	2.65	0.68
<i>mt-Atp6</i>	1.63	2.11	0.48	<i>mt-Atp6</i>	2.69	3.36	0.67
<i>Rpl38</i>	2.55	3.03	0.48	<i>Cd74</i>	3.09	2.44	0.65
<i>Cxcl9</i>	0.45	0.01	0.44	<i>Mmp9</i>	0.83	0.20	0.63

Lyz1 Macrophages				T-cells			
Gene ID	Control	VNMAA	Differential Expression	Gene ID	Control	VNMAA	Differential Expression
<i>Plac8</i>	2.19	1.24	0.95	<i>Gzmf</i>	0.00	1.80	1.80
<i>Rps28</i>	2.03	2.78	0.75	<i>Igkc</i>	1.83	0.13	1.70
<i>Slpi</i>	1.99	1.33	0.66	<i>Ighg1</i>	1.47	0.00	1.47
<i>S100a9</i>	3.52	2.87	0.65	<i>Gzma</i>	1.17	0.00	1.17
<i>S100a8</i>	3.38	2.75	0.63	<i>Mcpt1</i>	1.13	0.00	1.13
<i>AC160336.1</i>	1.16	1.77	0.61	<i>Il1b</i>	1.02	0.21	0.80
<i>mt-Atp6</i>	1.32	1.91	0.59	<i>Gzmd</i>	0.00	0.77	0.77
<i>Hdc</i>	1.58	1.01	0.58	<i>Gm11808</i>	0.50	1.25	0.75
<i>Rpl38</i>	2.56	3.11	0.55	<i>Ly6a</i>	1.71	1.00	0.71
<i>Gm11808</i>	0.29	0.84	0.55	<i>Rps27rt</i>	0.91	1.60	0.69

B-cells				Cst3 Dendritic Cells			
Gene ID	Control	VNMAA	Differential Expression	Gene ID	Control	VNMAA	Differential Expression
<i>Ighg2c</i>	1.60	0.00	1.60	<i>Cxcl9</i>	1.78	0.19	1.59
<i>Ighg1</i>	1.54	0.00	1.54	<i>Siglech</i>	1.12	0.00	1.12
<i>Ly6a</i>	2.33	1.18	1.15	<i>Ly6a</i>	1.67	0.62	1.05
<i>Jchain</i>	1.11	0.00	1.11	<i>Ly6d</i>	1.30	0.28	1.02
<i>Rps27rt</i>	0.96	1.87	0.92	<i>Cox6a2</i>	1.13	0.18	0.95
<i>Ifit3</i>	0.96	0.11	0.85	<i>Ly6c2</i>	1.22	0.33	0.89
<i>Gm11808</i>	0.56	1.35	0.79	<i>Bst2</i>	2.06	1.17	0.89
<i>Irf7</i>	1.11	0.35	0.76	<i>Ctsl</i>	1.67	0.82	0.85
<i>Ifi27l2a</i>	2.59	1.88	0.71	<i>Irf8</i>	2.24	1.45	0.79
<i>Stat1</i>	1.22	0.51	0.71	<i>Cd8b1</i>	0.79	0.02	0.76

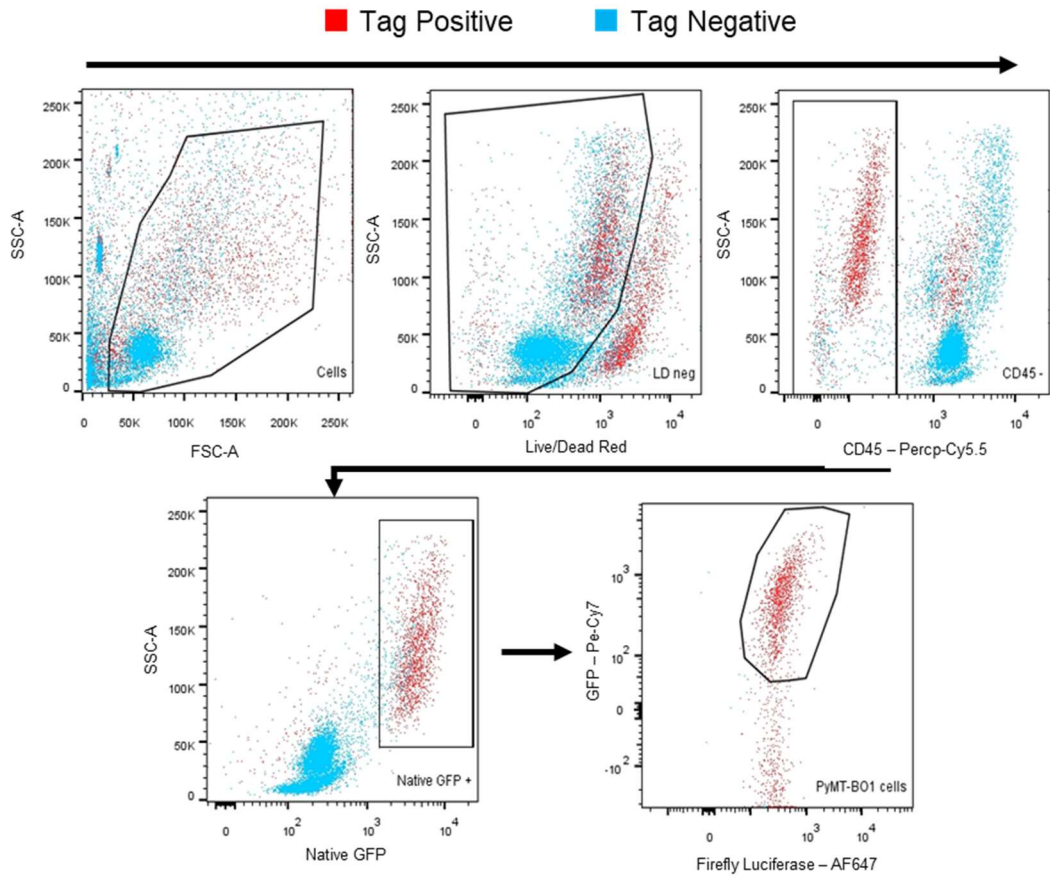
Fscn1 Dendritic Cells				Fibroblasts			
Gene ID	Control	VNMAA	Differential Expression	Gene ID	Control	VNMAA	Differential Expression
<i>Rrad</i>	1.80	0.28	1.52	<i>Rps28</i>	1.97	2.65	0.69
<i>Apol7c</i>	1.64	0.38	1.25	<i>Mt1</i>	1.09	1.68	0.58
<i>Jun</i>	2.56	1.55	1.01	<i>Rpl38</i>	2.55	3.04	0.50
<i>Rps27rt</i>	0.37	1.37	1.01	<i>mt-Atp6</i>	1.46	1.94	0.48
<i>Klf2</i>	1.05	0.05	1.00	<i>AC160336.1</i>	0.59	1.06	0.47
<i>Stk17b</i>	1.09	0.11	0.98	<i>Rpl36al</i>	1.30	1.72	0.43
<i>mt-Rnr1</i>	1.93	2.92	0.98	<i>Cx3cr1</i>	0.60	1.02	0.41
<i>Rps28</i>	2.04	3.02	0.98	<i>Fos</i>	1.43	1.02	0.41
<i>Tnfrsf9</i>	1.26	2.23	0.97	<i>Rps29</i>	3.09	3.49	0.40
<i>Serpinb1a</i>	1.00	0.05	0.95	<i>Rps27rt</i>	0.34	0.73	0.39

Luminal Cell 1				Luminal Cell 2			
Gene ID	Control	VNMAA	Differential Expression	Gene ID	Control	VNMAA	Differential Expression
<i>Rps28</i>	1.98	2.59	0.62	<i>Ltf</i>	0.00	2.90	2.90
<i>Fos</i>	1.11	0.56	0.55	<i>Mgp</i>	0.77	2.93	2.16
<i>Mt1</i>	1.58	2.07	0.49	<i>Sprr1a</i>	2.11	0.04	2.07
<i>mt-Atp6</i>	1.50	1.93	0.42	<i>Mt2</i>	2.33	0.56	1.76
<i>Lyz2</i>	0.51	0.93	0.42	<i>Clca3a2</i>	1.71	0.00	1.71
<i>AC160336.1</i>	0.57	0.97	0.40	<i>Neat1</i>	4.27	2.55	1.71
<i>Cx3cr1</i>	0.32	0.72	0.40	<i>Mt1</i>	3.43	1.80	1.63
<i>Jun</i>	1.84	1.44	0.40	<i>Atf3</i>	2.60	1.02	1.58
<i>Rpl38</i>	2.61	2.99	0.38	<i>Fgg</i>	1.51	0.00	1.51
<i>mt-Nd3</i>	1.54	1.90	0.36	<i>Csnk1g1</i>	0.30	1.76	1.46

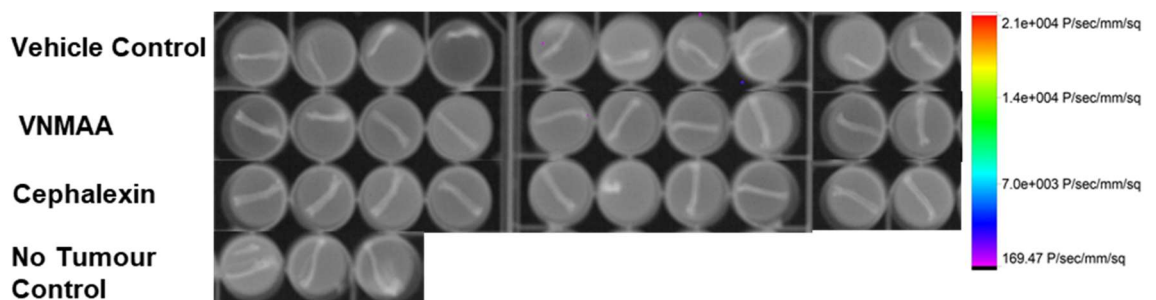
Proliferating Cell				Stromal Cells			
Gene ID	Control	VNMAA	Differential Expression	Gene ID	Control	VNMAA	Differential Expression
<i>Rps28</i>	1.87	2.45	0.58	<i>Glycam1</i>	1.19	0.00	1.19
<i>Mt1</i>	1.14	1.58	0.44	<i>Fabp4</i>	2.56	1.55	1.01
<i>mt-Atp6</i>	1.40	1.82	0.41	<i>Egfl7</i>	1.35	0.48	0.87
<i>Rpl38</i>	2.38	2.78	0.40	<i>Cxcl14</i>	2.46	1.61	0.85
<i>Fos</i>	0.59	0.20	0.39	<i>Igfbp3</i>	1.82	0.97	0.85
<i>Egr1</i>	0.81	0.43	0.38	<i>Col15a1</i>	2.12	1.34	0.78
<i>AC160336.1</i>	0.73	1.10	0.36	<i>Postn</i>	3.34	2.56	0.78
<i>Rps29</i>	3.01	3.34	0.33	<i>Igfbp7</i>	3.14	2.36	0.78
<i>Rpl37rt</i>	0.34	0.66	0.32	<i>Krt8</i>	1.51	2.28	0.77
<i>Mt2</i>	0.36	0.67	0.31	<i>Plvap</i>	1.25	0.49	0.77

Col3a1 Stromal Cells				Stressed Cells			
Gene ID	Control	VNMAA	Differential Expression	Gene ID	Control	VNMAA	Differential Expression
<i>Rps28</i>	2.02	2.81	0.78	<i>Rnd1</i>	1.51	0.02	1.49
<i>Fos</i>	1.56	0.79	0.77	<i>Lyz2</i>	0.04	1.52	1.47
<i>Mgp</i>	2.32	2.94	0.62	<i>Ntn1</i>	1.58	0.21	1.37
<i>mt-Atp6</i>	1.31	1.90	0.59	<i>Steap4</i>	1.73	0.42	1.31
<i>Ibsp</i>	2.05	1.49	0.55	<i>Htra3</i>	1.83	0.58	1.25
<i>Rpl37rt</i>	0.44	0.99	0.55	<i>Usmg5</i>	1.13	2.32	1.19
<i>Gm8624</i>	0.36	0.90	0.54	<i>Ptpre</i>	1.40	0.22	1.18
<i>Eln</i>	0.06	0.56	0.51	<i>Cd74</i>	2.22	1.04	1.18
<i>Cx3cr1</i>	0.45	0.95	0.50	<i>AC160336.1</i>	0.24	1.42	1.18
<i>Rps27rt</i>	0.31	0.81	0.50	<i>Mst1r</i>	1.57	0.41	1.16

Supplementary Figure 4.1.2.2. Tables comparing the most differentially expressed genes between treatment conditions for each of the 14 cell-type clusters. Differential expression was only considered different when the difference between the two conditions was ≥ 2 . Only C1qC Macrophages and the luminal cell 2 clusters exhibited genes which were significantly differentially expressed and those are highlighted in green.

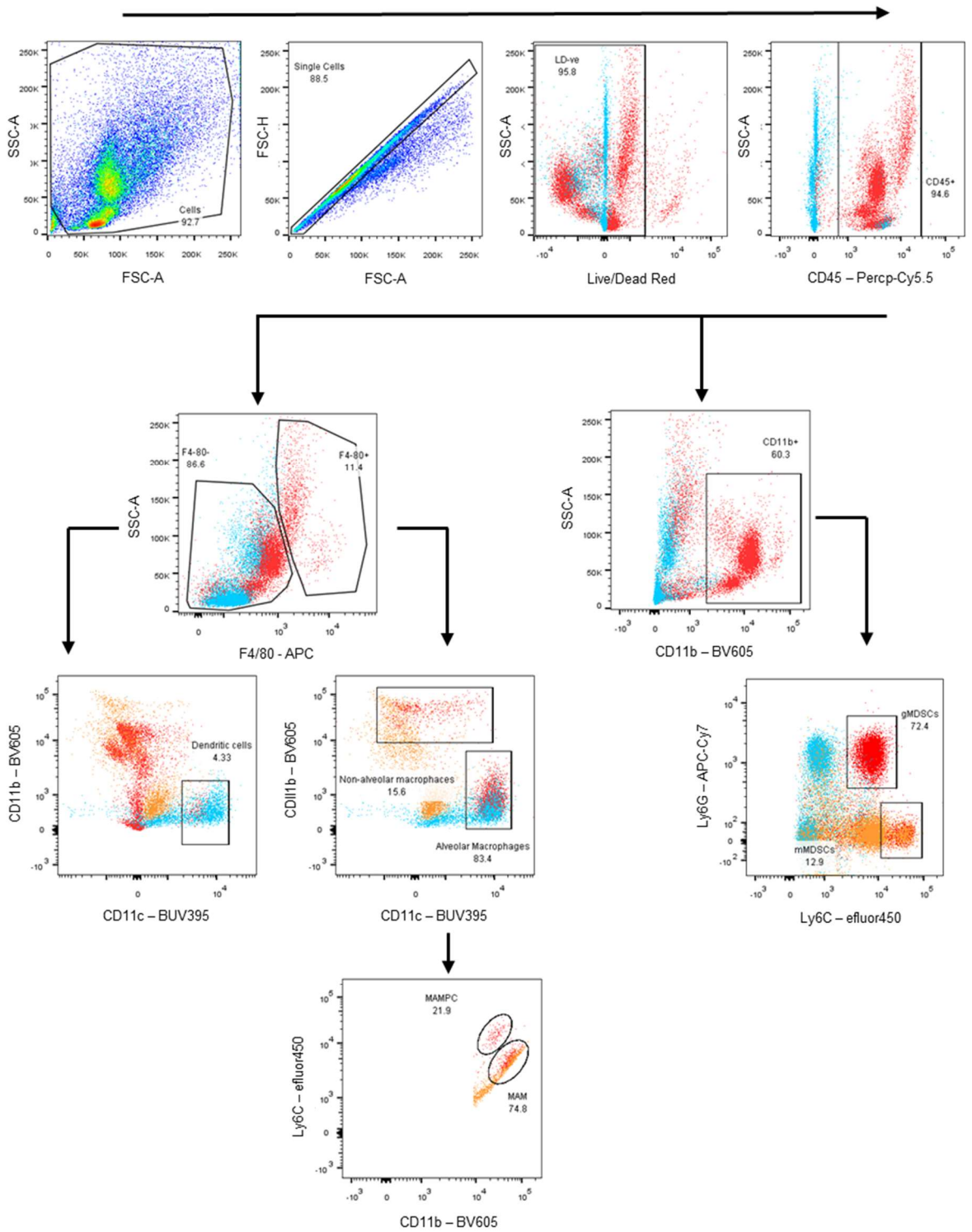


Supplementary Figure 5.2.2. Gating strategy for identification of PyMT-BO1 populations in blood and lung tissues. Lung tissues spiked with either tag positive (red) or tag negative (Blue) PyMT-BO1 cells were subject to flowcytometry to prepare gating strategies. Metastatic cells were gated from Live/Dead-, CD45- and native GFP+ populations and identified as being (anti-)Firefly Luciferase+ and (anti-)GFP+.

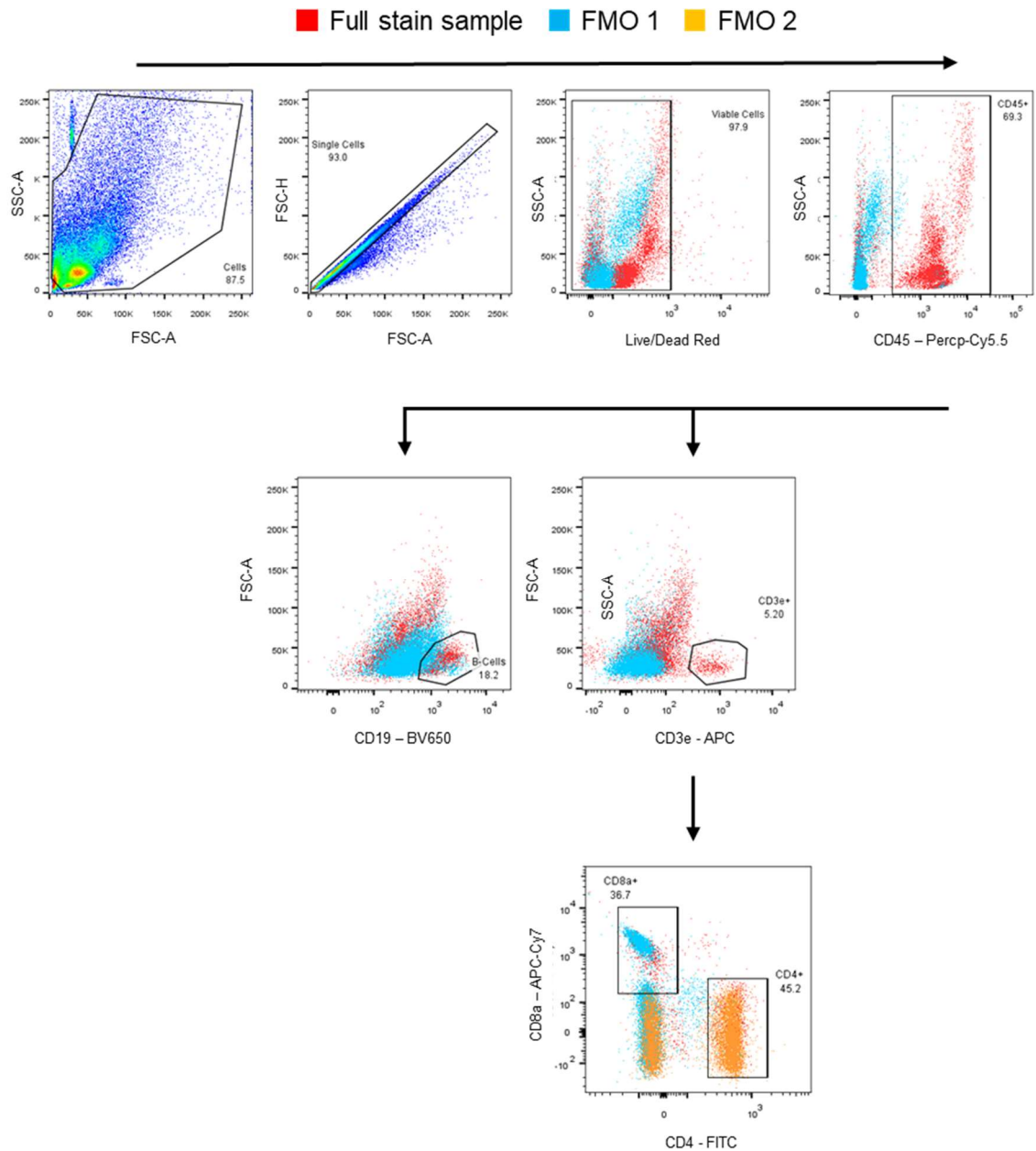


Supplementary Figure 5.2.3. imaging of bones for metastasis. Bioluminescence imaging was performed on bones harvested, at day 15 post tumour induction, from PyMT-BO1 tumour bearing animals at treated with either a vehicle control, VNMAA or cephalexin bathed in luciferin and imaged using the Bruker In Vivo Xtreme. No bioluminescence was observed in any of samples imaged.

■ Full stain sample ■ FMO 1 ■ FMO 2



Supplementary Figure 5.4.1. Gating strategy for identification of myeloid populations in solid tissues. Lung and tumours were subject to a similar myeloid gating strategy. Viable CD45+ leukocytes were gated from Live/Dead- cells. CD11b+ myeloid cells were gated from CD45+ cells and, subsequently, granulocytic cells (Ly6G+, Ly6C^{low}) and monocytic cells (Ly6G-, Ly6C^{high}) were gated from CD11b+ myeloid cells. The expression of the macrophage marker F4/80 was identified within CD45+ leukocytes and gated into F4/80+ and F4/80- cells. Dendritic cells (CD11b-, CD11c+) were gated off of the F4/80- population while two macrophage populations, alveolar macrophages (CD11b+, CD11c-) and non-alveolar macrophages (CD11b-, CD11c+) were gated from the F4/80+ population. The non-alveolar macrophages were further gated into metastasis-associated macrophages (MAMs) (CD11b+, Ly6C^{low}) and metastasis-associated progenitor cells (MAMPCs) (CD11b+, Ly6C^{high}).



Supplementary Figure 5.4.2. Gating strategy for identification of lymphoid populations in solid tissues. Both Lung and tumours were subject to the same lymphoid gating strategy. CD3e+ T-lymphocytes and CD19+ B-lymphocytes were individually gated from Live/Dead-, CD45+ populations. CD3e+ lymphocytes were further gated into CD4+ T-cells and CD8a+ cytotoxic T-cell populations..